Recreating Daylight for Vehicle Interior Evaluations

Innovation Report

Claire White

5th October 2017

This work is submitted in partial fulfilment of the requirements for the degree of Doctor of Engineering (EngD(int))

ABSTRACT

Daylight changes from moment to moment, in brightness, colour and direction. Under changing bright daylight, in-vehicle displays can become unreadable due to washout or glare, causing driver distraction or masking safety critical information. With an increasing number of vehicle systems being controlled through a centralised display, the legibility of automotive displays under ambient lighting conditions has become an important consideration for engineers in terms of perceived quality, safety and driver distraction.

Due to the dynamic nature of the sky, testing under natural daylight would not give the control required for meaningful measurements. Therefore, the challenge for the automotive industry is to standardise the simulation of illumination for performing assessments and to make the process controlled, repeatable and comparable to real daylight situations.

The main objective of this project is to propose a method for recreating a daylight-comparable lighting environment to enable the evaluation of vehicle interiors under high ambient lighting conditions and to propose best-practice for illumination used in legibility evaluation for design and validation activities.

This is achieved with a measurement and simulation approach, to evaluate current procedures and determine the gap between real world, simulation and lab-based assessments, and bring them closer to the real-world.

There are two main outputs from this project; a comparative simulation study which verifies digital tools for use by JLR in display design and evaluation activities, and the recommendation to align physical and digital methods to move evaluations earlier in the new product development process.

A concept has been included to enable controlled measurements as part of physical evaluations, as are the critical factors required for a repeatable physical environment for physical testing as the basis of continuous improvement of digital simulations.

ACKNOWLEDGEMENTS

This research has taken me on a long and varied journey. Along the way I have had some excellent support and advice which has seen me through to the end. I would first like to thank my academic mentors Alex Attridge and Mark Williams for their continued advice, support and academic direction during this project.

I would also like to thank Jaguar Land Rover; my industrial mentors Lee Skrypchuk & Elvir Hasedzic for their contribution to this project; Jas Pawar for facilitating the placement at Gaydon and the OCAE team, Kranthi Puppala, Pratap Yelamanchili and Ajay Kanwar, for their continued interest and support.

To those who offered technical support through this project; Claire Pietu and David Aymond from OPTIS for support and advice concerning SPEOS; Mark Tucker for making my calculations work as a Matlab script; and Peter Tandy and Andrew Minehane for transforming ideas and specifications in CAD models and drawings. Thank you!

Thank you to my wonderful friends and fellow winners, Courtney Thornberry and Matthew Pitts, for allowing me to have a good moan over a massive pub lunch.

I would also like to thank everyone who ever came for a run at 7.30am from IIPSI, especially Amy Burdis who was always there – I miss our runs.

Finally, I would like to thank the people who made this possible; my family. Your love, support and encouragement have enabled me to keep going.

Thank you Mum and Dad, for believing in me and for everything else! Thank you Dude for understanding and holding everything together while I've been busy.

Thank you, Bobbin and Cookie, I owe you so much time (and a build-a-bear) you are both amazing. I love you so much.

CONTENTS

LIST OF FIGURES

LIST OF TABLES

DECLARATION

All material in this Innovation Report is the original work of the author and has not previously been submitted for the award of a degree by this or any other University.

GLOSSARY

TERMS

	Illuminance	Concentration of total light (flux) upon a surface over a unit area. SI units are lumen per square metre (lm/m²) or lux
	Luminance	Light emitted or reflected from a surface in a given direction SI units are candela / square metre (cd/m²) or lumen per steradian per square metre (lm/sr/m²)
	Luminous flux	Total light emitted (power), independent of direction SI units are the lumen (lm)
	Luminous intensity	The total light (flux) from a given direction (generally only applied to a point source) SI units are the candela (cd) or lumen per steradian (lm/sr)
	Photometer	Light measurement device weighted for the response of the human eye
	Photometry	The measurement of light weighted for the response of the human eye
	Radiometry	The measurement of electromagnetic radiation in the optical spectrum
	SPEOS	Physics based rendering and light simulation software from OPTIS
BRDF	Bidirectional Reflectance Distribution Function	This is a relationship between radiance and irradiance expressed as a function of angle of incidence and angle of reflection, describing the diffuse and specular components of reflected light per wavelength
DUT	Display under test	
CCD	Charge Coupled Device	Light sensor technology used in modern cameras and imaging photometers

CIE	Commission Internationale de l'Éclairage	International Commission on Illumination
CSF	Contrast sensitivity function	A description of the visual system's ability to detect low contrast pattern stimuli, usually measured as a frequency response using sine wave gratings
CCT	Correlated colour temperature	A description of the colour appearance of a light source based on its position on the CIE 1931 (x, y) chromaticity diagram, relative to the Planckian locus. CCT is expressed in Kelvin (K).
FPD	Flat panel display	Modern display screen
FTC	Fast transmission caustics	Function in SPEOS for calculating the behaviour of transparent materials
HLDF	High line display front	Touch-screen technology
HMI	Human Machine Interface	This is a system that presents information to user with a mechanism for acting on that information to control a function. This can be in the form of switches and sensors, indicator lights, displays and haptic systems.
HVA	Human Visual System	This is a system that presents information to user with a mechanism for acting on that information to control a function. This can be in the form of switches and sensors, indicator lights, displays and haptic systems.
JLR	Jaguar Land Rover	UK's largest automotive manufacturer and sponsor of this project
LMD	Light measurement device	Such as a lux meter, photometer, spectro-radiometer etc.
NGI	Next generation instrumentation	Touch-screen technology
NPD	New Product Development	The process used by a company to control the development and launch new products
PCDS	Product Creation & Delivery System	The name given to the new product development system in operation at Jaguar Land Rover
PVCIT	Premium Vehicle Customer Interface Technologies	Facility that is part of the Product Evaluation Technologies group at WMG, University of Warwick

PJND	Perceived Just Noticeable Difference	A function of human visual function and contrast to describe the legibility of a display
RVP	Relative Visual Performance	A model linking visual performance to the influence of contrast and luminance defined by Rea (1986a, 1986b) later expanded to include age and target size (Rea and Ouellette, 1991)
RCS	Relative contrast sensitivity	A model of visual performance based on threshold visibility measures taking into account age, contrast, target size and shape, and eccentricity
SPD	Spectral Power Distribution	A chart to represent the radiant power of a light source emitted at each wavelength
VP	Visual performance	A model of visual performance, as defined by CIE 145 (2002), based on the 1945 studies by H. C. Weston

UNITS

cd	Candela	SI unit of luminous intensity also lumens per steradians (lm/sr) defined as the *luminous intensity in a given direction of a source that emits monochromatic radiation of frequency 540×1012Hz and has a radiant intensity in that direction of 1/683W/sr* (DiLaura et al., 2011)
cd/m²	Candela per square metre	SI unit of luminance
lm	Lumen	SI unit of luminous flux
lm/m²	Lumens per square metre	SI unit of illuminance (also known as lux)
lux		Unit of illuminance (lm/m²)
sr	Steradian	SI unit of solid angle

1 INTRODUCTION

This innovation report is an executive summary of the research presented in this portfolio. It serves as an outline of the key outcomes and innovations of the research and discusses them in the context of the sponsor company and the automotive industry. This first section gives an overview of the research and acts as a guide to the portfolio for the reader.

1.1 RESEARCH PROBLEM

Daylight is dynamic. The path of the sun influences the changing characteristics of daylight across the sky, as does the weather and atmospheric conditions. These changes in lighting conditions affect our perceptions yet mostly they are subtle and go unnoticed, however, other conditions interact with our surroundings to make visual tasks uncomfortable, distracting or impossible (Bell and Marsden, 1975; Boyce, 2003; Clear, 2012; Kent et al., 2014; Sawicki and Wolska, 2015).

The ambient lighting, can affect a driver of a vehicle in several ways; specular reflections from surfaces such as mirrors and chrome trim (Caberletti et al., 2010), veiling glare of the dash topper into the windscreen can obscure the driver's view (Bhise and Sethumadhavan, 2008; Dunsäter and Andersson, 2007; Schumann et al., 1996), and components of apparently the same colour when selected, appear different under natural daylight (BSI, 1967; Li et al., 2016). Some of these effects are mildly annoying, whereas others are potentially dangerous. The focus of this research are the effects of daylight at the centre console display which has the potential to be either.

In-vehicle displays can become illegible due to washout or glare, causing driver distraction by increasing the dwell time when reading information or masking safety critical information (Birman et al., 2013; Pala, 2007; Weindorf and Hayden, 2013). With an increasing number of vehicle systems controlled through a centralised display, the legibility

of automotive displays under high ambient lighting conditions has become an important consideration for engineers in terms of perceived quality, safety and driver distraction.

The methods employed to evaluate display legibility will vary depending on the auto manufacturer, however international standards are in place to guide such assessments.

Ford Motor Company refer to the SAE recommended practice in performing physical assessments under high ambient conditions (O'Day and Tijerina, 2011). They consider the character size of the information displayed (BSI, 2009), luminance, contrast polarity and colour contrast under high ambient conditions with respect to SAE J1757-1 (2007).

Research sponsored by BMW defines a figure of merit to link user preference of luminance, contrast and colour to physical measurements at suprathreshold conditions and to describe the ambient conditions that affects the display image quality as perceived by a driver (Wolf, 2014). This involved the application of visual performance models to the results of user subjective assessments.

Following the recommended practice from a standard will give greater confidence in producing a meaningful assessment however there are still issues in creating a controlled testing environment such as mimicking ambient daylight illumination and controlling the geometry of test equipment and ensuring the tests align with human vision. The issues associated with assessing the visual performance of displays are also considered by automotive tier one suppliers such as Visteon (Weindorf and Hayden, 2013), Continental (Birman et al., 2013) and Denso (Pala, 2007).

The challenge for the automotive industry as a whole, is to define the high ambient lighting conditions encountered by a vehicle and reliably reproduce them to evaluate their effects within the vehicle and assess the potential impact of these effects on the driver.

This research focuses on the methods in use at Jaguar Land Rover in order to define best practice in terms of their processes for new product development.

1.1.1 New product development process

New product development (NPD) is the strategy and process implemented by a company that guides the development and launch of new products into the market place. The purpose of implementing such a process is to obtain a competitive advantage through managing the development of new products in a structured way; by allocating resources appropriately, capturing the requirements of the target customer, and ensuring that the conditions of the marketplace are conducive to the launch of the new product (Cooper, 1988; Cooper and Kleinschmidt, 1993, 1988).

Traditionally, the system adopted by many industries to manage NPD and innovation was a phased review process which split the development of products into phases. These phases were designed in a linear sequence; when one function finished, the project would be handed over to the next department to implement their function and so on, until the product was released. While simple and still in use (Hart et al., 2003), this method produces a long development time due to the linear nature of the process. It also engenders the 'silo' mentality where each function is separate without any accountability to the project as a whole (Cooper et al., 2002). Other models have since been developed to make NPD more efficient by encouraging activities within phases of development to be implemented simultaneously by multi-functional teams.

One such system is commonly used in the automotive sector is the Stage-Gate® system (Figure 1-1).

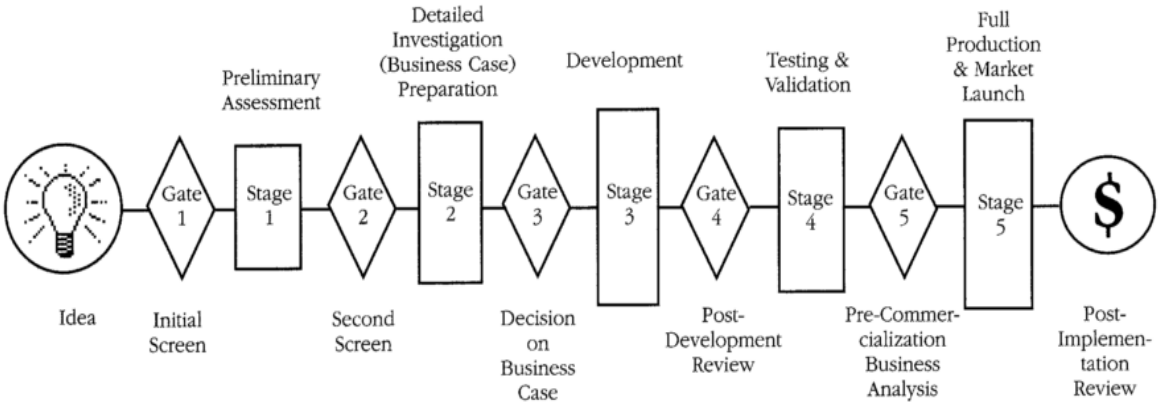

Figure 1-1: The Stage-Gate® process (Cooper, 1990)

Established in the early 1990s by Cooper (1990), Stage-Gate® was developed and refined to be a "*conceptual and operational map for moving new product projects from idea to launch and beyond*" (Cooper, 2008). The model consists of several information gathering stages separated by gateways at which 'Go/Kill/Modify/Recycle' decisions on the program can be made. The gateway becomes a key part of the decision-making process whereby risk and uncertainty are reduced which is a fundamental part of risk management. Decisions can be made to reduce investment when the risk is perceived to be high permitting further development/analysis prior to continuing with the funding (Van Oorschot et al., 2010).

The number of gateways and stages will be different for each company but the general model acts as an overarching roadmap for each program of work.

A criticism of the Stage Gate process, likens it to a traditional linear model with all the drawbacks of such a process (Unger and Eppinger, 2009), however, if used correctly it is a flexible and customisable process, with each stage containing concurrent activities performed across functions. The gateways are not a point at which the project is handed over to another team, but acts as a quality checkpoint where the status of the project is assessed on the progress made in the preceding stage, based on the deliverables at each gateway. A plan is then made on what actions are required to continue to the next stage (Cooper, 2008). This simple, sequential representation of the model does not depict the

flexibility or cross functional nature that is intended; it fails to communicate the importance of feedback and iteration in the process, and how the model should be put into practice.

It has also been said that the Stage Gate process is too rigid due to *"strictly enforced and objective evaluation criteria"* resulting in a lack of lessons learned from projects and stagnation in terms of innovation (Sethi and Iqbal, 2008). There is also the possibility that a project's potential to succeed will be killed early in development if resource is allocated incorrectly or if budgets are too tight (Van Oorschot et al., 2010) or due to a low level of knowledge held by the decision makers at the gateways (Trott, 2008).

Even with its limitations, Stage Gate is only a framework on which to base the process; most criticisms come down to how the process is implemented. No process is perfect which is why the NPD process of any company should be continually evaluated, and improvements made to ensure the process works efficiently and effectively for the workings of the company.

1.1.1.1 NPD at JLR

Jaguar Land Rover (JLR) is a global leader in premium luxury vehicles and have become the largest automotive manufacturer in the UK in 2016 by production volume (Jaguar Land Rover, 2016; SMMT, 2016).

As a technology and innovation led business, JLR invested £3.1bn in technology, infrastructure and talent for product creation in 2016 (Jaguar Land Rover, 2016), enabling them to offer new technologies to produce highly competitive vehicles.

There is a trend in the premium automotive sector, of a greater number of derivatives off a single platform, this results in the introduction of new models at an increased frequency which ties into customer demands for greater choice and technology and features expectations. However, over the past few years the increase in vehicle list price has risen in line with inflation, which equates to net prices remaining 'flat'. Along with the increase in cost for new vehicle improvements and additional features, this has led to a decline in the profits per vehicle (Mohr, D; Muller, N; Krieg, A; Gao, P; Kaas, H W; Krieger, A; Hensley,

2013). To remain profitable, JLR and other premium OEMs need to find ways to reduce cost whilst maintaining basic customer demands. As costs start to escalate during the new product development process, JLR continually evaluate their projects' business potential and focus on ways to reduce cost to meet the original targets.

JLR inherited many systems from their time under Ford ownership, including their NPD system (Mcfadden, 2012). However, the JLR system and the Ford system are very different due to JLR continually adapting their process, to improve efficiency, incorporate new systems and reduce the time to market without compromising the quality of the product. According to Loch (2000), NPD best practice is not 'one size fits all', instead it is a collection of processes aligned by an NPD strategy that best suits the needs of the company. The current NPD structure at JLR is known as the "*Product Creation & Delivery System*" (PCDS). As with many OEMs, JLR's PCDS is based on a stage-gate framework, with multiple levels to account for the various business functions which contribute to the product at different stages, as demonstrated in Figure 1-2**Error! Reference source not found.**. Each work stream will have their own deliverables and milestones but will be aligned to the main programme gateways in each phase of production. PCDS for each programme is managed by a cross functional team with representatives from each work steam. This ensures that a single function or department is never responsible for any one phase of development, and encourages collaboration and team work across the business and a sense of ownership (Cooper, 2008).

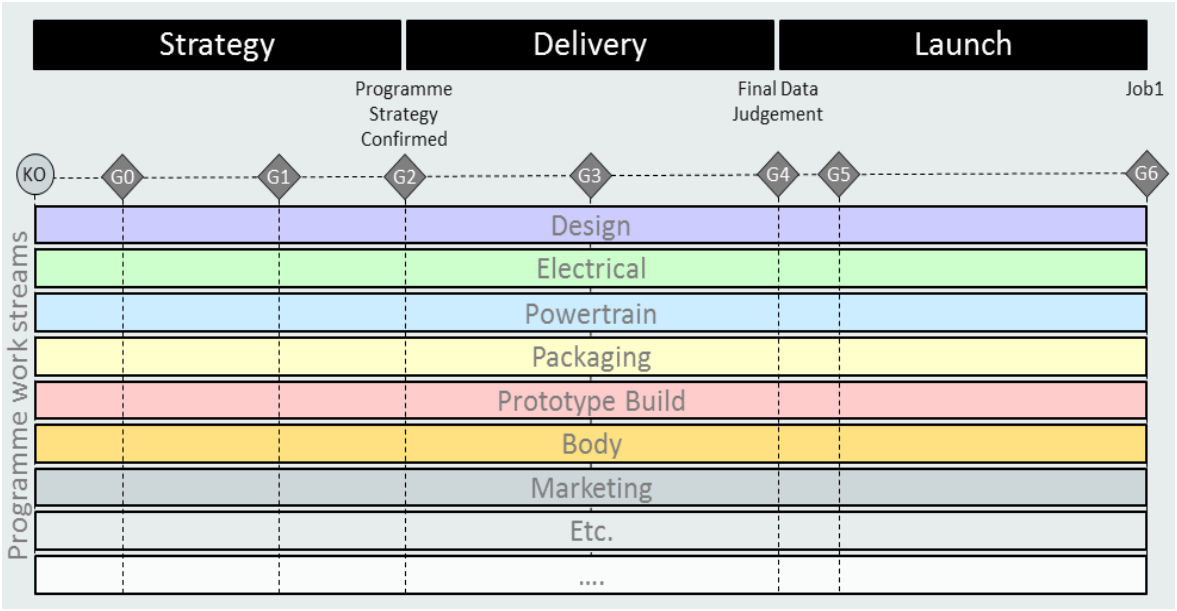

Figure 1-2: General PCDS structure (Freeman and Gaylard, 2008; Ogewell, 2015; Transport Knowledge Transfer Networks, 2012; Williams, 2008; Yazdani, 2006)

Delivery is the phase of detailed engineering. The first gateway of which, G2, signals the end of the phase of discovery (Strategy) where concepts and themes have been developed and styling and functionality of the product are narrowed down and finalised. The culmination of this phase is the freeze of design data where no further changes can be made and all product target have been proven digitally or through physical prototypes. Final Data Judgement at G4, indicates the start of the launch phase which finalises all testing, costing and marketing plans up to Job1 where the first production ready vehicle is produced. Launch is not the end of the process; following this stage the product enters production and finally the market (*Stage 5* of Figure 1-1). These phases of the product lifecycle are also managed under PCDS just as in Figure 1-1, a 'post implementation review' will capture lessons learned from the programme, to be fed back into future programmes and iterations of the PCDS.

Jaguar land rover have digital tools to allow a shift away from the traditional effort model of product development to a 'Front Loaded' model whereby effort in the development of a product is shifted to the left of the NPD process (Figure 1-3**Error! Reference source not found.**).

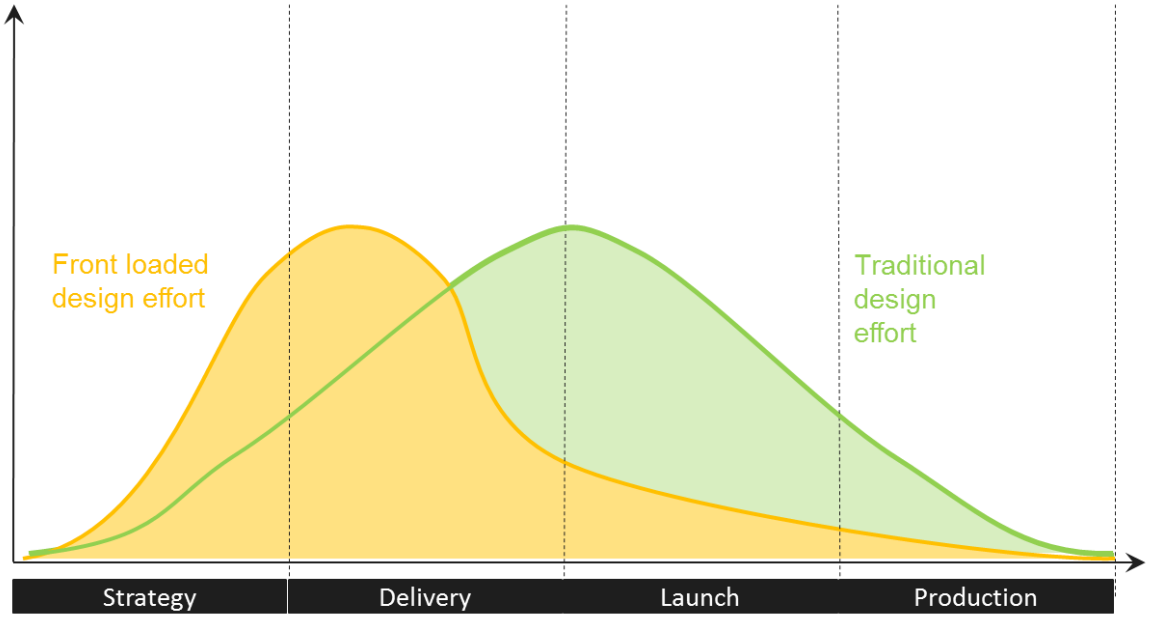

Figure 1-3: 'Front loading' or moving effort to the left of the NPD process

With effort shifted left, decisions can be made earlier and potential failure modes can be identified at a stage where they can be resolved with minimal cost, effort and impact on the timing of the programme. This shift can also lead to a more innovative solution, as multiple solutions can be evaluated reducing the conservative practice of carrying over proven parts, and can avoid the risk of obsolescence of using physical prototypes later in development (Trombini and Zirpoli, 2013).

At JLR, the daylight performance of the vehicle is assessed through physical and digital evaluations which are performed at different stages of development of the vehicle programme, with different teams responsible for the delivery of each.

Digital lighting evaluations are the purview of the Optical Computer Aided Engineering team (OCAE), part of Inter-Attribute Engineering (IAE). The OCAE team uses SPEOS to perform lighting simulations to support development, from G1 to G6 (see Figure 1-4**Error! Reference source not found.**), with bespoke checks and full assessments of functional lighting, displays and other lighting effects as the design progresses. These assessments are to aid with material selection and/or application that may impact the view of the driver, the positioning of display components and functional lighting to ensure quality targets will

be met, and reflections into the windscreen and side windows are outside critical areas of the driver's field of view. Requests for assessments are made as and when required throughout the programme from different attribute or project teams to support their delivery.

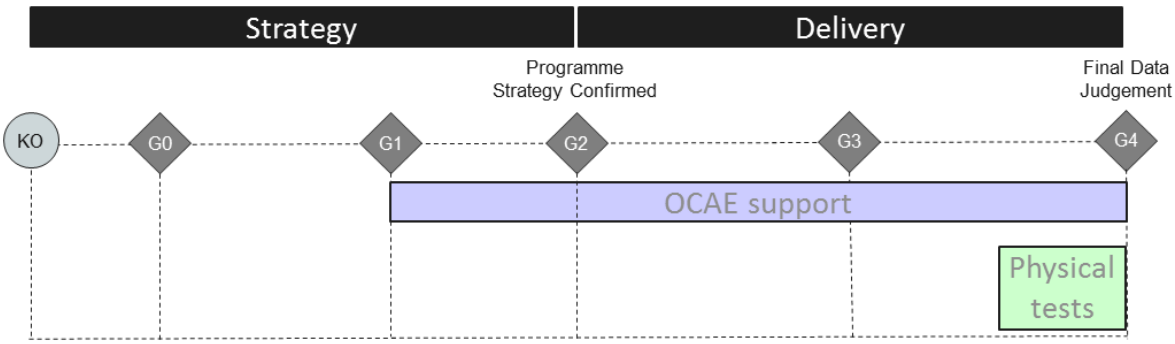

Figure 1-4: Optical performance assessments timing

For the current validation and sign-off of a vehicle programme physical tests are required, but as with the experience with crash testing, multiple scenarios can be modelled and simulated with digital tools and a single scenario can be verified with testing (e.g. crash one car). This reduces cost and uncertainty.

Physical evaluations are the responsibility of the Human Factors and HMI attribute teams. They set the performance criteria and ensure the quality, safety and legislative standards are maintained through physical measurement of the attribute. These tests are generally performed on one of the later prototype builds where the upper-body development is as close to production intent as possible. Testing includes the minimum requirements of functional lighting, night-time/daytime visibility of illuminated features and the high ambient legibility of displays (see Section 2.2).

1.1.1.2 Moving to the left

Automotive development is a complex and lengthy process; the development time for a new vehicle is between 24 and 36 months (Gibbs, 2015). In that time the requirements of the customer and the introduced technologies and innovations of competitors are changing. It is therefore important to keep the 'voice of the customer' at the forefront of

development to ensure the product released into the market is 'fresh' and a delight for the customer, to maintain or exceed the brand image and competitive advantage of the company (Chen et al., 2005; Chong and Chen, 2010).

Changes made to the product as a result of late marketing decisions can substantially impact the cost and timing of the project. It is not only market fluctuations that incur costs for change; one of the greatest sources of cost is late design changes due to the detection of failure modes such as errors or the unforeseen behaviour of the design. Failure modes detected late, or by the customer are costly or not possible to remedy, as depicted by Figure 1-5.

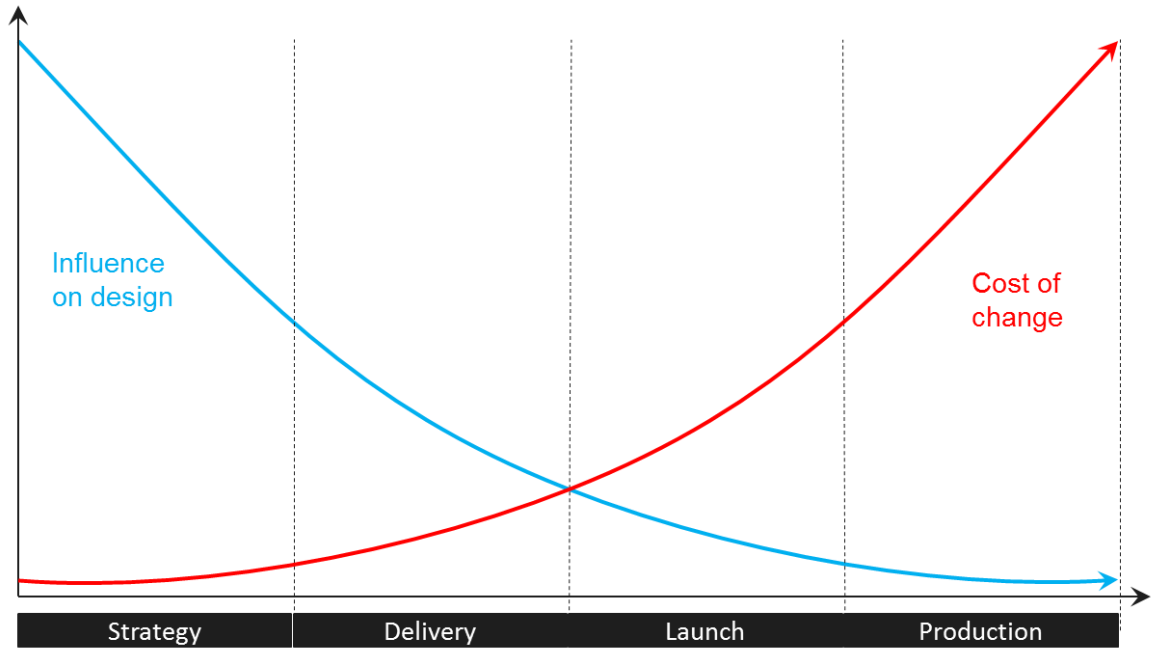

Figure 1-5: The cost of making design changes and the amount of influence on changing a design as a project progresses (based on (Boehm, 1976; Paulson Jr., 1976)*)*

Based on experiences in the construction industry, Paulson (1976) notes a decreasing level of influence as the uncertainty of the project is reduced over time. Concurrently, investigations in software engineering observed that as the stages of development progressed so did the relative cost to correct any errors detected (Boehm, 1976). This is due to the product becoming more 'fixed', therefore seemingly small changes can have a large impact across the entire design. This is especially true of more complex products and

it becomes more difficult and more expensive, in time or expenditure, to make any changes in the later stages of development. To avoid these late changes, it is a widely-held view that the greatest impact on cost, time and quality of the product is for failure modes to be detected in the earlier phases of development while the design is still flexible (Becker et al., 2005; Thomke, 2007, 1998; Thomke and Fujimoto, 2000; Wheelwright and Clark, 1992a; Zorriassatine et al., 2003).

JLR are continually making improvements in their NPD and establishing the failure modes earlier in the process as a way of 'Moving to the Left' their development process (or left shifting the development timeline). This is achieved through the investment of digital tools and techniques, with a goal of new vehicles being entirely developed through digital methods, prior to the tooling phase, by 2020 (Gibbs, 2015).

1.1.2 Recreating daylight for vehicle interior evaluations

Initially, in line with current industry practice, this research focussed on physical methods for recreating daylight, with a view to achieving a controlled lighting environment, comparable to real-world daylight, for the physical evaluation of performance of in-vehide displays, as well as other interior assessments. However, as the research progressed, this focus has shifted to consider in-vehicle display evaluation as a system of the virtual world of evaluations and testing (physical and digital), and the real world experienced by the driver (Figure 1-6) to make the greatest impact on NPD and shift evaluations earlier in the process (El-Sayed, 2011; King, 2002).

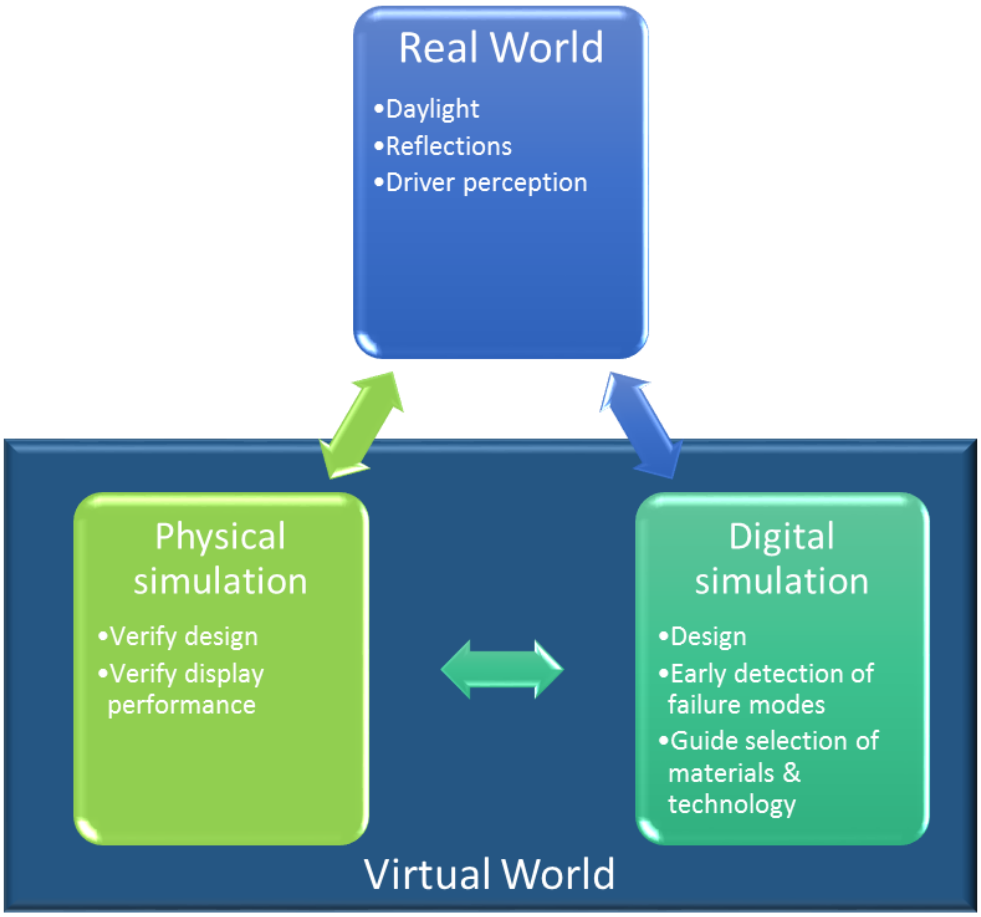

Figure 1-6: In-vehicle display evaluation system

The description of the real world relates to the experiences of the driver; how daylight interacts with the vehicle and how the driver perceives this. The virtual world tries to emulate these experiences to evaluate how a new design or technology will behave in the real world (Zorriassatine et al., 2003).

Physical evaluations are generally used to verify the design using prototype vehicles, and must mimic these qualities of the real world through a controlled artificial environment with a view to verifying the display performance as quoted by suppliers and to verify the design of the optical layout and HMI. Evaluations involving measurement must be repeatable and be able to be reproduced by other operators meaning a controlled environment and measurement procedure (BSi, 1994; Gawlik and Rewilak, 1999; Vitek and Kalibera, 2011). This is to minimise the variation in the testing and to yield consistent and comparable measurements.

Digital methods of assessment can be used at any point in the NPD process to detect potential problems with the display position and technology choice. If these assessments are performed early enough in the process, costly changes can be avoided later in development or failures which could lead to customer dissatisfaction, can be prevented (Becker et al., 2005). Digital methods are inherently repeatable and reproducible; however, care must be taken to ensure the correct inputs are used in each scenario to ensure consistent simulations with an output comparable to the real world.

Physical evaluations at buy-off and digital simulations to guide the design are currently employed within the automotive industry however, these must not be viewed as independent assessments, but part of the same process. For example, performing the analysis of the effects of ambient lighting on display legibility during the design stage, can guide the orientation and positioning of the display and the selection of technology used, considering established 'design rules' to avoid specular reflections from the display that will distract or even injure the driver.

Digital simulations must be representative of the real world in terms of the geometry of the vehicle and the behaviour of daylight within the vehicle. This must then correlate to the physical evaluations performed as part of the buy-off procedure (Zorriassatine et al., 2003). As with any design there will be variation in the finished product, the purpose of buy-off is to ensure that the technology performs as expected and that the final product meets the design within tolerance. Buy-off procedures must also reflect the assumptions of the design and the digital assessments, and be comparable to real-world daylight conditions as well as the physical geometry and viewing conditions of a driver (Czichos et al., 2011). These assessments are for the benefit of the end user; the driver. It is therefore critical that any measurement/simulation be sympathetic to human vision and the viewing position of the driver. For meaningful measurements/simulations, the quantification of how close the model performs in relation to the real world is required (Zorriassatine et al., 2003).

1.2 AIMS AND OBJECTIVES

1.2.1 Aim

The aim of this research is to *recreate daylight for the evaluation of in-vehicle displays*. As stated above, it is important that both physical and digital methods be considered to ensure correlation to each other and to the real world. Both are required to have a high level of control and be a representation of the real-world scenario with comparable inputs and outputs for consistent and meaningful assessments.

1.2.2 Objectives

With this aim in mind, the following objectives have been devised in order to achieve this in a robust manner:

Objective 1. Define the 'real-world' in terms of automotive displays; the environment in which they are viewed, how they are perceived by the driver and their performance.

Objective 2. Assess current in-vehicle display evaluation methods.

Objective 3. Define an appropriate method for recreating daylight and performing evaluations of in-vehicle displays.

Objective 4. Propose best-practice for display legibility assessments for design and validation activities in Jaguar Land Rover.

1.3 METHODOLOGY

To address the objectives of this research a quantitative approach using experimental and simulation methods has been followed to the steps outlined below:

Simultaneous measurement of display and sky

The luminance across an in-vehicle display was recorded simultaneously with the sky luminance and colour distributions. A total of 31 unique data sets were captured in Australia January 2015 including; a photometric image of the display (containing luminance

and colour data per pixel), a photometric image of the sky (containing luminance and colour data per pixel), the global horizontal illuminance (outside the vehicle) and the horizontal illuminance within the vehicle cockpit. This gives the reflections at the display and the daylight conditions which cause them to establish a real-world benchmark.

Development of models and simulations

Models are generated using physics-based rendering and light simulation software (SPEOS), based on JLR procedures and measurement geometry. Simulations are performed with standard settings and by varying the skies under which the displays are viewed to compare to the effects recorded in the real-world.

Simulations of the sky are also performed and a method developed in order to extract the luminance distribution to compare with those measured.

Comparison between measurements and simulations

The data captured in Australia are processed with a view to performing a comparative simulation study between measured and modelled displays. This study is to determine the influence of simulated dynamic skies on display legibility and to verify the use of digital methods for use in in-vehicle display assessment by establishing the difference to real world conditions.

1.4 PORTFOLIO STRUCTURE

This portfolio contains four submissions which document the research performed and are referred to in this innovation report. The process followed in this research is split into 6 steps (Figure 1-7); defining the problem, formulating the objectives, constructing the data collection instrument, collecting data, processing data and analysis, and implementation.

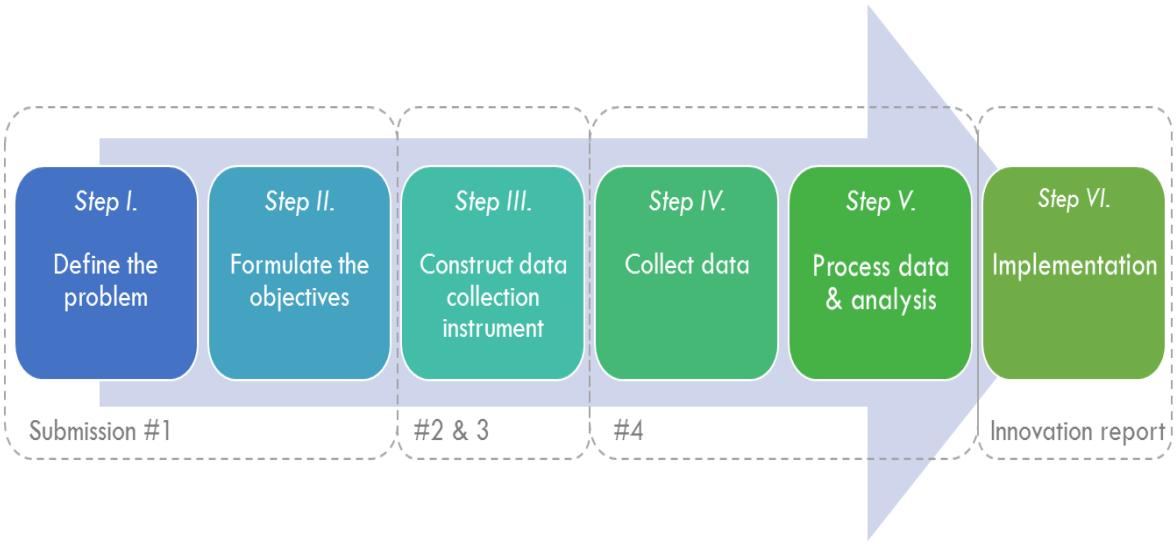

Figure 1-7: Research steps reported in the EngD portfolio

Figure 1-7 illustrates the steps and indicates where they are reported in the portfolio. The following is a brief synopsis of the content of each submission:

Submission #1: Artificial Skies (Step I & II)

The first steps of this research were based on literature and industrial and academic site visits. The outcome was a review of current technologies with the potential for recreating a daylight comparable environment and a set of basic considerations for performing vehicle interior evaluations, documented in Submission #1. One of the important actions that resulted from this review was the requirement to measure displays under real skies. This was with a view to defining the characteristics of the sky to be reproduced artificially in an evaluation facility and evaluating current method of recreating daylight against the real world.

Submission #2: Sky Capture (Step III)

Submission #2 details the sky capture trials performed to determine the procedure for collecting photometric data from the sky using an imaging photometer with a circular fisheye lens. These trials identified and overcame issues associated with operation of the photometer under high luminance conditions. The use of additional filters was rejected in favour of masking the sun and circumsolar region

with a view to reconstructing the data in post-processing. Due to the equisolid angle mapping function of the lens optics, it is possible to map the flat image of the sky to corresponding to angles of equal projection onto the curved hemisphere of the sky. This allows for the sky images to be sub-divided and luminance averages taken of discrete sky 'patches' to give a simplified distribution to be used in defining the influence of the sky on in-vehicle displays and to contribute to a specification of artificial daylight.

Submission #3: Display Assessments (Step III)

This submission details a lab based trial for in-vehicle display measurement. This was setup to determine the worst-case lighting angles to prioritise data capture under real-world conditions and to determine any issues with setting up and performing measurements. Due to the low intensity of the lamp used, it was not possible to identify the lighting positions with the greatest influence on display legibility. This setup did however, highlight the low repeatability of measurements and the variation in alignment between measurements, which can be attributed to movement in the photometer position and issues in the alignment geometry. Greater control can be introduced into the setup by replacing the reliance on tripods with dedicated mounting systems.

Submission #4: Displays under Dynamic Skies (Step IV & V)

Reflections of an in-vehicle display were recorded simultaneously with the sky luminance and colour distributions. This data was collected in Australia, January 2015. A total of 31 unique data-sets were captured which included: A photometric image of the display (containing luminance and colour data per pixel), a photometric image of the sky (containing luminance and colour data per pixel), the global horizontal illuminance (outside the vehicle) and the illuminance of cockpit.

The data captured in Australia is processed with a view to performing a comparative simulation study between measured and modelled displays. Display simulations are

run with standard settings on models generated based on JLR procedures and measurement geometry. Additional simulations are performed to vary the skies under which the displays are viewed. In addition, simulations of the sky are performed in order to extract the luminance distribution to compare with those measured. This study determines the influence of simulated skies on display legibility and also verifies the use of SPEOS for this application by establishing the difference to real world conditions.

1.5 Guide to Innovation Report

This report is designed to be a stand-alone document, however where further detail is required, the reader will be directed to the submission that contains this information. Even though the report contains details from the submissions, it does not follow the structure of the portfolio.

Section 2 gives the background of this research in terms of the real-world effects of daylight on in-vehicle displays and the current practice of display metrology and in-vehicle display evaluations.

Section 3 gives an overview of the measurements performed in this research. It contains a summary of trial measurements and details the field measurements of displays under high ambient daylight conditions in Australia.

Section 4 assesses the gap between the real-world measurement and virtual assessments. This assessment is in terms of physical measurement procedures such as the lab trial from (Section 3) metrology best practice (Section 2) and simulations compared to the measured skies and displays (Section 3).

Section 5 discusses the gaps identified in the previous section and proposes a way to address them; both in terms of physical and digital evaluations.

Section 6 discusses the research in terms of the New Product Development (NPD) process; where it fits currently at JLR, where it should be implemented and the implications of the implementation.

Section 7 concludes this report and highlights the impact and innovation of this project, where it has added value and the potential for future research.

2 AUTOMOTIVE DISPLAYS UNDER HIGH AMBIENT ILLUMINATION

Research into automotive displays under high ambient light conditions is a multidisciplinary field which touches on many research areas, the most relevant to this research are illustrated in Figure 2-1.

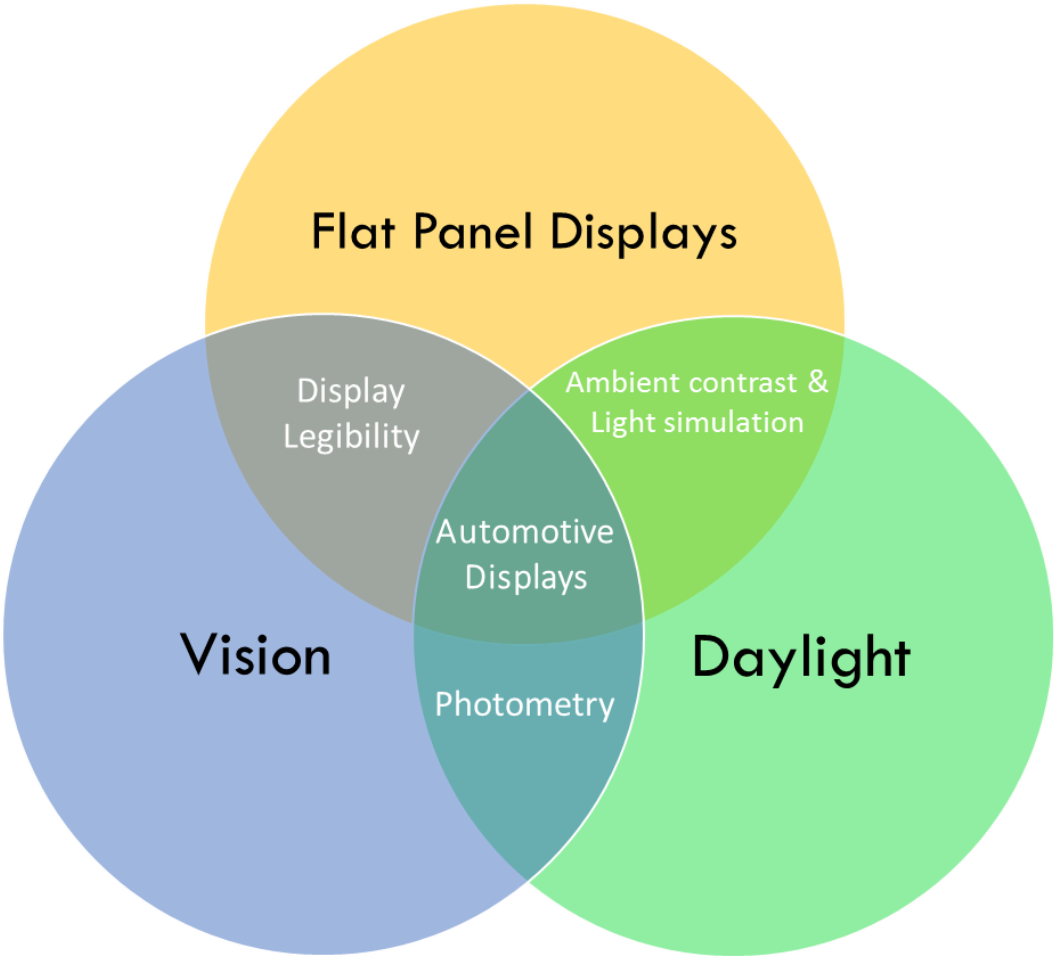

Figure 2-1: Automotive displays research areas

Common to all flat panel displays (FPDs) are the fundamentals of display metrology and determining the legibility of information presented. This research also considers the effects of daylight on the display, it is therefore important to understand how light behaves in a space, from fundamental optics to the characteristics of daylight and human visual perception.

To address *Objective 1: Define the 'real-world' in terms of automotive displays; the environment in which they are viewed, how they are perceived by the driver and their performance,* this section describes the techniques used to characterise the behaviour of in-vehicle displays under high ambient conditions; display metrology standards, legibility metrics and procedures to evaluate legibility at Jaguar Land Rover.

2.1 AMBIENT CONTRAST PERFORMANCE OF IN-VEHICLE DISPLAYS

Daylight is a combination of direct sunlight and diffuse skylight resulting from sunlight scattered by the atmosphere. The diffuse light from the sky forms a non-uniform distribution of luminance and colour which is continually changing depending on time of day, time of year and location (latitude). Though nominaly 'white' , the spectral characteristics of daylight are irregular and vary constantly throughout the day depending on the position of the sun and atmosperic conditions.

Daylight is strongly dependent on the elevation of the sun above the horizon and affects how the intensity and colour of light reaching the ground and its reflections are perceived by the observer. This angle determines the length of the path of light reaching the ground; lower altitudes equate to a longer path travelled through the atmosphere with a greater amount of solar energy being absorbed and more blue light to be scattered, resulting in lower intensity warmer (yellow-red) light.

Daylight within the vehicle is reflected from different surfaces in all directions. Reflected light at the central display becomes a problem when it travels back to the driver's eye point, and is perceived as any combination of the three components of reflection (Kelley et al., 1998a);

- Lambertian (see Figure 2-2a). Diffuse reflections independent of direction. A uniform wash of light is superimposed on the image of the display resulting in a loss of contrast.
- Specular (see Figure 2-2b). Directional reflections that produce mirror-like images at the display.
- Haze (see Figure 2-2c). Diffuse reflections in the direction of the source of illumination that produces a fog-like effect over the display image.

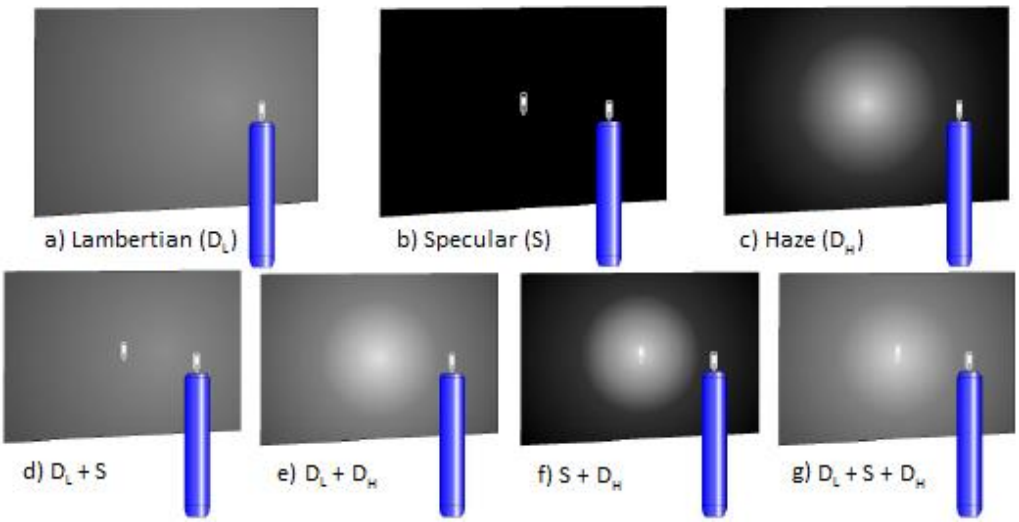

Figure 2-2: Components of reflection (ICDM, 2012) *illustrated by light source reflections on a screen*

Both the specular reflections (also known as glare) and diffuse reflections (commonly referred to as washout) degrade the performance of the display.

The performance of in-vehicle displays is evaluated on several criteria to do with the physical characteristics of the display, such as surface defects, pixel/luminance uniformity etc. However, arguably the most important performance criterion is the legibility. Legibility is the relative ease by which the driver can recognise each character and distinguish it from its surroundings (Ambrose and Harris, 2006; O'Day and Tijerina, 2011). Readability is a concept linked to legibility but is mostly concerned with the layout and design of the text and images displayed to convey information to the driver in a timely manner (Ambrose and Harris, 2006; Dale and Chall, 1949). Legibility is a combination of task and lighting and depends on the effects of luminance (including contrast and colour), the size of the target information displayed and the functions of human vision (including the effects of age of the observer).

2.1.1 Display metrology

To determine the characteristics of a given display under a specific set of conditions requires measurement. With respect to the legibility of displays, the measurements of interest are reflections of ambient light which are used to define the *'ambient contrast'*; the contrast of the display under ambient lighting conditions. These measurements can be complicated, with set-up geometry being critical for quality measurements (Jones and Kelley, 1998; Kelley, 2002; Kim et al., 2009). This is mainly due to the the non-lamberian scatter of light from the display surface as the magnitude of reflections are non-uniform and are heavily dependant on the incident angle of the light and viewing direction of the observer. Therefore standards have been established to advise on performing quality measurements (BSI, 2014, 2012, 2009; ICDM, 2012; SAE, 2007).

For these measurements to be useful and comparable to a standard, it is important to establish a measurement method that controls the variables of the environment and measurement condition for precise and reproducible results. The simpler the method the better, which is one of the reasons that performance characteristics of displays measured under dark room conditions are usually quoted by display manufacturers to give a way to compare different displays, and are useful benchmark measurements. However, few displays have an intended application in a darkroom environment it is therfore a better indication of performance to perform assessements in the presence of light which mimics the enviromnent of the end user.

Diffuse ambient contrast measurements, to simulate viewing conditions of an ovecast day, were proposed via a number of methods (Kelley, 2001a) but with the same general premise and set up geometry (Figure 2-3**Error! Reference source not found.**). Full screen black and full screen white luminance measurements were taken of a display under test where the ambient light was simulated with a light source reflected from a surface surounding the display, to give an even distribution of light. The contrast ratio of the display under these conditions is then calculated and scaled to the illuminance.

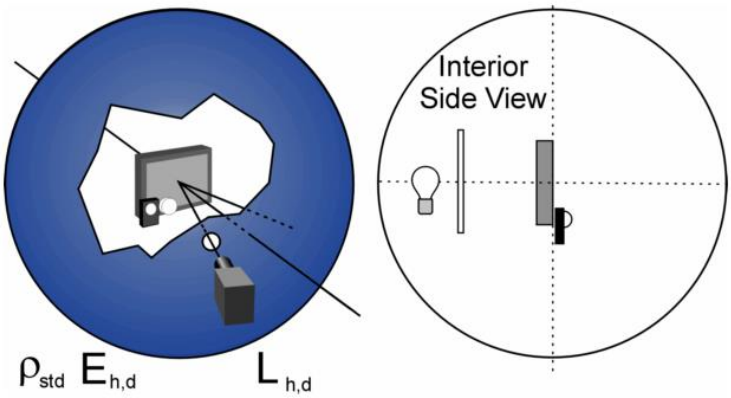

(a)

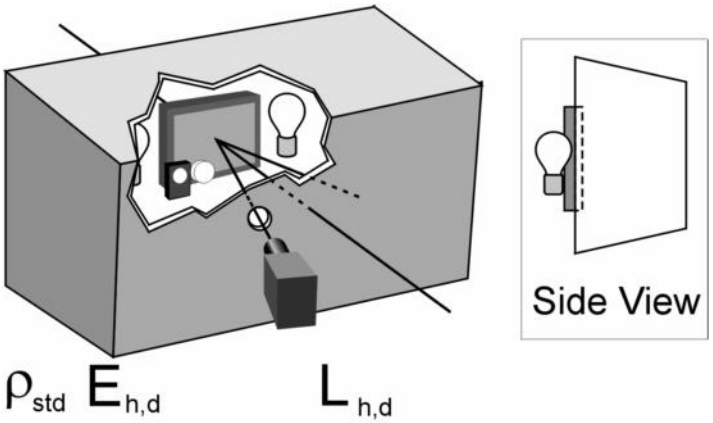

(b)

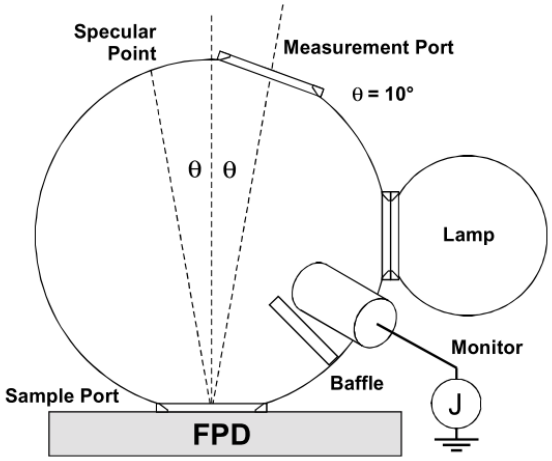

(c)

Figure 2-3: Setup for diffuse ambient contrast measurements; (a) integrating sphere, (b) open box method (c) sampling sphere (Kelley, 2001a)

Kelley, Lindfors, & Penczek (2006) determined that for realistic daylight measurements of displays it is not enough to use a spot light of sun-level illuminance to represent daylight. Their method to determine daylight ambient contrast of the display involves measurements under a diffuse sky condition and a direct sun condition. The diffuse sky measurements are performed using a setup as shown in **Error! Reference source not found.**(c) with a tungsten-halogen source filtered to achieve a CCT of 16,500K. The direct sun condition is setup with the geometry demonstrated by Figure 2-4**Error! Reference source not found.**. The direct source is to subtend 0.5° to the centre of the display, and uses a filtered tungsten-halogen lamp of 5,500K.

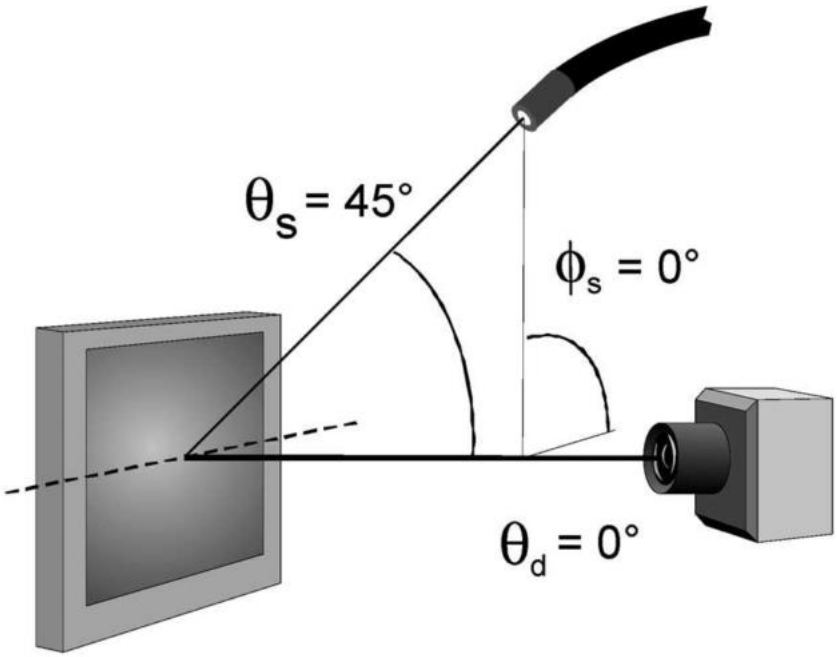

Figure 2-4: Fixed sun daylight measurement configuration (Kelley et al., 2006)

The individual measurements of luminance from these setups are used to determine the contribution of the sun and sky components, then combined and scaled to give an overall impression of display contrast under daylight illumination with CCT 6,500K. This method has been developed further and has been adopted by a number of international measurement standards (BSI, 2014, 2012; ICDM, 2012).

Under dark room conditions, their display under test exhibits high contrast yet when viewed under daylight conditions, the value drops to a fraction of the dark room contrast.

When viewed as the individual measurements, the effects under the direct sun setup demonstrates a better ambient contrast than that measured from the diffuse setup. They conclude that the contribution of sky light is not negligible and it is therefore important to also consider the diffuse contribution of the sky in addition to the direct component for any ambient contrast measurements.

For automotive applications, these standards are slightly different due to the viewing angle of the driver. Generally, for display metrology, the set-up geometry of the light measurement device (LMD) is positioned normal to the display centre, however this is not representative of the typical viewing direction of the driver which is at an oblique angle. This viewing angle affects how the display is perceived due to the directionality of the scattered light, therefore specified performance compared to the view from the normal direction would not be a true indication of performance in use. Automotive standards have therefore been drafted to take viewing angle into consideration to assess the daylight legibility of a display. ISO 15008 (BSI, 2009) and SAE J1757-1 (SAE, 2007) define the minimum requirements for legibility and outline methods to perform 'High Ambient Illumination Contrast Ratio Measurements' of displays, specifically for automotive applications, recommending two measurement methods similar to the Kelley method; an in-situ measurement set-up and using an integrating sphere or a smaller sampling sphere.

The sampling sphere setup simulates the diffuse ambient condition; daylight without direct sun exposure to the geometry shown in Figure 2-5**Error! Reference source not found.**.

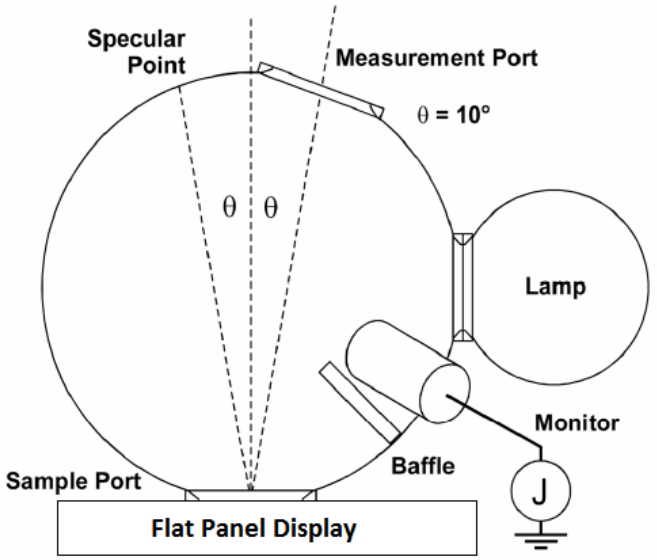

Figure 2-5: Measurement set-up using a sampling sphere (SAE, 2007)

Depending on the size of the sampling sphere and a method to place the equipment at the display surface, it may be possible to perform this measurement within the vehicle if necessary, however it would be simpler to perform this measurement on the test bench with sturdier and more stable mounting of equipment without the constraints of the vehicle architecture. Therefore the only advantage to an in-vehicle setup would be if it is not possible to remove the display under test from the vehicle.

The method for in-situ measurement simulates two situations; diffuse sky and direct sun which are simulated separately (see Figure 2-6**Error! Reference source not found.**).

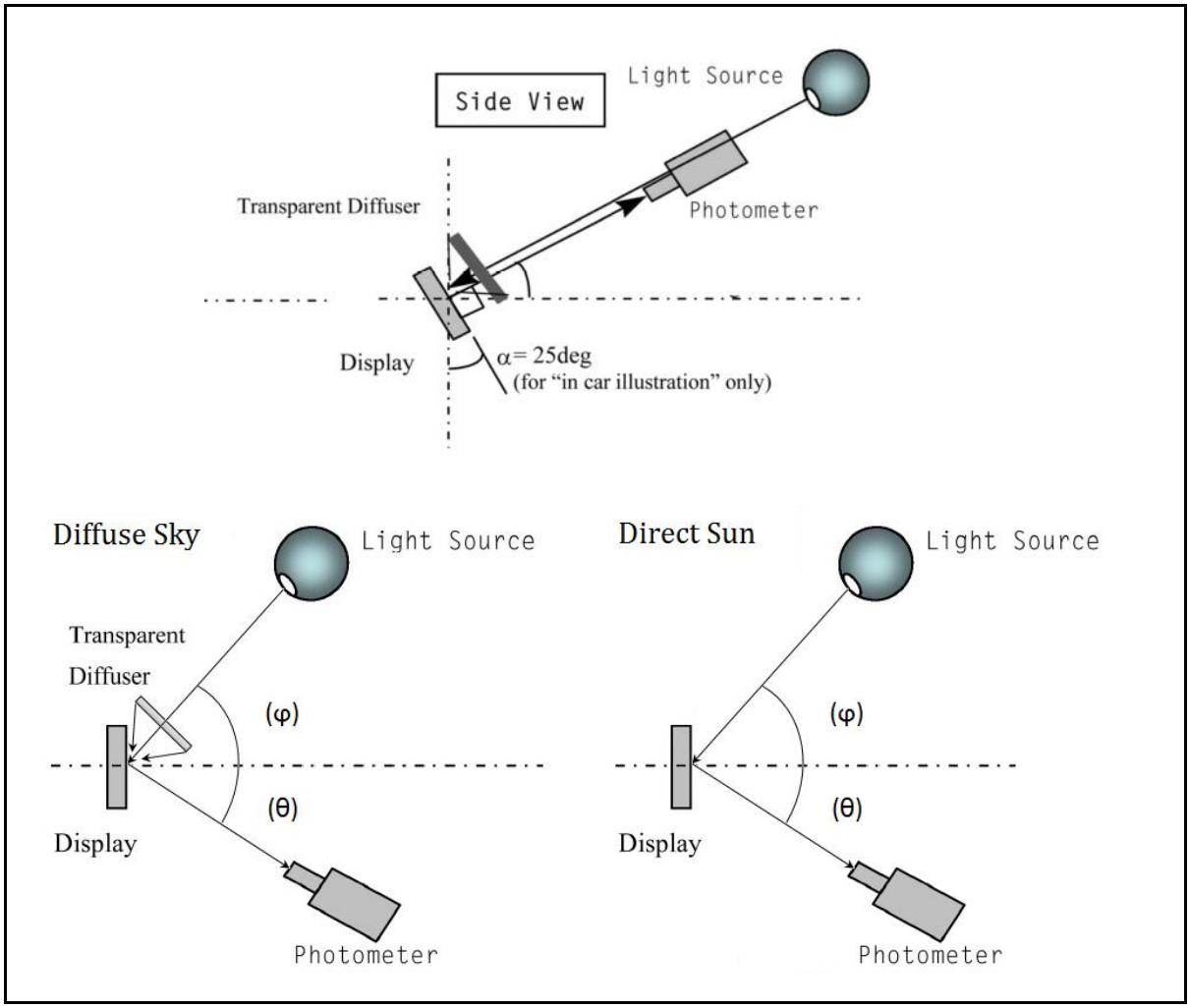

Figure 2-6: SAE J1757-1 real life/in car measurements using high ambient light illumination simulation geometry: Side view of diffuse sky setup shown (top) & plan view (bottom) for diffuse sky (left) and direct sun (right) (based on (SAE, 2007)*)*

This method has the advantage of being able to be performed within the vehicle under assessment with the photometer placed at the driver eyellipse as defined by ISO 4513:2010 (BSI, 2010). It is also possible to set up these tests using known vehicle geometry on the test bench.

Use of the sampling sphere neglects the vehicle geometry in the test, and only the performance of the display under a theoretical overcast sky can be evaluated. This method can be used to assess the legibility at the display by assuming that the patch sampled is under the influence of the sky. It does not assess the display as a whole under any specific daylight conditions. The in-situ method allows an evalution closer to the use case and

assessment of the performance of the entire display rather than only across the sample port. It also takes into account the viewing geometry of a driver and recommends measurements in a range of positions within the viewing cone (SAE, 2007). However even this method is not a truly realistic representation of daylight within a vehicle due to measurements under direct sun and diffuse sky being taken separately and only for a single source geometry (Blankenbach, 2012).

The in-situ method can be used as a basis to build a representitive in-vehicle assessment under a range of sun positions that could impact the legibility of the display. This would need to incorporate both the direct sun and diffuse sky components along with the vehicle geometry and specific display orientation with respect to a driver's viewing position.

2.1.2 Visual Performance

The human visual system (HVS) comprises the functions of the eye and brain to process the signals generated by optical radiation to produce an image. As with any system, the HVS has a limit to its capabilities described by boundary conditions called the 'thresholds of vision', which indicate where a visual task becomes difficult. Visual thresholds are the point at which a stimulus can just be discriminated by the visual system under various conditions (P. Boyce & Raynham, 2009; Lee, 2005) in terms of the minimum detectable light or the minimum discernible differences, as opposed to stimuli which are easily visible which is known as a suprathreshold measure. According to Boyce (1973) *"A threshold condition is described by the value of the stimulus for which the required response (e.g., detection of the stimulus) is 50 per cent correct. This 50 per cent criterion is a matter of convenience and convention."*

Between individuals of a population, threshold measures are highly variable yet there is a general trend in visual performance for lighting, target conditions and age that allow these measures to be used to describe the general functions of the HVS (Blackwell, 1946; Boyce, 2003). Thresholds can be categorised as either *spatial threshold measures*, *temporal threshold measures* or *colour threshold measures*. These relate to the ability to discriminate a target from its background (*spatial*), the detection of fluctuations and the

speed of response (*temporal*) or the ability to just discriminate colours as separated on a chromaticity diagram (*colour*). These threshold measures describe the main visual functions of the HVS; adaptation, contrast perception and visual acuity.

Adaptation: The HVS can function over a large range of light intensity levels from bright daylight luminance of 10^8 cd/m² to dark night-time luminance of approximately 10^{-6} cd/m², however it cannot operate over all over all of these levels simultaneously. Adaptation is the function by which the visual system changes its sensitivity dependant on the level of illumination.

Contrast perception: As the luminance of the environment increases, fully light adapted cone photoreceptors become less sensitive to light with rods becoming saturated and insensitive to further light signals. This decrease in sensitivity at the retina is attributed to the photochemical process of bleaching and regeneration and the neural process of lateral inhibition. Lateral inhibition is where the signal generated by neighbouring photoreceptors are not transmitted to the ganglion cells if activated at the same time; only the signal from the cell at the centre of the receptive field will be transmitted resulting in an overall reduction in sensitivity (Schreuder, 2008). This neural process not only ensures that under changing luminance the brain receives a consistent signal but it is also the process by which 'edges' and differences in luminance are perceived.

The luminance of a target is not the only factor which determines whether or not the target can be 'seen', rather it depends on the threshold luminance being achieved as well as the difference in luminance or colour between the target and its immediate background. This difference is known as the contrast.

Visual acuity: Visual acuity is a measure of how well the HVS discriminates fine detail of a target. Acuity tests use high contrast, high luminance targets, where the smallest target can be identified on 50% of occasions presented.

It is usually expressed as a threshold of separation denoted by the angular measure (measured in minutes of arc) of the smallest discernible target. This figure is quoted

as one minute of arc for normal foveal vision (Peter R. Boyce, 2003; Schreuder, 2008), however this is dependent on the method used to measure acuity. Measurements of acuity use targets such as gratings, Landolt rings or alphanumeric characters.

Physiological changes in the HVS occur over time; even with healthy eyes, visual perception can deteriorate. With age, the crystalline lens density increases; it becomes less flexible and a greater amount of light entering the eye is absorbed. This leads to a reduction in retinal illuminance resulting in a lower contrast sensitivity in older adults. Weale (1961) noted that by the age of 60 an observer will have a contrast sensitivity of approximately 1/3 of that at age 20. Also, the light absorbed is not uniform across wavelengths; primarily shorter wavelengths are absorbed due to an accumulation of yellow pigments in the lens which results in a shift in colour perception in older observers (Boyce, 1973; Salvi et al., 2006).

There is an increase in intraocular light scatter in the aging eye that can reduce image contrast and increase sensitivity to glare effects (Boyce, 1973; Owsley, 2011) which are more pronounced in observers with increased opacity of the lens (age related cataracts) (de Waard et al., 1992).

Predominantly attributed to the slight variation in radii and asphericity of the crystalline lens with age, the eye loses the ability to compensate for ocular aberrations; the geometric imperfections of the optical system that affect performance (Berrio et al., 2017). The muscles that control the iris weaken with age, causing the maximum diameter of the pupil to be reduced. This condition, Senile Pupillary Miosis, contributes to the reduction in retinal illuminance, yet it has also been linked to a lessening of the effects of high order aberration in older eyes (Mathur et al., 2010).

As the lens thickens and the ciliary muscles (that control lens shape) weaken, the ability of the eye to focus on objects of varying distance (accommodation) is diminished and the closest point at which the eye can focus (the near point) recedes, so that by age 45 most people can no longer focus on objects nearer than approximately 40cm (Owsley, 2011).

Along with these optical factors there are neurological changes, such as a reduction in ganglion cell density at the retina, which affects contrast sensitivity. However, for photopic vision neural changes have been found to be a minor influence on the contrast sensitivity when compared to the optical factors (Burton and Sloane, 1993; Owsley, 2011). Whereas for scotopic and mesopic levels, it is suggested that neurological changes are a contributory factor to the reduction in visual performance in older observers. This is due to optical changes not being able to fully account for the higher magnitude of vision losses at lower lighting levels (Burton and Sloane, 1993).

What is known of the performance of the human visual system is based on psychophysical measurements. Psychophysics is the study of the human response to physical stimuli, as such it is highly subjective. It is also difficult to measure the response of a single stimulus without the influence of other variables. There has been a wide range of studies on human vision and the perception of light that have resulted in various models and laws which can be used in defining visual perception. However, in appreciating how the human visual system responds, it is important to keep in mind the experimental conditions under which the models hold true, in order to extrapolate these conditions to the real world.

2.1.2.1 Visual performance models

Every task is a unique combination of visual and non-visual components of performance, making it impossible to generalise the visual performance from the effects of light on one task to another task. However, an early attempt to do this by Weston was to use a simulated task using Landolt rings to measure visual acuity (Weston 1945 in Boyce, 2003). Rings of varying gap size (measured in minutes of arc) and contrast were presented to subjects on a chart under different background illuminances. Subjects are then asked to read through the chart and mark all rings with a specific orientation. The time taken and accuracy of the task were recorded, minus the time taken to mark the chart to isolate the motor component from the visual aspect of the task. Measures of Speed and Accuracy were defined which were then multiplied to give a performance score. The results of this

study are displayed in Figure 2-7 as a plot against illuminance for different ring gap sizes and contrast.

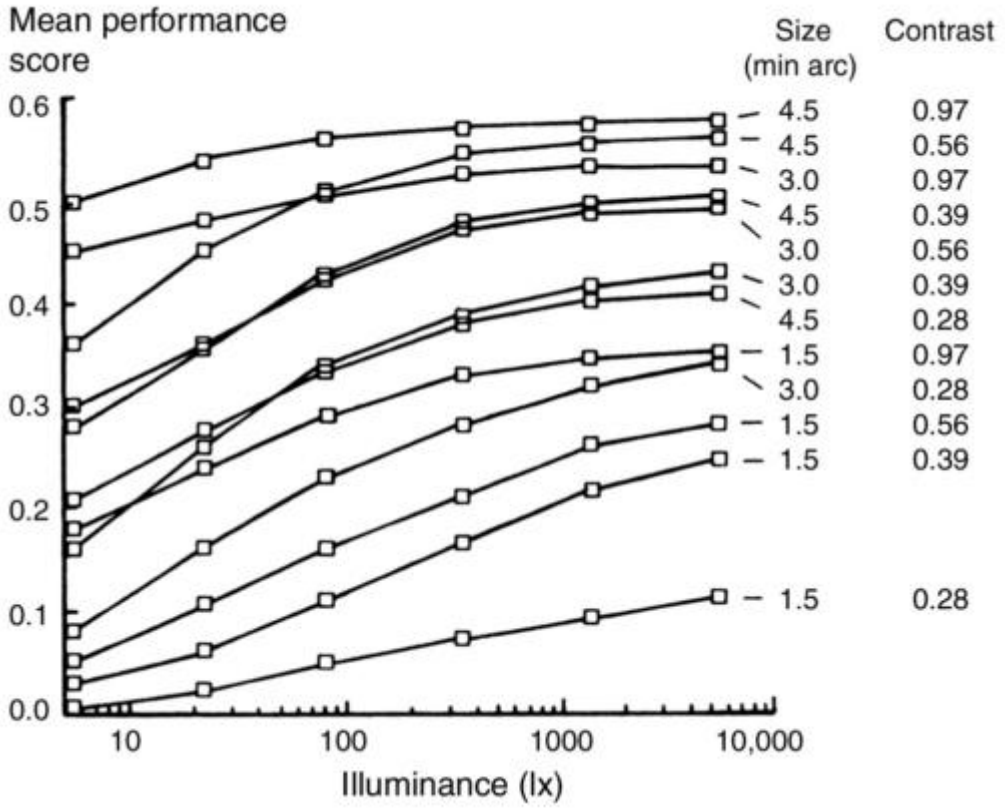

Figure 2-7: Weston's visual performance vs illuminance for different critical size and contrast (CIE, 2002)

From these results, it can be seen that visual performance or the visibility of the task, generally increases with contrast, target size and illuminance. However, criticism has been directed at this model from Rea (Rea, 1986a; Rea and Ouellette, 1988) due to inconstancies between results from Weston's earlier work and the arbitrary multiplication of two task performance parameters, speed and accuracy, which he believes should be dealt with separately. Boyce (2003) suggests that this multiplication skews the effects of two difference aspects of task performance and that this is therefore not a model to describe visual performance, but is rather an indication of general trends in performance.

Rea (1986a, 1986b) attempts to create a generalised model from measuring simplified real tasks where the non-visual component of the task is low, and the performance can be

extrapolated for a set of conditions. His experiment involved subjects reading and comparing a list of five-digit numbers of fixed size with varying contrast and background illuminance. The time taken, as well as the accuracy of the comparison was recorded, however only the reading time data was transformed and used in the development of the model as it was the more stable measure of visual performance. The first model of Relative Visual Performance (RVP), linking visual performance to the influence of contrast and luminance, is demonstrated in Figure 2-8.

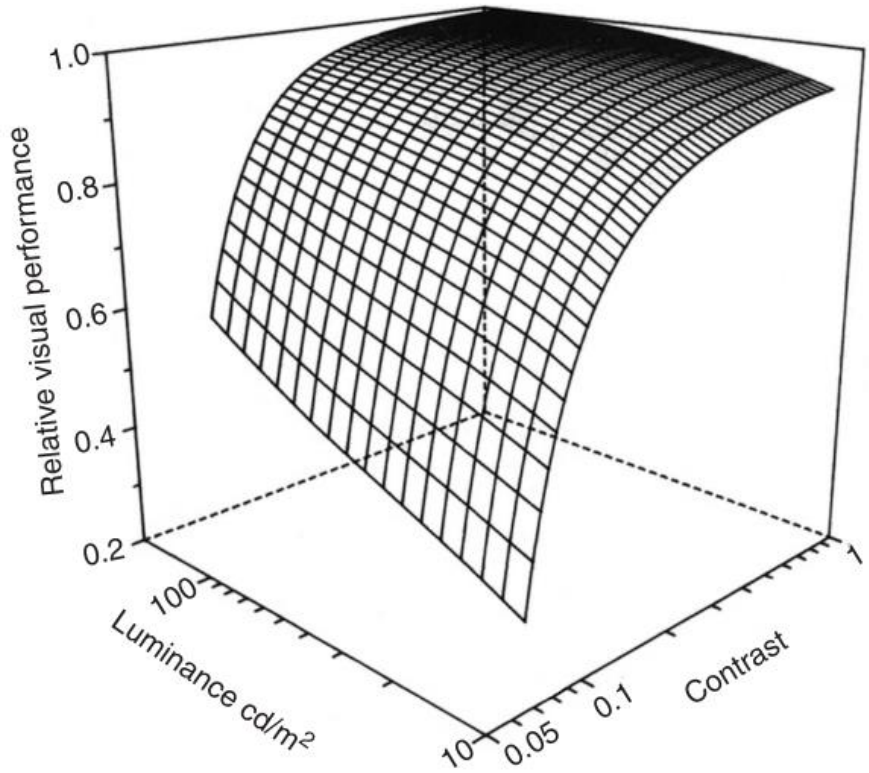

Figure 2-8: The RVP model of visual performance (Rea, 1986b) *plotted for a single size of task element based on response times of reading task*

As with the Weston model, this model demonstrates that visual performance is high with increased contrast and greater background luminance, but rapidly drops as one of the factors becomes too small for discrimination of the target. It does not, however take into account the effect of target size, or for situations of light text on a dark background and is

only applicable to young subjects. These limitations are noted by the author as points for further investigation.

Rea & Ouellette (1988) build on this work with two experiments measuring reaction time of a presented target; one for targets lighter than their backgrounds and one for targets darker than their backgrounds. The variables of the experiments were target size defined by the solid angle (measured in steradians), target contrast, and retinal illuminance which was calculated from background illuminance and controlled with an 'artificial pupil'; a 2mm diameter aperture to limit the amount of light entering the eye. These were then linked to differences in visual processing time, ΔT_{vis}, in a new model to describe visual performance.

Both of these models, RVP and ΔT_{vis} were still limited to young subjects and not directly comparable due to the differing measures of visual performance.

Both sets of data were unified into a single model through deriving an equal set of stimulus conditions of subject age, target size, target contrast, and retinal illuminance (Rea and Ouellette, 1991). These conditions allowed the two independent models to be related to each other by a linear scale transformation and generalised for the prediction of visual performance of older observers. The result was a final visual performance model based on reaction time, RVP_{RT}, as shown in Figure 2-9.

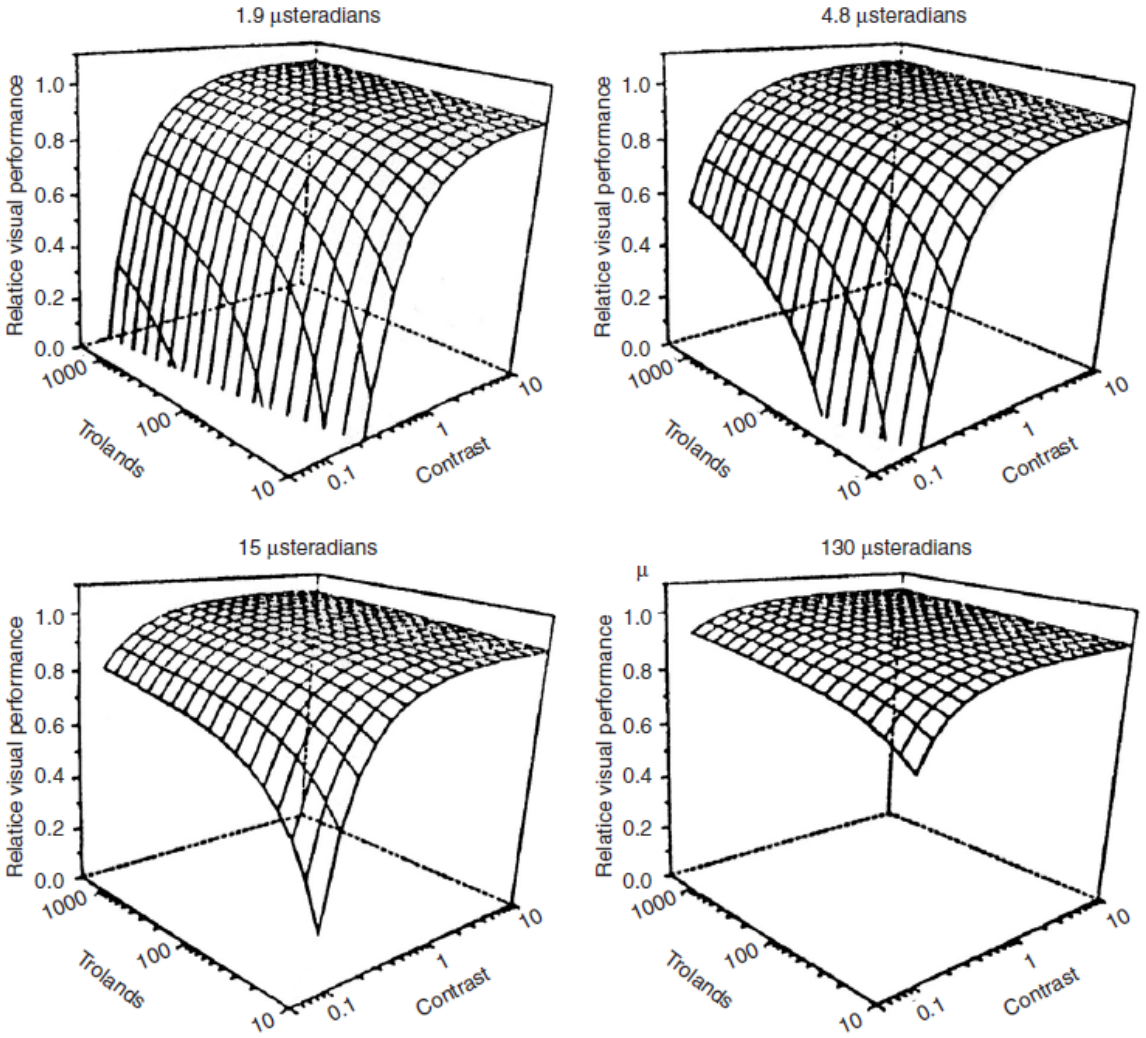

Figure 2-9: The RVP model of visual performance based on reaction time data. RVP plotted for varying contrast and retinal illuminance (trolands) for a fixed target size (µsteradians) (Rea and Ouellette, 1991)

This model gives a good description of visual performance for tasks dominated by the visual component and can be described by the effects of visual size of the target, luminance contrast and background luminance limited to values within the ranges used in production of the model. This model should also be limited to foveal tasks where there is no dependence on peripheral vision or search, as noted by Boyce (2003), the model is based on conditions where subjects were presented with a stimulus and knew where to look for information.

A criticism of the RVP model comes from CIE145 (CIE, 2002) in that the model does not consider the influence of visual acuity and how it is affected by age of observer. The document states that the RVP model erroneously disregards the influence of age by using a calculation for pupil size that is only valid for young subjects, and only considers the changing transmittance of the ocular media with age, thus reports an incorrect value for retinal illuminance for older observers. However, this is not strictly true as the RVP model incorporates a function to lower the retinal illuminance due to reduced transmittance as *well as* an increase in scatter. This function is based on estimates of age dependant thickening of the crystalline lens and reductions in pupil area (Weale 1961 & 1963 in Rea and Ouellette, 1991). The basis for this criticism may be in the control of the pupil diameter in the reaction time experiments and that all measurements are based on young subjects. Indeed, the VP model of visual performance as recommended by CIE 145:2002 is developed from studies that only use natural pupils and involves the resolution of fine detail, which the reaction time experiment did not. The VP model of visual performance is based on the 1945 studies by H. C. Weston, with the incorporation of an Age Factor, to predict speed and accuracy of performing the Landolt ring task.

CIE 145 seems to have misrepresented the RVP models which calls into question its dismissal in favour of Weston's data, based on the claims that RVP and ΔT_{vis} are incongruent when the final model is not presented. It does however make some valid points for application. The RVP model uses complex factors in its calculation; retinal illuminance and solid angle of the target. In practice, it would be simpler to use the CIE 145 recommendation but the selection of a model would need to be made based on the requirements of the application and the boundary conditions to be considered.

2.1.2.2 Legibility evaluation

As has already been stated, legibility depends on the luminance, contrast, target size and the visual perception of the observer. Modern research into flat panel displays has contributed to defining these parameters such as the optimal character height of text (Cai and Green, 2009, 2005) and the effects of colour and contrast under different illumination

(Kelley et al., 2011; Wang et al., 2012), resulting in the development of a number of methods to evaluate display performance under varying ambient lighting conditions.

Wang et al. (2012, 2010, 2009) use the method of Minimum Separable Visual Angle (MSVA) in a number of their studies. This method involves participants identifying the direction of Landolt rings in 9 seconds, and using the minimum size distinguishable to evaluate visual performance of electronic displays. These studies vary the size of the target and the ambient illuminance in order to measure visual acuity under changing illuminance levels for different technologies. As a user trial, this method would be a useful tool to compare the performance of a number of displays or to establish pass/fail criteria for future evaluations. Alone, however, it would time consuming and impractical for automotive testing as there is no clear metric for evaluation of the legibility of characters of a specific size defined, just that one display is better than the other under different illuminances. A metrological method used in conjunction with a visual performance model would be better suited to the evaluation of display performance for automotive applications.

The work of Edward Kelley and a number of collaborators, has defined display performance evaluations, focusing on the characterisation and metrology of display reflections and ambient contrast (Hertel and Kelley, 2014; Kelley, 2007, 2002, 2001a, 2001b, Kelley et al., 2011, 2006, 1998a, 1998b; Kelley and Penczek, 2004; Kim et al., 2009; Penczek et al., 2015). In the evaluation of 'daylight readability' Kelley et al. (2006) propose the use of the VP model of visual performance, as defined by CIE 145 (2002), as the metric to define performance of displays under daylight ambient conditions (see Submission #3 for more details on the human perception).

The visual performance was calculated for a 20, 50 and 75-year-old observer using the equations from CIE 145, which are defined in terms of contrast (C), background luminance (L_{ave}) and critical detail size (arc minutes), then scaled with an age factor. This model is plotted as displayed in Figure 2-10, normalised to the performance of a 20-years-old observer at 1,000cd/m² with the critical target size of 1.5' to give a relative visual performance of P=1, or 100%, to indicate 100% accuracy of the visual task. In this case, the

smaller target size of 1.5' is employed, as opposed to 4.5' defined in CIE 145, in order to represent the character size common on many electronic displays.

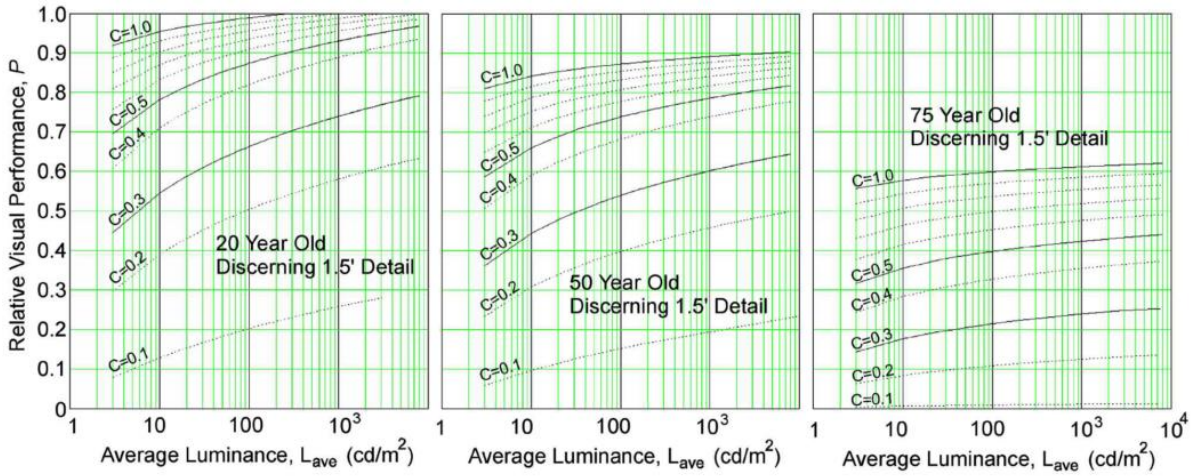

Figure 2-10: Visual Performance to the CIE VP model as calculated by Kelley et al. (2006)

Measurements of luminance were taken for the foreground target and the background of a full display to calculate the luminance contrast, this is then used with the plotted model to allow the prediction of display performance for the same display of defined contrast under different adaptation luminance levels for different observers.

An alternative to this is the Perceived Just Noticeable Difference method (PJND). The PJND method was developed by British Aerospace specifically for legibility assessments of aircraft displays and was derived through physical simulation of display reflections (Vassie, 1998). The daylight environment of an aircraft cockpit, under which the display would be viewed was characterised to calculate the light reflected to the eyepoint of a pilot.

The threshold contrast luminance and chromaticity were determined for a task with a critical target size of 4 minutes of arc and considers the changing performance of the human visual system with luminance level based on the relative contrast sensitivity function (RCS), as defined by Blackwell (Blackwell, 1946) and used as the basis for CIE Report 19/2 (1981), normalised to 10,000cd/m². For the luminance contrast, this threshold was determined to be 0.0051 which is the value required for 50% of the population to discern a difference. On the same basis, the chrominance threshold, to discern a difference

in colour as plotted on the UCS diagram was determined to be 0.0042 (Sharpe et al., 2003; Vassie, 1998).

The result was two functions; one to determine the Luminance Just Noticeable Difference (Equation 2-1) and the other for the Chrominance Just Noticeable Difference (Equation 2-2). These functions are then combined to give the overall Perceived Just Noticeable Difference (PJND) as shown in Equation 2-3.

Equation 2-1: Luminance Just Noticeable Difference

$$LJND = \frac{\log_{10} Contrast \times RCS}{threshold}$$

Equation 2-2: Chrominance Just Noticeable Difference

$$CJND = \frac{\sqrt{(u'F - u'B)^2 + (v'F - v'B)^2} \times RCS}{threshold}$$

Equation 2-3: Percieved Just Noticeable Difference

$$PJND = \sqrt{LJND^2 + CJND^2}$$

Where contrast is the ratio of target luminance to background luminance, $u'F$ and $v'F$ are the foreground colour co-ordinates and $u'B$ and $v'B$ are the background colour co-ordinates as plotted on the UCS diagram, and RCS refers to the relative contrast sensitivity.

This is not a generic model of human vision such as the VP model, but that of a specific use case. It is therefore limited for daylight ambient legibility of a display with the same reflectivity characteristics as that used in the experiment. It is also a simplification in that it assumes visual performance at threshold levels hold true at suprathreshold conditions.

However, the PJND as calculated from these equations were then linked to subjective measures of acceptability defined at suprathreshold levels to extend the use of the metric to any display. This was determined via user subjective assessments of simple and complex graphical and numerical information displayed with various luminance levels. The participants of the original study were five test pilots, reported as being young, mainly male with good visual acuity (Sharpe et al., 2003; Vassie and Christopher, 2000). This was expanded in a further study with both male and female participants between the ages of 24 and 57 with an average of 34. A cockpit mock-up of a fast jet was set up under artificial

lighting producing 100,000 lux of illumination at the display surface. The display under test had a luminance of more than 3,500 cd/m² which participants were asked to adjust the luminance and grade the display as either *'acceptable'* or *'desirable'*. The luminances were recorded and used to calculate PJND values for those conditions indicated. The pass levels ascertained for the Eurofighter jet can be seen in Table 2-1.

Table 2-1: Acceptance PJND values for different functions on Eurofighter (Sharpe et al., 2003)

Function	Minimum PJND value	Description
Attention getter	120	This data requires attention getting quality that must be maintained beyond the para-foveal limit and into the peripheral vision areas.
Warning and caution	90	This data contains warning information or cautionary information requiring predominate attention.
Dynamic complex	70	This data contains complex formats with small alphanumeric characters and/or fine line analogue or graphic presentations. This data is *not* fixed in location.
Static Complex	60	This data contains complex formats with small alphanumeric characters and/or fine line analogue or graphic presentations. This data *is* fixed in location.
Status	50	This data consists of dual state (on-off) information. Its location is fixed.
Informative	40	This data is fixed format single state information. This provides background information supporting controls or more complex presentations.

In these applications, the major component of PJND is from the LJND due to the chrominance difference being determined for shades of white/black. The CJND will be more applicable for design of colour formats such as coloured backgrounds and symbols.

Automotive displays operate under lower ambient illumination than above cloud situations and are generally enclosed in the vehicle rather than exposed under a clear canopy (with the exceptions of a convertible or a panoramic roof). The adaptation luminance of the driver is therefore lower, requiring a lower display luminance for the display to be visible and comfortable. Automotive displays typically emit at luminances of 400 to 800cd/m². Under these conditions the calculated PJND acceptability classes would differ from the fast

jet application. For automotive applications, the PJND scale needs to be adjusted to take these deviations into account, as well as to define the acceptance criteria of a driver.

For use by Jaguar Land Rover, this PJND scale was determined in a project led by National Physical Laboratory. User trials were performed with an unbiased sample population of 31 male and female participants with an average age of 46. Luminance levels of a display were adjusted by the participants for the display to fall into one of the performance categories shown in Table 2-2 with the luminance of the display measured and the corresponding PJND value calculated using Equation 2-1 to Equation 2-3.

Table 2-2: General acceptance criteria for JLR display assessment (according to JLR test procedure)

Performance categories	Description
Easily readable	The driver is able to read the display instantaneously when glancing at the display. The background colours will be more visibly discernible and thus is consequently more visually appealing than "Readable".
Readable	The driver is able to read the display almost instantaneously when glancing at the display. It will appear as largely monochromatic and consequently is not visually appealing.
Just Readable	This requires the driver to dwell momentarily in order to read information from the display.
Unreadable	The driver is unable to read information from the display.

The acceptance levels were defined based on the foreground luminance that 95% of the population would consider the display to be either, *'Just Readable*, *'Readable'* or *'Easily Readable'*. A critical value of PJND 32 was determined to correspond to the legibility class 'Readable' and any display found to be less than this is deemed unacceptable.

Generally, the results of industrial research and procedures are deemed proprietary and are not largely disseminated to the wider research community as it would be with academic research. Therefore, there is no published evidence to suggest that this model is used outside of BAE Systems and Jaguar Land Rover, which suggests that it has not had the rigorous testing by the academic community that the VP model has benefited from such as evaluating the fit of the model to the data collected from other studies, however the

model has been referred to in other studies when selecting a figure of merit (Aydın et al., 2009; Wolf, 2014).

Both the VP model of CIE 145 and the PJND model are based on character size, contrast and luminance to define the visual performance. PJND is a simplified metric based on reasonable assumptions for application in practice. However, this simplicity affects the flexibility of the model as the critical target size is fixed and cannot be used to assess larger or smaller characters than those subtending 4 minutes of arc. PJND uses the relative contrast sensitivity as a variable with background luminance to model the change in performance. RCS as defined by CIE 19 (CIE, 1981) incorporates an age factor, similar to that used in CIE 145 however, it is not clear if this has been set to the average age of the trial participants, or whether the RCS calculation used in this PJND model is based on the earlier version of CIE technical report #19 which does not include an age factor which means that this model holds true for young observers only.

Ultimately, for use in the evaluation of legibility at JLR, PJND has the advantage of being scaled with a suprathreshold acceptance; for *VP* or any other model of visual performance to be applied to automotive assessments some form of pass/fail criteria would be required for the in-vehicle situation to be useful.

2.2 In-vehicle displays evaluations at Jaguar Land Rover

Evaluations of the centre console display are made to verify that a minimum legibility/visual performance is achieved under various lighting conditions. At Jaguar Land Rover (JLR), these evaluations follow a test procedure designed to identify the potential optical failure modes of the display from the following three stages:

1. Digital simulations: An analysis on simulations performed using the optical ray-tracing and physics-based rendering tool, SPEOS.
2. Physical evaluations: Measurements performed on a production level vehicle to assess the legibility based on the PJND method. This stage generally conforms to

SAE J1757-1*: Standard Metrology for Vehicular Displays.* This standard is also recommended as a reference to aid the set-up of measurement conditions.

3. Real world assessment: A test drive to verify the performance under real world conditions.

2.2.1 Digital simulations

SPEOS is an optical ray-tracing and physics-based rendering tool integrated into CAD software such as Catia V5, NX Creo and SolidWorks, and is widely used in the automotive industry by OEMs and tier 1 suppliers for light modelling and visual ergonomics (Delacour et al., 2005; Dunsäter and Andersson, 2007; OPTIS, 2017).

At Jaguar Land Rover, SPEOS is used to perform optical failure mode analysis on a number of attributes such as veiling glare into the windscreen, interior reflections, Head Up Display (HUD) assessments and display legibility and reflection studies. The SPEOS display evaluations, highlight areas at the display where there is the potential for specular reflection and identify specific sun directions that may cause issues. In terms of legibility, a PJND simulation is performed on a display with no graphic which assesses the display under 360 sun positions, corresponding to a rotation from 0° to 360° and an elevation from 0° to 90° at 10° intervals. A SPEOS output file (.xmp) is produced for each result where specific issues can be investigated. These 360 .xmp files are then processed with a proprietary macro that runs within SPEOS to calculate the PJND based on the contrast between the specified value of background luminance of the emissive display used in the simulations and the foreground luminance, which is a combination of the specified luminance and the reflections of the simulated daylight. For these calculations, the CJND component is neglected as there is no graphic included in the simulations due to there being no method included to discriminate the chromaticity values of foreground and background characters.

The output of the macro is processed to produce two polar plots which display the PJND acceptance levels as areas that span sun positions with respect to the vehicle. One is generated from the average luminance across the entire display and the other is calculated

with the maximum luminance on the display at each condition. These plots give an approximation of legibility for the whole display surface therefore the two results give a more balanced picture of performance, with the maximum showing the worst-case condition but will not be able to show the area of the display affected.

For example, areas of Figure 2-11 that are green or yellow are sun angles (rotation and elevation) which produce a PJND of greater than 32 at the display, indicating acceptable legibility, whereas dark red indicates areas of potential specular reflection.

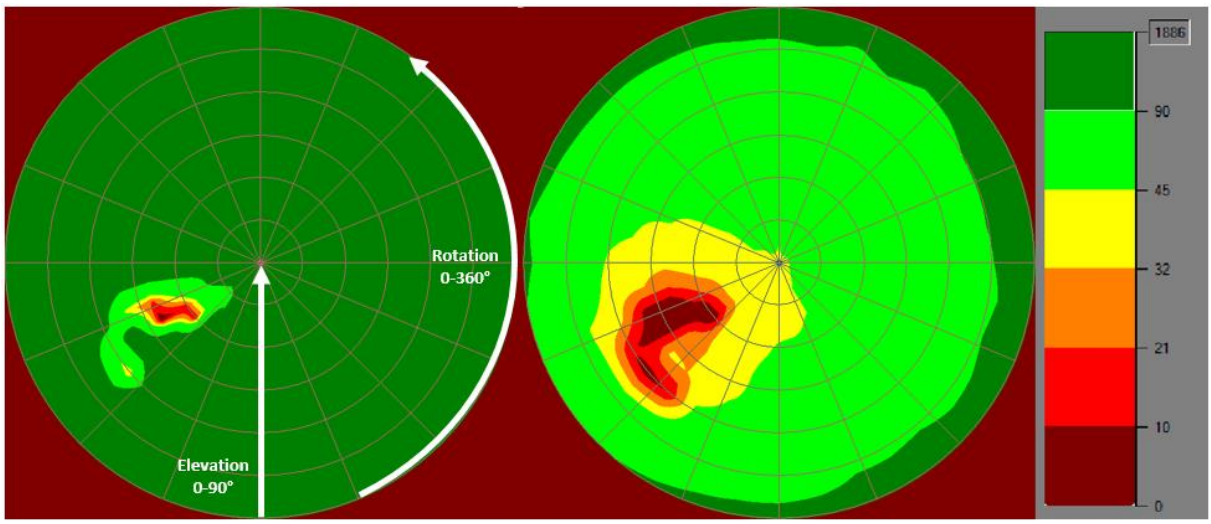

Figure 2-11: Conoscopic plot of PJND for 360 sun positions (Left: average, Right: maximum)

These plots identify critical sun positions which can be used with the images of individual results to evaluate potential issues to inform and guide the design, and advise the next stage of testing. A sun position is provided, specified as angles of azimuth (rotation) and elevation for five situations; sun forward, sun passenger, sun rear, sun driver and sun specular.

A method to determine the critical specular direction is specified by SAE J1757-1. This procedure uses a mirror at the display surface to determine if the driver can see any daylight openings (DLOs) from which direct specular light may reach the driver if reflected from the display. This step is not required here due to the information provided by the SPEOS evaluations.

SPEOS has the capability to produce high quality renders however there is a trade-off between time and noise in the resultant image. Physics-based rendering using ray-tracing is a time-consuming process. For 'photo-realism' there are techniques that can be employed to speed up the simulation time however this is at the expense of physical accuracy (Martinez, 2010; Müller et al., 1995).

SPEOS has been validated by Ecole Nationale Des Travaux Publics de l'Etat (ENTPE) (Labayrade, 2014) against CIE 171:2006 test cases (CIE, 2006). The recommended standard test cases assess the accuracy of light propogation in lighting simulation tools. SPEOS accurately simulates the spatial aspects of light as defined in the test cases and also spectral aspects of light propogation (Labayrade and Launay, 2011). These tests give confidence that the software will give results based on the physical behaviour of light in the prediction of reflections and appearance. Even with physically accurate results, there is no guarantee that the image produced will appear 'realistic'. This is due to the difference in dynamic range of human vision (10^8:1 cd/m²) and the display on which the image is viewed (typically 100:1 cd/m²) (Devlin et al., 2002). It is also unclear what the accuracy of the high ambient use-case based on comparisons to empirical data.

As a commercial product embedded into CAD software, SPEOS is limited by its configuration. Licenced by modules, the full suite of tools are not available as standard and it is not possible to apply sky models other than those programmed or to import measured sky data. This limits the use of SPEOS for research purposes and excludes the user from incorporating the latest lighting techniques for rendering real world lighting such as .

2.2.2 Physical evaluations

The metrological procedure for display evaluations under high ambient illumination at JLR outlines the setup of equipment to the measurement geometry and to the lighting situations to be evaluated.

2.2.2.1 Measurement geometry

Measurements are performed using a Radiant Zemax PM-1613F-1 series imaging photometer/colorimeter with a 50mm lens calibrated to a working distance of 75cm. The photometer is mounted on a photographic tripod and positioned on the driver's seat to the Driver's Reference Eyepoint, and aligned to the display centre (see Figure 2-12).

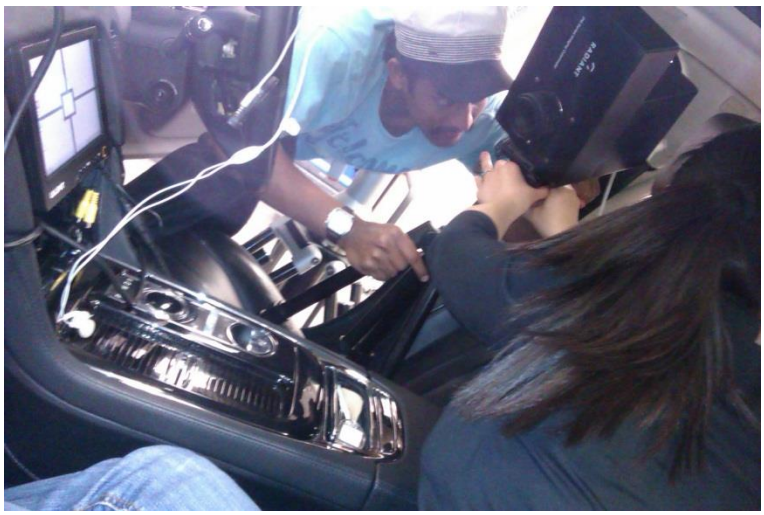

Figure 2-12: Photometer alignment following JLR procedures

There is no advice included in the procedure as to how to achieve the positioning of the photometer to the Driver's Reference Eyepoint, however a procedure to align the photometer to the display centre is detailed. This setup involves presenting a target pattern on the display and dropping a plumbline so that it is positioned over the centre when viewed by a 'target driver'. The photometer is then adjusted to view the plumbline over the target using functionality of the control software.

2.2.2.2 Lighting setup

Electrical lighting is required to simulate daylight illumination from a diffuse sky and a direct sun component. The procedure used within JLR specifies target illumination at the display which should be monitored using an illuminance meter such as the Minolta T10. The levels required are dependent on the situation under test, taking into account whether the display is subject to direct illumination by the sun (see Table 2-3).

Table 2-3: Illumination levels for situations tested at target locations accordng to JLR test procedure

	Illumination levels at target locations (lux)		
Situation	Display	Manikin	Roof
Sun Forward	5,000 to 10,000	70,000-90,000	100,000-120,000
Sun High	5,000 to 10,000	70,000-90,000	100,000-120,000
Sun Rear	70,000-90,000	N/A	100,000-120,000
Sun Side	70,000-90,000	N/A	100,000-120,000
Sun Specular	90, 000-120, 000	N/A	N/A

The lamp representing the direct component of the sun, is set to angles recommended by the SPEOS evaluation for each of these situations. In addition to this, several lamps (a minimum of three is recommended) are positioned around the vehicle with diffuser panels to supply a background diffuse component to the illumination. These levels are recorded with an illuminance meter throughout the measurement process.

The setup of the lamp position is dependent on the recommendation from the SPEOS assessments. There is no advice included in the procedure as to how to achieve the required angles of the light sources. The test procedure recognises this limitation and the impact this will have on measurement accuracy on and therefore recommends measurements be performed at WMG, University of Warwick in the PVCIT Centre of Excellence.

The lamp specified for daylight simulation is a representitive lamp such as an ARRI Daylight Compact. These lamps have a CCT 6000K and are capable of achieving the illuminance levels specified (ARRI, 2005).

2.2.2.3 Measurements

Measurements are taken of predefined test patterns and HMI images, such as the Home screen, Navigation screen etc. under each of the specified conditions in Table 2-3. The exception to this is the specular condition, which is evaluated with the display switched off

in order to assess the area of the display affected by the external light source from a specular direction.

From the standard conditions, luminance and colour data is extracted and used to calculate the PJND at the display for specified test images and HMI interactions. From the measurements taken for the specular condition, the area and magnitude of the specular reflections are extracted in order to establish compliance with the standard.

These results are recorded and any deviation from the standard or the SPEOS simulation raised as a concern. A further SPEOS study may be undertaken with the measurement conditions, in order to understand the failure modes.

2.2.3 Test drive

The final stage of evaluation is a series of UK test drives in a vehicle with the same build and trim level as assessed by the previous two stages. This step allows the display performance and overall legibility at maximum display luminance to be assessed subjectively for the sun positions evaluated in physical test (defined in Table 2-3). When the display becomes difficult/impossible to read, the display performance is rated and comments on the legibility, display condition and test situation are recorded.

Two drivers are required to assess the display legibility over a ten-hour period on a sunny day. The route taken is flexible but requires sun location corresponding to the physical test condition to be covered. During the test the sun location with respect to the vehicle is noted and the daylight illuminance is logged with an illuminance meter positioned on the roof or on the dash within the vehicle. Assessments are made when the illuminance is in excess of 50 klux. Weather conditions are also monitored; the amount of time during the test drive where the conditions change are noted especially in the case of cloud cover. Even with these conditions being monitored, a test drive is not a repeatable test due to the variability of daylight conditions both in weather, the time of year and the geographic location. A UK test drive may not encounter the sun elevations that cause an issue however if the vehicle under test is for the UK market these failure conditions will be sufficient for the evaluation.

The test drive is not reliant on the perception of a single driver, however the procedure does not outline any requirements for the characteristics of the drivers involved, such as the height, age, gender and vision of the driver.

The height of the driver will affect their viewing position with respect to the display, which will affect where reflections from daylight will be seen to fall meaning that an area of the display which is obscured by reflections for one driver will be clear for another.

The visual acuity and whether the driver has normal vision or any visual defects or aberrations will affect the visual performance of the driver. There are large differences in human visual performance between individuals , particularly between age groups where older observers become more sensitive to glare effects and have a reduced contrast sensitivity meaning that an older driver performing the test is more likely to perceive the failure modes at the display than a younger driver, as such two drivers are not likely to be the 'average' driver and would not be a representative sample of common drivers therefore a single test drive will not be enough to establish whether the appropriate failure modes will be encountered.

The test drives can give the engineer an appreciation for the view of the end user and the potential legibility issues that a driver will encounter. It is especially useful to identify failure modes that have not been tested for in the physical and digital simulations. However, this is for one specific condition that cannot be replicated and does not guarantee that the situation where a failure mode will occur being encountered during the drive. It is also unclear the number of test drives that are recommended and whether the drivers remain the same for each session.

2.3 SUMMARY

The daylight conditions under which an in-vehicle display is viewed will affect the visual performance of the display depending on the angle of the sun with respect to the vehicle.

Reflections at the display surface can degrade the performance of the display by lowering the contrast of displayed information. In order to evaluate the ambient contrast

performance of in-vehicle displays, simulations are performed digitally and physically under controlled conditions which mimic the viewing environment of the in-vehicle display.

This section has partially addressed *Objective 1: Define the 'real-world' in terms of automotive displays; the environment in which they are viewed, how they are perceived by the driver and their performance*, by describing the metrics to assess ambient contrast performance and the physical and digital methods employed by JLR to determine display performance. However, in order to do this fully, measurements are required of in-vehide displays under high ambient light to characterise the reflections under real daylight conditions.

3 DAYLIGHT AND DISPLAY DATA CAPTURE

Measurements of the sky and display are required to characterise the real-world environment to fully address *Objective 1: Define the 'real-world' in terms of automotive displays; the environment in which they are viewed, how they are perceived by the driver and their performance*.

Trial measurements were performed to become familiar with the equipment and to establish a method for performing photometric measurements of the sky and the in-situ measurements of display reflections. Submission #2 details these trials for measuring the sky and Submission #3 details the trial setup of in-vehicle display evaluations following JLR procedures.

The lab-based measurements of in-vehicle displays were also required to understand the challenges of performing in-vehicle display assessments. The aim of performing the trial was to identify areas that require greater control in the setup geometry for display measurements both for preparation for the field measurements and as the basis for evaluating current in-vehicle evaluation methods to address *Objective 2: Assess current in-vehicle display evaluation methods.*

Field measurements were performed as part of the International Placement in Australia. This location was chosen for the sky conditions at the time of year to facilitate measurement, as well as access to academic experts in the fields of lighting in fulfilment of the requirements of the international placement.

This is a crucial step of the research, without which the gap between current methods of recreating daylight for in-vehicle display evaluations and the real-world environment could not be assessed.

3.1 MEASUREMENT EQUIPMENT

In order to capture photometric measurements of the sky and an in-vehicle display, photometric measurement equipment is required. Photometers are devices used to measure visible light. They use photoelectric detectors to convert the power of light into an electrical signal which is proportional to the amount of light detected and calibrated to the spectral region to be measured.

The photoelectric detectors in photometers are usually photomultiplier tubes or silicon photodiodes that require the incoming light to be scaled to the spectral response of human vision (the *V(λ)* function) and the range of wavelengths outside the visual spectrum to be suppressed. This is usually done through the application of specialist filters.

The equipment considered for use in this research are sky scanners, imaging photometers/colorimeters and commercial digital cameras.

3.1.1 Sky scanners

Sky scanners are specialist photometers for the measurement of sky luminance distributions. Specified for use in the international daylight measurement programme (IDMP) by the CIE guide to recommended practice for daylight measurement (CIE, 1994), these instruments scan the sky vault and record measurements at 145 sky points as defined by the Tregenza sub-division of the sky (Tregenza, 1987). There are two main producers of sky scanners; PRC Krochmann (Figure 3-1a) and EKO Instruments (Figure 3-1b).

(a) (b)

Figure 3-1: (a) PRC Krochmann Sky Scanner and (b) EKO MS-321LR Sky Scanner

The PRC Krochmann comprises a luminance sensor in a fixed position. Scanning optics with an acceptance angle of 11° rotates in the vertical and horizontal directions to scan the sky vault every 15 minutes. Each scan starts in the direction of the sun meridian takes approximately 25 seconds and records 150 luminance readings for 145 sky points, plus an addition five zenith readings. This equipment was developed as the reference instrument for the IDMP therefore its measurement parameters match those specified by the CIE.

The luminance sensors saturate at high luminance values resulting in an underestimation of luminance in the sun and circumsolar region. It is recommended that an exclusion zone of 12° about the sun are extracted from the results to avoid the sun's direct influence on measurements (Beyer et al., 2009; Ineichen, 1992).

The EKO MS-321LR scanner is a similar instrument with twin detectors with an acceptance angle of 11° mounted on a motorised tracker. It also scans 145 sky points but with the first measurement taken at the southerly horizon. Scan times are longer, at approximately four minutes to perform a full scan of the sky vault, but each scan records both luminance and

radiance data and a shutter automatically blocks direct radiation to avoid saturation which can affect measurements and damage the sensor (EKO Instruments, 2006).

3.1.2 Imaging photometers/colorimeters

Imaging photometers are CCD based instruments which include filters to spectrally adjust the incoming light to the *V(λ)* function for the measurement of illuminance, luminance, and luminous intensity. In contrast to the photometers mentioned above, which measure luminance/illuminance at a single point, these instruments are capable of capturing data across each pixel on the CCD sensor.

Imaging colorimeters are imaging photometers which additionally measure colour characteristics of the light such as chromaticity, correlated colour temperature and dominant wavelength. However, the CCD does not distinguish between different wavelengths of light therefore the light incident on the sensor must first be split into its constituent wavelengths. This can be done in a number of ways such on-detector filters, prismatic beam splitters or with a filter wheel. On-detector filters are generally used in commercial digital camera and with *Interline Transfer* CCDs. They apply an array of red, green and blue filters across the surface of the sensor called the 'Bayer pattern'. This has the advantage of being a low cost method without the need for additional hardware however this method allows each pixel to only capture one colour, therefore the other two colours are interpolated from the surrounding pixels, and are generally not a close match to CIE tristimulus values (Hubel et al., 2004; Pro-Lite Technology Ltd, 2007).

The method used by most suppliers of imaging colorimeters on the market (Instrument Systems and Konica Minolta, 2014; Photo Research Inc., 2002; Radiant Zemax, 2014; TechnoTeam, 2014) incorporates the use of a filter wheel, as demonstrated in Figure 3-2.

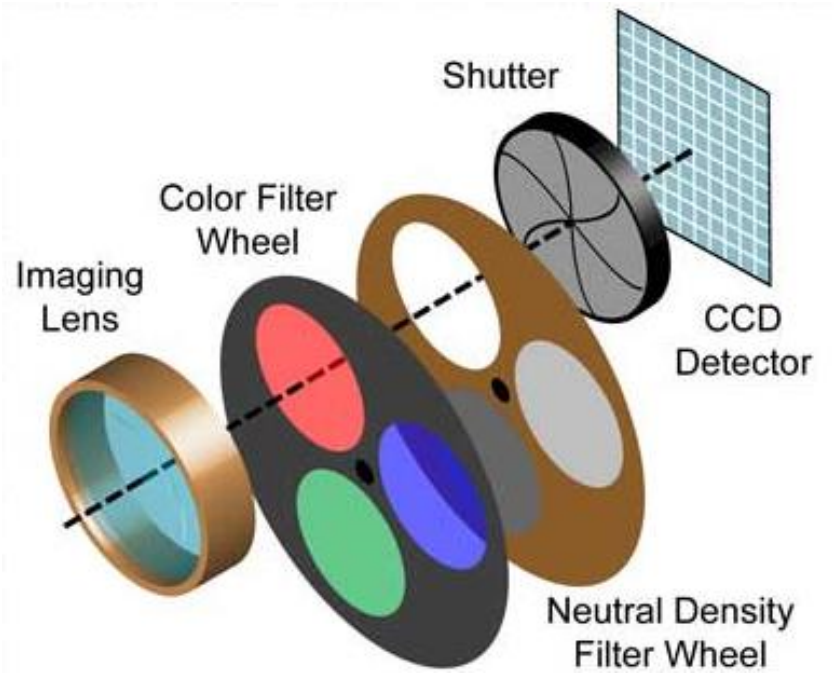

Figure 3-2: Typical construction of an imaging colorimeter (Rykowski and Kostal, 2008)

This technique uses filters that are closely matched to CIE colour matching curves mounted on a wheel that moves the filters sequentially over the sensor that enables lossless capture of light. This technique also requires a mechanical shutter to block light from the sensor between each colour exposure resulting longer measurement times in a larger, heavier, more complex system which is generally more expensive. However, depending on the CCD detector selected, these devices can deliver a high dynamic range, spatial resolution and with appropriate cooling and efficient electronics, low noise. They also offer the best match to the CIE colour matching curves.

Generally used for light source evaluation, display metrology and instrumentation analysis but with the addition of a fisheye lens, this type of equipment has also been used in luminance mapping of the sky (Kenny et al., 2006).

3.1.3 Commercial cameras

There has been active research for many years to find alternative methods to measure sky luminance distributions with commercially available, non-specialist equipment. This is due

to the high cost of precision equipment and the limited availability of sky scanners, with the PRC Krochmann being no longer available, and most being part of sky monitoring station, many of which are now inactive since the IDMP finished. Table 3-1 summarises a number of these methods.

Table 3-1: Research into alternative methods of measuring sky luminance distributions

Research	Equipment	Calibration equipment	Techniques
Bellia, Cesarano, Minichiello, & Sibilio (1997)	CCD Camera with fisheye lens	Spectroradiaometer Precision photometer Standard source	This was an investigation into the validity of using solid-state video cameras with wide angle optics for sky luminance mapping. At the time the method was not proven and there were no systems available commercially therefore the uncertainty of the technique was taken as ±10%. It recommends calibration for spectral response, geometric accuracy and uniformity of the sensor response and a final calibration to sky zenith luminances
Roy, Hayman, & Julian (1998)	Nikon/Fuji E2 CCD Camera Nikon Nikkor 8 mm f/2.8 full-field lens	Krochmann Sky Scanner	Developed a method to extract luminance information from sky images using RGB pixel values and camera metadata using a calibration derived from sky scanner data.
Inanici & Galvin (2004)	Nikon Coolpix 5400 CCD Nikon FC-E9 fisheye lens	Konica Minolta LS110 Luminance meter 3 standard sources and a darkroom OceanOptics Spectrophotometer	Uses HDR imaging techniques where multiple exposure photographs taken to capture the wide luminance variation within a scene. The camera response function for the R, G and B channels are derived from the multiple exposure image in Photosphere, then used to fuse these photographs into a single HDR image. A luminance calculation for each pixel is derived from these curves and calibrated with a reference physical measurement.
Spasojević & Mahdavi (2005)	Digital camera and fisheye converter	Array of 12 illuminance sensors	This research used RGB values and camera metadata to calculate luminance values as (Roy et al., 1998) and calibrated the images with a correction factor derived from the measured horizontal illuminance levels.

Research	Equipment	Calibration equipment	Techniques
Kobav & Dumortier (2007)	Nikon Coolpix 5000 and fisheye lens	EKO sky scanner	This describes the process of extracting luminance data from digital images using Photolux software and a camera calibration function calculated from the sky scanner data. They recommend for the system to be placed under a sealed glass dome for continuous use, and protected from direct sunlight with a shadow band or disk. They also note that performance of the system may vary with temperature fluctuations.
Shahriar, Hyde, & Hayman (2009)	Nikon Coolpix 5400 FC-E9 fisheye lens converter	*None quoted*	Luminance was extracted from RGB values using the relationship developed by **Inanici & Galvin** (2004) and automatically applied to images with a Matlab script. They also highlight a geometric distortion in the fisheye lens.
Tohsing, Schrempf, Riechelmann, Schilke, & Seckmeyer (2013)	Canon PowerShot G10 Dörr DHG fisheye lens	Ocean Optics S2000 spectro-radiometer Standard source	Developed a hemispherical sky imager based on commercial CCD cameras to measure luminance, radiance and cloud cover. A 10° exclusion zone of the sun and circumsolar region in defined in order avoid saturation of the sensor. Luminance was calculated from RGB values of pixels, ISO number, shutter speed and f-stop number (Roy et al., 1998) and calibrated using constants derived from lab measurements of a known standard. HDR imaging techniques were used to compensate for the low dynamic range of a single image.
Rogers, Thanachareonkit, & Fernade (2013)	Nikon Coolpix 5400 digital fisheye lens	Minolta LS-110 luminance meter illuminance measurements	Use HDR imaging techniques, calibrated to sky zenith luminance and global / diffuse horizontal illuminance measurements. These were used in the generation of computer simulations

3.1.4 Equipment selection

There are a number of different types of equipment to capture photometric data; this research requires equipment for sky luminance capture and display measurement

Sky scanners are valuable instruments for daylight measurement, however their major drawbacks are the high cost of the equipment, the complex calibration and setup times, and the duration of each scan.

Even without these drawbacks, to be useful in this research an active sky monitoring station would need to be available for use in this research and would need to be able to perform measurements simultaneously with equipment for use in display measurement. As a sky scanner was not available, the equipment to be considered for both sky and display measurements are commercial cameras and imaging photometers.

Commercial cameras have been proven to be effective in sky luminance mapping with results comparable to traditional photometric methods. The imaging techniques of commercial cameras and imaging photometers allow the instantaneous capture of data across the entire sky vault and commercial cameras with fisheye lenses are an affordable solution to most research projects. However, filters on commercial sensors are not calibrated to CIE tristimulus values and errors are generated due to the Beyer pattern used to discriminate wavelengths, therefore they are not recommended for colour measurements.

Many of the images captured in the daylight studies referred to in Table 3-1 suffer from a limited dynamic range due to the 8-bit cameras, this would cause greater errors in higher luminance conditions and applications where fine detail needs to be resolved but would generally be sufficient for overcast sky measurements (Lee and Devan, 2008). The goal of many of these studies was proof of concept, investigating the suitability of using CCD cameras for sky luminance mapping, and therefore did not tackle the complex calibration procedures, most of which were device dependant, time consuming and required other expensive equipment and expertise. Inanici & Galvin's (2004) study using HDR imaging gave a more transferable solution, not only by extending the dynamic range using multiple exposures but by using their algorithm in conjunction with the camera response function generated by Photosphere. They have made calibration simpler and applicable to potentially any device, although it would still be advisable to use a physical measurement in the calibration and therefore a photometer is still necessary.

HDR imaging techniques, while useful in sky luminance mapping, still have their limitations. To be effective, HDR imaging needs to be performed under stable lighting conditions. Due

to the need to capture multiple exposures, dynamic lighting conditions introduce errors if there are significant changes to lighting conditions between exposures.

The limitations of using commercial cameras in sky measurements are also of concern for use with display measurements, though this would be a method to explore. However, investigation into this application is outside the scope of this research, leaving conventional photometers to be considered. Imaging photometers are also the simplest to use and capture the entire sky vault or display area in a single measurement.

The imaging colorimeter selected for this research was the Radiant Zemax PM-1613F-1 (Figure 3-3) fitted with a 50mm lens for use in display measurements and an 8mm F3.5 EX DG Sigma lens for capturing the sky.

The PM-1613F-1 is a 16-bit full-frame CCD-based imaging photometer/colorimeter, used in conjunction with Radiant Zemax ProMetric® 10.7 software, which controls measurement operations and offers a suite of tools for post-processing operations on captured images.

Figure 3-3: PM1600F imaging colorimeter

This equipment is capable of capturing photometric and colorimetric data through the application of RGB filters, closely matched to $V(\lambda)$ and CIE Colorimetric Observer. Filters are applied with the use of specialist motorised filter wheels, including a neutral density (ND) filter wheel. With ND filters fitted, this photometer is capable of measuring luminance

up to 10^{10} cd/m² (Pro-Lite Technology Ltd, 2011; Radiant Zemax, 2012), which exceeds the stated luminance of direct sunlight ($1.6x10^9$ cd/m²) (DiLaura et al., 2011).

The 16-bit CCD sensor has a high dynamic range and pixel resolution of 1,024 x 1,024 (1,048,576 pixels), resolves 65,536 different shades of grey and is thermoelectrically cooled to reduce dark noise. This equipment delivers high dynamic range and spatial detail, for low noise and greater precision in measurements (Radiant Zemax, 2012).

The 8mm F3.5 EX DG Sigma lens is a fully circular fisheye lens, with a field of view of 180° when used with full-frame imaging equipment. The Special Low Dispersion (SLD) glass used in its construction compensates for potential colour aberration and the multi-layer optical coating reduces flare and ghosting common in use with digital cameras. This lens is recommended by the manufacturer for measurement applications due to its equisolid angle mapping function, giving a known angle/area relationship of image artefacts as such it has been used in other sky research (Feister et al., 2000; Inanici, 2010; Kenny et al., 2006; Shimono et al., 2011).

3.2 TRIAL MEASUREMENTS

Trial measurements to guide field measurement were performed separately for the sky capture and in-vehicle display measurements.

3.2.1 Sky capture

The imaging photometer and lens were trialled three times at WMG as shown in Figure 3-4 using a laptop to control the photometer and a portable generator supplying power to the equipment.

Figure 3-4: PM 1613F-1 video photometer and Sigma 8mm fisheye lens

The first trial on 14-May-2014 identified an issue with measuring daylight directly. The PM-1613F-1 colorimeter is quoted as being capable of measuring luminance of up to 10^{10} cd/m² with appropriate ND filters (Radiant Zemax, 2012). This should allow the capture of sun and sky luminance, as the published terrestrial luminance of the sun is 1.6 x 10^9 cd/m² (DiLaura et al., 2011). However, even using the ND4 filter the CCD sensor became saturated (Max luminance recorded across all images captured = 1.53 x 10^6 cd/m^2) around the sun and circumsolar region.

Luminances were of an order that the photometer was not able to capture without saturation of the sensor or 'blooming'; seen as a line across the image originating at the solar disc as these pixels also become saturated (see Figure 3-5). There is also the possibility that other pixels in this area are showing erroneous measurements due to excess charge from the saturated pixels. This effect could also be due to lens flare or a combination of the two phenomena.

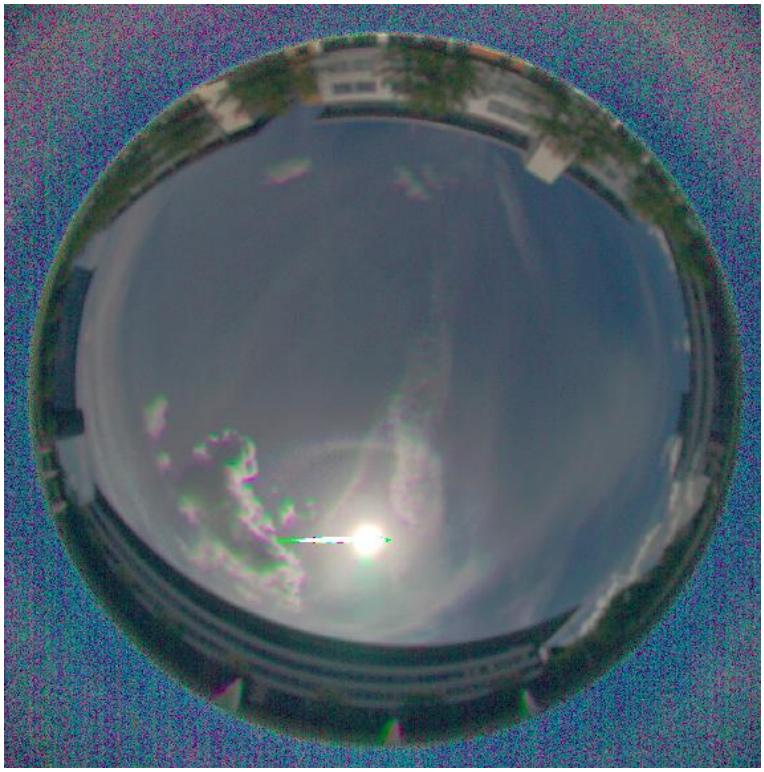

Figure 3-5: True colour image of the sky captured with PM 1613F-1 at WMG (11:24am on 14/05/2014)

Blooming arises in CCD sensors when the level of illumination detected generates more charge than can be accommodated by the pixel. This excess charge then spreads to surrounding pixels which results in an error in measurements. To combat this phenomenon, sensors are available with embedded 'anti-blooming' structures. These sensors give an upper limit on the luminance measured by limiting the charge accumulated in the pixel and removing the risk of blooming by providing a path for excess charge to 'drain' (Hubbell, 2013). However, anti-blooming structures are not typically incorporated into scientific devices due to non-linearity, a lower quantum efficiency, lower spatial resolution (by reducing the active area) and a lower overall sensitivity of the sensor (Andor, n.d.; Hubbell, 2013).

In this case, due to the lack of anti-blooming structure in the camera and the requirement for accurate measurements, it is desirable to avoid the saturation condition, therefore two further trials were performed to try to overcome this either by reducing the overall

incoming light with additional filters or by blocking the area of highest luminance (the sun) from the measurements with a mask.

3.2.1.1 Masking

On the 22nd July 2014 a second set of clear sky luminance data were capture from the lower roof level of Car Park 15 at the University of Warwick. The set-up remained the same as for the 14th May measurements with the addition of a paper mask applied to the front of the lens over the location of the sun to see if the 'blooming' effect could be mitigated and how the interference of the incoming light would affect the surrounding sky. One image was taken without the mask (Figure 3-6**Error! Reference source not found.**) and three successive measurements were taken with the mask in place (Figure 3-7**Error! Reference source not found.**).

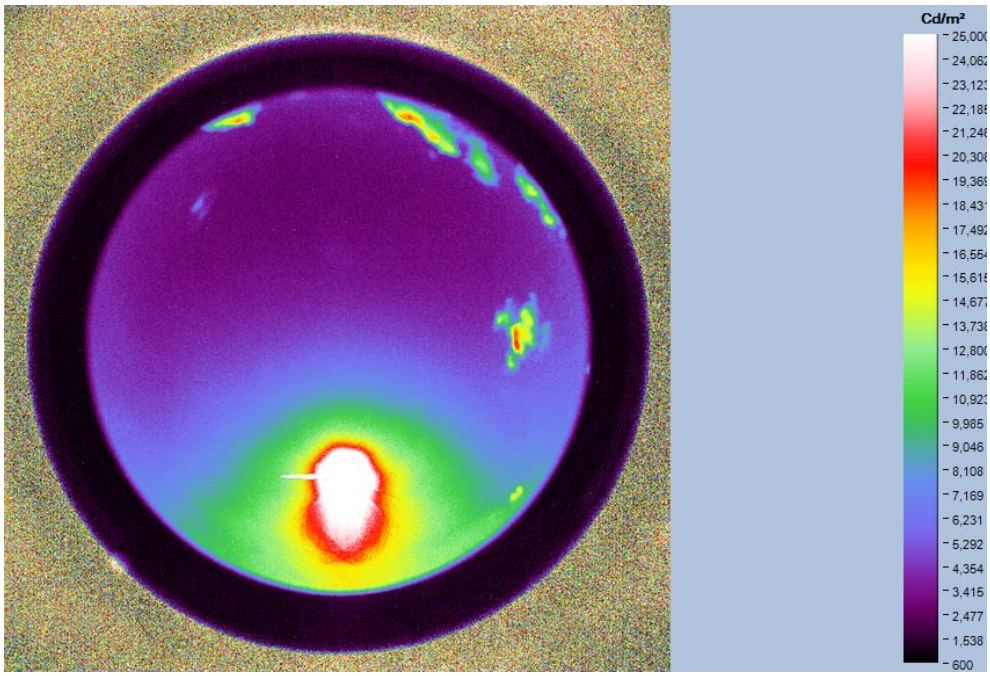

Figure 3-6: False colour image without mask (Car Park 15, 11:15am on 22nd July 2014)

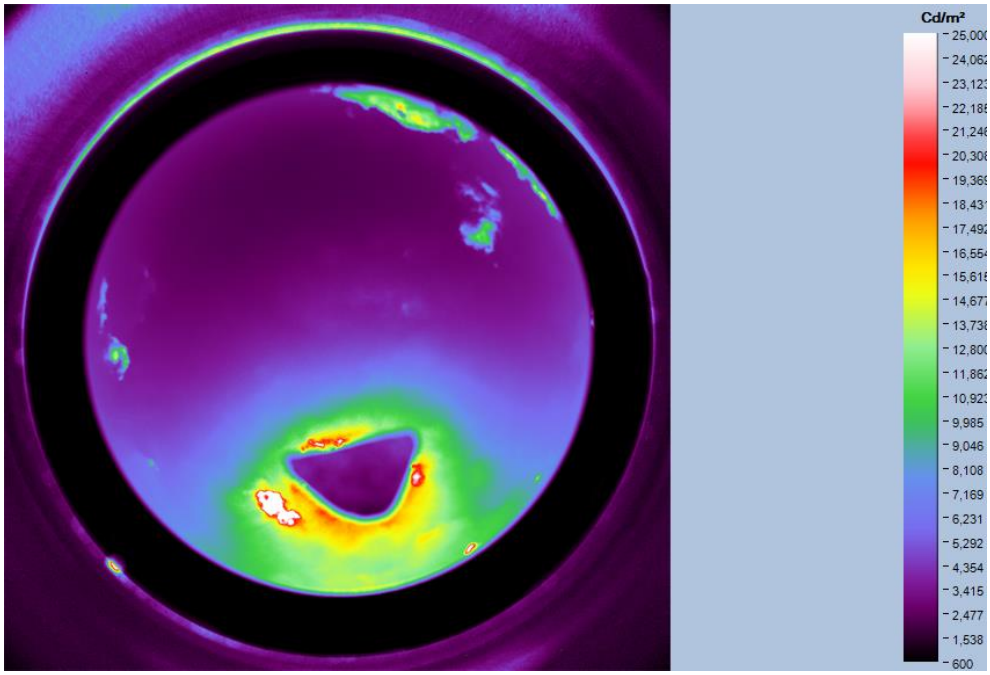

Figure 3-7: False colour image with mask (Car Park 15, 11:25am on 22nd July 2014)

With the mask in place, the sensor does not become saturated and the maximum luminance measured across the three images is 39,936 cd/m².

This is not ideal as data is removed from the measurement, however if an anti-bloom structure were available that did not affect the sensitivity and accuracy of the sensor, it would still remove this data by limiting the luminance detected.

3.2.1.2 Filters

Due to the curvature of the lens used, it was not possible to add filters in front of the optics. Therefore, to attempt to eliminate saturation, a set of gelatine ND filters were trialled on the 2nd September 2014. A benchmark measurement was attempted using only the internal filters, however, exposure could not be set correctly due to saturation of the sensor.

The gelatine filters were cut to fit the slot at the rear of the 8mm lens and measurements were taken for 0.9ND, 1.2ND and 2.4ND. However, even though the exposure could be set with the use of additional filters, the bloom observed in the first trial is still evident. It is suspected that this is due to the physical optics and is contributing to saturation of the CCD

at measurement. The filters used in this trial were inexpensive gelatine ND filters which do not have the uniform qualities of scientific grade glass filters. This was observed in the 2.4ND measurements where filtering was achieved with a double layer 1.2ND filter; not all wavelengths were attenuated equally resulting in a purple colour cast of the images, demonstrated in Figure 3-8.

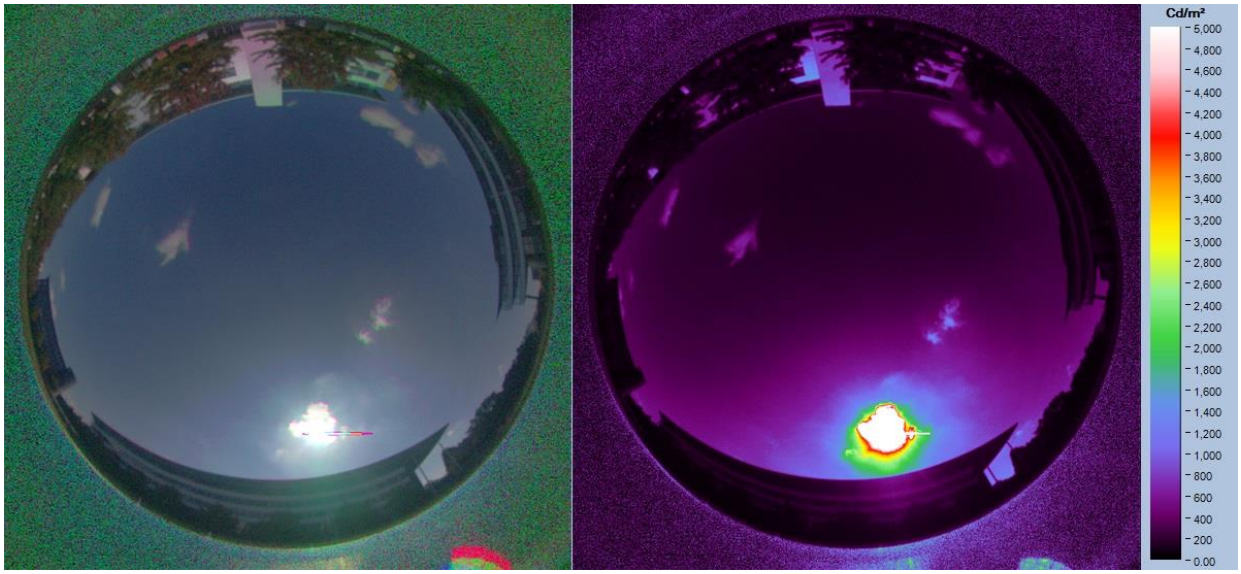

Figure 3-8: 1.2ND gel filters - true colour (left) and false colour (right) images (11.07am on 2nd September 2014 at WMG)

Of these two systems, the masking was the only one that removed the bloom and the saturation of the sensor. The filters did not address this issue and added colour errors in the form of a purple cast to the images. Therefore, a solar mask is required to make measurements of the sky with this imaging photometer and fisheye lens.

3.2.2 In-vehicle display measurement

On 14th and 15th August 2014, a set of lab based measurements were taken to understand the challenges of performing in-vehicle display assessments. Guided by JLR test procedures, the aim was to identify areas that require greater control in the setup geometry for display measurements to aid in the planning of recording displays under dynamic skies.

The floor of the PVCIT Centre of Excellence at WMG was mapped out in 15° intervals around a central point (Figure 3-9) to indicate the azimuth positions of the lamp representing the

sun. The vehicle under test was then positioned along the 0° line with the display aligning with the 90° line.

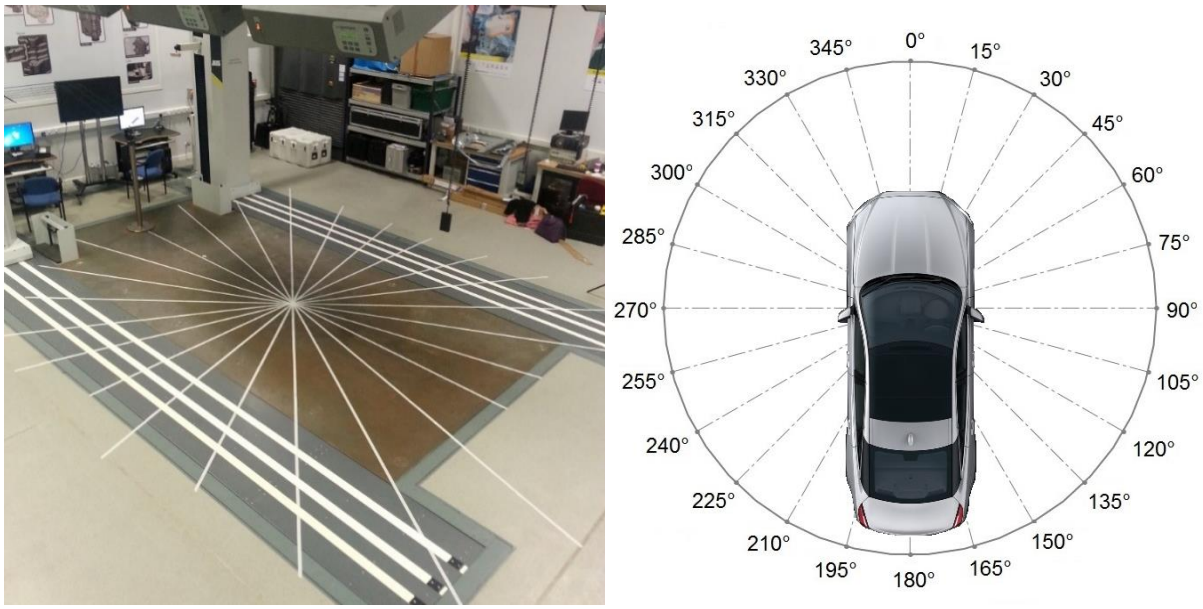

Figure 3-9: Floor layout (left) and positioning of vehicle (right)

Measurements were made using a PM1613F-1 imaging photometer, mounted on a tripod and positioned on the driver's seat to record the driver's point of view when viewing the centre console display. The JLR procedure requires the photometer position to be set to the centroid of the 95th percentile eyellipse (defined by SAE J941 (2010)) and aligned to the centre of the display (Figure 3-10). This is consistent with the recommendation in SAE J1757-1 (2007).

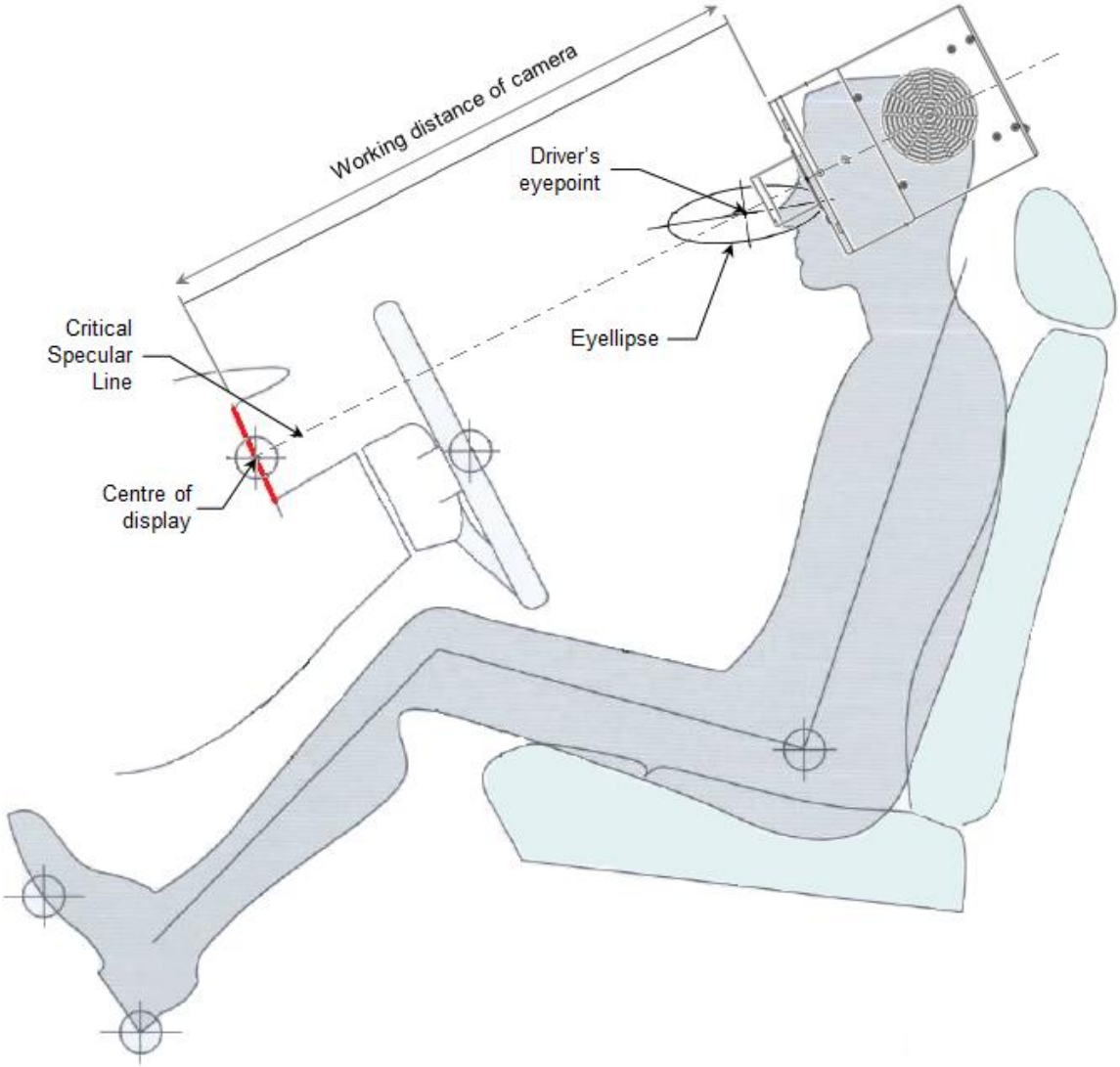

Figure 3-10: Photometer alignment from driver's eyepoint to centre of display

According to BS ISO 4513:2010 (BSI, 2010) the eyellipse is a "*statistical distribution of eye locations in three-dimensional space located relative to defined vehicle interior reference points"* for use in design and evaluation of in-vehicle visual tasks. It is defined based on 50/50 gender mixed user population (see Table 1 of BSI, 2010).

The eyepoint for a specific vehicle is determined from the hip point location which for JLR is defined with the driver's seat set in its lowest and rearmost position. The tripod was set with two legs on seat and one forward in the footwell (Figure 3-11) with the imaging photometer positioned with the front face set to the working distance of 75cm from the

display surface, using a tape measure. Alignment was then made by eye through the 'focus mode' of the Pro-Metric software and with manual adjustments made to the tripod.

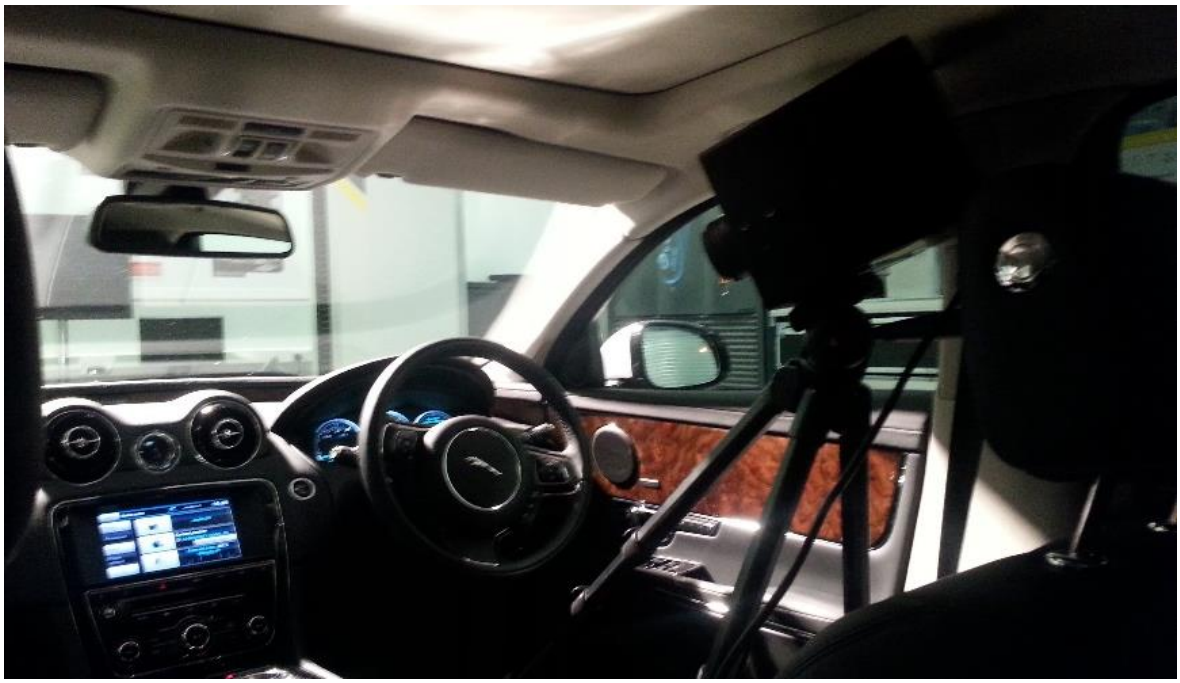

Figure 3-11: Photometer position on driver's seat

The Driver's Reference Eyepoint for the vehicle under test in this trial was not available, therefore the height and inboard position of the photometer was set arbitrarilty based on the view of a reference driver. However even if the position were available, there is no clear advice in the JLR test procedure on how to position the photometer in this position. Alignment of the photometer to the centre of the display followed steps of the procedure, whereby a plumbline is dropped over the central area of the display as viewed from the driver's eyepoint. The photometer is then adjusted to 'see' the plumbline over the display centre, as demonstrated by Figure 3-12.

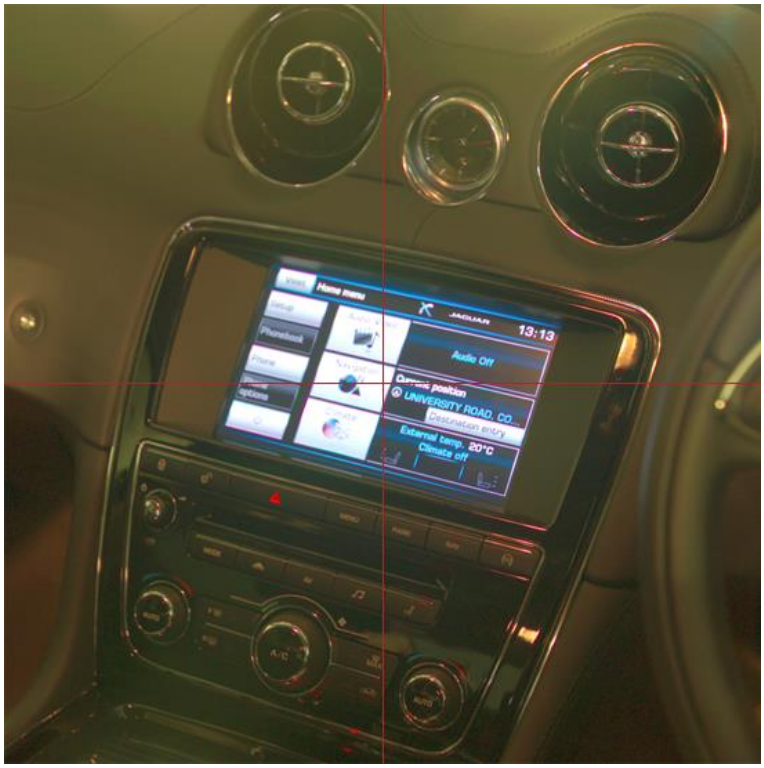

Figure 3-12: Image of display through focus mode

A specific lamp is not specified by JLR for use in this application, however there is a recommendation to use a daylight representative lamp such as the 'ARRI Daylight Compact'. The luminaire used during the trial was an ARRILITE 2000, which is not a daylight simulator as it does not follow the SPD of the daylight illuminant and its CCT is warmer than average daylight. These characteristics are important for correct colour rendering and will play a role in the perceived just noticeable difference (PJND) evaluations of legibility at the display, in this case however, it is sufficient just to indicate an effect on display legibility. The position of the lamp is set to represent the position of the sun, as illustrated in Figure 3-13.

Figure 3-13: Direct lighting high-nearside - Azimuth 300°, Elevation 60°

The angular position marked out on the floor (see Figure 3-9 above) in 15° intervals, is used to set the azimuth, and the angular elevation is set based on the linear distance from the centre point and the height of the tripod. The range of measurements were taken for an elevation of 20°, 40° and 60° to give a sun low, mid and high. A total of 59 measurements were taken over the two days.

To verify the alignment of the photometer to the centre of the display, the centre point of the measured image is plotted across all measurements using the 'points of interest' function in the ProMetric software.

The centre point of the display is assigned coordinates *0,0*. This is from the initial setup of the photometer and the first recorded measurement. The variation in subsequent measurements is tracked using the navigation arrow icon as a datum feature (see Figure 3-14) and adjusted to give the centre of the display with respect to the origin of the initial measurement.

Figure 3-14: Points of interest: centre point locations of navigation arrow across all measurements shown on image taken of original display alignment

Whilst the vehicle was under test, the photometer was not removed from the vehide. However, due to the short length of the cables for the photometer and the lamp, power leads and data cables had to be moved from one side of the vehicle to the other when taking measurements between the passenger and driver side. For this reason, the centre points have been grouped by the side of the vehicle that the equipment was plugged when taking measurements and then plotted in Figure 3-15.

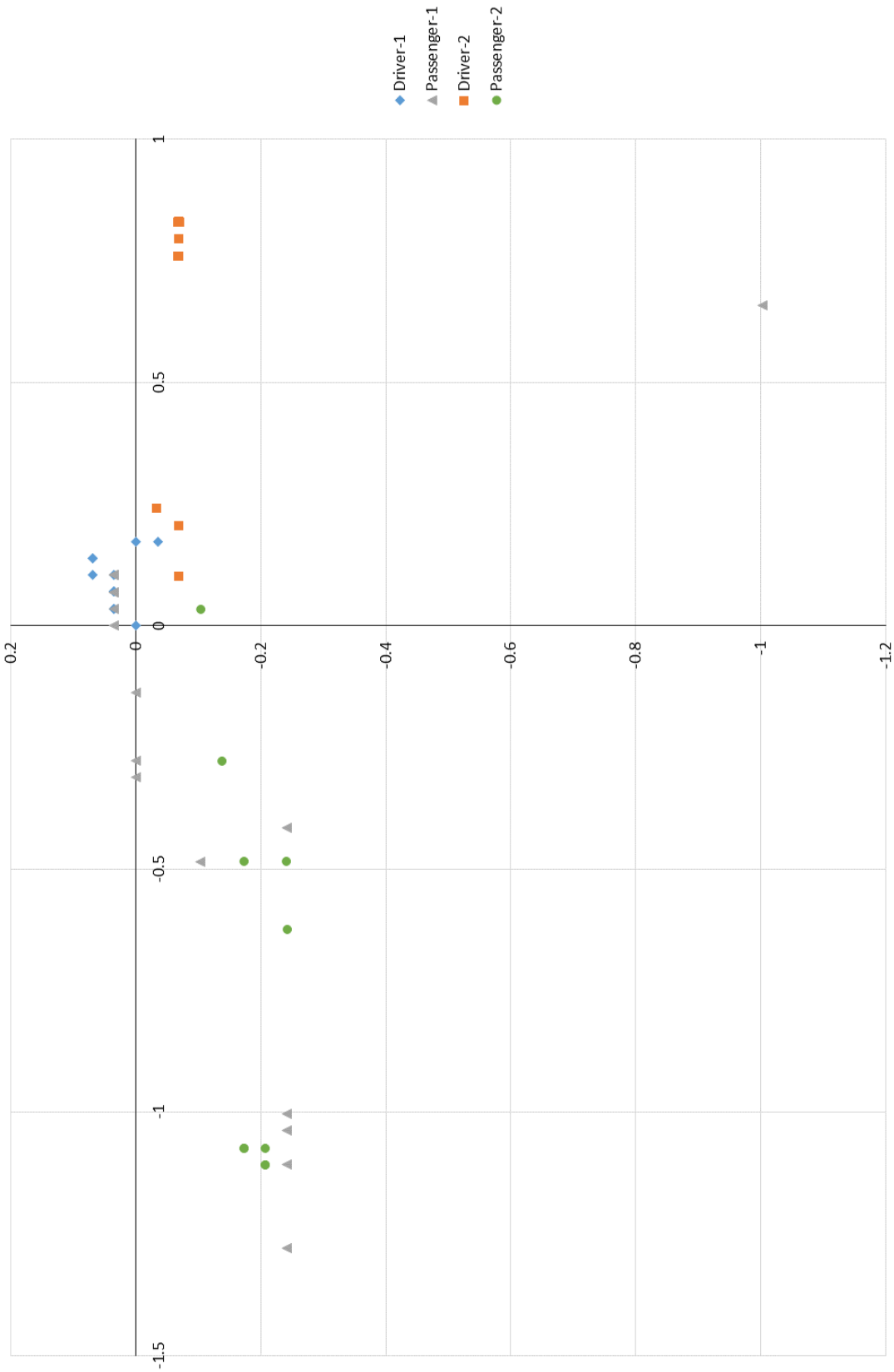

Figure 3-15: Plot of location of crosshairs off centre of display

A one-way ANOVA was performed using Minitab on the distance off centre of the alignment. Due to the different number of measurements in each set, it is assumed that the variance between samples is unequal and that there will be a difference between the means. Welch's t test is used to quantify this difference between the means, the results of which are displayed in Table 3-2.

Table 3-2: Results of One-way ANOVA from Minitab

One-way ANOVA: DRI-1, PASS-1, DRI-2, PASS-2

Method

Null hypothesis	All means are equal
Alternative hypothesis	At least one mean is different
Significance level	α = 0.05

Equal variances were **not** assumed for the analysis.

Welch's Test

Source	DF Num	DF Den	F-Value	P-Value
Factor	3	23.0818	27.43	0.000

Model Summary

R-sq	R-sq(adj)	R-sq(pred)
28.66%	24.70%	18.49%

Means

Factor	N	Mean	StDev	95% CI
DRI-1	11	0.1118	0.0481	(0.0795, 0.1441)
PASS-1	18	0.451	0.466	(0.219, 0.683)
DRI-2	19	0.6157	0.2960	(0.4730, 0.7584)
PASS-2	10	0.767	0.385	(0.491, 1.042)

The variation within groups, indicated by the standard deviation, demonstrates a drift in alignment of the photometer when the equipment has not purposefully been moved. This demonstrates the influence of the compressibility of the seat on the stability of the alignment.

The initial setup (DRI-1) exhibits the lowest mean and standard deviation. The low mean value can be attributed to being early in the measurements; over the course of the measurements the mean drifts further from the position of the photometer at alignment. The low standard deviation could be an indication of a relatively stable setup, with limited

effect from the compressibility of the seat, however it is more likely to be due to the limited interaction with the vehicle at the beginning of the measurements. This interaction increases over the course of the measurements; cables to the photometer and lamp are moved and the display is reinitiated after going into power save mode.

There is a statistically significant difference between means of each group of measurements as indicated by the ANOVA ($p < 0.05$) which suggests that the movement of the cables contributes to the variation observed.

One of the limitations was the range of measurements taken due to the geometry; positions close to the vehicle were inaccessible, such as for sun-high positions (Figure 3-16) due to the luminaire being mounted on a tripod. This system was also top-heavy and likely to topple while in use with this style of tripod.

Figure 3-16: Greatest elevation able to test at rear of vehicle - Azimuth 0°, Elevation 20°

Another concern was the precision and accuracy in positioning the tripod both on the ground and for angular positioning of the lamphead. The floor was marked to give the tripod positions with respect to the azimuth and elevation angles, and the lamphead was then angled down and set at the height of the corresponding elevation angle using an angle finder. These were manual adjustments with little precision that could not be verified.

3.3 MEASUREMENTS: DISPLAYS UNDER DYNAMIC SKIES IN AUSTRALIA

Field measurements were performed in in Sydney, Australia in January 2015 as part of the EngD(int) International Placement (documented in the *International Placement Report* of this portfolio). The purpose was to measure the luminance distribution of summer skies and the resulting reflections across a centre console display within a vehicle. To perform these measurements, specialist photometric imaging equipment was borrowed from JLR and hired from Pro-Lite Ltd and a test vehicle was supplied by Jaguar Land Rover Australia.

3.3.1 International placement

The purpose of the international placement is to develop international relationships with a view to developing research collaborations, whilst developing doctoral candidates in a number of core competencies (WMG, 2013). For this project, the international placement was used as a dissemination and networking exercise where this research was discussed with experts in similar fields and also gave the opportunity to select a location to perform the main data collection activities under high ambient daylight conditions.

The decision was made to go to University of Sydney, to visit a leading academic in illumination design to discuss available technologies for recreating daylight luminance and colour, and to visit the university's research class daylight monitoring station.

This project has an automotive focus and application, however there are also many parallels and crossover with daylighting design, illumination design and research visualisation. These visits and discussions have opened up the possibility of collaboration in the future, especially with the CAVE2™ at Monash University to explore the application

of visualisation in automotive evaluations from the simulation results and renderings from this research.

3.3.2 Measurement setup

The in-vehicle measurements were setup as defined in Submission #3 with the exception of the specified photometer; due to availability and funds it was necessary to find an alternative to the PM-1613F-1. Measurements were performed with a Radiant Zemax PM-1423F imaging photometer with a 50mm lens. There is not much difference between the two photometers as they use the same CCD technology; the PM1423F has a lower dynamic range but a greater spatial resolution due to the size of the active sensor. Both use the same lens therefore the field of view remains the same but the calibrated working distance is 50cm rather than the 75cm of the PM1613F-1.

The photometer was positioned in the cockpit on a tripod and aligned with respect to the driver's eyepoint (centroid of the eyellipse) of the 95th percentile man and the centre of the display under test. This geometry allows measurements to be taken from the perspective of the driver and also correlates with the geometry of the virtual simulations performed in SPEOS during the design of the vehicle. The eyepoint and its axis to the display centre (Critical Specular Line) were taken from the CAD geometry for the Range Rover Evoque, supplied by Jaguar Land Rover for this purpose. There were three dimensions used to align the photometer:

- The angle of the photometer pointing down (pitch)
- The angle of the photometer pointing inward (yaw)
- The working distance of the photometer (X direction)

A digital angle finder was used to set the pitch and yaw angles and the working distance was measured using a laser range finder placed at the display and aimed at the front face of the photometer. Once these dimensions were set the final adjustment was to align the view of the photometer to the centre of the display, indicated by the target image (Figure 3-17), by adjusting the tripod in the Y (in/outboard) and Z (up/down) directions.

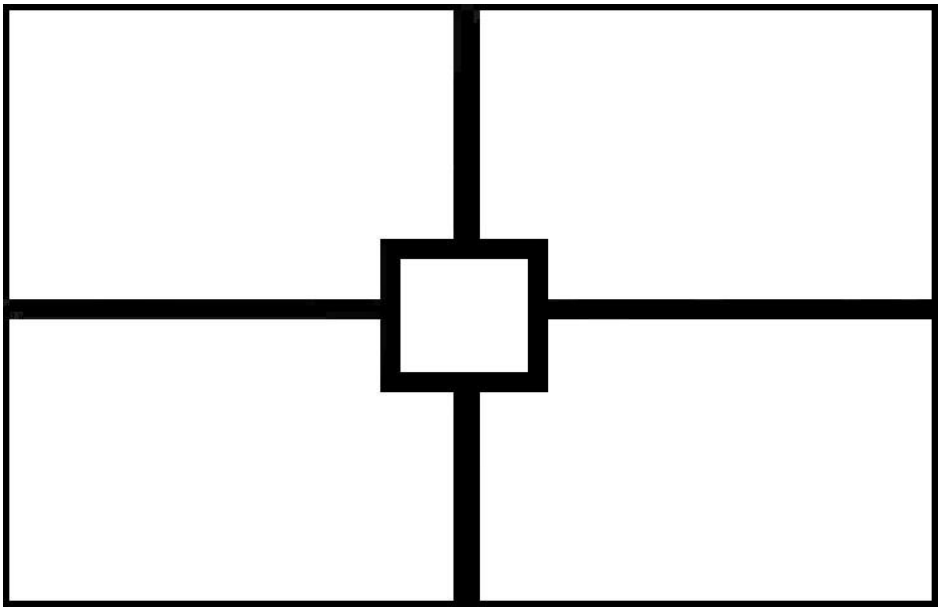

Figure 3-17: Target image for alignment of photometer at centre of display

The 500mm working distance of this photometer was too close to the edge of the driver's seat to be stable on a tripod and did not allow for the entire display to be viewed. Therefore the photometer was positioned in the footwell behind the driver's seat, 1m from the display, with the driver's head restraint removed; the final setup can be seen below in Figure 3-18.

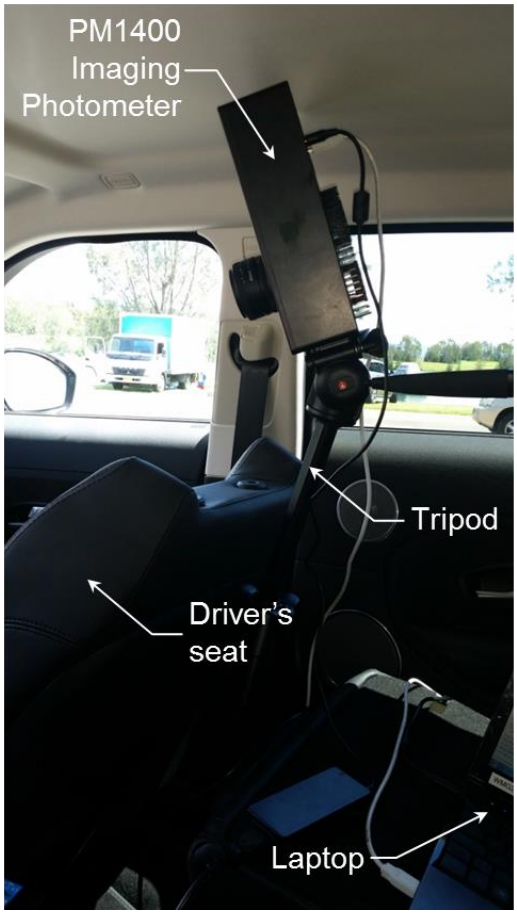

Figure 3-18: In-vehicle setup

To maintain a good flat field calibration, the working distance needs to be maintained to within a 10° rotation of the focus ring which equates to a range of approximately +15cm and -10cm. Positioning outside of this range, as in this case, will cause there to be flat-field dropout around the edges of the measured images, however these effects will be in the corners of the image which do not fall on not fall on the display surface [private communication with Pro-Lite Ltd 07/04/2014]. As well as capturing the reflections at the centre console display, a Konica Minolta T-10 lux meter was used to record the total illuminance at the centre of the cockpit.

A second imaging photometer was set on the roof of the test vehicle to capture the luminance distribution of the sky (see Figure 3-19). The sky measurements were performed following the setup defined in Submission #2, using a Radiant Zemax PM-1613F-1 imaging

photometer with an 8mm Sigma (fisheye) lens, and controlled through the ProMetric version 10.7 software. The photometer was set on a tripod with a shading disc in front of the lens and setup on the roof of the test vehicle to capture the dynamic skies causing the interior reflections. The shading disc allowed the luminance distribution of the sky to be captured without saturation of the CCD sensor in the photometer.

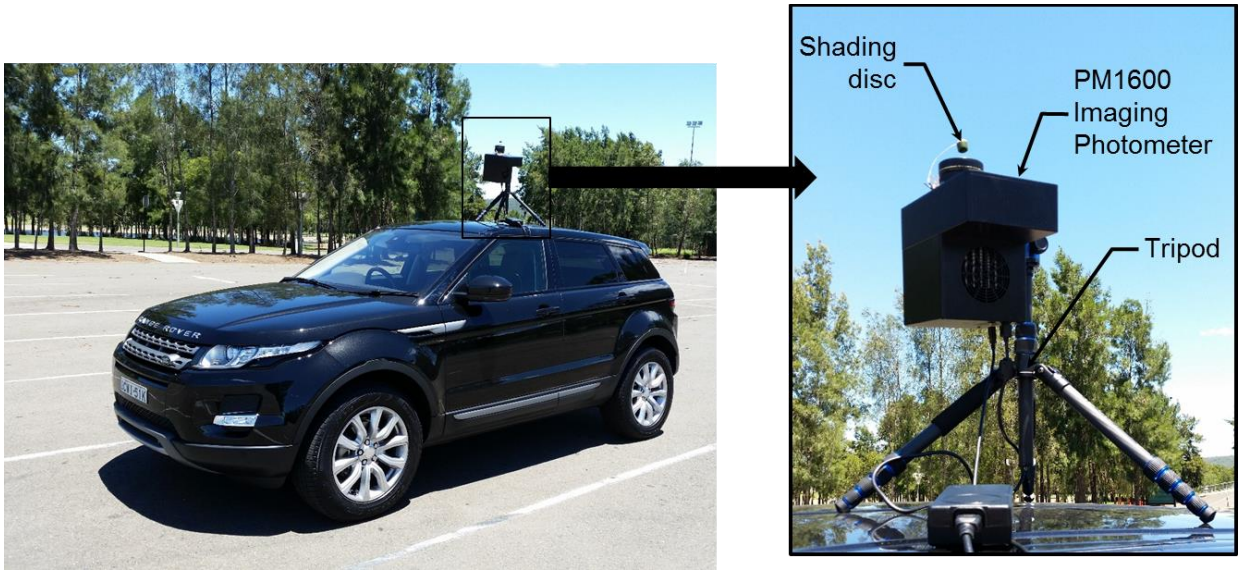

Figure 3-19: Sky capture setup

Due to the sun being masked from the measurements, a second illuminance meter (Konica Minolta T-10) was used to record the global horizontal illuminance; the total daylight reaching the roof of the vehicle. Over a 3 day period, 31 unique data sets were captured including:

- Photometric image of the display (Figure 3-20) containing luminance and colour data per pixel.
- Photometric image of the sky (Figure 3-21) containing luminance and colour data per pixel.
- Global Horizontal Illuminance, measured with lux meter outside the vehicle and logged in Table A.1 of Appendix A.
- Illuminance of cockpit, measured with lux meter within the vehicle and logged in Table A.1 of Appendix A.

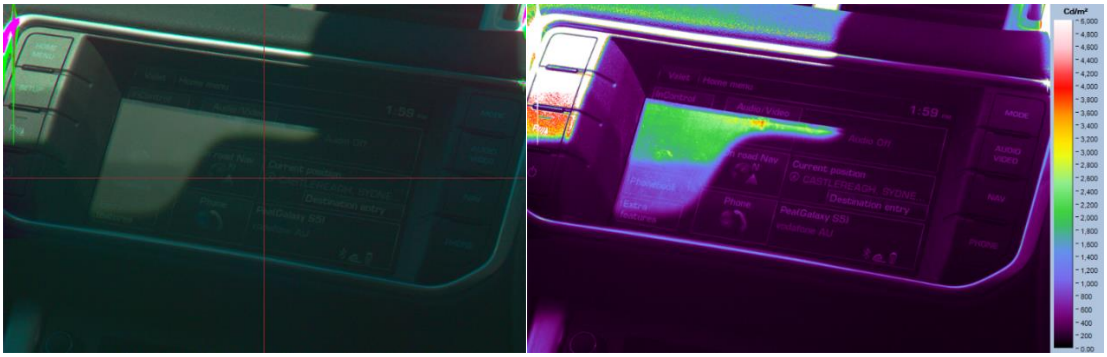

Figure 3-20: Example of captured image of display (left) and false colour image depicting luminance distribution (right)

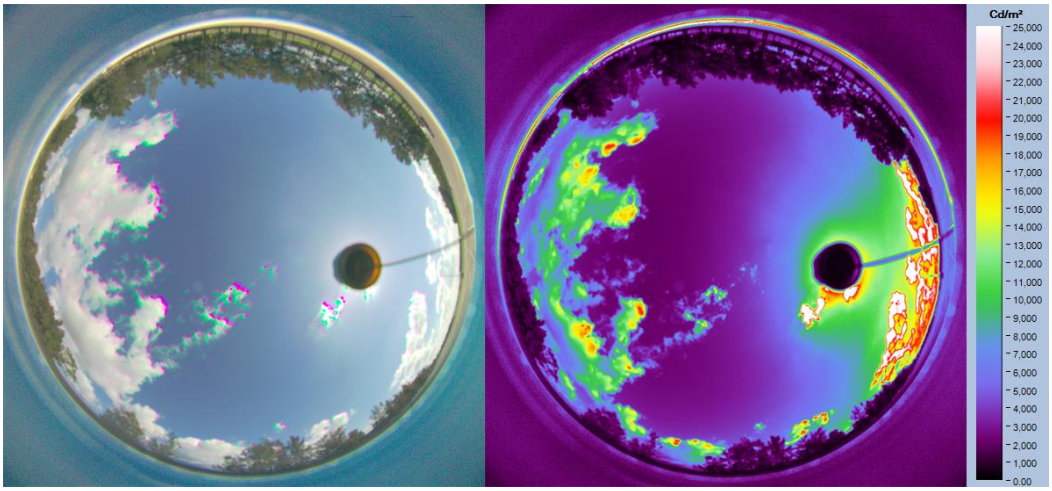

Figure 3-21: Example of captured image of the sky (left) and false colour image depicting luminance distribution (right)

3.3.3 Measurement uncertainty

All measurements are subject to uncertainty. This is the doubt associated with the value of the measurement and its dispersion from the 'true' value. Uncertainty can be related to the equipment used in the measurements, in this case the imaging photometer to capture the display reflections. It is also due to how the stability and accuracy of the equipment is effected by the position and orientation of the equipment.

In this study, the expanded uncertainty for the sky measurements was estimated to be approximately 3%. This is based on the quoted calibration uncertainty of the PM1613F-1

and an estimate of repeatability based on the standard deviation of the mean from measurements made in the lab.

For the display measurements, an expanded uncertainty of approximately 4% was estimated based on the target specifications of the equipment, an estimate of the experimental repeatability and the sensitivity of measurements to variation in alignment of the photometer.

The reported expanded uncertainty is based on the standard uncertainty multiplied by a coverage factor *k = 2*, providing a coverage probability of approximately 95%. This uncertainty evaluation is based on methods outlined in *UKAS document M3003* and *NPL Measurement Good Practice Guide No. 11* (Bell, 1999; UKAS, 2012). Details of this uncertainty estimation can be found in Submission #4.

3.4 SUMMARY

The trials performed facilitated field measurements by establishing the equipment and techniques necessary for sky capture and performing in-situ measurements of in-vehide displays. These trials have highlighted areas where more control is needed to perform good measurements, such as the influence of vibrations and seat compressibility on alignment of the photometer.

Field measurements captured the 'real-world' displays and the environment in which they are viewed, with an estimated expanded uncertainty of less than 4%.

The trials and field measurements detailed in this section will be used to evaluate the gap between the real world and current assessment methods.

4 THE GAP BETWEEN THE REAL & VIRTUAL WORLD

This section addresses *Objective 2: Assess current in-vehicle display evaluation methods.* To do this, it is necessary to compare these virtual methods to the conditions which the assessments are designed to replicate.

The gap between physical evaluations and the real world are determined through the comparison of the lab trial detailed in Submission #3, display evaluations at Jaguar Land Rover and the best practice in display metrology in international standards.

The digital gap is assessed by comparing the measured displays under high ambient daylight, detailed in Submission #4, to digital simulations of each measurement using the tools and techniques in use at Jaguar Land Rover.

4.1 PHYSICAL GAP

As established from Section 2.1, measurements for display assessments require a controlled measurement geometry and a controlled environment in which to perform repeatable and reproducible measurements.

4.1.1 Controlled measurement

The lab trial highlighted the low reproducibility of measurements and the variation in alignment between measurements, due to movement in the photometer and the setup geometry (see Figure 4-1). This drift in alignment can be attributed to the compressibility of the driver's seat; either from physically interfering with the seat or through vibrations from door closure. It is also affected by the movement of cables from one side or the vehicle to another.

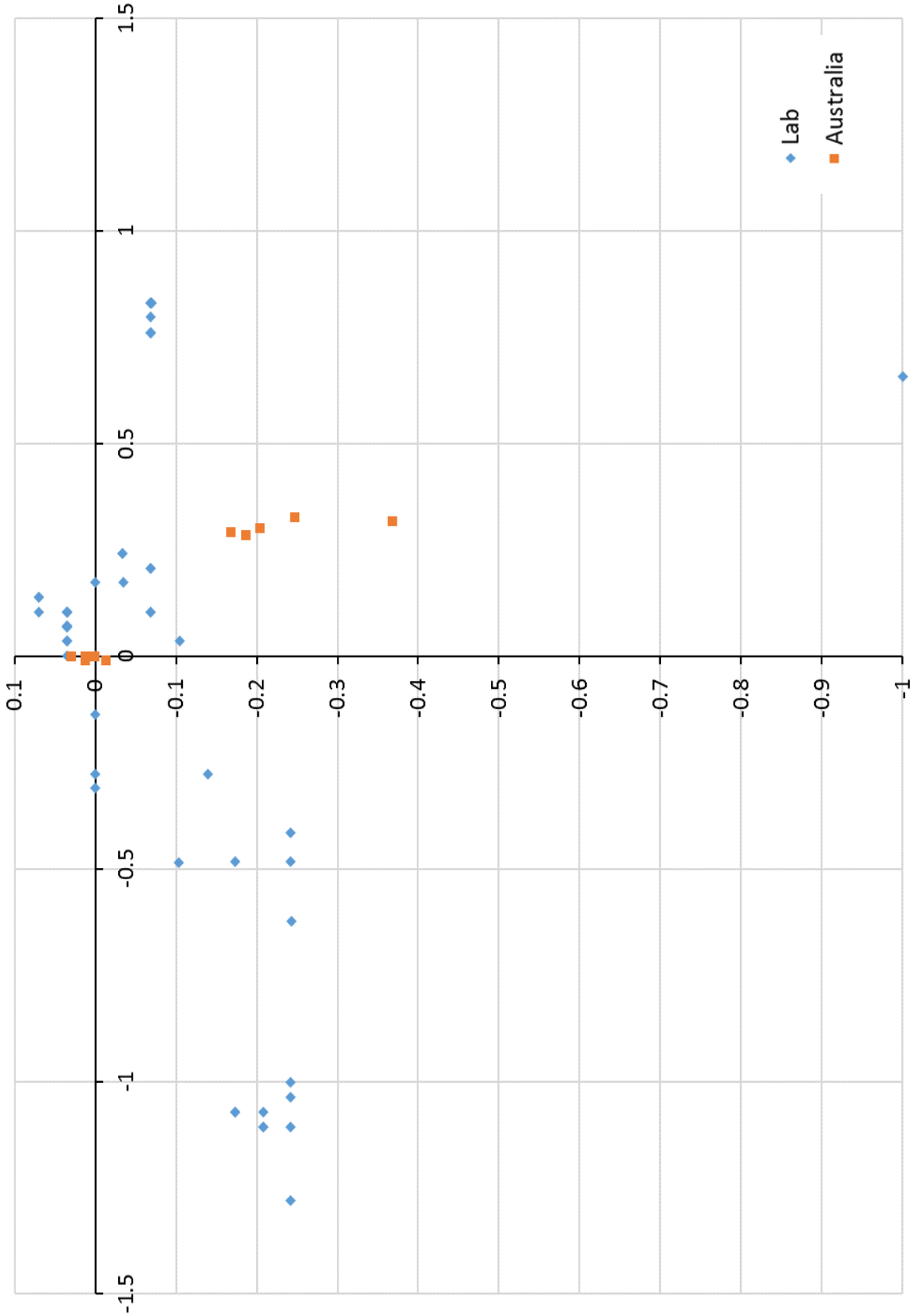

Figure 4-1: Linear shift in centre point of image (scale in mm relative to image plane of measurement)

Figure 4-1 is a plot of the movement of centre positions of the display relative to a datum measurement for both the lab measurements and the field measurements taken in Australia. However, the vehicle and alignment geometry were different for the trials and field measurements. The shift in alignment is comparable if treated as two separate populations and if scaled to consider the difference in working distance of the photometer. The linear distance from the centre is converted into the angular shift subtended from the photometer (shown in Table 4-1) and plotted for each measurement in Figure 4-2, to demonstrate the comparable magnitude of shift.

Table 4-1: Angular distance off display centre of field and trial measurements (radians)

Field measurements		Trial			
4.88E-04	1.66E-05	0.0	1.51E-03	2.91E-04	1.11E-03
4.12E-04	1.66E-05	6.60E-05	1.74E-03	2.91E-04	1.46E-04
3.66E-04	1.66E-05	6.60E-05	4.15E-04	3.26E-04	4.13E-04
3.39E-04	1.66E-05	1.04E-04	3.69E-04	3.26E-04	6.85E-04
3.39E-04	2.90E-05	1.04E-04	1.84E-04	1.02E-03	7.22E-04
3.41E-04	1.20E-05	1.04E-04	4.67E-05	1.02E-03	8.93E-04
3.41E-04	1.20E-05	1.46E-04	6.60E-05	1.02E-03	1.46E-03
0.0	1.44E-05	1.67E-04	1.03E-04	1.02E-03	1.50E-03
0.0	1.44E-05	2.08E-04	1.03E-04	1.07E-03	1.45E-03
0.0	1.44E-05	2.08E-04	1.46E-04	1.11E-03	1.50E-03
0.0	1.44E-05	2.31E-04	1.46E-04	1.11E-03	1.45E-03
0.0	0.0	2.35E-04	1.46E-04	1.11E-03	
0.0	0.0	1.60E-03	1.46E-04	1.11E-03	
0.0	0.0	6.41E-04	6.61E-04	1.11E-03	
0.0	0.0	1.38E-03	1.65E-04	1.11E-03	
0.0		1.42E-03	1.65E-04	1.11E-03	
Mean	9.04E-05	6.49E-04			
SD	1.56E-04	5.41E-04			

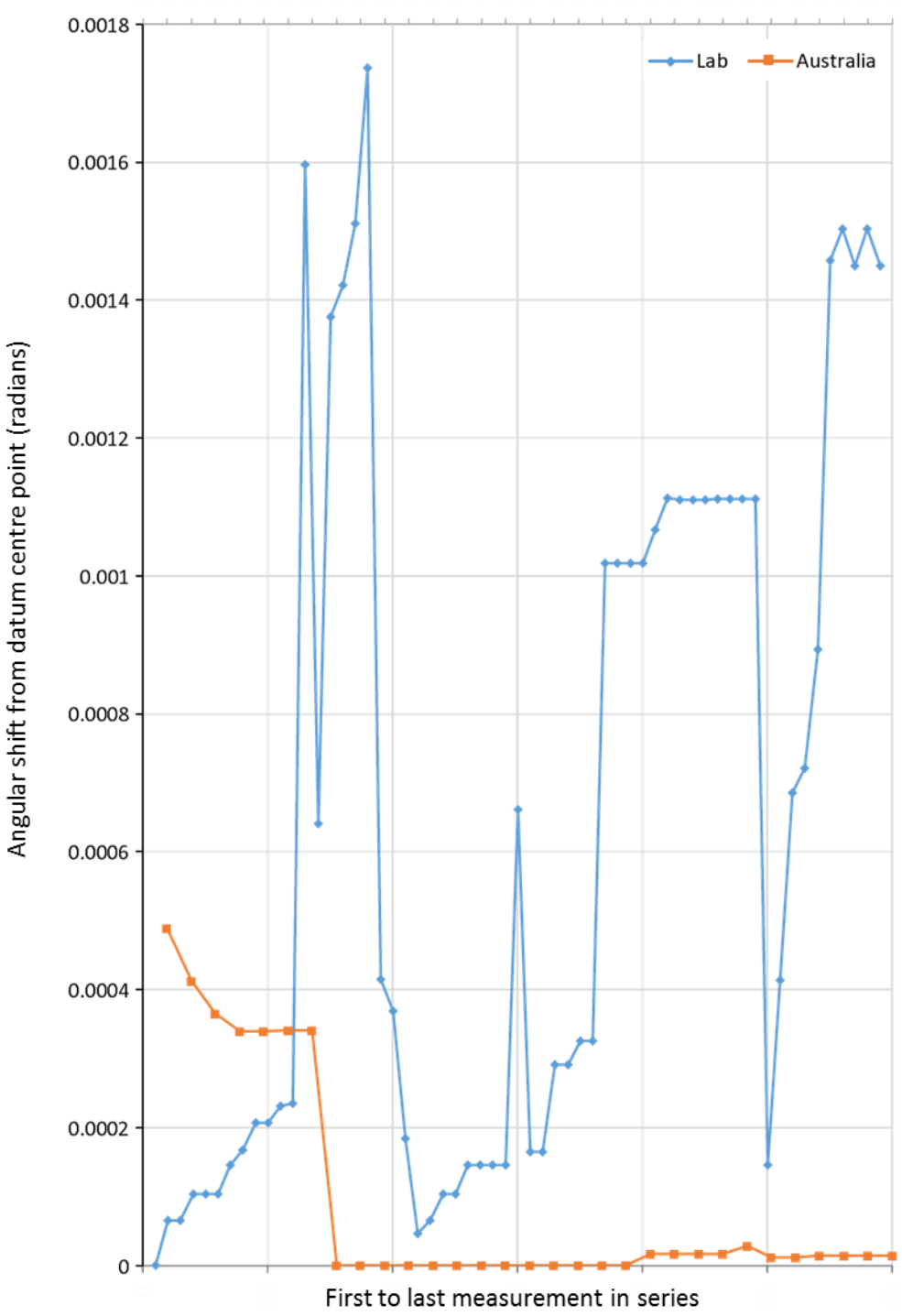

Figure 4-2: Angular shift of each measurement point (radians) relative to datum measurement

The first set of measurements taken during the lab trial appear to steadily shift away from the display centre, with few measurements take at the same position. This is similar to the first set of field measurements, except that they are further off centre and after a few

measurements they stabilise. The trial set-up becomes increasingly erratic with only a few areas of stability before a dramatic shift.

Overall, the field setup proved to be more stable, as demonstrated by the lower standard deviation (Table 4-1). This can be attributed to the photometer being positioned behind the driver's seat, with the feet of the tripod mounted directly to the floor, subsequently reducing the influence of seat compressibility. However, there was still variation in the field measurement from alignment of the photometer to the display centre and some influence from vibrations from door closure and accessing the photometer on the roof of the vehicle.

The alignment process of the photometer to the diplay centre is not a simple or a repeatable task. Alignment of a plumbline over the target area is dependant on the point of view of the operator; the position will be aligned to the reference eyepoint if viewed from the reference eyepoint. If however the plumbline is viewed from any other position it will appear to align to a different area of the display due to paralax. As the plumbline is not of specified dimensions or placed in a specified position, the operators of the test will need to judge the alignment from their own view point. This means that the photometer will not be aligned to the Driver's Reference Eyepoint but to the eyepoint of the operator and for different operators this will be a different position. Repeatability is compromised due to variability between operators and no standard plumb line definition. The testing setup is difficult to reproduce due to the minimal likelihood of operators having the physical proportions of the 95th percentile standard and achieving the Driver's Reference Eyepoint.

The lab trial demonstrated that the use of a tripod to mount the photometer on the unstable surface of the driver's seat, the weight of the photometer and the level of adjustment in the tripod also contribute to the difficulty in making fine mechanical adjustments. This was also the experience of the alignment during field measurement, however greater control was attempted by setting the angular position and working distance of the photometer from the CAD data. The height and in-board position of the photometer still relied on the subjective alignment of display centre through the view

finder. It is not possible to say whether this step increased the level of control in the measurements as the driver's eyepoint is a theoretical point not related to physical geometry of the vehicle. This compounds the difficulty of setting up the photometer and verifying its position as there is no datum feature to facilitate alignment.

4.1.2 Controlled environment

The controlled environment is required to provide stable lighting conditions that are comparable to the spatial and spectral distribution of natural daylight, with a direct component to represent the sun and diffuse lighting to represent the sky, with respect to both the levels and geometry of daylight on a vehicle. Table 4-2 outline the characteristics of daylight to be considered for a controlled lighting environment.

With the exception of the illuminance measurements which included the effect of direct sunlight, the measurements taken are for sky light only. In general, the luminance of artificial daylight sources is not specified, instead it is the relative value of illuminance depending on the geometrical positioning of the luminaire.

SAE J1757-1 (SAE, 2007) recommends illumance levels of 45 klux at the display surface when it is subject to direct sun light and 5 klux when only diffuse light is considered. These values are lower than the measurements taken at the roof, which is likely due to transmittance of glass and light blocked by the vehicle body, however it is lower than expected which is recognised by the specification. The JLR setup comes closer to representing daylight as it combines both diffuse light and a direct daylight lamp with illuminances representitive of measured and specified levels. There are however several deviations from an ideal setup for both the direct and diffuse light which are illustrated by Figure 4-3 and Figure 4-4.

Table 4-2: Daylight characteristics from measurement, specifications, research and used in JLR high ambient evaluations

Characteristic	Measurements (Sydney 2015)	Specifications/ Research	JLR
SPD (Daylight)	N/A	SPD of standard phases of daylight (Judd et al., 1964) (see Figure D-5 in Appendix D) D65 is recommended as the best representation of average daylight (CIE 2010) SPD of sources should fall within 20% of that specified by CIE 85 Table 4 (see Figure D-4 in Appendix D) without any sharp peaks in the spectrum (SAE, 2007) to be considered a daylight simulator	ARRI Daylight Compact 1200 (fitted with HMI® 12000 W/SE lamp) (ARRI, 2014)
Luminance (Sky)	Min. 2,622 cd/m² Max. 6,987 cd/m² Mean 4,097 cd/m²	N/A	N/A
Illuminance (Daylight)	Min. 85,200 lux Max. 129,800 lux Mean 112,682 lux	5,000 lux from diffuse and 45,000 lux from direct light (SAE, 2007)	Illuminance set to 70-90 klux (Direct), 5-10 klux (diffuse) at the display surface and 100-120 klux at the roof
CCT (Daylight)	N/A	D50: 5,000 K D55: 5,500 K D65: 6,500 K D75: 7,500 K (CIE 2010) Based on Standard phases of daylight 4,800 K, 5,500K, 6,500 K, 7,500 K, and 10,000 K determined by Judd et al (1964). The CCT is secondary to the SPD (SAE, 2007).	6,000 K (OSRAM, 2016)
CCT (Sky)	Min. 11,728 K Max. 31,660 K Mean 19,637 K	CCT of the sky is not specified, however Kelley et al (2006) use 16,500 K (diffuse) and 5,500 K (direct) to give overall impression of 6,500 K, for assessing daylight legibility of displays – see also (Mardaljevic, 2013)	N/A
Chromaticity	Chromaticity of sky plotted with Plankian locus and isothermal lines of CCT (see Figure D-1 to Figure D-3 in Appendix D)	Tolerance ellipse for daylight illuminant plotted on The CIE 1931 Chromaticity Diagram (BSI, 1967) (see Figure D-1 to Figure D-3 in Appendix D)	N/A

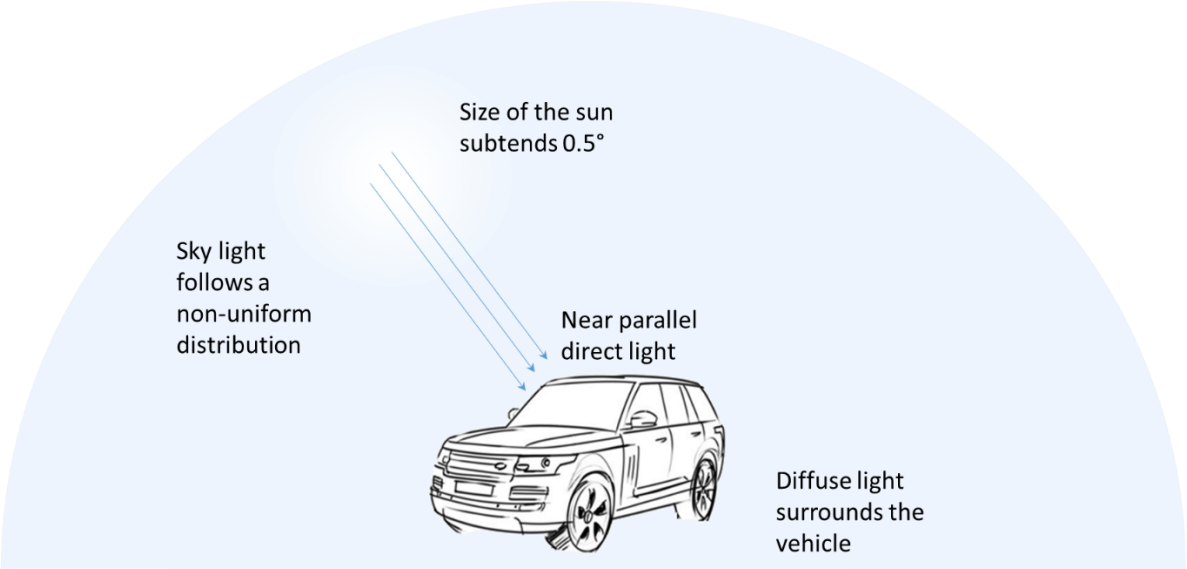

Figure 4-3: Representation of daylight geometry

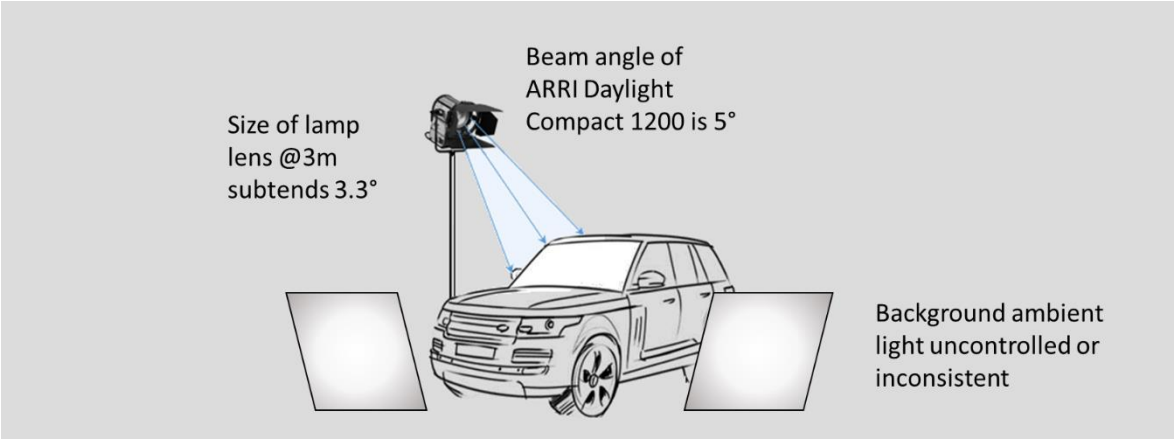

Figure 4-4: Representation of lab setup geometry

The specified sun lamp from the JLR setup does not simulate the apparent size of the sun and is not collimated to represent close to parallel rays of the sun. These parameters of daylight are recognised in the SAE specification but not put into practice in either the JLR or SAE specification.

The same lamp is used in each test; however, as highlighted by the lab trial discussed in Section 2.2.2.2, the precise position of the lamp cannot be controlled therefore the

situation under test does not repeatably replicate a given direction of light. This is due to the instability of the tripod and the lack of method to make fine mechanical adjustments; both to the downward angle of the lamphead and the rotational position with respect to the vehicle under test.

The ARRI Daylight Compact lamps are daylight simulators with a CCT of 6000K, with eight different versions available (ARRI, 2005). The ARRI Daylight Compact 1200W used by JLR, appears to be a good visual fit for D65 SPD (Figure 4-5) however it is not determined how well it meets the specified 20% of CIE 85 Table 4 as this data is not included in the data sheet, and there is a peak in the blue and green regions of the spectrum and contains less red light.

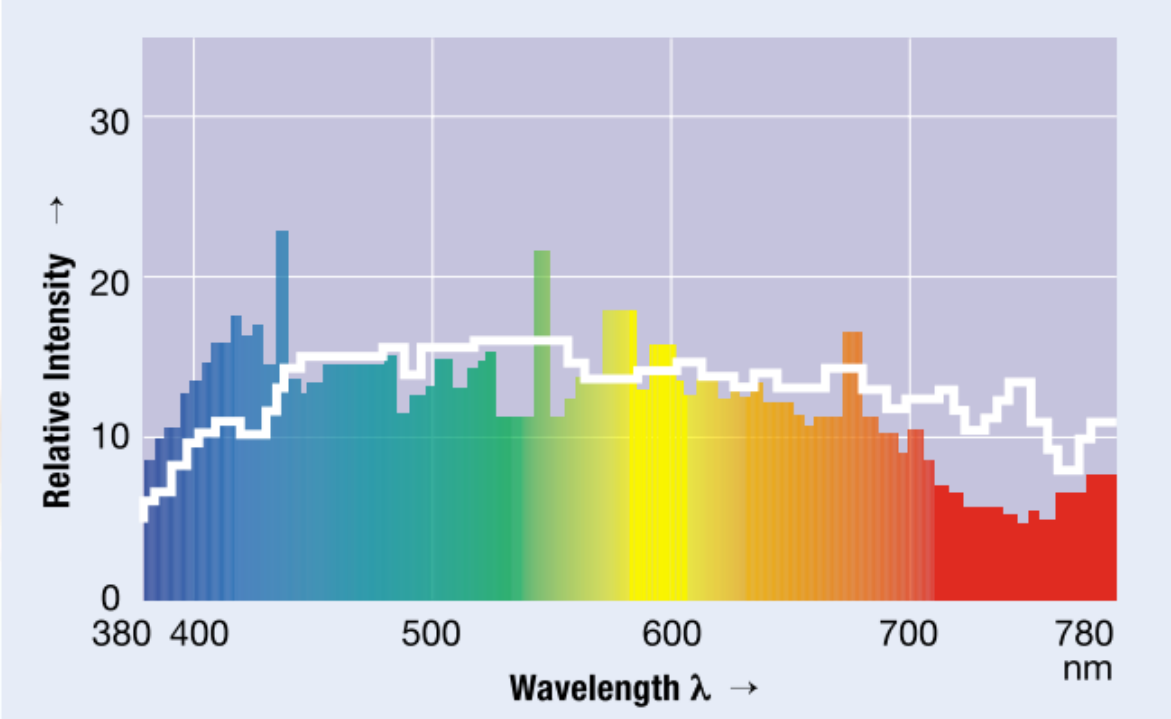

Figure 4-5: Spectral power distribution of OSRAM lamp used in ARRI Daylight Compact (coloured SPD), compared to D65 (white line) (OSRAM, 2016)

The CCT of the ARRI lamp is 6000K, which is considered to be a good representation of daylight. Both the diffuse and direct light are specified as D65 simulator lamps rather than a lamp to simulate the sun with a cooler colour temperature and lamps of a warmer colour temperature to simulate the diffuse sky light.

International standards for display metrology simulate diffuse uniform light to represent sky light to encompass the display. This is not appropriate for evaluation of the final system as vehicle architecture will block incoming light causing shadows at the display and reduces the daylight levels of illuminance within the cockpit, resulting in different daylight illuminance conditions outside and inside the vehicle. Ideally this diffuse light needs to encompass the vehicle to ensure that all daylight openings into the vehicle are covered.

The illuminance levels must be stable and the same levels for each test. The target levels for JLR's tests are comparable to real-world however the diffuse light generated for the JLR setup does not follow a recommended distribution and is not specified to be uniform, this means that other than the specified target illuminance levels there is no specified size, orientation, number or location of diffusor screens. This will result in different illuminance levels for each setup.

4.2 DIGITAL GAP

As noted in Section 2.2.1, SPEOS simulations are performed at JLR as part of the evaluations on in-vehicle display legibility. These digital simulations create daylight scenarios to assess the ambient contrast effects at the display for different sun positions and sky conditions, to guide the positioning of the display and give the critical sun locations to be assessed during physical testing.

Using the display data collected in Australia, simulations of the display are performed to compare to the measurements. This is to ascertain the degree to which SPEOS represents real world high ambient conditions. These simulations are based on the on the standard procedures for display legibility assessments at Jaguar Land Rover, with parameters that generate data comparable to the measured displays such as geometry, material properties and sun positions.

4.2.1 Results comparison

Figure 4-6, Figure 4-7 and Figure 4-8 are examples of the measured and simulated displays. The examples selected, demonstrate the effect of high ambient daylight conditions in each

orientation of the vehicle; with the sun high and in the direction of passenger side, driver's side and rear respectively.

Figure 4-6: Measurement (top) and simulations (bottom) of configuration #3

Figure 4-7: Measurement (top) and simulation (bottom) of configuration #14

Figure 4-8: Measurement (top) and simulation (bottom) of configuration #23

A visual comparison between the measured displays and their simulations suggests that the software gives a good approximation of the real world with respect to shadows falling

where expected and the area of lowest contrast of the display demonstrated. It is easily seen, however, that the graphic is still highly legible in comparison to the captured image.

The presented images extracted from the measurements and simulations give an impression of the effects, however do not give enough detail especially without a calibration to the device that displays the results. For a meaningful comparison, the photometric data is required in the form of the foreground and background luminance (as defined in Submission #4) in addition to the calculated contrast and PJND of the display.

To evaluate the measured and simulated displays, like for like points were defined to perform the assessment. There are no set guidelines in the JLR test procedure on how to do this other than the requirement to *"ensure each of the important HMI interactions is assessed"*. The assessment could be performed by selecting each HMI interaction (e.g. clock, phone, Nav etc.) or by sub dividing the display.

With this in mind, it was decided to sub divide the display into patches that span the full area of the display and cover all of the main HMI interactions. Guided by the main display graphic a set of 16 patches were defined to achieve this (Figure 4-9).

Figure 4-9: 16 sample patches of the display area

Of the 16 patches, four have been disregarded (#5, #9, #10 and #14) due to only low contrast features in these areas or a corresponding feature not being available between the measured and simulated displays, which would make comparison difficult.

For a PJND evaluation, foreground and background colour and luminance data is required. Therefore, within each of the remaining 12 patches, a foreground and background feature is identified.

A sample of 12 pixels is selected from each feature (Figure 4-10) from which the mean luminance (cd/m^2) and colour (Cx, Cy) can be extracted. A minimum sample of 10 pixels at the smallest feature is recommended by the camera supplier, to ensure an accurate measurement. This reduces the variability of the measurement especially at the edges where the dark surrounding pixels will reduce the average luminance of the lit area.

Figure 4-10: Sample of 12 pixels of a foreground and a background feature in patch #1

4.2.2 Performance metrics

Common metrics for determining the accuracy of a simulation in relation to measured data are the relative error (Equation 4-1), the mean bias error (Equation 4-2) and the root mean square error (Equation 4-3).

Equation 4-1: Relative Error (RE)

$$RE = \left(\frac{x_s - x_m}{x_m}\right)$$

Equation 4-2: Mean Bias Error (MBE)

$$MBE = \frac{1}{N}\sum\left(\frac{x_s - x_m}{x_m}\right)$$

Equation 4-3: Root Mean Square Error (RMSE)

$$RMSE = \sqrt{\frac{1}{N}\sum\left(\frac{x_s - x_m}{x_m}\right)^2}$$

Where, N is the number of data points, x_s is the predicted (simulated) value and x_m is the measured value.

These metrics are widely used in sky modelling (Angus, 1995; Cucumo et al., 2010; Gueymard and Myers, 2008; Ineichen et al., 1994; Kobav, 2009; Littlefair, 1994; Mardaljevic, 2008, 1999) and were amongst the metrics chosen for benchmarking of sky measurement equipment (Beyer et al., 2009).

The relative error (*RE*) describes individual data points; illustrating the difference between measured and simulated values to give an indication of accuracy for each measure. Whereas the mean bias (*MBE*) and the root mean square error (*RMSE*) describe the performance of the entire model. *MBE* gives an indication of the overall bias of the modelled data; whether there is a tendency for the model to under or over predict values and the *RMSE* is a good measure of the overall error and the fit of a model. It reflects the magnitude of errors and the amount of scatter or deviation from the measurement. It differs to variance and standard deviation in that it is a measure of how far on average the error is from 0 rather than the spread about a mean.

For a perfect fit, $x_s = x_m$ and the *RMSE* would be equal to zero. Therefore, lower values of *RMSE* indicate a better model. The form presented in Equation 4-2 and Equation 4-3 give relative values normalised with the mean of the measured data.

In terms of lighting simulation, it is suggested that a high accuracy is achieved with an RMSE <10% and medium accuracy if <25% (Mardaljevic, 2008, 2002, 1999).

4.2.3 Performance evaluation

Figure 4-11 to Figure 4-13 plot the luminance of the foreground features of the display at each of the 12 sample patches to indicate the reflection profile of displays #3, #14 and #23. Figure 4-14 to Figure 4-16 are the equivalent plots for the background sample luminance of these displays.

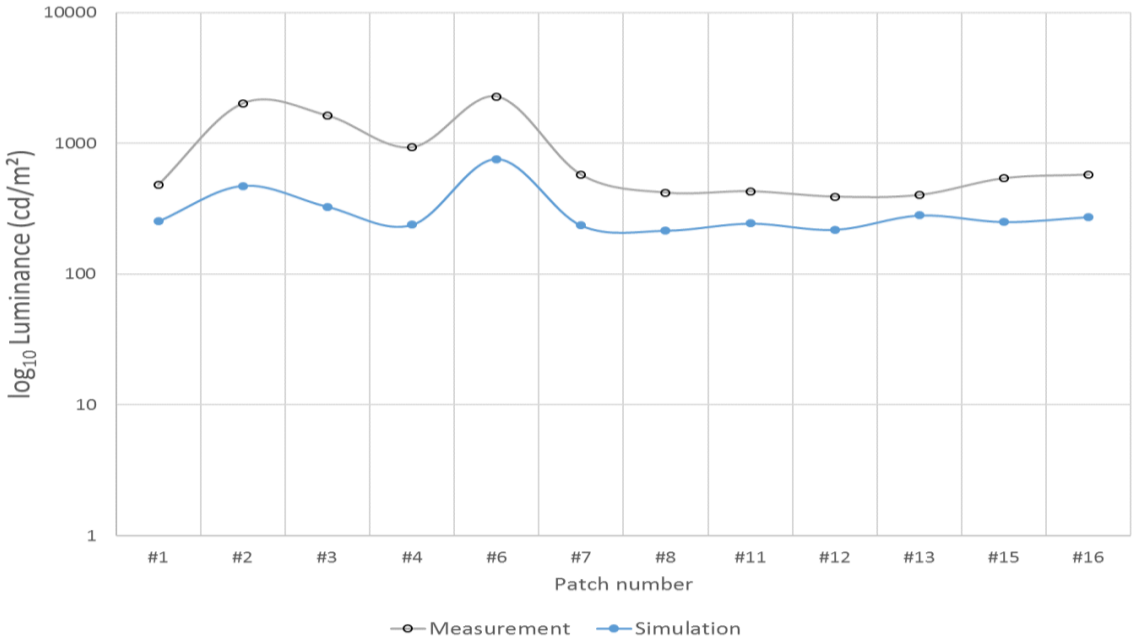

Figure 4-11: Foreground Luminance per sample patch at Display #3 plotted on a log $_{10}$ scale

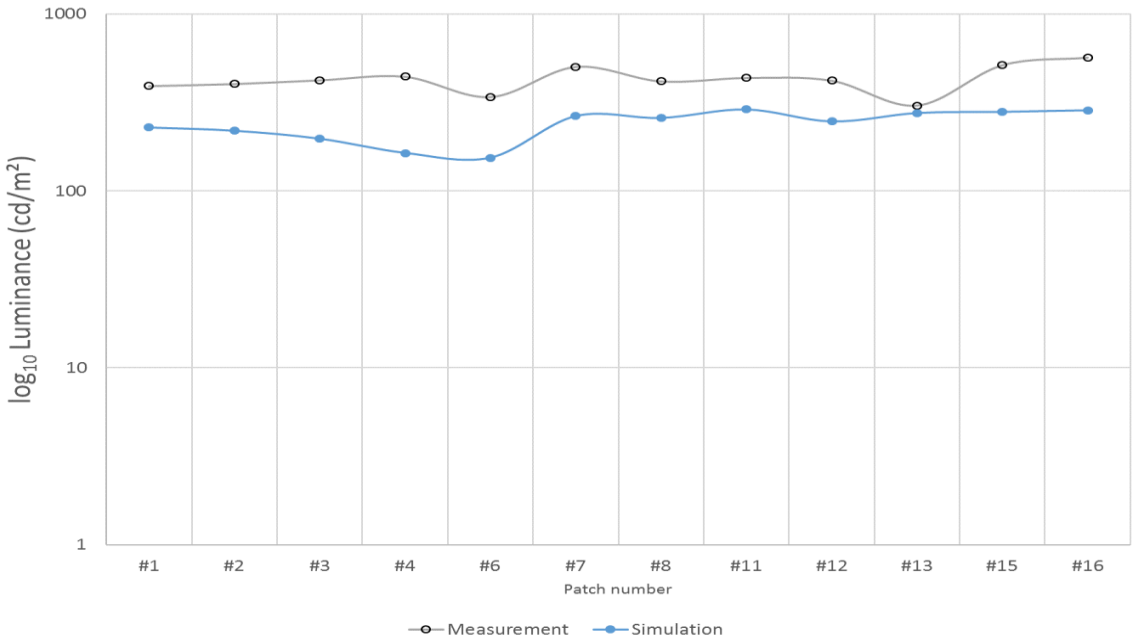

Figure 4-12: Foreground Luminance per sample patch at Display #14 plotted on a log $_{10}$ scale

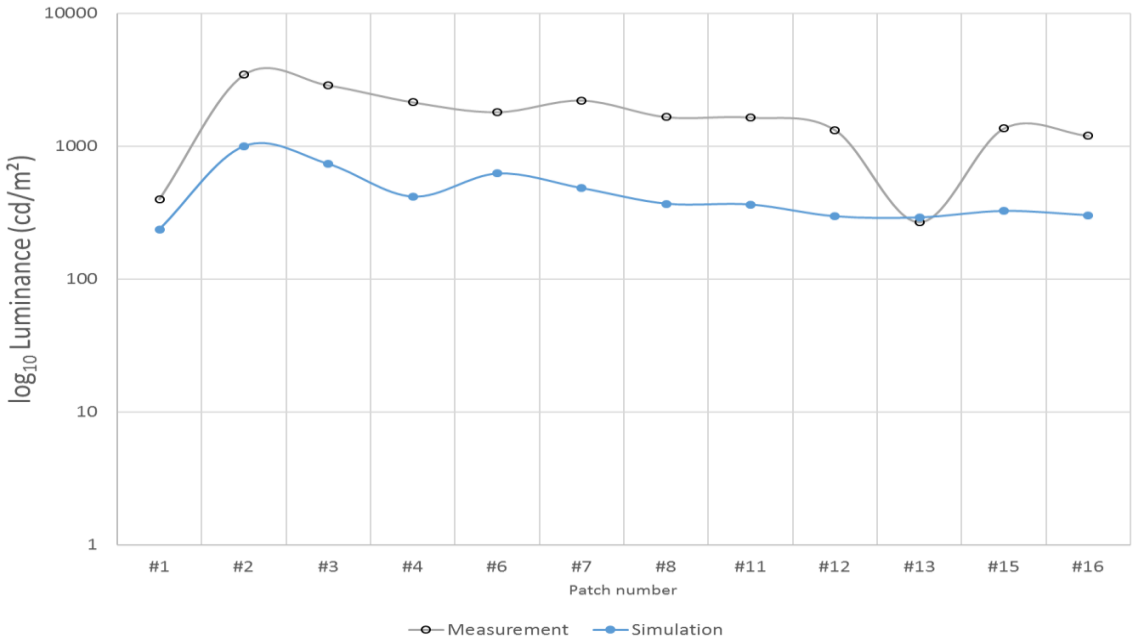

Figure 4-13: Foreground Luminance per sample patch at Display #23 plotted on a log $_{10}$ scale

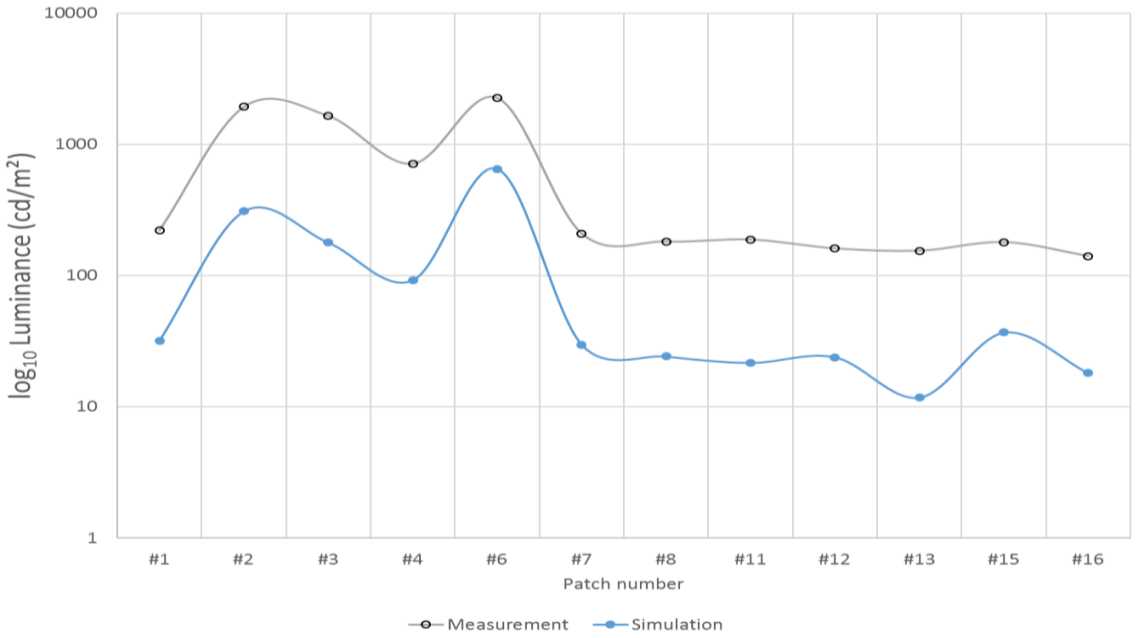

Figure 4-14: Background Luminance per sample patch at Display #3 plotted on a log $_{10}$ scale

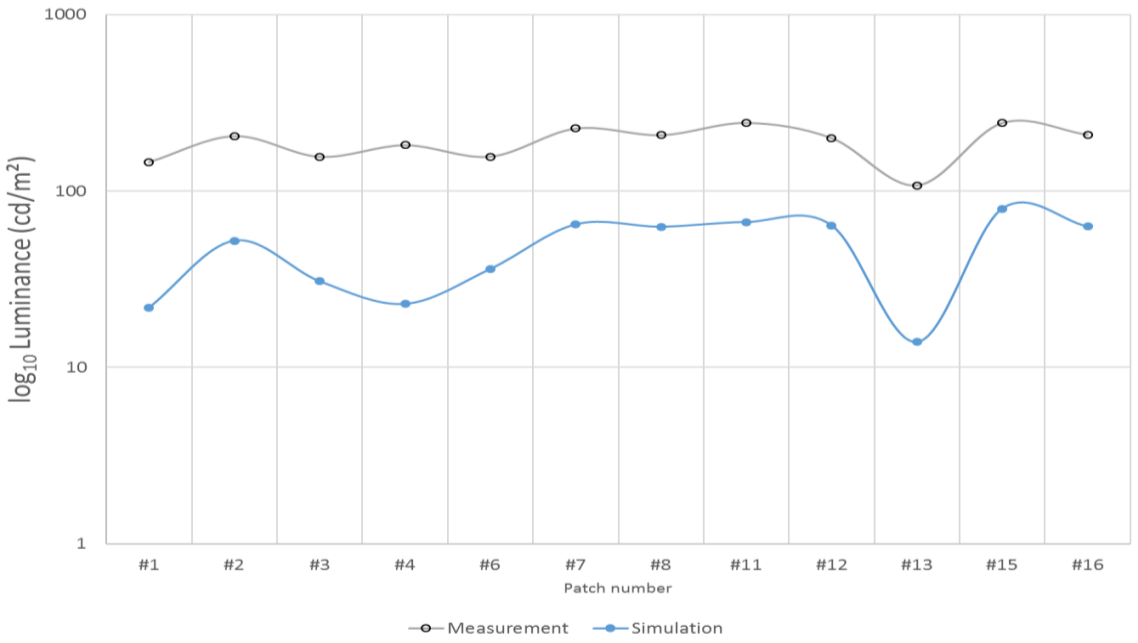

Figure 4-15: Background Luminance per sample patch at Display #14 plotted on a log 10 scale

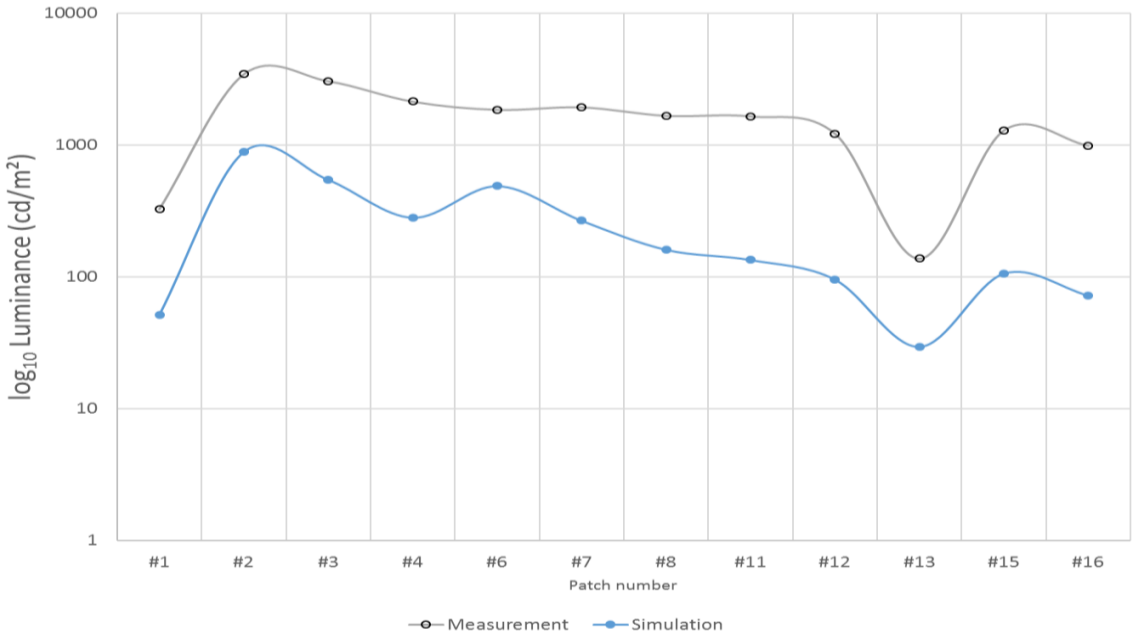

Figure 4-16: Background Luminance per sample patch at Display #2 3 plotted on a log 10 scale

From the foreground and background luminances of the sample displays, it can be seen that the measured and simulated data follow a similar profile. The measured luminance is, however, consistently greater. An indication of the magnitude of these differences is illustrated by the $\log_{10}$ scale, as the log function addresses the skew of large values and therefore highlights where peaks span an order of magnitude.

It appears that Patch #13 is an exception that does not follow the trend of the luminance profile in both the fore and background charts. This is most evident in the plots of foreground luminance for Display #14 (Figure 4-12) and #23 (Figure 4-13), however, this will be the case for Patch #13 across all measurements, as demonstrated by Figure 4-17.

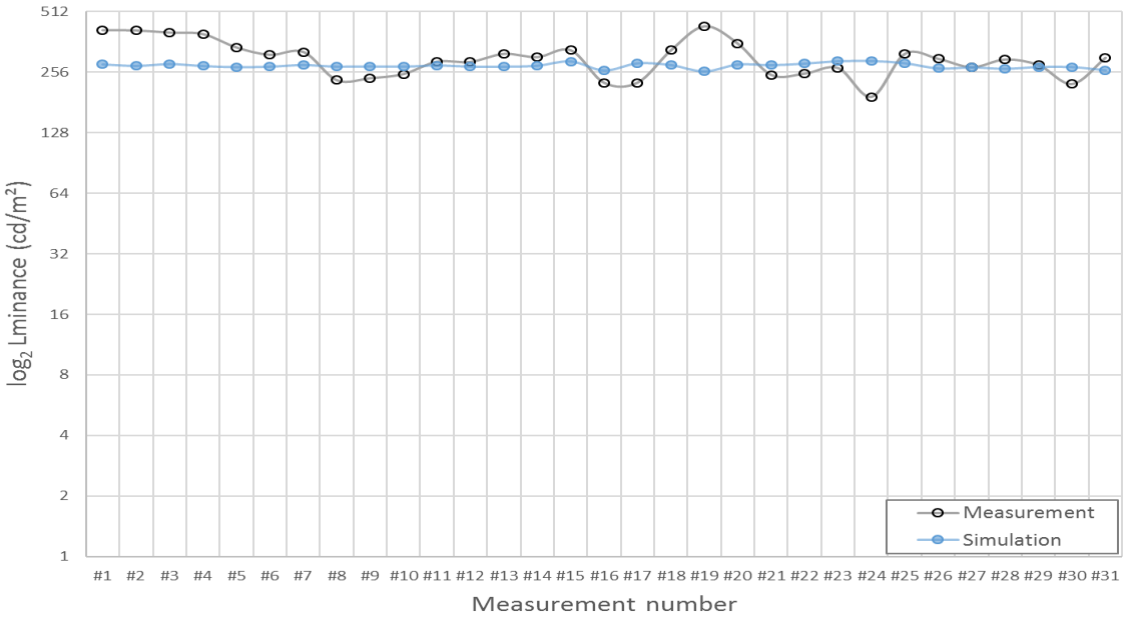

*Figure 4-17: Foreground Luminance of **Patch #13** across all measurements plotted on a $\log_2$ scale*

The simulations predict that the foreground luminance in the area of Patch #13 will remain steady regardless of sun position, which is consistent with the measurements. From the display images, it can be seen that Patch #13 is easily visible with good luminance contrast; in this area, the display falls into shadow due to the display being slightly recessed with the shadow falling along the top of the display, also affecting the areas of Patch #1, #5, and #9.

The two central patches along the top of the display (Patches #5 and #9) were disregarded due to non-comparability of graphics, however the foreground luminance across all measurements at Patch #13 can be compared to Patch #1 (Figure 4-18).

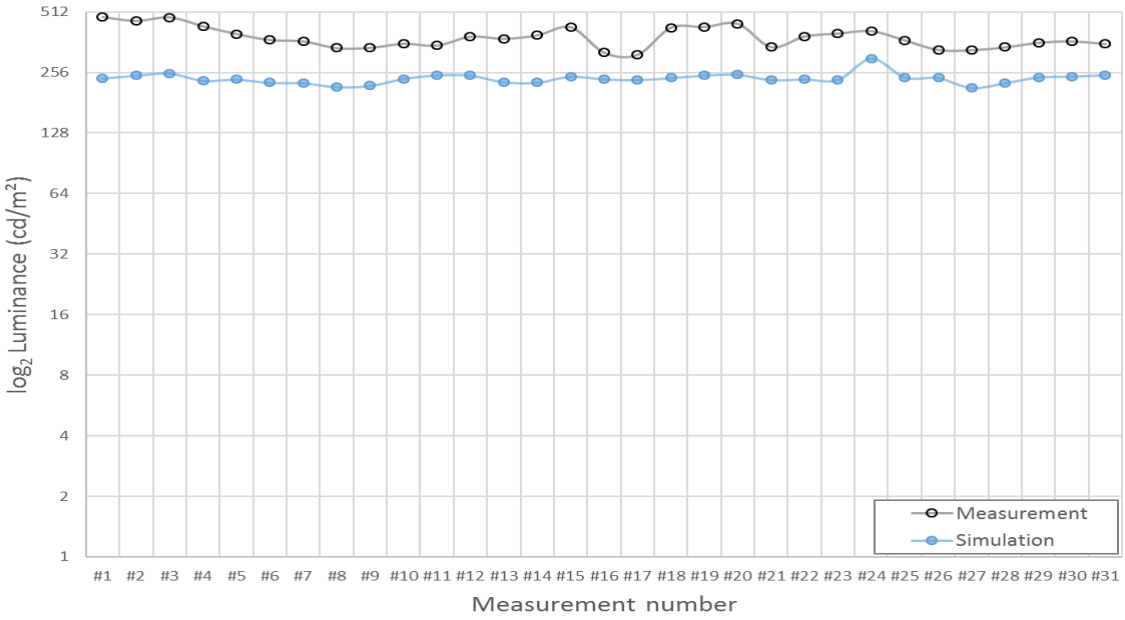

*Figure 4-18: Foreground Luminance of **Patch #1** across all measurements plotted on a log₂ scale*

From this plot, a similar trend can be seen where the foreground luminance is consistently lower and the simulation prediction is closer in magnitude to the measurement. This suggests that Patch #13 is not an anomaly.

The performance of the simulations can be further demonstrated by the *RMSE* and *MBE* (listed in Table 4-3).

Table 4-3: Root mean square error and mean bias error of foreground and background luminance (displays #3, #14 and #23)

Display	Foreground luminance		Background luminance	
	RMSE (%)	MBE (%)	RMSE (%)	MBE (%)
#3	58	-56	85	-85
#14	45	-44	76	-76
#23	70	-66	86	-85

As already stated above, the simulations under predict the fore and background luminance of the displays, as indicated by the negative bias of the *MBE*.

An indication of performance of the model for the entire display is the RMSE. Display #3 is a complex area of shadows and bright patches which has an RMSE of 58% for foreground luminance and 85% for the background lumiance.

From the measured image in Figure 4-7, it can be seen that information on Display #14 is ledgible as is that of the simulation result. This gives the impression that the simulations are a closer fit to measurements as indicated by the RMSE of 45% for the foreground luminance and 76% for backgound luminance. Whereas Display #23, which demonstrates near complete washout under real world conditions, has the greatest deviation of foreground and background luminances, 71% and 88% respectively. This can be further demonstrated by Figure 4-19 to Figure 4-21 which show the contrast of the sample displays at each patch, and Figure 4-22 to Figure 4-24 which present the PJND. Both the contrast and the PJND are indications of the legibility of the HMI features of the display. The contrast is the ratio of foreground to background luminance; the greater the difference between these two figures, the greater the contrast and therefore the legibility is increased. The PJND is a function of the contrast which is scaled to the threshold response of human vision.

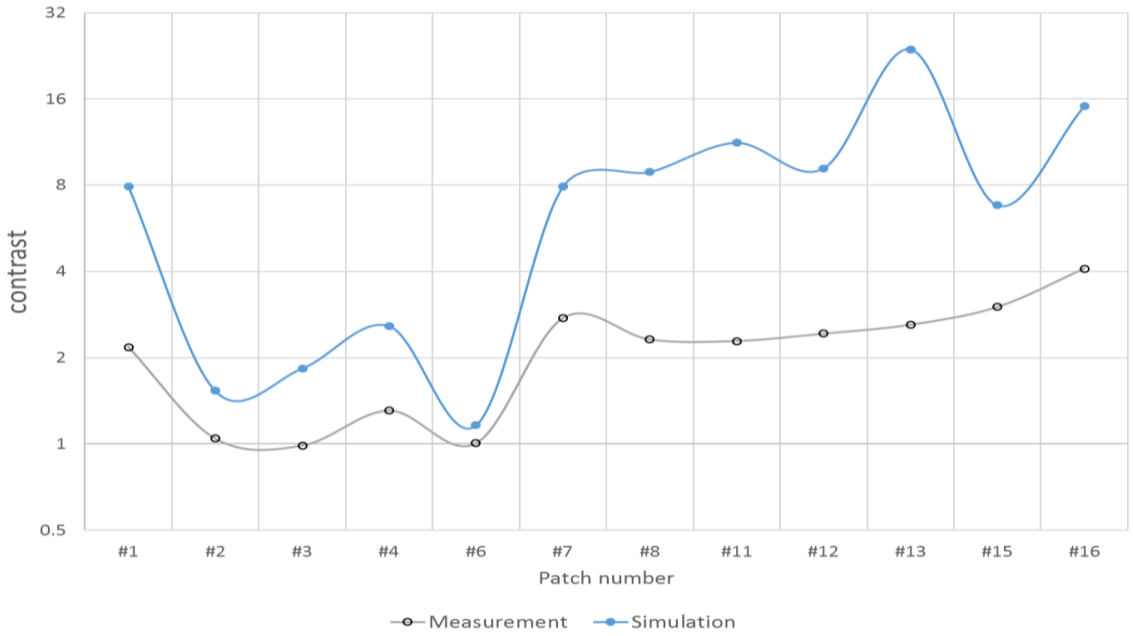

Figure 4-19: Contrast per sample patch at Display #3 (log_2 scale)

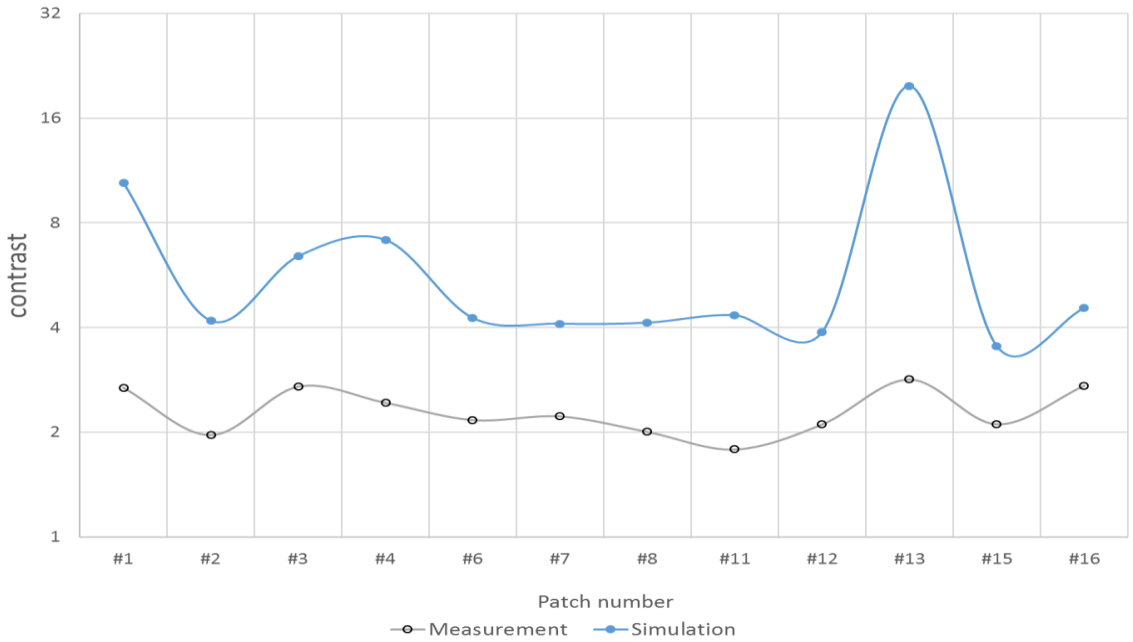

Figure 4-20: Contrast per sample patch at Display #14 (log_2 scale)

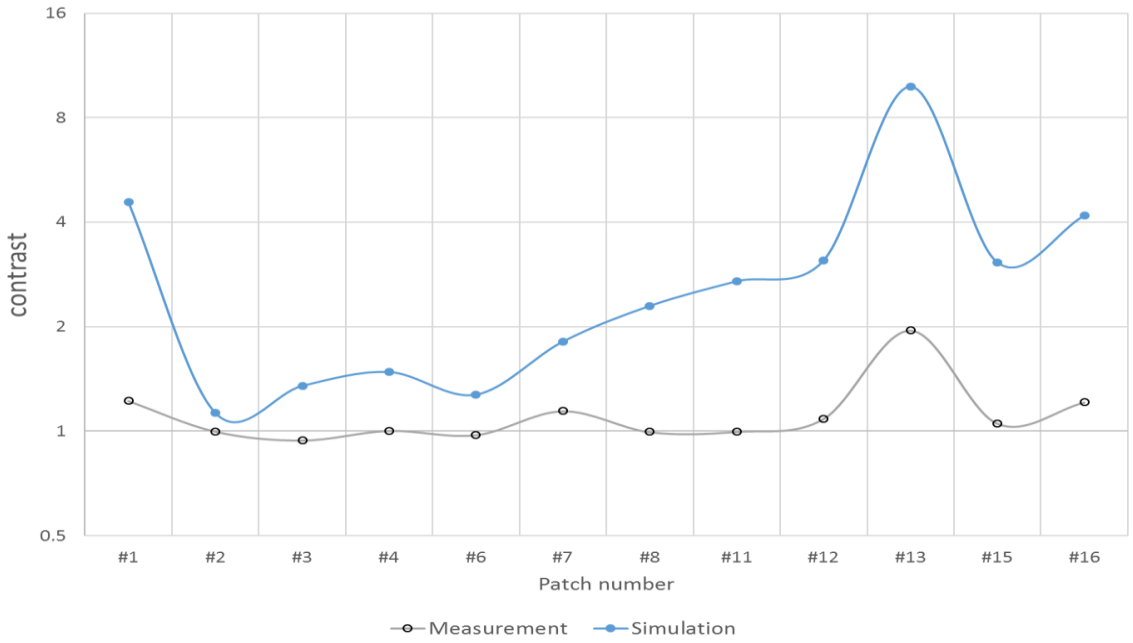

Figure 4-21: Contrast per sample patch at Display #23 (log_2 scale)

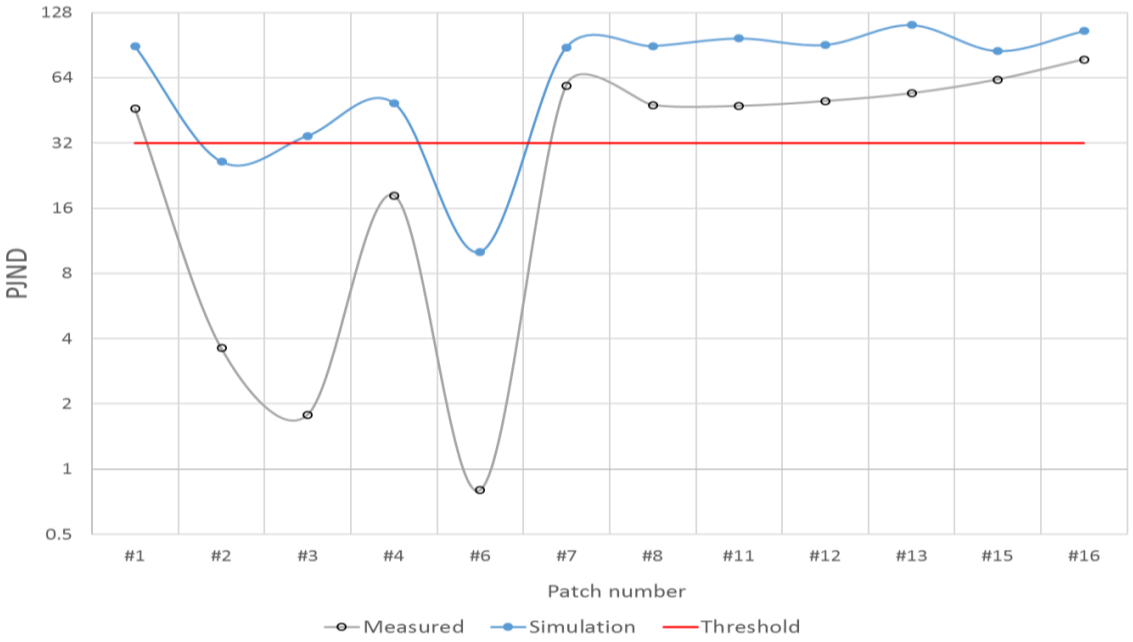

Figure 4-22: PJND per sample patch at Display #3 plotted on log_2 scale

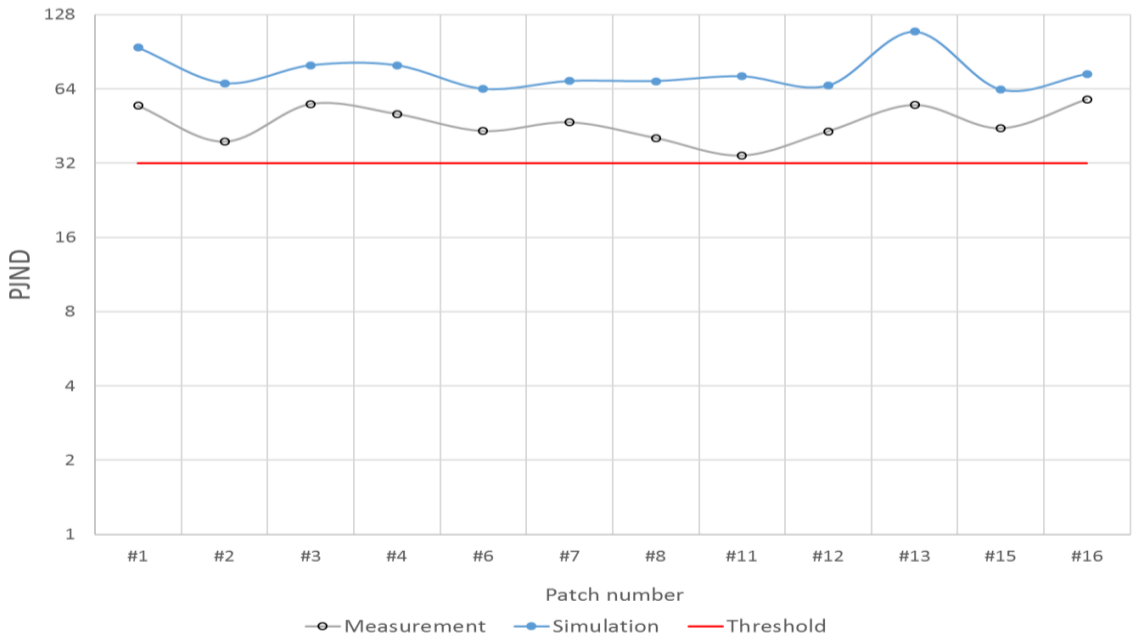

Figure 4-23: PJND per sample patch at Display #14 plotted on log_2 scale

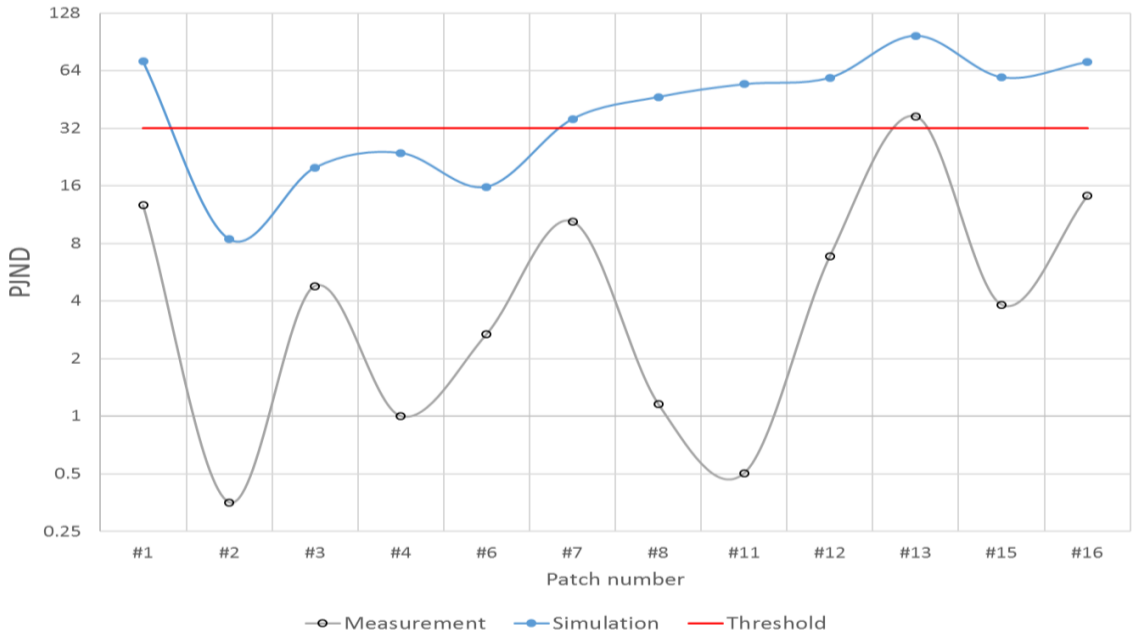

Figure 4-24: PJND per sample patch at Display #23 plotted on log_2 scale

These figures are plotted on a $\log_2$ scale to highlight areas of skew. A base of 2 was selected rather than $\log_{10}$ due to the small range of values for PJND. A threshold line has been included at the PJND value of 32, which has been established as the pass criteria for PJND evaluations at JLR. Above this line the HMI interaction under evaluation is deemed to be 'Easily Readable'.

The PJND plot for Display #14 confirm that both the measured and simulated displays are fully legible at all sampled patches with the simulated result following the profile of the measurements, as do the plots of PJND on the other two displays. However, the simulation gives a prediction of PJND an order of magnitude greater, as indicated in the plots of fore- and background luminance. It can also be seen from the measured displays with areas of low contrast that are illegible, have corresponding points on the simulated displays that will give a result that exceeds the threshold of required legibility. Therefore, it is possible for the simulations to underestimate the effects of sunlight at the display. This effect seems to be greatest for displays adversely effected by high ambient daylight and could be due to the behaviour of the material properties or the source definition in the simulation.

4.4 SUMMARY

This section has evaluated the gap between current evaluation methods and the real world by comparing the measurements to and the trial setup and simulations of the field measurement situations, in fulfilment of *Objective 2*.

The current method of performing physical assessments on in-vehicle displays are not repeatable, reproducible and are not comparable to daylight conditions. The lack of controlled measurement is attributed to the method of setting up the photometer to the driver's reference eyepoint and alignment to the centre of the display. The difference in environment is mainly due to the undefined geometry in diffuse illumination and the lack of control in positioning the direct light source.

Overall the digital simulations are found to give a good visual approximation of daylight effects with the foreground and background luminance following similar profiles to the measured reflections. The measured luminance is however consistently greater with an RMSE of 45% to 70% at the foreground and 76% to 86% at the background of the presented sample displays. The greatest errors occur where the display is affected by high ambient illumination.

The gap in the simulations could be due to the daylight definition of the software or the properties of the materials in the simulation.

5 VIRTUAL ASSESSMENTS OF DISPLAY LEGIBILITY

Section 4 discussed the gaps that currently exist in in-vehicle display evaluations and proposed areas that potentially cause or contribute to these differences. This section looks to address *Objective 3: Define an appropriate method for recreating daylight and performing evaluations of in-vehicle displays* by evaluating these factors, and where possible, closing the gaps in digital and physical methods of performing virtual assessments of display legibility.

5.1 DIGITAL EVALUATIONS

The digital gaps in automotive display evaluations at JLR could be due to the definition of the sun and sky in the simulations influencing the luminance of reflections at the display surface. It is also possible that the material properties of the display surface do not represent the behaviour of the real-life display resulting in incorrect reflection characteristics. These potential sources of error in the digital evaluations performed at JLR are investigated with a view to closing the gap.

5.1.1 Source definition in SPEOS simulations

The daylight source generated in SPEOS is defined using a combination of the sky model and spectral parameters to describe the sun, which are listed in Table 5-1.

Table 5-1: Properties of the sun in SPEOS simulations (OPTIS, 2016)

Properties	Values
Apparent diameter	Approx. 0.5°
Correlated colour temperature	Approx. 5800K
Luminance	1.6 x10^9 cd/m²
Illuminance at the ground (normal)	Approx. 10^5 lux
Spectral range	380 to 780nm

These parameters are consistent with the characteristics specified for the generation of artificial daylight as outlined in Section 4.

As no direct sun measurements were taken, the daylight source generated by SPEOS will be evaluated in terms of the daylight illuminance and the luminance distribution of the sky. To facilitate this comparison, simulations were performed to extract comparable data. Ideally, the simulations would be generated from the measured sky data, however the control over the sky definition in SPEOS is not configurable, therefore it is not possible to input the measured sky luminances from this study directly into the program without the assistance of developers from OPTIS. As such, other methods are required to compare measured and simulated daylight illuminances and sky luminance distributions.

5.1.1.1 Daylight illuminance

For each of the 31 display scenarios, a 50 x 50mm irradiance sensor was positioned at the roof of the vehicle in the CAD model to capture the simulated daylight illuminance for each configuration under test. The sensor in the simulation was defined to replicate the operation of the sensor of the Konica Minolta T-10, which has a sensor aperture of 25mm radius. Figure 5-1 plots the results of the simulations and the global horizontal illuminance recorded in Australia (see Table A.1 of Appendix A).

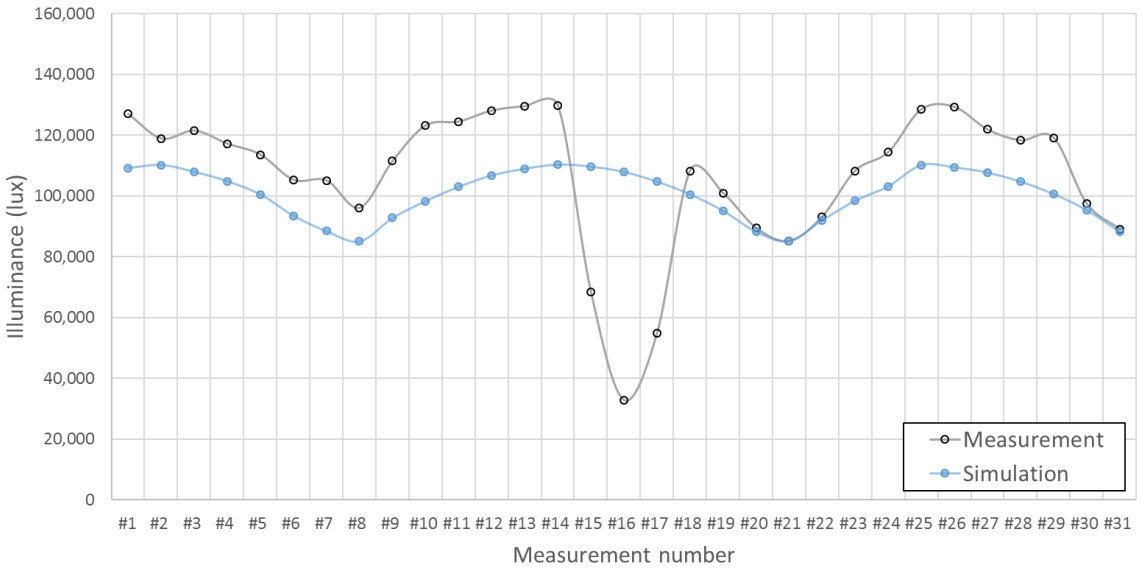

Figure 5-1: Measured and simulated global horizontal illuminance

The smoother curve of the simulation is expected due to being based on a mathematical model, whereas the illuminance from real skies fluctuates depending on atmospheric conditions. The first half day is indicated by measurements #1 to #7. This shows how the illuminance falls from the solar noon through the afternoon; this trend is demonstrated by both the measured and simulated illuminances. Day 2 was a full day of 13 measurements from #8 to #20, demonstrating the rise of illuminance in the morning until solar noon around measurement #14 and the decline in the afternoon. The illuminance of the measured dataset displays a dip in the illuminance for #15, #16 and #17. From looking at the images taken of the sky at these data points (Figure 5-2), it can be seen that there is a high level of cloud around the circumsolar region that is obscuring the solar disc.

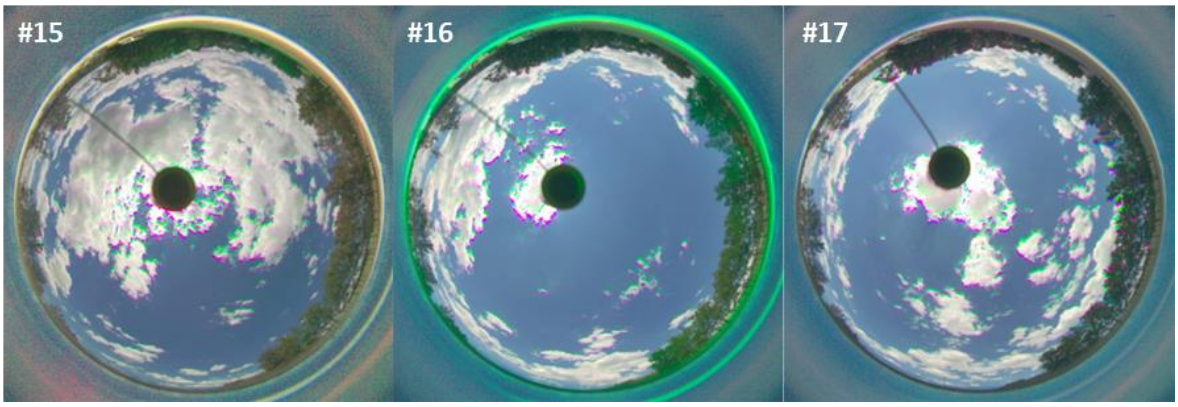

Figure 5-2: Images of skies for measurements #15, #16 and #17

These data points are removed (Figure 5-3) due to the high level of cloud which is not simulated by the software.

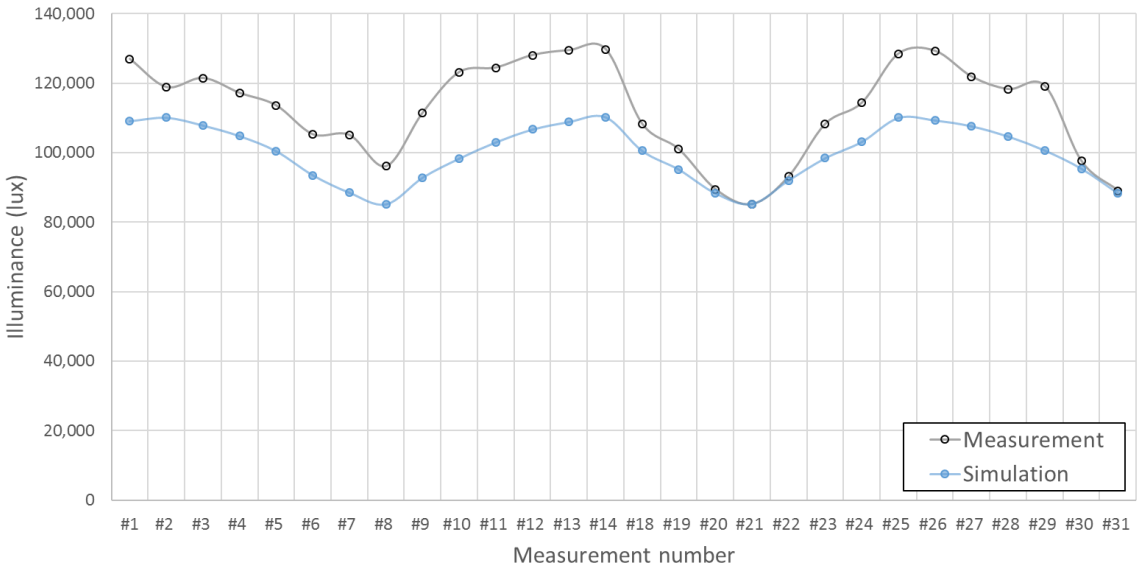

Figure 5-3: Measured and simulated global horizontal illuminance excluding measurements #15, #16 and #17

The removal of these points has truncated the curve between points #14 and #18 which is also evident between points #24 and #25 where there are missing measurements due to equipment failure. The predicted illuminance follows the profile of the measurements however other than points #20 to #22 the illuminance is generally underestimated, which is indicated by the negative MBE of -11%. The gap between the model and the measurements is quantified with a RMSE of 12%; demonstrating that the model gives a good approximation of illuminance.

5.1.1.2 Luminance distribution

To compare the measured luminance distributions to those generated in the simulations was not straightforward. One option was to produce the luminance distribution from the mathematical model used by the software; a practical application of the Perez model defined by Preetham, Shirley, & Smits (1999). However, the software documentation did not explicitly refer their sky models to this paper, so without confirmation from OPTIS there was a possibility that another model was used. Therefore, the distribution was extracted though simulations.

5.1.1.2.1 Generating simulated distributions to compare to measurements

Extracting the sky luminance distribution requires a sensor setup within the simulation comparable to the photometer and optics of the measurements. The option to create camera sensor with a fisheye lens, which would be required to capture the full 180° of the sky vault is part of the *'Digital Vision & Surveillance'* package within SPEOS. However, this module it not part of the SPEOS product licenced by WMG or JLR, and these options are not embedded in the *'Light Modelling'* and *'Visual Ergonomics'* modules available. To overcome this limitation, a sphere was modelled with mirror optical properties, and a luminance sensor placed directly above it, looking down to capture the reflected sky as depicted in Figure 5-4. This would mimic the circular output of the measurements taken with a fisheye lens.

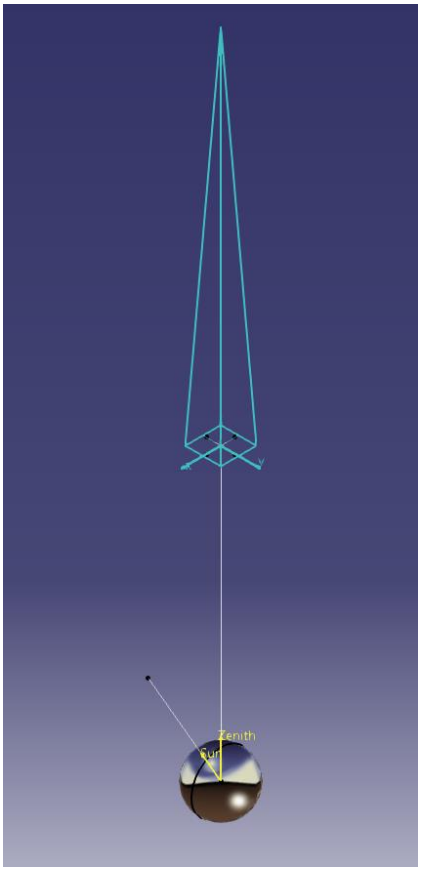

Figure 5-4: CAD model of mirror sphere and sensor

To be comparable to measurements, the simulation needed to match the parameters of the photometer and fisheye lens, with the same number of pixels (1020 x 1020), sensor size (24.45mm x 24.45mm), and the same active area of the image (R11.3mm).

The active area of the image was calculated using the mapping function of the lens (Equation 5-1) which occurs at the maximum value of r at the simulated horizon, which occurs at the maximum inclination angle, $\theta = \frac{\pi}{2}$.

Equation 5-1: Equisolid angle projection of the fisheye lens used for measurements

$$r = 2.f.\sin\frac{\theta}{2}$$

Where:

r *is the radial distance from the centre of the image*

f *is the focal length of the lens (8mm)*

θ *is the inclination angle of the incoming ray of light (from* $\frac{\pi}{2}$ *at the horizon to 0 at the zenith)*

The sphere is set at an arbitrary distance from the sensor and the geometry of the mirror sphere is then calculated assuming a perspective projection, as illustrated in Figure 5-5. The sensor parameters can then be used to calculate the size of sphere required (Equation 5-2 and Equation 5-3).

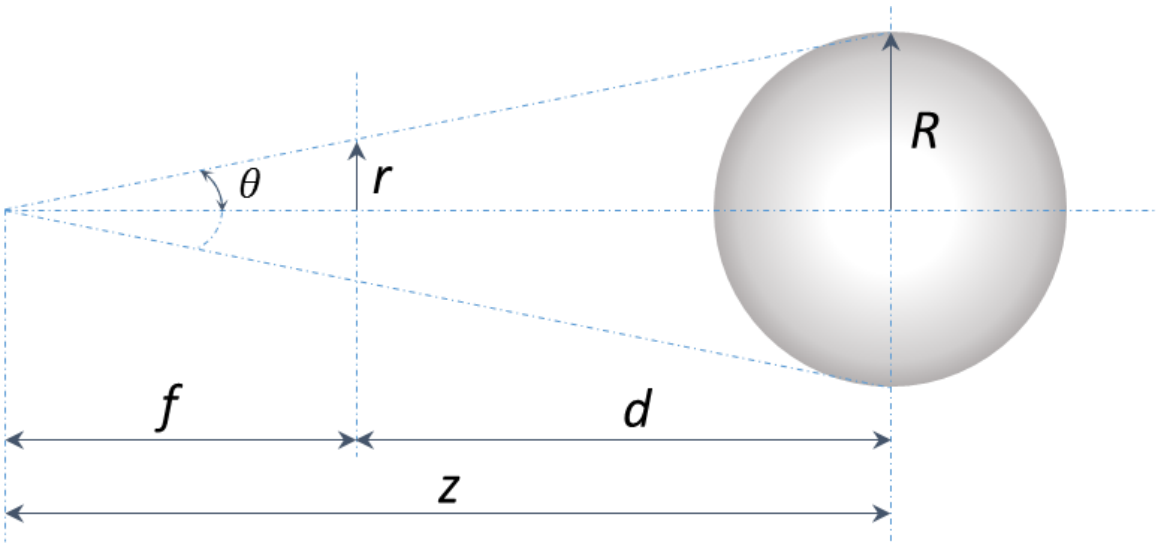

Figure 5-5: Perspective projection of Mirror Sphere

Equation 5-2: Perspective projection at r

$$r = f.\tan\theta$$

Equation 5-3: Perspective projection at R

$$R = Z.\tan\theta$$

Where:

r *is the active area of the image (as calculated by* Equation 5-1*)*

f *is the focal length of simulated lens*

θ *is the projection angle*

Z *is the projection point and the sphere centre*

R *is the radius of the sphere*

However, due to the curvature of the mirror, the distance Z is adjusted to achieve the correct image size. By tracing a ray of light from the sky hemisphere reflected to the sensor from the mirror sphere (Figure 5-6), the relationships in Equation 5-4 and Equation 5-5 can be discerned (for more detail on derivation see Submission #4).

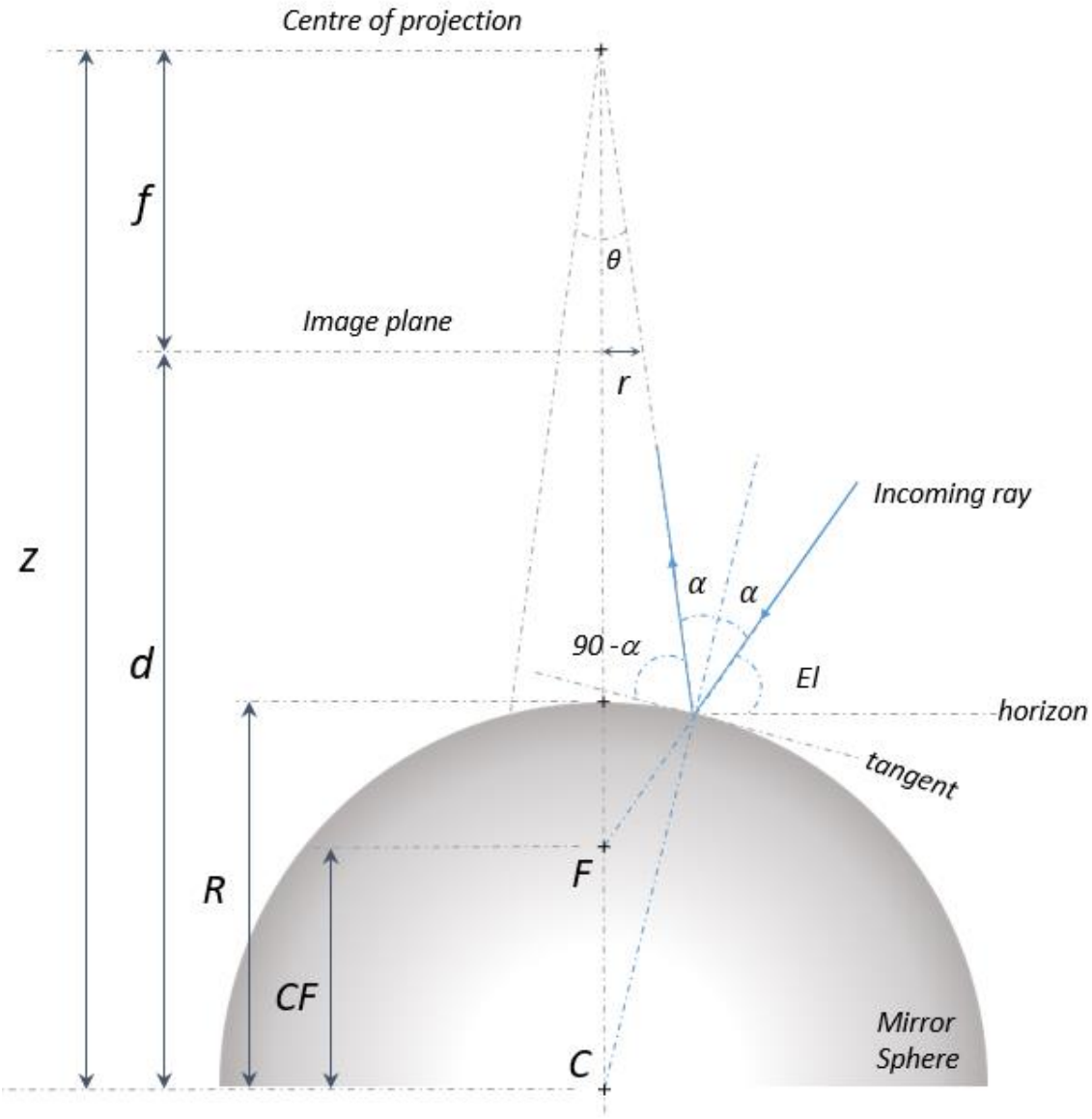

Figure 5-6: Ray diagram of incoming ray from sky hemisphere mapped back to the image plane

Equation 5-4: Relationship between angle of incidence and elevation

$$\alpha = \frac{1}{2}\left(\frac{\pi}{2} + \theta - El\right)$$

Equation 5-5: Distance of sphere from projection point of lens

$$Z = \frac{R.\sin\alpha}{\sin\theta}$$

Where:

α *is the angle of incidence of an incoming and reflected ray*

θ *is the projection angle (as calculated by Equation 5-2)*

El *is the elevation angle of the incoming ray of light (0 to* $\frac{\pi}{2}$*)*

R *is the radius of the sphere (as calculated by Equation 5-3)*

Z *is the distance of sphere centre of curvature from projection point of lens*

The outer radius of the image denotes the horizon where the angle of elevation, *El* = 0. Therefore, α = 0.808 (according to Equation 5-4) which can then be used in Equation 5-5 to give *Z* = 325.6mm (or *d* = 75.6mm) for the apparent size of the simulated image to be 11.3mm.

For each sky measurement, a mirror sphere sky is generated and the luminance distribution is extracted per pixel for both the measurement and simulation results. The text files containing these data are processed using a Matlab script written to perform several operations to the raw data to enable meaningful comparison between the measurements and simulations; data is aligned, cropped and subdivided into 145 discrete patches of average luminance.

Figure 5-7 illustrates these steps with measured data. The process for subdividing and averaging the data in the simulations follows the same procedure, the only exception is the difference in the mapping functions applied; perspective projection as opposed to the equisolid angle projection of the measurements.

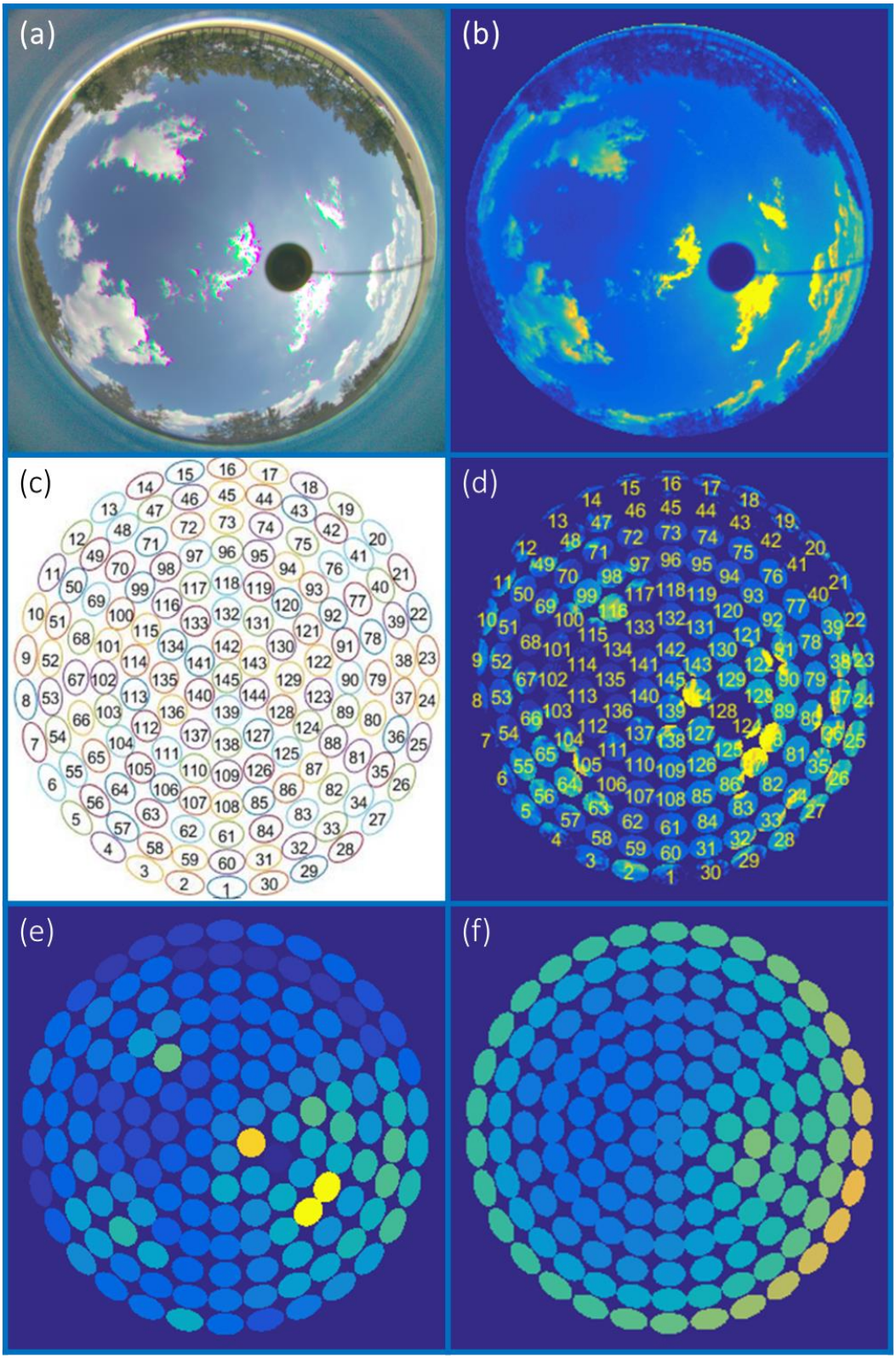

Figure 5-7: Matlab processing of sky data; (a) Original image, (b) Matlab generated aligned and cropped, (c) identify patch size and locations, (d) Isolate luminance data within patches, (e) Average luminance within patches (Measured sky), (f) Average luminance within patches (Simulated sky)

Align image to real world coordinates

The first step is to ensure that the pixel locations on the flat sensor plane can be mapped to the real world. This is done by converting the x,y pixel locations into polar coordinates, then linking these points to the spherical coordinates of the real world using the mapping function of the lens/simulation (Equation 5-1 to Equation 5-5) and correcting for any geometric inconsistencies between the coordinate systems. The rotation, or azimuth, in the 2D and 3D systems are now aligned and the radial distance on the image, r, relates to an elevation of an element of the sky.

Crop data

The relationship established in alignment is used to crop the data to the size of the active area of the image. This follows the process outlined in Section 5.1.1.2 where the size of the active area of the image is calculated using Equation 5-1 (page 116). The maximum value of r is calculated to be 11.3mm at the maximum inclination angle, $\theta = \frac{\pi}{2}$ and the focal length of the lens is 8mm.

Even though there is no stray light from the lens in the simulation, there are a large number of pixels of the sensor with a null value in the data matrix. For this reason, the simulation data is also cropped in this manner, to only show the active pixels and facilitate a simpler comparison. The aligned and cropped data is then exported to text and as an image.

Subdivision of the sky and extraction of mean luminance of sky patch

For each pixel on the active are of the CCD sensor there are data associated with the luminance and colour of the sky, which even cropped, gives over 600,000 data points. To make this more manageable the sky vault is divided into 145 discrete zones following the Tregenza subdivision of the sky (Tregenza, 1987). Each patch subtends to a solid angle of 11° which gives an area of approximately 3000 pixels. The centre location for each patch is given in Appendix B.

5.1.1.2.2 Comparison of sky luminance distributions

Figure 5-8 to Figure 5-10 are the sky luminance distributions extracted from the measurement and simulation data. They present both data sets as a Matlab generated image and a visualisation of the average luminance per sky patch, for the skies corresponding to the sample displays chosen in previous section; #3, #14 & #23.

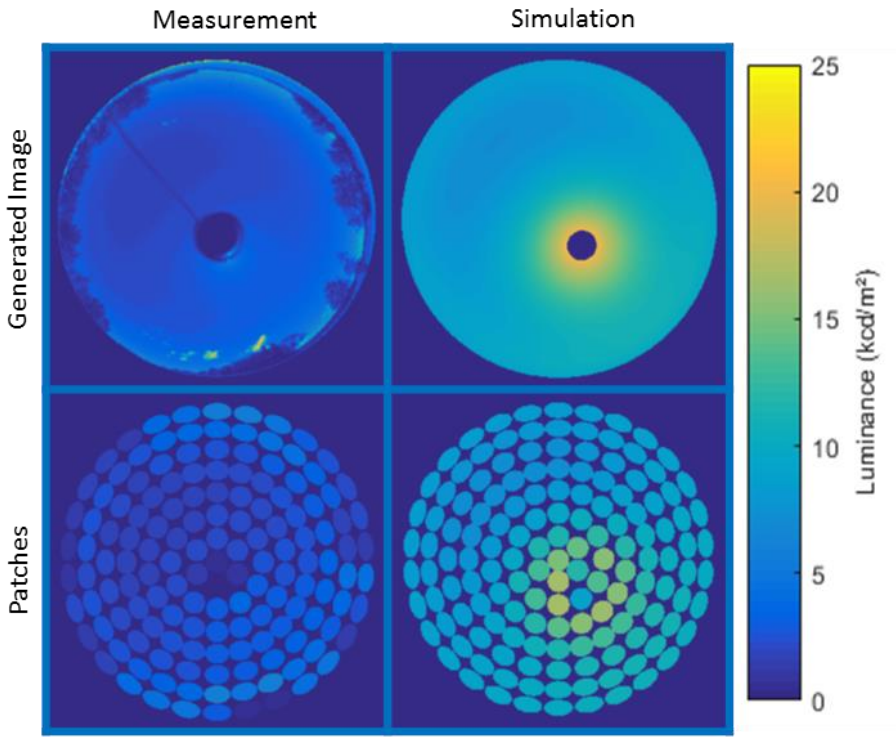

Figure 5-8: Luminance distribution of measured and simulated data (Sky #3)

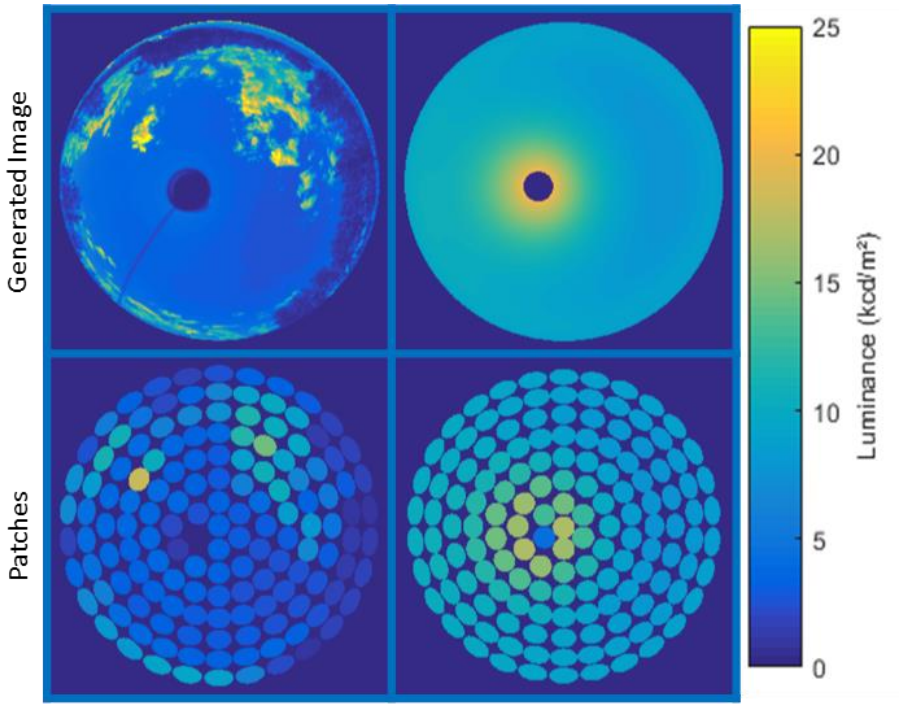

Figure 5-9: Luminance distribution of measured and simulated data (Sky #14)

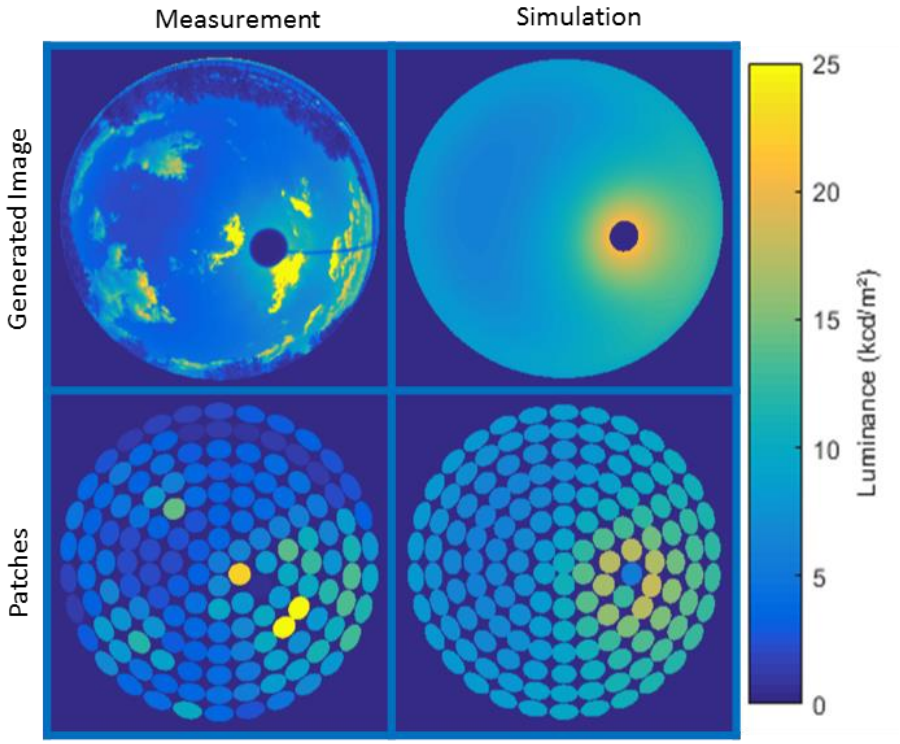

Figure 5-10: Luminance distribution of measured and simulated data (Sky #23)

The images illustrate that in general the simulated skies appear to be brighter than the measured skies. The exceptions are bright patches in the measured skies, due to reflections from clouds which become brighter as the clouds approach the circumsolar region. This is highlighted by the very clear sky condition of Sky #3 in Figure 5-8.

The mean luminance per sky patch is plotted for these skies in Figure 5-11; as a comparison of performance of the simulation, the first row of patches containing trees and obstructions are excluded, as are the patches masked from the sun. Due to variation in the size of the real mask with respect to the simulation, the number of patches excluded is not equal.

From these plots, it appears that the simulations and measurements are very different with the measurements exhibiting fluctuations.

When the luminance distributions are plotted on a $\log_{10}$ scale (Figure 5-12) a common trend becomes evident, especially in the clear sky, #3.

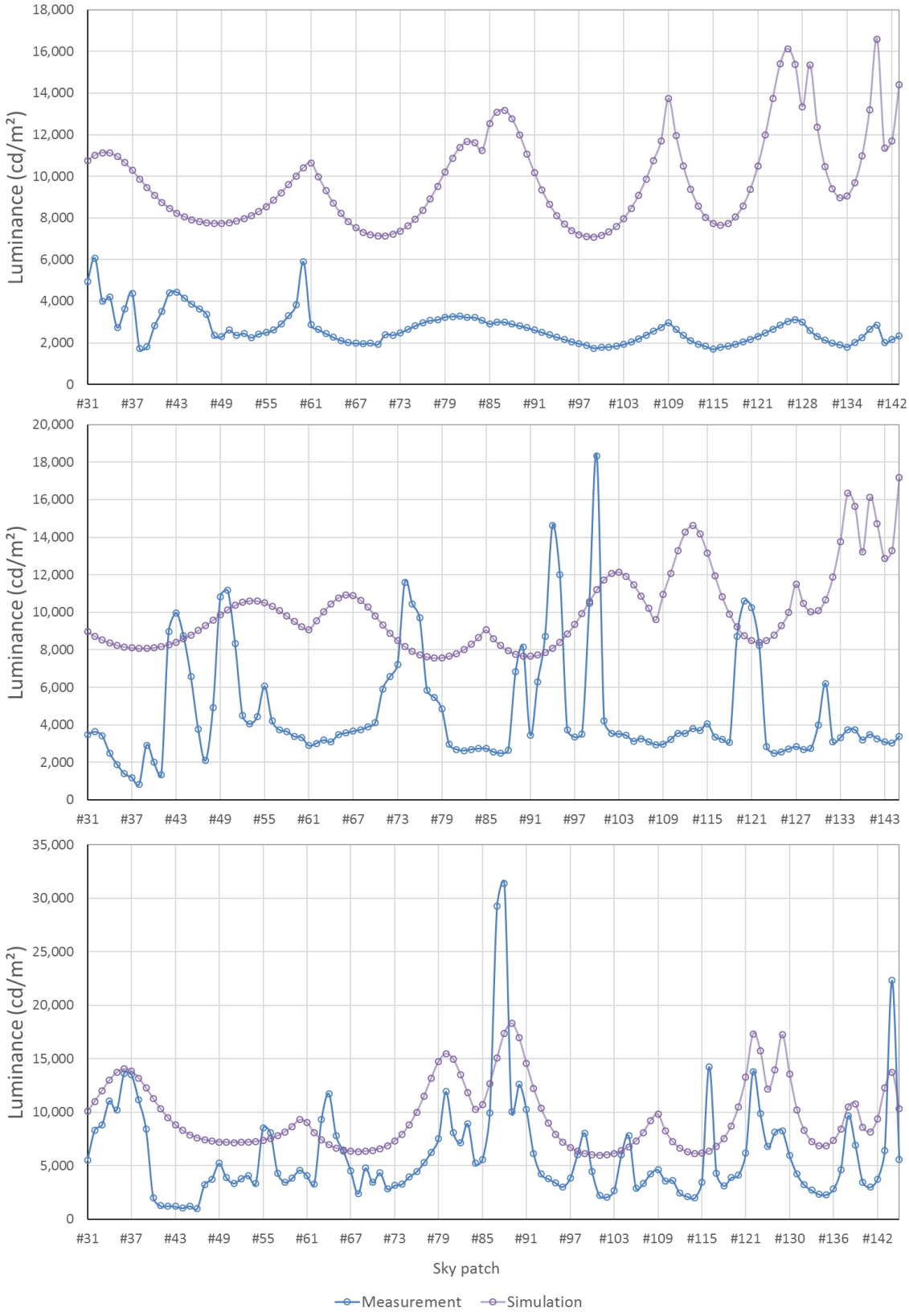

Figure 5-11: Plot of average luminance per patch for measured and simulated data (excluding masked patches); Sky #3 (top), Sky #14 (mid), Sky #23 (bottom)

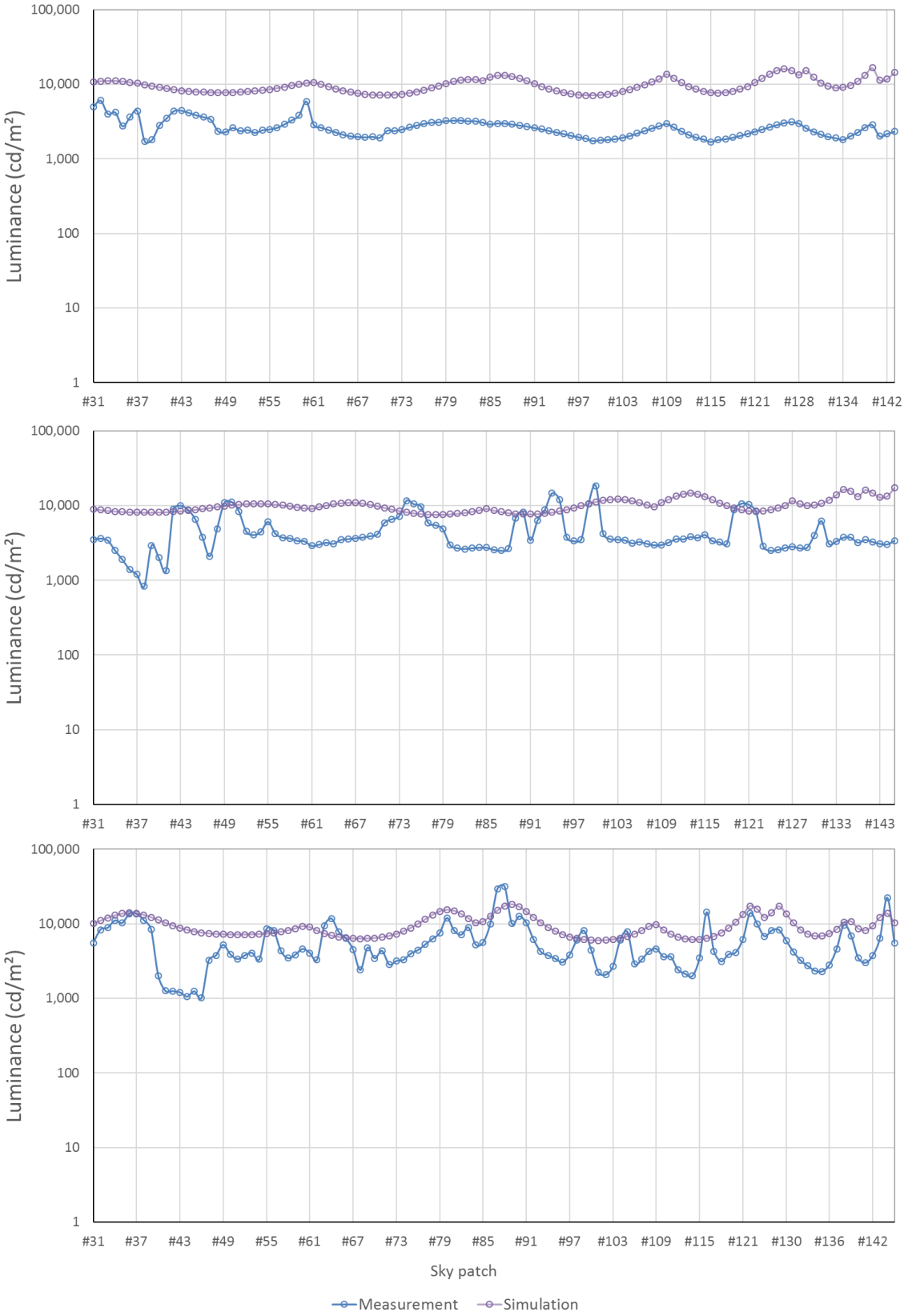

Figure 5-12: $\log_{10}$ plot of average luminance per patch, Sky #3 (top); Sky #14 (mid), Sky #23 (bottom)

The simulated skies follow the profile of the measurements but are of a greater magnitude and are skewed by the peaks in luminance caused by clouds.

The SPEOS generated skies do not appear to be a close approximation of the real skies as demonstrated by the large RMSE and the difference between the mean luminances of the unobscured sky vault (Table 5-2).

Table 5-2: Root mean square error and mean luminance (sky #3, #14 and #23)

Sky #	Mean Luminance (cd/m²) *		RMSE	RMSE
	Measurement	Simulation	(%)	(kcd/m²)
#3	2,678.39	9,788.04	300	7.43
#14	4,731.85	10,039.39	232	6.31
#23	6,081.83	9,586.28	187	5.02

* for all sky patches excluding masked data

From these figures, it would suggest that even with the large gap, the simulation of Sky #23 is closest to the measurement, however the lower RMSE is due to the skew of high luminance clouds, as can be seen by the overlap in profiles in Figure 5-12.

This is trend is consistent across all data points; the mean luminance is overestimated as illustrated in Figure 5-13.

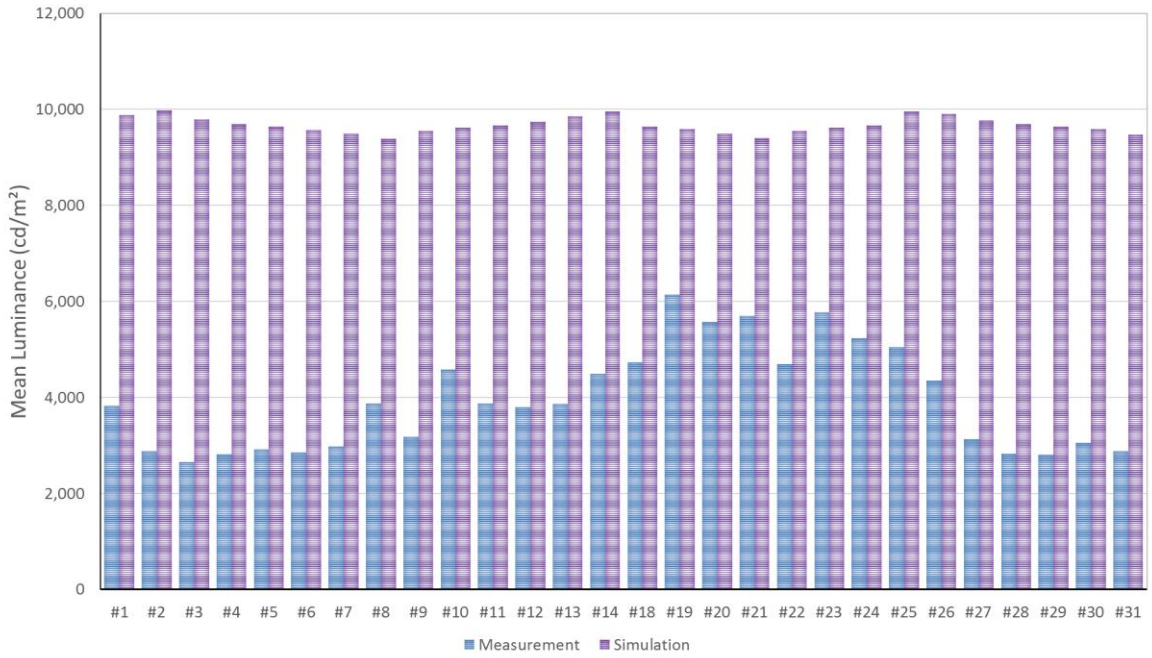

Figure 5-13: Mean luminance of measured and simulated skies excluding obscured sky patches

5.1.1.3 Performance of SPEOS daylight source

The definition of the sun in SPEOS is consistent with the spectral and spatial characteristics of the sun quoted by the literature and international standards for daylight simulators (BSI, 2005; CIE, 2010; DiLaura et al., 2011; Wyszecki and Stiles, 1982), and are comparable in terms of luminance and normal illuminance at the ground.

The SPEOS sky models, however, predict the luminance distributions of the sky to be up to 3.5 times greater than those recorded in Australia. The behaviour of the measurements is consistent the representations of measured luminance distributions from daylight measurement stations as reported by Ferraro et al. (2011). The results of their study reported RMSE values of between 21% and 45% for all sky model and data sets evaluated. This comparison deviates from the Ferraro study as it does not scale the mathematical models to a measured global horizontal illuminance value, and is based solely on a single modelled sky type; does match a specific sky type other than to exclude the measurements where there is a high level of cloud in the circumsolar region that effects the measured illuminance at the ground.

Other studies to compare sky models are for use in software simulations to rate the ability of the program to simulate illuminance. A study by Vezifeh et al. (2015) reports on the limited use of the CIE and Perez all weather models to predict illuminance at a vertical plane and quote RMSE values based on the luminance of model sky patches of 3.54 and 4.32 kcd/m² respectively. This is comparable to the 5.02 kcd/m² RMSE for Sky #23.

Mardaljevic (1999) notes that the models he evaluates do not perform well in terms of matching measured sky distribution yet the RMSE for illuminance in some cases is low enough (<10%) to indicate a good prediction of measured vertical illuminances. This is consistent with the SPEOS generated daylight illuminance; even with a general under estimation, the simulations of horizontal daylight illuminance still give an approximation of the measurements with an RMSE of 12%. This suggests that the daylight model may underestimate the contribution of direct sunlight, and where the sky model over estimates the luminance distribution, the effect on the overall illuminance at the ground is negligible.

5.1.2 Measured display materials properties

It is also possible that the gap between measured and simulated display reflections is due to the definition of material properties in the simulations.

The optical simulations performed at Jaguar Land Rover have an extensive library of material files based on the measured BRDF of a material sample. There are very few material definitions used within the SPEOS simulations that rely on approximations in the form of simple scattering files. One such approximation is the material for the HLDF display surface. In order to establish whether this significantly effects the behaviour of the simulated reflections, a measured sample of a display surface is required to compare to the simulations using the simple scattering material file.

Unfortunately, even though sample displays were available to measure, the equipment for capturing the BRDF properties was not. To test the hypothesis that the application of measured materials would perform better than approximated materials, a comparison is made by performing simulations with a comparable BRDF file and an approximation of this material. The BRDF file was of a Satin Black plastic with a low gloss level and strong Lambertian characteristics. The results from these simulations are presented in Figure 5-14 to Figure 5-17.

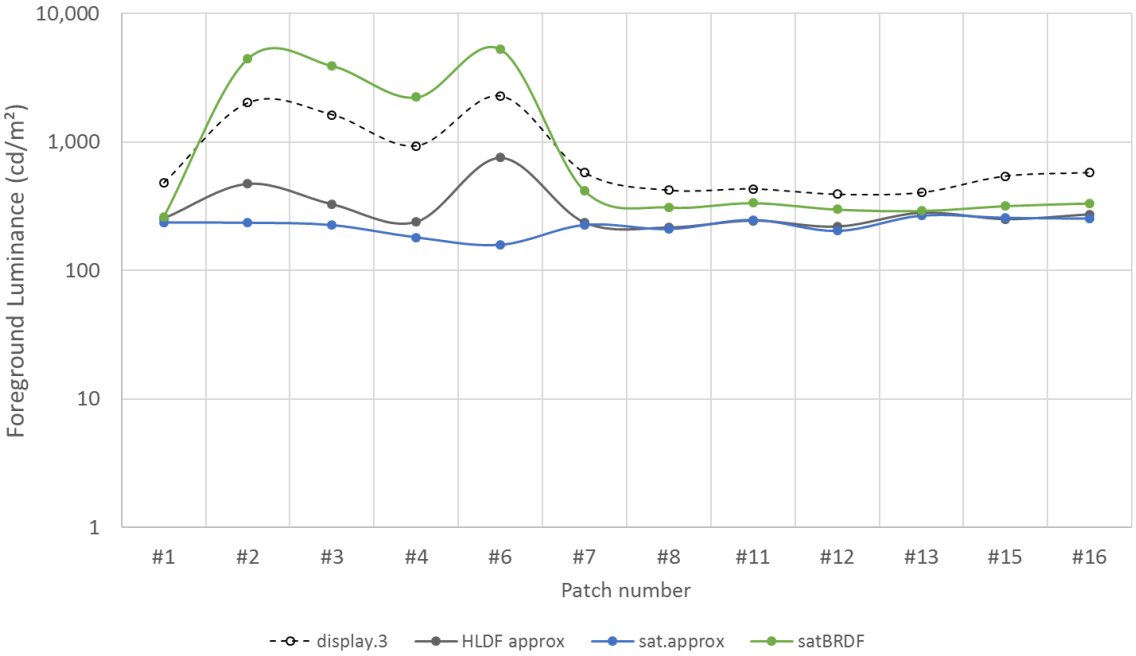

Figure 5-14: Foreground Luminance per sample patch at Display #3 plotted on a log $_{10}$ scale

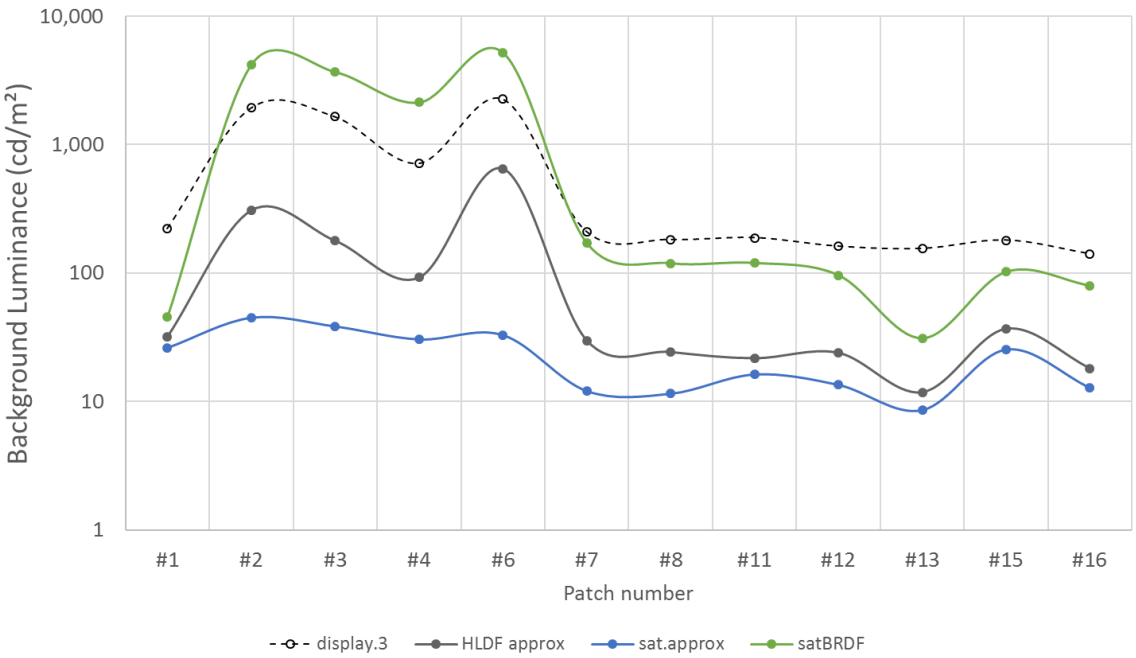

Figure 5-15: Background Luminance per sample patch at Display #3 plotted on a log $_{10}$ scale

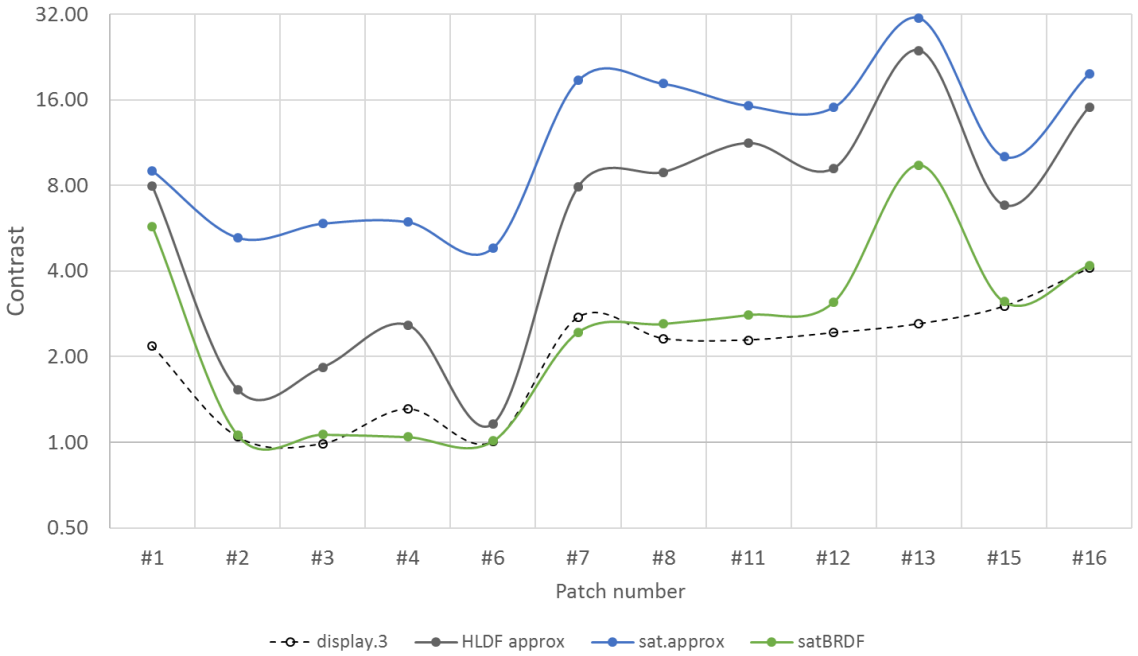

Figure 5-16: Contrast per sample patch at Display #3 plotted on a log_2 scale

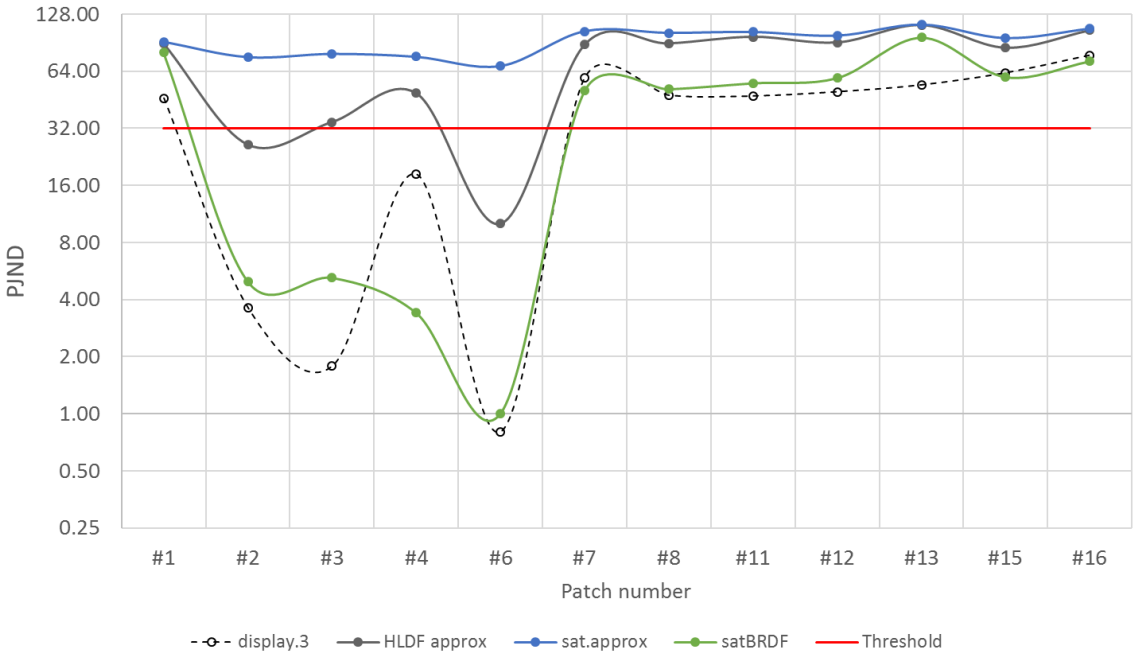

Figure 5-17: PJND per sample patch at Display #3 plotted on a log_2 scale

The BRDF and approximate material appear to follow on either side of the HLDF approx. profile, with the approximation underestimating the reflected luminances and over estimating the performance of the display, demonstrated by the contrast and PJND curves.

The BRDF file performs closer to how the measured display indicates which can be seen from a visual comparison of the simulations (Figure 5-18 and Figure 5-19). The low contrast area on the display is hardly visible on the result of the approximate material and completely illegible on the BRDF result.

Independent-samples t-tests were performed to compare the foreground luminance and the background luminance for the materials. The results suggest that there is a statistically significant difference between the BRDF and the simple-scattering foreground luminance profiles ($t(11) = 2.37$, $p = 0.037$) and the background luminance profiles ($t(11) = 2.33$, $p = 0.04$).

The difference between the behaviour of the two material files suggests that the type of material characterisation used will significantly impact the results of the simulation.

Figure 5-18: Simulation Display #3 using measured BRDF of a Satin Black material

Figure 5-19: Simulation of Display #3 using simple scattering file of Satin Black material

5.1.3 Simulation adjustments

To attempt to close the digital simulation gaps identified, modifications are made to the simulations in areas that allow user adjustment without the need for intervention from the software developers to enable short-term improvements. The main gap is seen as underestimation of the reflections in the foreground and background luminance of the display, therefore the overall luminance of the simulation is adjusted by changing the sky definition and altering the luminance levels of all sources in the simulation in post processing.

5.1.3.1 Changing the sky definition

The SPEOS *sky type* is defined by a mathematical model to several options including CIE standard general skies, uniform luminance or a natural sky which is defined by the atmospheric parameter of *turbidity*. The turbidity is a simplified measure of the 'haziness' of the sky caused by particles of various size in the atmosphere and is a ratio of "*the optical thickness of the haze atmosphere (haze and molecules) to the optical thickness of the atmosphere with molecules alone*" and can be estimated based on the contrast of distant objects against the background of the sky. Figure 5-20 shows the relationship between Meteorological range (distance at which target contrast tends to the threshold contrast of the observer) and turbidity (Preetham et al., 1999).

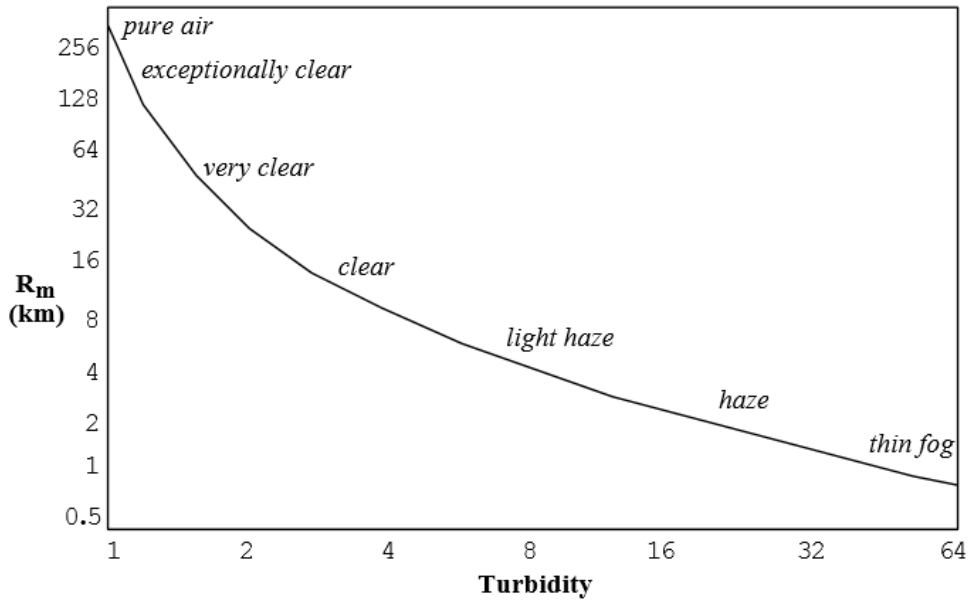

Figure 5-20: Meteorological range vs turbidity (Preetham et al., 1999)

The standard simulations were run with a sky turbidity of 2, giving a very clear sky. To determine whether the sky type will affect the outcome of the display simulations, two further sets of simulations were run with skies of a turbidity of 4 and 6, which are still clear skies but approaching a light haze. The results of these simulations for display #3 is presented in Figure 5-21 to illustrate the difference between the effects of different turbidity in simulated skies.

(a) Measurement #3 (PASS_1358.bmp)

(b) Simulation with a sky turbidity of 2

(c) Simulation with a sky turbidity of 4

(d) Simulation with a sky turbidity of 6

Figure 5-21: Measurement and simulations of display #3

The clearer skies (turbidity of 2) give a crisper definition to the edge of the shadow and also appear to have the most legible areas within these shaded regions. The higher turbidity simulation, tends to have softer edges to shadows and a perception of lower contrast across the shaded regions. From the images alone it cannot be seen if the sky definition is a significant factor in simulating in-vehicle displays, therefore the foreground and background luminance values for display #3, #14 and #23 are sampled as detailed in the previous section and plotted below in Figure 5-22 and Figure 5-23.

In general, the profiles of the different sky types appear to follow each other closely with greater deviation in the background luminance. The performance of each model, indicated by the RMSE (Table 5-3) does not seem to be very different from each other.

Table 5-3: Root mean square error for different sky turbidity models (Display #3, #14 and #23)

Display #	Sky turbidity	RMSE	
		Foreground profile	Background profile
#3	2	58%	85%
	4	57%	83%
	6	56%	80%
#14	2	45%	45%
	4	42%	42%
	6	38%	38%
#23	2	70%	70%
	4	70%	70%
	6	71%	71%

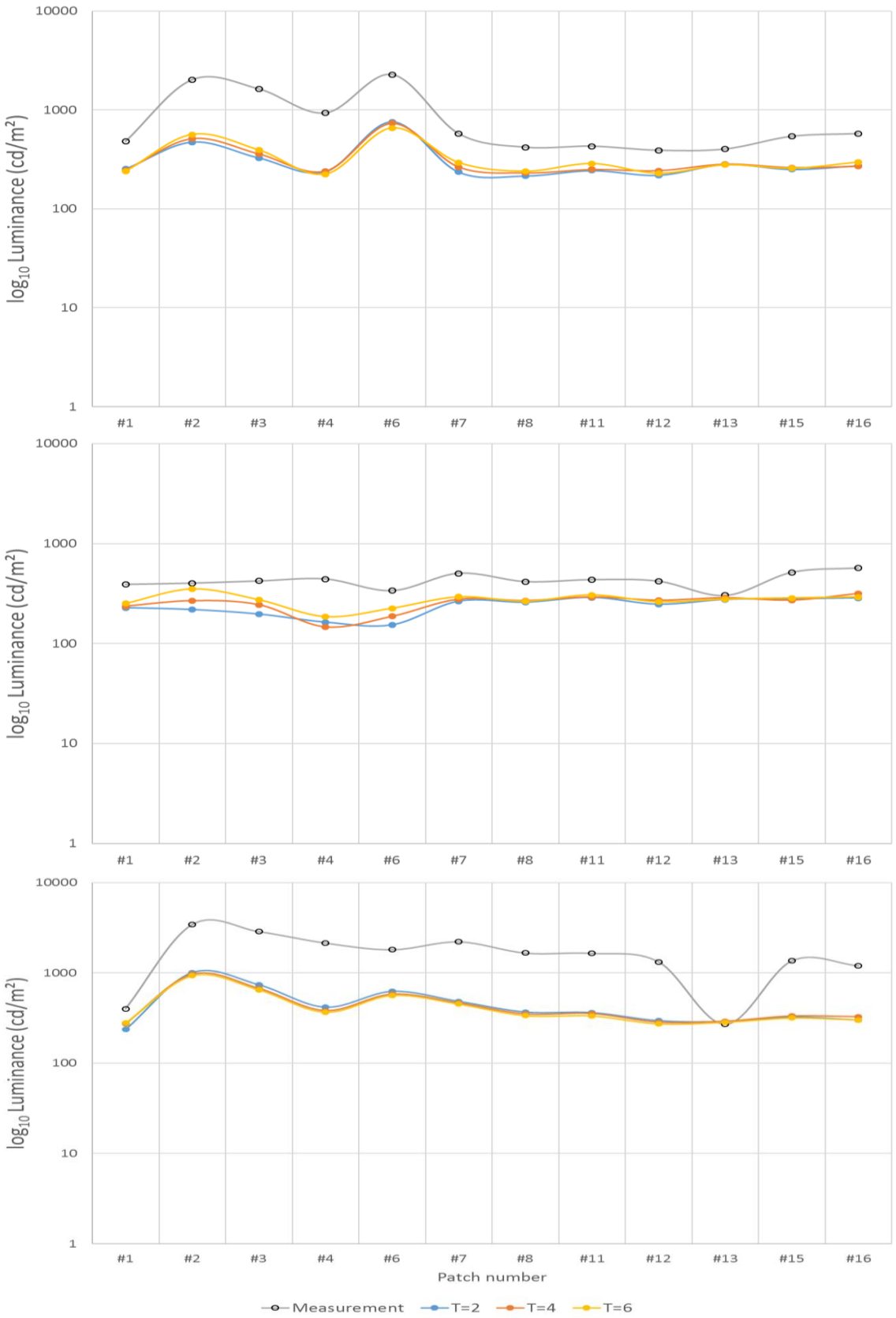

Figure 5-22: Foreground Luminance per patch at Display #3 (top), #14 (mid) & #23 (bottom) plotted on a $\log_{10}$ scale

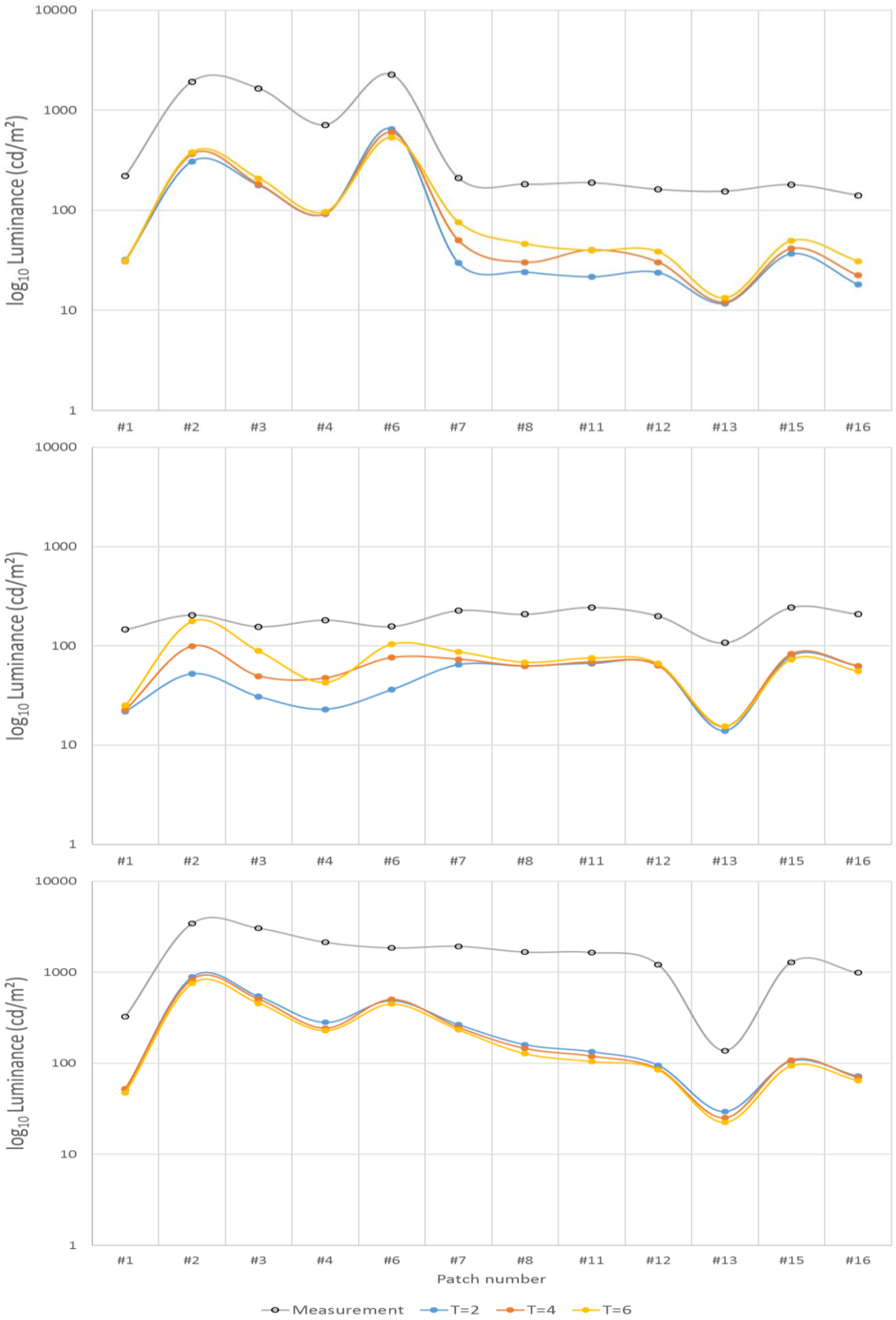

Figure 5-23: Background Luminance per patch at Display #3 (top), #14 (mid) & #23 (bottom) plotted on a log $_{10}$ scale

A test for equal variance confirm that variances could assumed to be equal (see Appendix C for more detail) and one-way ANOVA of all data points was used to compare the effect of the different sky models on the display luminance. There is not a statistically significant difference in the effects of the different turbidity models on the simulated display reflections indicated by foreground ($F(2, 1113) = 0.38$, $p = 0.686$) and background display luminance ($F(2,1113) = 0.55$, $p= 0.575$). This suggests that the sky model used is not the factor of greatest impact on display reflections.

5.1.3.2 Post processing

The results of the SPEOS simulations have several post processing operations that can be performed. This allows for lighting conditions to be assessed or adjusted without the need for re-running simulations. For this assessment, the processes applied to the light sources present in the simulation results, involved increasing the luminance of a combination of the sky, display and an additional sun (no sky). These combinations, detailed in Table 5-4, are applied to Display #3 to observe the effect on the display reflections. The performance of the adjustments can be seen from the RMSE of the foreground and background luminance, plotted in Figure 5-24 and Figure 5-25.

Table 5-4: post processing operations applied to simulation results of Display #3

Condition	100%	200%	400%	600%	800%	1000%
Increase sky luminance (HLDF at 100%, no additional sun)	T2	a	b	c	d	e
Increase sky luminance (HLDF at 200%, no additional sun)	f	g	h	i	j	k
Increase sky luminance (HLDF at 100%, additional sun at 100%)	T2+sun	l	m	n	o	p
Increase sky luminance (HLDF at 200%, additional sun at 100%)		q	r	s	t	u
Increase sky luminance (HLDF at 100%, additional sun at 200%)		v	w	x	y	z
Increase sky luminance (HLDF at 200%, additional sun at 200%)		aa	ab	ac	ad	ae
Increase luminance of additional sun (HLDF at 100%, sky at 100%)		af	ag	ah	ai	aj
Increase luminance of additional sun (HLDF at 100%, sky at 200%)			ak	al	am	an
Increase luminance of additional sun (HLDF at 200%, sky at 200%)			ao	ap	aq	ar

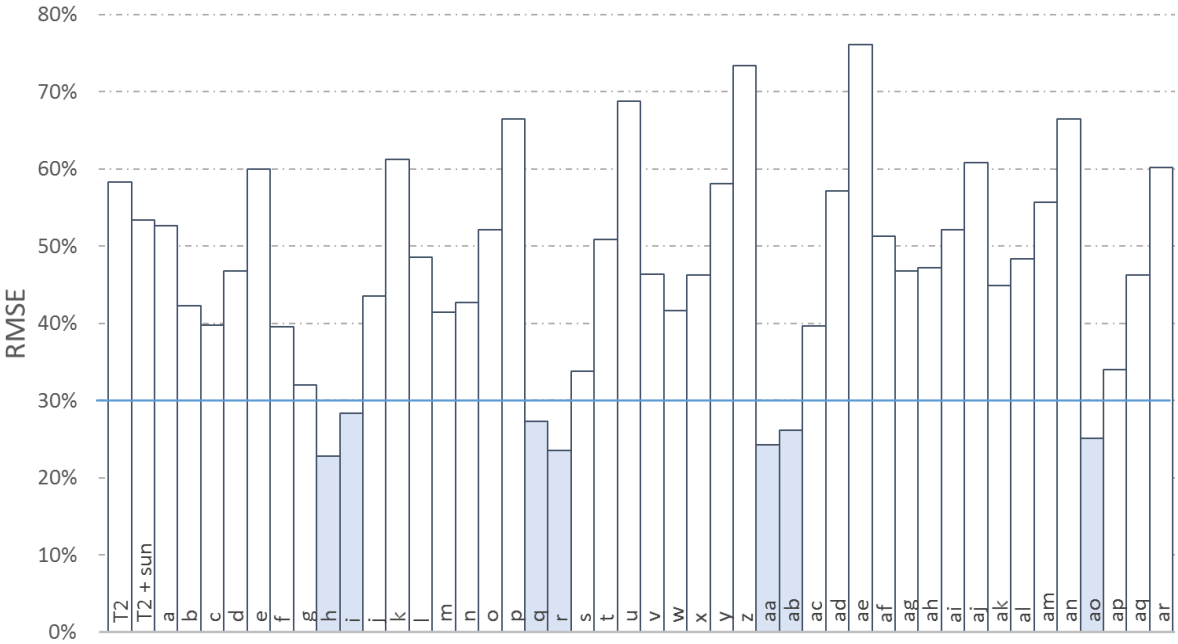

Figure 5-24: Foreground luminance RMSE of post-processes – blue highlights values below 30%

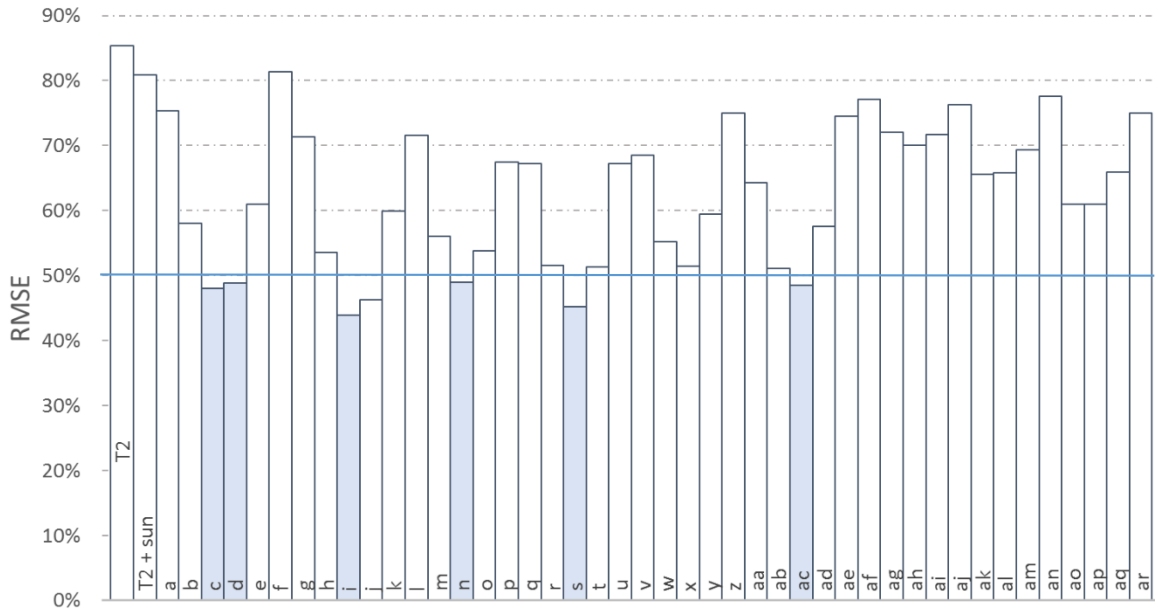

Figure 5-25: Background luminance RMSE of post-processes – blue highlights values below 50%

The additional sun appears to slightly improve performance of the model (T2+sun) whereas some of the operations are detrimental to performance (e.g. 1000% increase in luminance). The operations that appear to improve performance the most fall below and RMSE of 30% for foreground luminance (Figure 5-26) and 50% for background luminance (Figure 5-27).

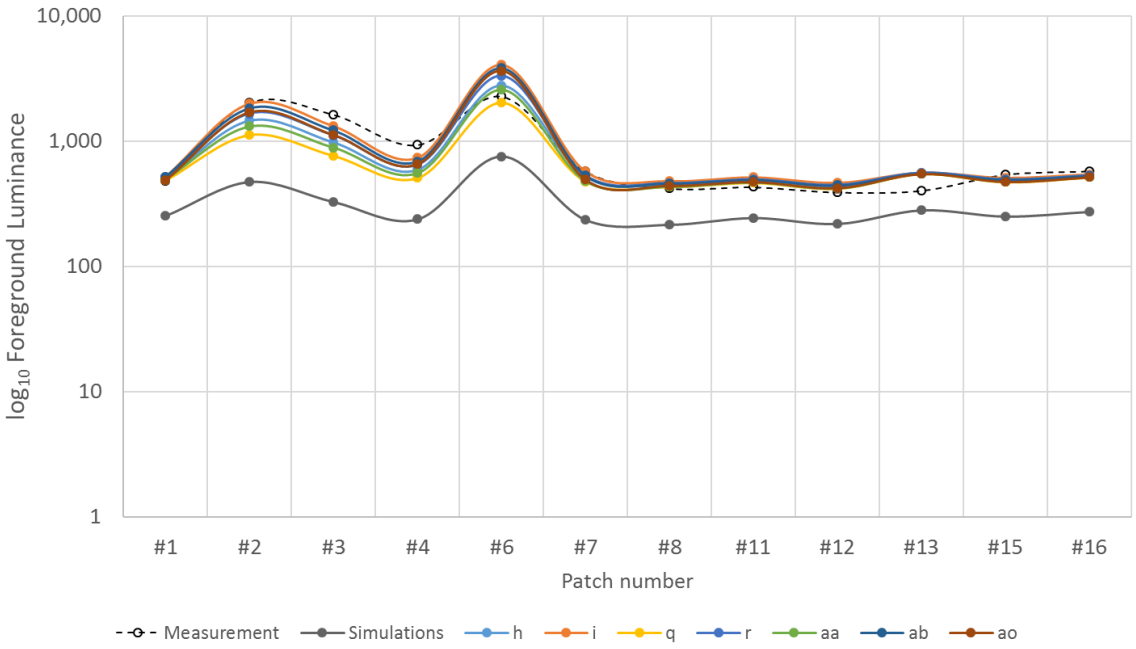

Figure 5-26: Foreground luminance of post-processes below 30% RMSE

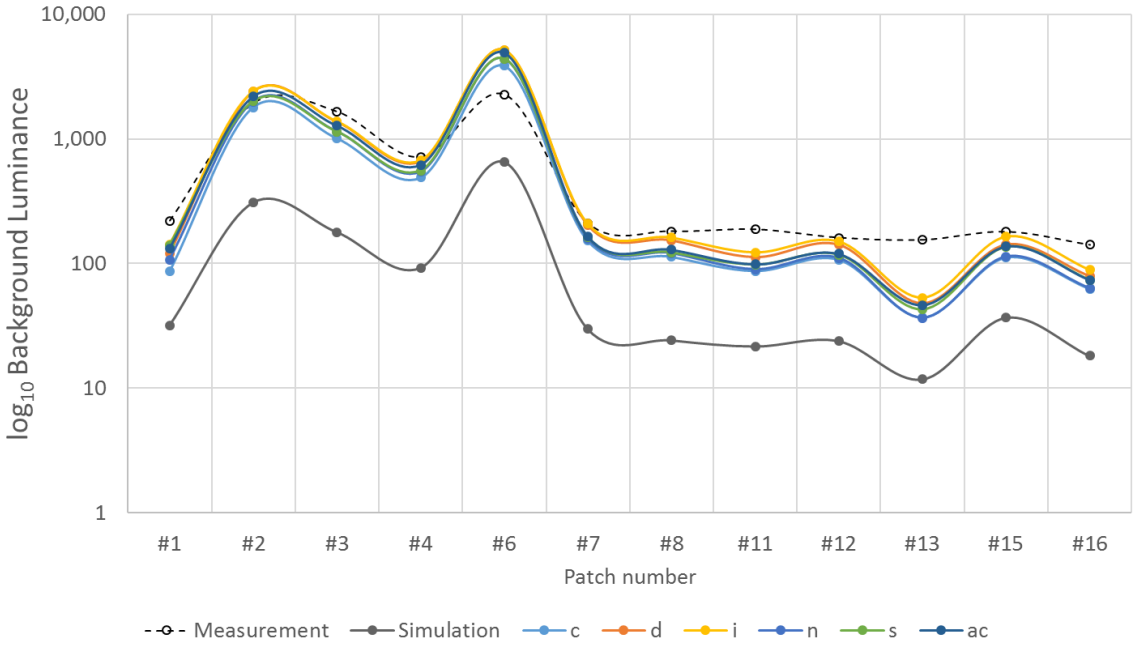

Figure 5-27: Background luminance of post-processes below 50% RMSE

Each of these post-processing operations brings the result closer to the measured data points. However, only process *i* falls into the group of best performing for both foreground and background luminance. This suggests that this process is the best adjustment to apply, which is further supported by the plot for PJND, where process *i* is one of the only profiles to achieve the pass fail criteria (see Figure 5-28).

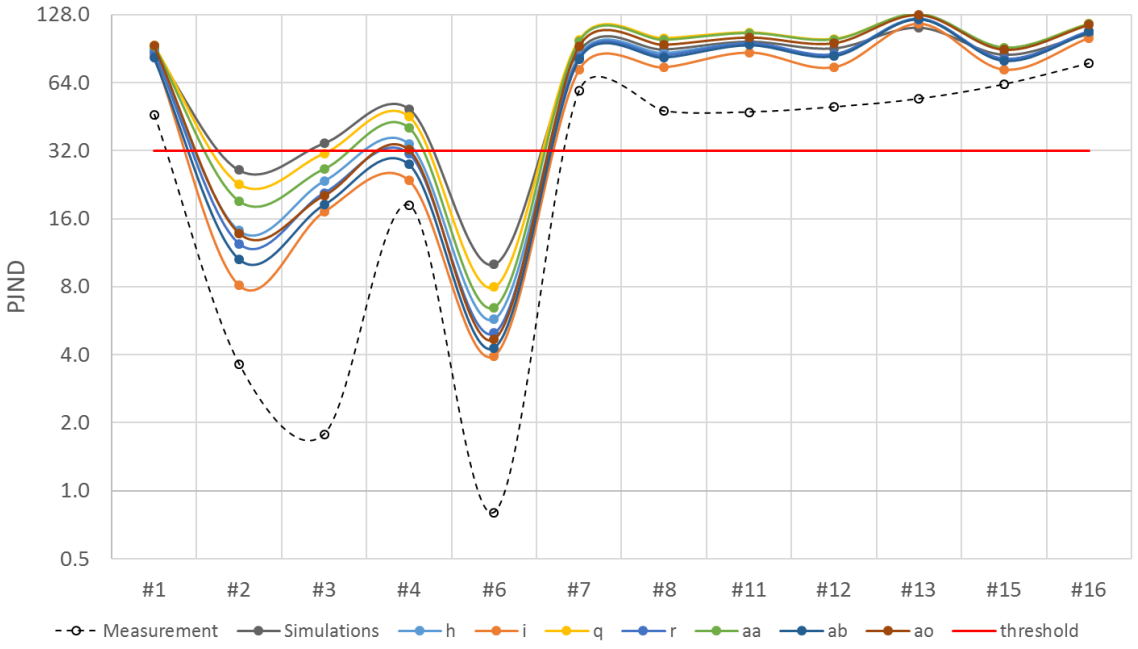

Figure 5-28: PJND for post-processes with RMSE <30% for foreground luminance

5.2 PHYSICAL EVALUATIONS

To close the gap in the current methods of physical evaluations of displays requires increased control in measurement geometry and a method to generate a stable lighting environment comparable to natural daylight.

5.2.1 Controlled environment

The controlled environment required for performing vehicle interior evaluations is a stable lighting environment comparable to natural daylight. The focus of automotive assessments has been on the direction and intensity of the sun lamp as the main source of glare and reflections at the display surface. However, the contribution of the diffuse light from the sky and the inter-reflections of light from all directions within the vehicle needs to be considered to achieve a more realistic lighting environment. Therefore, both a diffuse and direct component of daylight are required to be recreated.

The current method for creating the diffuse component involves illumiating diffuse screens with a minimum of 3 daylight simulator lamps yet the diffuser characteristics, size, number and location of these screens are unspecified. This does not create a stable reproducable environment.

Daylight enters the vehicle cockpit from all around, therefore to perform illumination evaluations within a vehicle, a fully immersive environment is required to allow for daylight from all directions. There are a number of methods available that can be employed for this purpose, as demonstrated by Table 5-5**Error! Reference source not found.**.

Table 5-5: Sky simulation methods

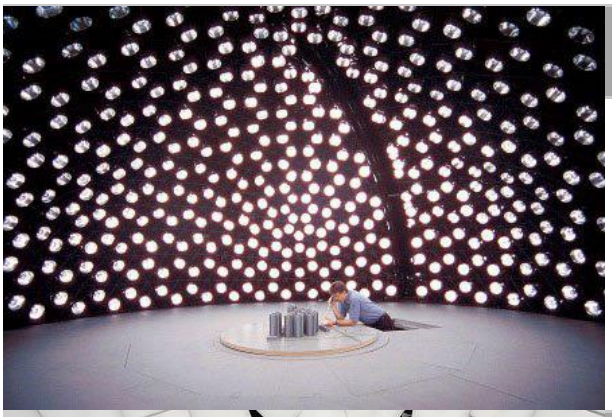	**Point source simulator** A complex array of individually addressible light sources which can recreate measured or modelled luminance distributions of the sky. This a is high maintence and expensive method, with high build cost and power consumption. It is however, the most faithful representation of sky light. This method would be more complex and evern more expensive to expand to the size necessary for an automotive application.
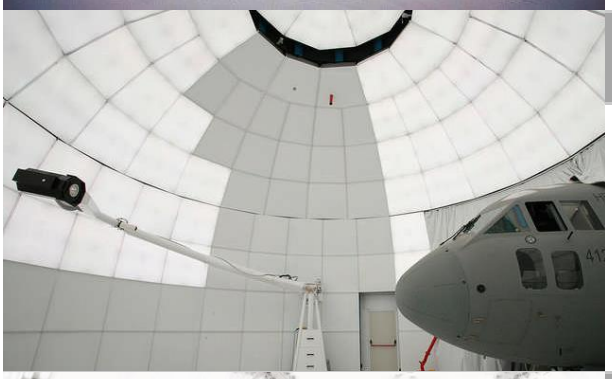	**Lumious panels** This simulator at Alenia Aeronautica, consists of 79 lumious panels and 112 reflective panels. Similar to a point source simulator, it can create lumiance distributions although to a less degree due to the lower number of addressable areas, but both build and maintenance costs will be lower.
	**Sky dome** A dome with a diffuse surface, lit either from the outside or from below. Is simpler in construction than the point source and lumious panel skies but does not have their control over distrubution.
	**Diffuse room** As with the sky dome, these simulators are diffuse surfaces lit from below but are generally a circular room and a domed ceiling to avoid shadow patches, rather than a dome. They can had a perimeter of lights at the floor or ceiling or a combination of the two. They are low maintenance with relatively low running and setup costs.

These types of facilities can be expensive and complex, especially those with a greater accuracy to real daylight. Darula & Kittler (2015) argue that artificial sky simulators are worth the high cost as they are capable of creating any daylight scenario and allow the assessment of interreflections of different materials and technologies. They do not support the use of computer simulation as an alternative, suggesting that current software is incapable of simulating complex geometric scenarios and fails to consider interreflections of interior and exterior surfaces. This assertion is contrary to the experience of even advocates of artificial skies, who acknowledge the accuracy of computer simulation tools but believe that this method lacks the subjective qualities of light interacting in a space (Bodart et al., 2008; Raynham, 2006). As with any mathematical modelling, the accuracy of digital simulations depends on the quality of the algorithms used in the program.

There are errors inherent to artificial sky measurements due to either too much or too little light reaching the interior surfaces (see Submission #1), limiting the validity of quantitative evaluations. Trying to mitigate or eliminate these errors can make the use of these simulators impractical and/or expensive. Mardaljevic (2006, 2003, 2002) questions the practicality of using artificial skies other than to perform validation exercises whereby the software predicts the performance of the artificial sky condition rather than the simulator predicting a real sky as digital simulations are a truer representation of daylight and can simulate a wider range of scenarios than physical simulations.

Real sky light has a variable, non-uniform luminance distribution however, the analysis of the simulations in which the sky type is adjusted, suggests that the distribution and turbidity of the sky has little effect at the display surface within the vehicle. Therefore, the subtle effect of the distribution of sky luminance, which is an important factor in the availability of daylight within a room, is negligible in this context.

This supports the use of a simpler sky dome or diffuse room. Although, care must be taken in the design to ensure that either a uniform lumiance is achieved or that the distribution pattern from the lamps is smooth and consitant in all directions. A simplified model would still be subject to errors, however the geometry and lighting levels would provide the

control required to be replicated digitally. Figure 5-29 identifies the critical features to include in a controlled daylight environment.

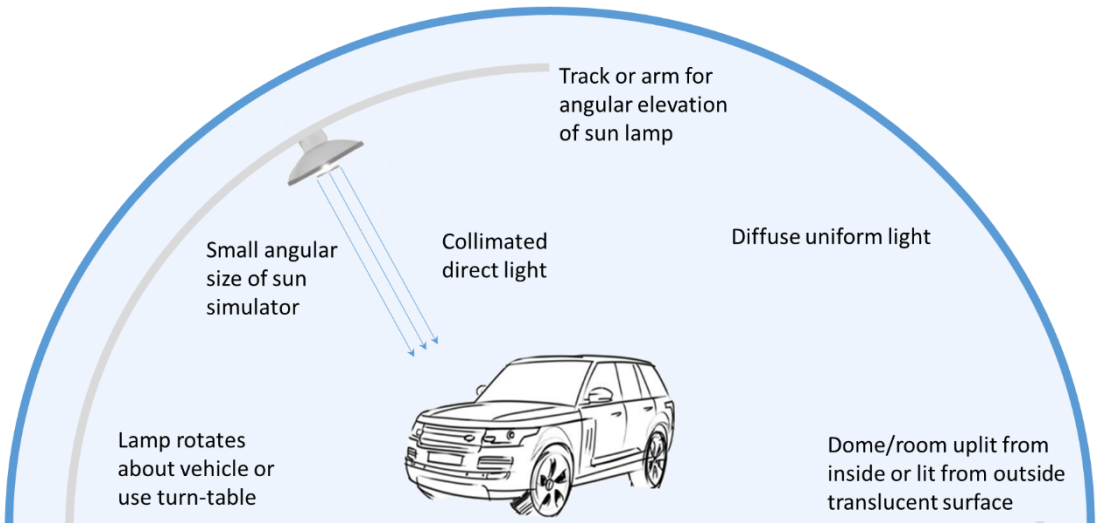

Figure 5-29: Artificial representation of daylight geometry

The 'direct sun' component of collimated light will need to be recreated with a sun simulator to control the position of the directional light with respect to the vehicle. As highlighted in Section 2.2.2.2 and Section 4.1.2, the use of a tripod as a means of support does not enable the lamp to be positioned precisely for a given sun direction in terms of angular elevation and rotation. The azimuth, or rotation angle with respect to the vehide can be achieved by either moving the lamp around the vehicle or rotating the vehicle on a turn-table.

To provide the elevation angle, a curved arm or track is required that will allow the lamp to travel in an arc at a fixed distance from the vehicle. The distance of the sun lamp from the vehicle will influence the angular size of the sun, the area of light coverage and the illuminance in this zone.

Based on the assessment in Section #4, the criteria critical to generating daylight comparable illumination for a controlled assessment environment are outlined in Table 5-6.

Table 5-6: Requirements for artificial daylight sources (based on measurements and specifications (BSI, 2011, 2005, 1967, CIE, 2010, 2009, 2004)*)*

Characteristic	Daylight	Sun light	Sky light
SPD	A close approximation of D65 illuminant CIE 19-2, to within 20% of that specified by CIE 85 Table 4. The SPD of D65 takes priority over CCT.	Corresponding to CCT	Corresponding to CCT
Illuminance	5 to 120 klux	70 to 120 klux	5 to 10 klux
CCT	6,500 K (average)	5,000 to 6,000 K [1]	11,500 to 21,500 K [1]
Chromaticity	Corresponding to D65 source; falls within ellipse specified by BS 950-1:1967	-	-
Beam angle	-	Parallel beam (~0.5°)	-
Apparent diameter	-	As small as possible (0.5°)	-

In order to select daylight sources to simulate diffuse light and direct light, a method is required to evaluate the capabilities of the source with respect to these characteristics. Therefore, each criterion has been given a weighting factor to reflect the importance of the characteristic of the lamp to meet the requirements. *'Must have'* requirements will be weighted as *nine* or *ten*, *'highly desirable'* features are weighted between *six* and *eight,* and *'nice to have'* features have been weighted at *four* or lower. The weighting of *five* has been avoided to minimise non-decisive scoring.

Each criterion will then be given an impact score of 0, 4, 7 or 10, with 0 being complete compliance or an excellent solution, and 10 being non-compliance or a poor solution.

Table 5-7**Error! Reference source not found.** outlines the characteristics to be evaluated, the weighting factors and a guide to selecting the impact scores.

[1] Range based on measured CCT and illuminance and calculated to give average daylight CCT of 6,500 K using method from Kelley et al. (2006) (see Appendix D.1)

Table 5-7: Daylight source evaluation guide

Characteristic	Weight	Description	Scoring
Illuminance	10	The levels of illuminance are critical to evaluating displays under high ambient conditions. This criterion is weighted at (10) to reflect its importance to the expected outcome of each assessment	0 = Source can achieve specified levels of illuminance 10 = Does not achieve the levels required
Spectral power distribution	9	It is important for the selected source to be able to represent average daylight levels of lighting, especially when it comes to rendering colours. Any peaks to the spectrum could result in deviation in perceived colour and relative brightness of a component under test. This criterion is weighted at (9) to reflect its importance to the expected outcome of each assessment	0 = Closely follows the D65 curve in the visible spectrum 4 = Gives a good approximation of a D65 illuminant in the visible spectrum 7 = Could be considered D65 but with a number peaks at various wavelengths 10 = Does not follow the D65 spectrum
CCT	7	The CCT of the sources selected are important when used in evaluations of colour displays. However, a weighting factor of (7) is assigned to reflect its lower importance relative to that of the spectra of the light source.	0 = is equal to CCT specified 4 = is close to specified CCT 7 = is CCT of daylight illuminant 10 = does not represent CCT of daylight
Chromaticity	4	The specified tolerance gives the chromaticities that are close to the CCT of the D65 illuminant. This criterion is assigned a weight of (4) to indicate that if the CCT and SPD are achieved then the chromaticity is of lower importance as daylight has a wide range of chromaticities and CCTs.	0 = falls within tolerance ellipse 4 = is outside tolerance 7 = is outside tolerance ellipse but is close to Planckian locus 10 = is outside tolerance
Beam angle (direct source luminaire)	8	A weight of (8) is given to this criterion to indicate that the beam angle of direct light needs to be as close to parallel as possible to represent the 0.5° beams of direct sunlight.	0 = Collimated light 4 = Spot light with narrow beam less than 3° 7 = Spot light with narrow beam greater than 3° 10 = Flood light with wide beam
Source size (direct source)	8	The size of source is compromise between illuminance and distance from the display. This criterion has been weighted as (8) due to the desire to achieve the apparent diameter of the sun but the need for flexibility.	0 = is equal to 0.5° 4 = is close to 0.5° 7 = is small<5° 10 = is large >5°

This table lists the functional criteria of a light source to recreate daylight levels for vehide interior evaluations. It is not an exhaustive list, as there are other factors important for consideration in design (such as uniformity over time, cost, lamp life, lead time etc.) that will need to be defined as part of the scope for a controlled lighting environment.

This scoring system can be used to select sources that will give the best solution depending on the functional and operational constraints which has been applied to a decision matrix**Error! Reference source not found.**.

Table 5-8: Light source selection matrix

		1 [lamp description – option 1]		2 [lamp description – option 2]		3 [lamp description – option 3]		4 [lamp description – option 4]	
Factor	Weight	Impact	Total	Impact	Total	Impact	Total	Impact	Total
SPD	9								
Illuminance	10								
CCT	7								
Chromaticity	4								
Beam angle	8								
Source size	8								
Uniformity of batch									
Uniformity over time									
Lamp life									
Disposal									
Maintenance requirements									
Power requirements									
Unit cost									
Order quantities									
NRE Cost									
Lead Time									
	Total	**xx**		**x**		**xxxx**		**xxx**	
	Place*	**2nd**		**1st**		**4th**		**3rd**	

Definitions

Impact (0 - 10) The deviation from specification

Weight (0 - 10) Likelihood of deviation from specification impacting daylight assessments

**Lowest score wins*

5.2.2 Controlled measurement

To address the need for controlled measurement, a design specification was drafted to guide the development of a photometer mounting system for use in in-vehicle display measurements. The scope of the specification was to define the necessary functionality of the system without prescribing how this functionality would be achieved. The purpose of the mounting system was to:

a. to make the test geometry consistent and repeatable
b. to reduce the time required to set up the test
c. to allow the camera to move to different 'head' positions for different views of the car interior (e.g. display screen, centre stack, door etc.)

The specification outlined the functional and environmental operating requirements of the system as well as the system interface for use in a vehicle.

As summary of the requirements are detailed in Table 5-9.

Table 5-9: Basic requirements for photometer mounting system

Performance specifications	Interface specifications
Installed without damage to surface or structure, and without removal of vehicle architecture	Interface to PM1600F photometer (size, weight and mounting positions) and clearance from fan
Camera position once set, not to be interfered with	Working distance of photometer and alignment tolerance
To be adjustable and allow inboard movement and alignment to measurement geometry	Adjustment in XYZ, pan and tilt and along camera axis to set working distance
Include measurement system to facilitate alignment	To fit within vehicle cockpit
Simple assembly by one person	

The specification was reviewed by three engineers from JLR and WMG, and modified to reflect their comments. This specification was then used to guide the development of a mounting concept for the photometer. Development of the system was first attempted by offering the problem as an MSc project at WMG however there was no useful solution that

could be taken forward. The concept development was finally facilitated through collaboration with two CAD engineers at different stages of the design.

Integral to the design from the beginning are the automated positioning controls, in the form of a motorised drive tower from Bosch Rexroth (Figure 5-30), supplying the adjustment in the Z direction. Fine adjustments in X and Y supplied by slide rails and a pan-tilt head were then established as shown in Figure 5-31.

Development of the vehicle interface (Figure 5-32) started as an integrated storage case, however difficulties with removing the influence of the seat compressibility moved to a simpler 'cage-like' concept which mounts from hard-points in the floor.

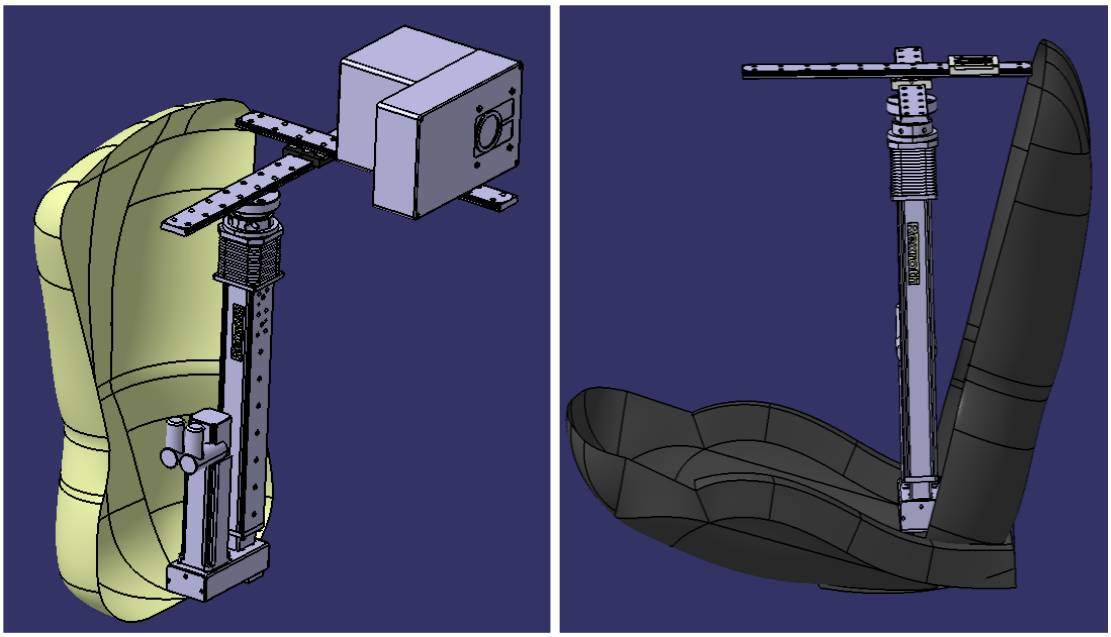

Figure 5-30: Automated positioning tower integral to design early in development

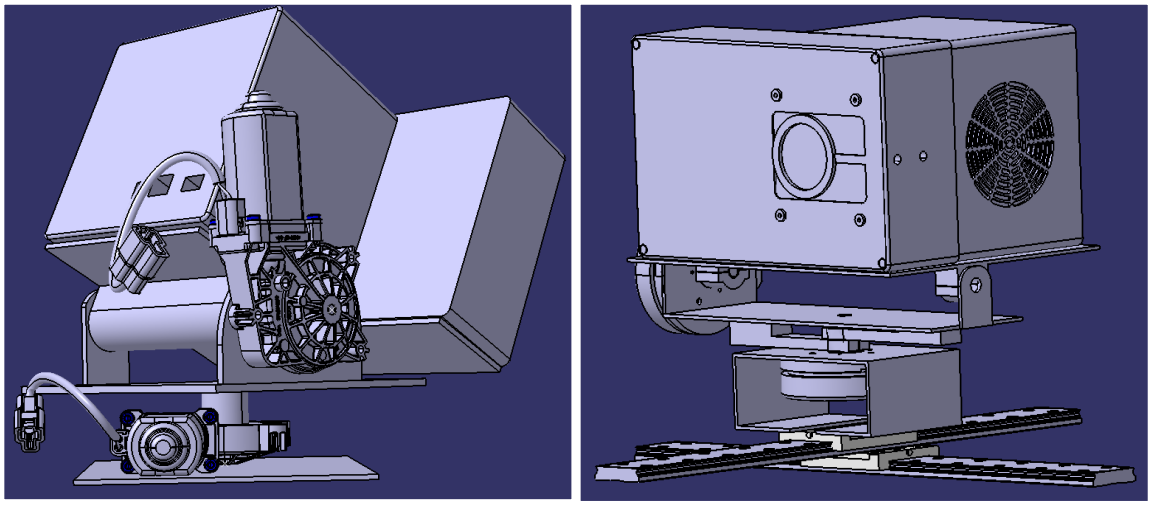

Figure 5-31: Motorised pan-tilt adjustment concepts; compact motors with rail & slider adjustment developed (right)

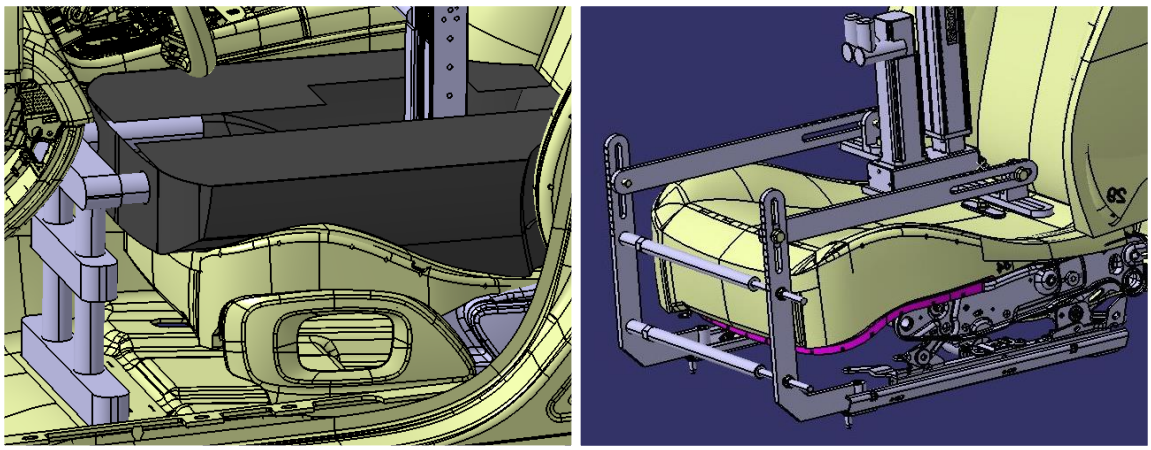

Figure 5-32: Interface options; contour seat base with stabilising strut (left) and rail mounted cradle (right)

The concept passed on to JLR (Figure 5-33) is a system consisting of two sub-assemblies; the seat cradle (blue) and the tower assembly (red).

The cradle is a mechanical assembly consisting of manufactured parts and the tower assembly is constructed from bought-in electronic control items from Bosch Rexroth. A full set of drawings and bought-in part numbers have been passed on to Jaguar Land Rover.

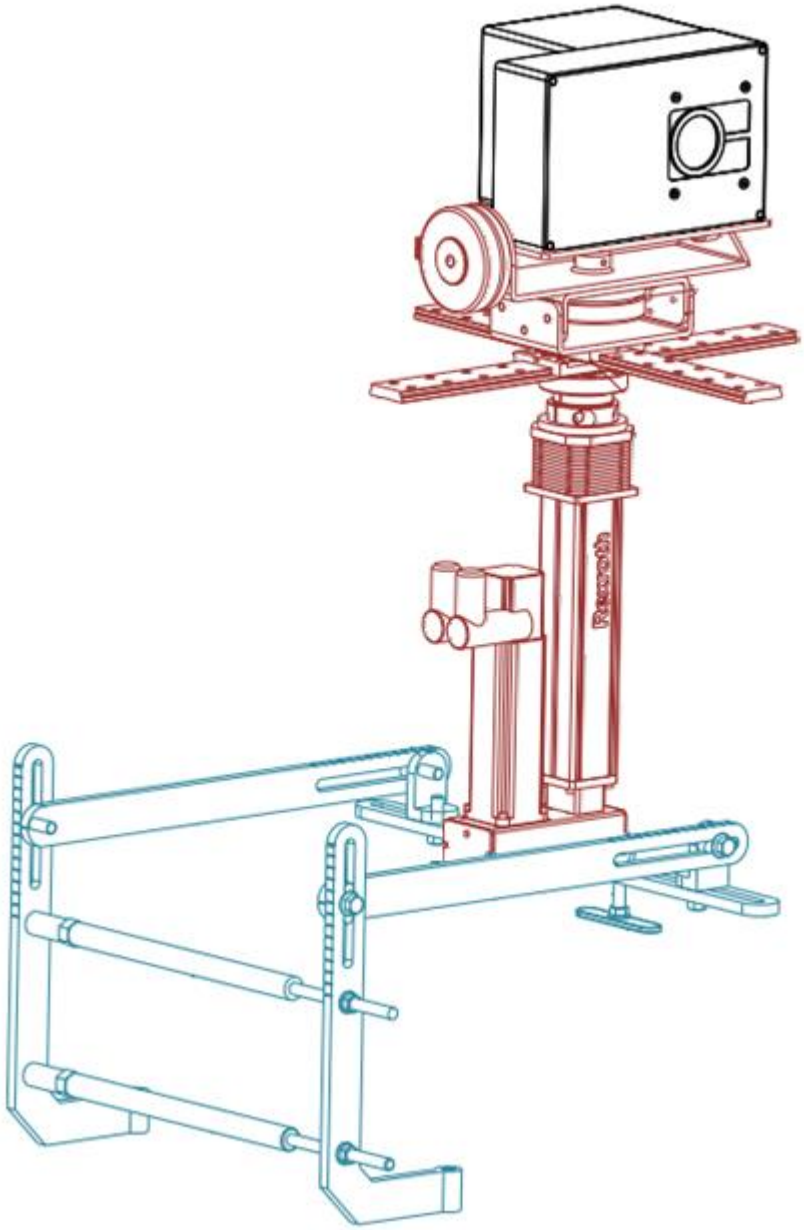

Figure 5-33: Final camera mounting system concept; Tower assembly (red) and Cradle assembly (blue)

The cradle is mounted off the front fixing points of the seat rails and stabilised with the seat pad at the rear of the assembly. The bosses which fit in the slots, allow for mechanical adjustment without twisting to keep the cradle stable and level.

The fixing points act as a datum feature to determine the reference eyepoint. From this point the X distance of the tower base can be set by making mechanical adjustments to the cradle. The tower height and slide rails are adjusted via the motor controls and can be

moved from their zero position to the Y and Z positions of the eyepoint from the datum feature. Pan and tilt are also motorised functions which allow fine adjustment to align the photometer to the point of regard. The slider rails are also to fine-tune the working distance of the photometer and allow for a corrective 'head' movement should the test require.

The advantages of this concept are:

- A more stable mounting solution than a tri-pod on the driver's seat as it is mounted directly from a hard point on the floor
- Reduces variation in alignment
- Increases repeatability of setup by reducing the influence of operator perception for alignment
- Allows fine adjustment
- Introduces a datum feature to set reference eyepoint position

There is still work required to develop this into a working solution; the distances to the eyepoint need to be calculated and worked into an algorithm to set the initial position of the cradle, as well as developing a graphical user interface to interact with the motorised components.

5.3 SUMMARY

This section has recommended ways of closing the gaps in digital and physical methods of performing virtual assessments of display legibility.

In the digital assessments, the simulated sky model overestimates the luminance distribution however the effect on daylight illuminance appears to be negligible. Post-processing operations are possible to bring the results closer to real-world measurements however the results of display simulations are sensitive to the material definition used. It is therefore recommended that approximations not be used when the display surface is the object of the evaluation. Further investigation is required when it is possible to measure the display surfaces and to incorporate measured skies directly into the simulation.

Physical methods of recreating daylight cannot replicate the wide range of scenarios and do not have the flexibility of digital tools. Moving forward the focus should be on digital methods for full system evaluation however this cannot be realised without a way to validate and give confidence in digital simulations. The physical methods suggested in this section outline what is required create a statement of work to produce a controlled lighting environment to facilitate this goal.

6 INTEGRATION OF LIGHTING SIMULATIONS INTO AUTOMOTIVE NPD

During the simulation and analysis of this research, the researcher was hosted by the Optical Computer Aided Engineering team (OCAE) at Jaguar Land Rover. From this perspective, the value of the research can be discussed in terms of the New Product Development (NPD) process; where it fits currently at JLR, where it should be implemented and the implications of the implementation, in order to address *Objective 4: Propose best-practice for display legibility assessments for design and validation activities in Jaguar Land Rover*.

6.1 OPTICAL PERFORMANCE EVALUATIONS IN PCDS

As stated in Section 1.1.1.1, optical performance is already a front-loaded activity in JLR; OCAE is utilised early in the NPD process (see Figure 1-4 for current OCAE timing) allowing early problem solving and iteration in design (Thomke and Fujimoto, 2000; Wheelwright and Clark, 1992a). However, the OCAE team are a small group of four engineers acting as a central resource for the analysis of lighting effects within the vehicle, supporting a wide range of functions and projects. As demand for lighting evaluation grows within the business, utilisation of this resource increases which can cause delays in responding to requests due to tasks queuing (Thomke, 2007).

These issues are modelled by Loch & Terwiesch (1999) in the context of change requests and the time to action them. They found that scarcity of resource with high utilisation and little 'slack' in the process to deal with bottle necks causes long queuing times. In addition

to this, congestion in the process is further exacerbated by the variability in task; number of requests made (adding to the queue) and complexity of task (adding to the lead time).

To address these challenges, they suggest five strategies to overcome these issues: flexible capacity (overtime work when needed), balanced workloads (preparation work shifted to non-specialists), merged tasks (multiple tasks actioned by single operator to reduce queue when passing task onto next operation), pooling (central resource of engineers to share the workload), and reduced set-up time and batch sizes. The OCAE team is already set up to use these strategies yet they are over stretched with the current resource (including engineers and processing capacity), and still need to prioritise incoming tasks depending on the programme making the request, the development phase of the programme and the capacity of the team to pick up the task at the expense of another task. More attention is required on the management of tasks with a focus on the deployment of resource (Wheelwright and Clark, 1992b) to optimise performance and allow for planning. For this to be achieved for OCAE, the process should be integrated to PCDS with deliverables set for OCAE during strategy and delivery. This will allow efficient use of current resource and provide greater evidence of where additional resource is required to alleviate over utilisation and incorporate slack into the process, resulting in greater flexibility in addressing a backlog in the task queue when a bottleneck forms.

Figure 6-1 gives a high-level overview of where optical performance could be aligned to PCDS; support through strategy and delivery with scheduled studies, early support for design and special request.

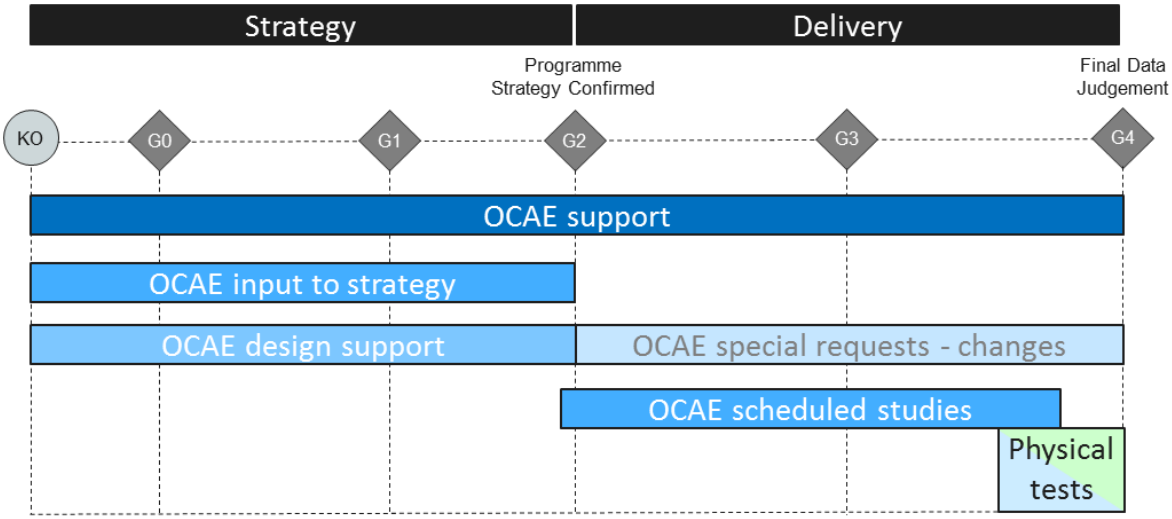

Figure 6-1: Aligning optical performance evaluations to PCDS

OCAE should be involved with the programme from the beginning and represented at project level to highlight where optical performance may be effected by decisions. For example, the material selected for interior surfaces will influence the behaviour of light within the vehicle; OCAE can advise from experience where the use of certain materials could cause an issue and should be assessed to ascertain the impact on HMI targets/driver vision. Early involvement with the project will also allow for scheduled support for each programme. Even though there will still be the need for bespoke assessment (such as in the example above) the strategic body of work for the project should be known and can therefore be planned; even the early design support can be planned to a certain extent using the general level of development and where it falls in the process. Contrary to making the process more rigid, this will allow OCAE to be more flexible as the scheduled studies will be anticipated, and the workload can be spread to key points in the process where the maturity of data is known. Planned, iterative studies throughout the development allows continual assessment to influence change until the design becomes mature enough to give results comparable to the final vehicle.

6.2 DIGITAL AND PHYSICAL INTEGRATION

Digital and physical evaluations of optical performance are considered as separate assessments performed by separate functions; there is input from digital to physical, in the form of SPEOS evaluations to show the specular condition to be tested, however there is no feedback from the physical evaluations back to the digital.

Becker et al. (2005) suggest unifying the physical and digital simulations into a single team populated by members responsible for the digital evaluations.

Integration of the two techniques can be achieved by producing a digital simulation of the physical set-up to show the correlation between the two systems. This would also provide a target pass criteria for the physical evaluation to achieve which is simpler to verify than through real-world measurement. Feedback from this assessment could be used to track variation in the physical setup and be fed back to enhance future digital simulations. Ideally this stage of evaluation should be performed by the same team; the OCAE team would be the best suited to do this as they have the expertise of the behaviour of light within a vehicle, experience of the simulations to know what to expect, and an appreciation for experimental control as they are responsible for BRDF measurements of materials to use in their simulations. However, due to the size of the team, their simulation workload supporting varied functions and the need for measurement of a number of different attributes, ownership of physical testing is not feasible under the current structure. For this to be done would require a growth in the resource of the team including engineers and measurement facilities. An alternative would be to perform collaborative assessments with input from both the attribute owner (HMI) and OCAE.

This still plays to the traditional paradigm of 'build it then test it' (Martin and Carvalho, 2006); a "new" approach shifts the physical test away from late assessments close to production and instead uses finished products from previous projects in the characterisation of digital simulations for new projects. The goal should be to continually correlate the digital to the physical simulation with a view to remove reliance on the physical model completely, in line with the company's desire to reduce the amount of time

spent on physical prototypes, reduce cost, and move decisions to earlier in the NPD process (Thomke, 1998). This would require complete shift in approach from traditional development which is based on physical prototypes as the validation of design.

6.3 OBSTACLES/RESISTANCE TO DIGITAL PROTOTYPE

Digital prototyping has been found to reduce the number of physical prototypes needed thereby reducing costs and development time (Martin and Carvalho, 2006; Thomke and Fujimoto, 2000; Thomke, 1998; Wheelwright and Clark, 1992a) by allowing a greater number of iterations and more diverse tests. This also provides greater insight into the behaviour of the physical system and components than with physical prototypes. This knowledge leads to design improvements and higher quality/more accurate digital models in future developments (Becker et al., 2005; King, 2002).

With the introduction of more digital tool-sets and a greater use of simulation in automotive NPD, it could be assumed that there is little resistance to the digital prototyping. However, within the automotive industry, there is still a heavy reliance on physical prototypes, usually with greater confidence placed in the results of physical testing (Elverum and Welo, 2014). Yet the physical prototype is still a simulation, and compared to a digital simulation, it is a lesser approximation of the real world (El-Sayed, 2011). A digital prototype is better able to control and simulate a greater number of variables than those accounted for with a physical prototype and also removes the errors associated with operators and deviations between physical models.

Some of this adherence to physical prototyping is due to organisational and cultural 'fixation', where development and validation has traditionally been reliant on physical methods and people are reluctant to change (Martin and Carvalho, 2006).

Becker et al (2005) suggest that "*in order to reap the full potential of virtual simulation tools, beyond cost and lead time effects, adapting the organization is required".* To tackle organisational resistance to digital prototypes requires evidence of success and validity of digital simulations to raise confidence in the use of such models and techniques. As with

any organisational change, this shift in attitude needs a champion and clear support and direction from management in the use of simulation (Murphy and Perera, 2002).

There are also limitations in some simulation methods and gaps in the correlation to physical prototypes which can restrict the use of digital prototypes (Martin and Carvalho, 2006). The accuracy of simulation outputs depends on how well the operating conditions are defined; the user environment, the product behaviour and human interactions all need to be modelled with a high level of detail and linked to corresponding physical measures (Zorriassatine et al., 2003). To achieve greater confidence in the results of digital simulations, effort is required to characterise the physical attributes of the system to be fed back into simulation and move correlation activities using physical prototypes to earlier in the NPD process (Zorriassatine et al., 2003).

A digital prototype however does not overcome the 'emotional barriers' associated with communicating a concept, which Elverum and Welo (2014) found to be the role of early physical prototypes; overcoming the resistance to an idea and influencing decision making with a physical mock-up. These types of physical prototype are not always feasible, especially where analysis is required for a complete system or subsystem of a vehicle. In terms of the automotive industry, the accuracy of the physical model would require a prototype vehicle of production intent. This level of prototype is produced towards the end of development which gives little opportunity for changes to be made and offers no insight to designers. Changes required due to the identification of a failure mode captured at this late stage would be costly to implement, if possible to do so.

According to Youmans (2011), designers have a *strong preference* to touch and interact with prototypes, resulting in better understanding and aiding communication for greater creativity. Where a physical prototype would be inappropriate, replication of the environment is achievable through visualization techniques. The advantage of visualization is that abstract simulation results and complex concepts can be presented in a familiar, and often interactive way (Rohrer, 2000).

The outputs of OCAE simulations are very visual and a real-world comparison will have a large impact on stakeholders. This could impress enough to encourage a greater confidence in digital simulation, however there is also the danger that if their experiences are different in the real-world they will doubt the results of the simulation without appreciating what the conditions they were viewing under compared to the conditions tested for in the simulation. Martin & Carvalho (2006) found that these cultural restrictions were one of the highest rated factors hindering the migration from physical to digital tools. Another factor identified was 'difficulty obtaining data'.

Data flow is not just one way; the results of assessments flow from the OCAE team to the attribute team but there is a requirement for data to flow into the team to allow the assessments to be performed. Data management tools give a central database of CAD data from design, however, OCAE need to know the components and level of data that are to be included in the assessments (part numbers, revision etc.). This data then needs to be processed prior to use in SPEOS and materials properties added. To facilitate the flow of data into OCAE, there needs to be a relationship with the design team and a point of contact for each programme. This can be established at the beginning of each programme, prior to data being required. This relationship is important as lack of data into the assessments contributes to the bottleneck, as does incorrect data. The design of a product is continually advancing, and parts and revisions can change without the OCAE team being aware, resulting in assessments being performed on incorrect data, increasing the lead-time of assessments and impacting the throughput of OCAE.

6.4 SUMMARY

Closing the gaps between simulation and the real world should be a priority to increase confidence in digital simulations. This work is the start of this process of continual improvement for optical performance assessments, contributing to the goal of a fully digital prototype for a vehicle programme. For now, physical testing is necessary, however with the future vision of zero physical prototypes, there should be an emphasis on the use of digital simulations and changing the attitudes of the business to embrace and improve digital prototypes.

7 SUMMARY & CONCLUSIONS

The aim of this research was to *recreate daylight for the evaluation of in-vehicle displays*. Current digital and physical practices for display legibility assessments were found to be lacking in control and representation of the real-world scenario. For the physical assessments, this was attributed to the test set-up and for the digital assessments the gap was a result of approximations in material definitions. This research includes recommendations to address these gaps and to bring digital and physical evaluations into a system for evaluations focused on correlation of digital methods.

This section will briefly re-examine the objectives stated in Section 1.2.2 and summarise the main findings of the research. It also serves to conclude the research and reflect upon how well the research objectives have been met and the value created for the sponsor company.

7.1 SUMMARY OF OBJECTIVES

7.1.1 The 'real-world' environment of automotive displays

The performance of in-vehicle displays is affected by the changing daylight conditions under which they are viewed. Under high ambient daylight, the contrast is reduced making the displayed information less legible. This reduction in contrast is dependent on the incident angle of the sun, the combined luminance at the display from reflections and emitted light, and the viewpoint and visual perception of the driver.

Metrological techniques have been established which characterise these reflections and determine their impact on legibility from psychophysical models of human vision. At Jaguar Land Rover, the metric used to evaluate legibility is Perceived Just Noticeable Difference which describes the point at which a difference in contrast can be perceived. This is

combined with physical and digital simulation methods to predict the optical performance of displays within new vehicles.

The field measurements performed in this study capture the real-world characteristics of daylight effects upon in-vehicle displays, from the point of view of a driver, to assess current performance evaluation methods.

7.1.2 Assessment of current in-vehicle display evaluation methods

The current methods of in-vehicle display evaluation are compared to the real-world characteristics that the simulations are designed to emulate. A gap is established, both in the physical and digital techniques.

The physical gap is determined from the lab-based trial and field measurements compared to standards of display metrology and the real-world lighting environment. It centres on the deficiency in controlled measurement (mainly from the alignment method of the photometer and the stability of mounting from the driver's seat), the positioning of direct lighting and the undefined diffuse environment. This lack of control results in the non-repeatability and inconsistency of the measurements taken.

A digital gap is found to exist between the measured display reflections and the SPEOS simulations of the same situation with the simulated result consistently underestimating the effect of daylight, quantified by the RMSE of foreground luminance (up to 70%) and background luminance (up to 86%). This difference produced by the digital simulations could be due to the daylight definition of the software or the properties of the materials in the simulation.

7.1.3 An appropriate method for recreating daylight and performing evaluations of in-vehicle displays

The proposal for an appropriate method of recreating daylight for ambient contrast simulations is based on closing the gap in existing methods.

Physical simulations of daylight can be complex and of limited accuracy, however it is possible to close the gap in current methods to establish a controlled and meaningful assessment method.

The digital simulations were found to overestimate the luminance distribution of the sky compared to the real skies measured in Australia, however this resulted in an underestimation of daylight illuminance at the ground of approximately 12%. This suggests that the direct solar component is also underestimated and the contribution of the sky luminance to simulated daylight illuminance is negligible. It is possible to align simulations closer to real-world measurements through post-processing operations, however this does not address the gap fully and further investigation revealed that the results of display simulations are highly sensitive to the material definition used.

It is therefore recommended that BRDF measurements of materials be used in place of approximations for the display surface when it is the object of the evaluation, and for physical methods to be developed for a controlled lighting environment to characterise a set of conditions to give confidence in the digital simulations.

7.1.4 Best-practice for display legibility assessments for design and validation activities in Jaguar Land Rover

Within Jaguar Land Rover, display legibility assessments are required to optimise design and ensure failure modes are identified and rectified before they reach the customer. The earlier in the NPD process that these failure modes can be detected, the easier they can be addressed with a reduced impact to time and cost of a project.

Digital evaluations are employed throughout the NPD process, with buy-off using physical prototypes during the later stages of development. However, to be most effective, digital and physical methods need to be integrated and aligned to the NPD at JLR. The focus of legibility evaluations, and all optical performance evaluations, should be the continual improvement of digital simulations with an attempt to move the verification exercises to earlier in the process with lower cost, more controlled physical simulations.

There should be an emphasis on the use of digital simulations and changing the attitudes of the business to embrace and improve digital prototypes.

7.2 IMPLEMENTATION, IMPACT & INNOVATION

This research has focused on providing value to JLR especially to Vehicle Engineering where there can be an immediate impact to processes. Accordingly, there are areas of the research that have had a direct impact on JLR, however aspects of the research are also of benefit to the wider industry.

7.2.1 Parameters of simulations for high ambient display assessments

This research has demonstrated the importance of the material definition used in SPEOS simulations. Consistent with previous research into simulation validity (Robinson, 1997; Sargent, 2011), the lack of quality inputs in these simulations has produced results that suggest an inaccurate model. A high level of detail is required in the parameters and assumptions made in building digital models to achieve high quality digital prototypes (Zorriassatine et al., 2003), the gap in material definition has the potential for failure modes to be missed or their severity to be downplayed resulting in poor performance systems to be implemented. The implication is that the failure mode will not be identified early enough to rectify without significant costs or it is possible it will not be identified until in-use by the customer (Becker et al., 2005), ultimately affecting customer satisfaction.

The OCAE team at JLR are committed to improving simulations and have implemented the recommendation of using measured materials for assessments of display reflections. The introduction of next generation display technologies, has instilled a greater urgency for this to be implemented for new vehicle programs. This work is ongoing, with equipment currently being sourced for the measurement of BRDF characteristics of displays. Until this is realised, an interim solution has been implemented whereby the surface coatings of displays have been scanned from a sample plaque for use in simulations; this will give a better approximation of performance based on more accurate data than the simple scatter files.

The immediate benefits to the OCAE team from the research are from the results that support the validity of past simulations while allowing for improvements to future simulations by closing the gap between simulations and real world. This confidence in the software is also a means to raise the profile of digital lighting evaluations throughout the business.

The material definition is an important consideration in building quality models, the results of this study therefore have the potential to benefit the wider industry; users of SPEOS and for OPTIS as the software provider. It is generally understood that greater accuracy models require higher accuracy inputs, however it is possible that the impact of using approximations is not appreciated. This study can be used as evidence of the need for greater accuracy in material definition for confidence in the tool for automotive applications.

The findings of this research show a gap in sky luminance measurements versus simulation. This concern over the definition of the ambient source has been raised with OPTIS who are developing a method to recreate a sky with measurement data as an ambient source within SPEOS. This will allow further testing and will make the software more compatible with research activities.

Quality models are also reliant on the *'reliability and credibility of the results obtained'* which requires verification to test cases and use case data (Becker et al., 2005; Reuding and Meil, 2004). The methodology followed by this research can be used in further studies in the continuous improvement and/or introduction of new digital tools. The data capture and comparison techniques, along with the method created for extracting and comparing simulated skies using a mirror-sphere. This is not limited to SPEOS applications but may also be employed with other simulation tools and adjusted to the mapping function of the optics used to capture the sky data. These methods will allow the empirical data capture and evaluation of new software tools for specific use cases.

7.2.2 Control and repeatability in assessments

One of the fundamentals of metrology is the control and repeatability of measurements (Czichos et al., 2011). With simpler test setups, such as bench-top simulations, the boundary conditions of measurements are easier to control however they can lack comparability to the use case. In automotive applications, the driver's view of a display and the ambient conditions of the environment under which the measurements are performed are important considerations and can be complex. This is especially true for luminance measurements due to the angular dependence of the measurement and sensitivity to setup geometry (Jones and Kelley, 1998; Kelley, 2002; Kim et al., 2009).

Experience in this research of setting up the measurement equipment suggests that without a dedicated mounting system, in-situ measurement will suffer from low repeatability. This is due to setting the measurement equipment at the reference eyepoint for the study which has no physical reference to the vehicle geometry, the unstable mounting surface and the variability in the method of alignment. A concept to mount a photometer in the vehicle is presented to counter these issues within JLR to make measurements more repeatable.

> *"What we were really keen to develop was a robust camera mounting device and procedure that would sit solidly in the right position in the vehicle and enable us to comfortably orient the camera correctly on the interior components we were interested in - anything that replaced the horrible wobbly tripod balanced on a seat."*
>
> David Smith, Jaguar Land Rover Vehicle HMI Attribute Team
>
> October 2013

The advantages of this concept are:

- A more stable mounting solution than a tri-pod on the driver's seat as it is mounted directly from a hard point on the floor
- Reduces variation in alignment

- Increases repeatability of setup by reducing the influence of operator perception for alignment
- Allows fine adjustment
- Introduces a datum feature to set reference eyepoint position

This mounting solution has value with other automotive suppliers but also for other industries and research where a sensor (such as the photometer) is required at a specific view point. An example of the application for research is from advice given, based on this research, for a project with the departments of Psychology and WMG at the University of Warwick (M Pitts 2017, personal communication, 8th August). A camera mount for a driving simulator is needed where accurate replication of a reference eyepoint from a virtual environment is required. There is also the potential for further value for use in research into the shift in use of vehicle interiors in autonomous vehicles, where the active driver becomes a supervisor to the driving task. The environment of such systems has not yet been developed, but it can be speculated that the viewpoint of the 'driver' may change and the user environment of display technology may be different to the current cabin due to larger and more varied displays and a larger glasshouse from transparent canopy; increasing the influence of sky light on a viewing task and the potential for the specular condition. For these new use-cases, correlation activities to simulation will be required (Reuding and Meil, 2004) which suggests the need for a controlled environment.

Even though current physical assessments of displays are later in the NPD process and require a production level physical prototype, a controlled lighting environment is of interest to JLR. Based on the recommended setup for high ambient display assessments in international standards (BSI, 2009; SAE, 2007) and experience presenting this research at 'electronic displays Conference (edC2015) where most questions from automotive display suppliers concerned lighting levels and the controlled environment for in-situ measurement, it can be assumed that establishing a stable lighting environment for in-vehicle evaluations is a challenge for the wider automotive community.

The emphasis in this research is for a controlled lighting environment to provide stable lighting conditions for repeatable measurements for display legibility assessments. The

recommendations in this research facilitate the definition and specification of this environment with suggestions for methods to control the position of the direct lighting and a weighting system to assess lighting technology. These recommendations are customisable to other controlled lighting environments depending on the needs of the industry and/or the specific testing required.

7.2.3 Integration of physical and digital prototypes aligned to NPD process

In line with JLR's desire to reduce the reliance on physical prototypes, reduce cost, and move decisions to earlier in the NPD process, this work recommends the integration of physical and digital methods for the assessment of in-vehicle display legibility.

There is still a high reliance on physical prototypes in the automotive industry; they can be touched and interacted with to enable the communication of abstract or complex concepts to external stakeholders and to solicit internal support for overcoming design challenges (Elverum and Welo, 2014). However, in terms of legibility and display reflection assessments, the prototypes required are of such maturity that they are only available in the very late stages of development, therefore digital simulations are taking the place of physical simulations in the early stages of development to aid design and the physical assessments are used as a final verification.

The advantages of digital simulation are a reduced development time, lower cost through reduction in the number of physical prototypes, and an increase in the number of scenarios/iterations tested with a wider range of possibilities (Becker et al., 2005; El-Sayed, 2011; Thomke, 1998). To stop this split in evaluations of early digital prototypes to support late physical prototypes, these simulation activities can be integrated into a single system. This would involve shifting the physical simulations to the left of the NPD process and using them in support of digital evaluations; physical prototypes made up of previous systems of known configuration, to test/measure specific attributes that can be transferred into digital simulations. The advantage of integrating assessments into a system of evaluations is that it takes advantage of the benefits of both digital and physical methods. According to El-Sayed (El-Sayed, 2011), the automotive industry have been successful in implementing

digital simulations and reducing prototype build time and cost yet due to the adherence to the 'physical build founded processes' this success will be limited. This suggests that it is an industry-wide attitude that focuses on physical prototypes therefore other OEMs would benefit from aligning their physical and digital assessments, not limited to display evaluations.

This systems approach is new to JLR, and the OCAE team and Human Factors are interested in trialling a digital model build of the physical simulation set-up as a verification exercise. This will enable the investigation of where verification activities can be planned earlier in the process and to align activities between the two groups to facilitate gateway deliverables. This alignment to the NPD process will then enable the planning and development of test procedures to run in parallel to the development of the design. This is consistent with previous research that suggests *"As the design evolves and is implemented, the corresponding tests should also evolve and be applied in parallel. Thus, at the end of the design, engineers are not merely relying on what they believe in, but also have a well-established set of results that demonstrate the continuous verification efficacy of the design"* (Murphy et al., 2008).

The recommended alignment of the process to PCDS and the barriers to implementation are being presented by the OCAE to senior leaders at JLR as evidence to expanding resource and the value of digital simulation in the NPD process.

> *"As front loading concept is pretty much embedded into the Optical CAE failure mode avoidance analysis, the requirements to assess the advanced technology is continuously in demand. Due to the fact that screen's technology evolution is rapid, the need to capture the potential readability issues is needed, the study conducted by Claire White is giving us enough proof to convey the message across business to measure the displays on regular basis."*
>
> Kranthi Puppala, OCAE Team Lead
>
> December 2016

7.3 LIMITATIONS & FURTHER WORK

As with any study there are limitations to this research. Throughout this project, there were several challenges encountered which could be consider 'limitations' but which shaped the direction of the research.

At the beginning of the project, the focus was on a physical solution to recreating daylight; partially from pre-conceptions of what the research should be and partially from the expectations of the sponsor company. Overcoming the assumption that a physical daylight test facility was the end goal of the research, led to consideration of digital simulations as the primary tool for performing daylight legibility assessments rather than being limited to physical simulations.

There were also a few assumptions made with respect to the software that were discovered to be incorrect, most notably that the captured sky data could simply be incorporated into SPEOS to evaluate the performance of the simulations and that all material definitions were based on measured BRDF files. The limitations of the flexibility of sky definition, although not ideal, led to investigating the capabilities of the software and developing a method to extract the simulated skies in a comparable format to the measured skies. It also shaped the processing techniques used for both sets of sky data. The lack of a BRDF file for the display surface was unexpected and meant that the study was not able to quantify the relative accuracy of the software to the measured data. It did however demonstrate the importance of the material definition and to show that they significantly influence the results of the simulations. To definitively attribute the digital gap to the characterisation of materials in the simulations, there is value in further investigation into the use of the measured materials, the techniques used to capture the data and any errors associated with the methods.

A weakness in the methodology is due to the use of highly variable real-world data in assessing the simulations. Due to the number of potential error sources, it is difficult to attribute gaps between the data sets to deficiencies in the software. Also, the comparison of the digital simulations was relative to the measured data. This would not be an issue for

validation of a controlled setup which would be correlation of the physical test setup to the digital simulations however in this case there was no correlation to a reference standard in the real world. It is recommended that future evaluations make comparisons based on an absolute value of daylight luminance/display luminance.

The collected data was limited to a single vehicle configuration under a limited number of skies. However, the procedures followed in this research lend themselves to verification exercises to form the basis for continued improvement. This can be done by expanding the dataset to include different vehicle configurations and various locations, combined with data captured in controlled environment. Future measurements would benefit from a method of verification of the driver's eyepoint location and greater control of the measurements to ensure correlation with digital simulations.

The results of the simulation comparison suggest that the sky luminance distribution plays a minor role in simulating the reflections at the display surface. However, being able to directly simulate the daylight conditions, through the incorporation of measured data would give a more direct answer as to the influence of the sky on display reflections not just on the simulations of reflections.

Though beyond the scope of this research, which focused on the physical and digital daylight recreation methods, it would be beneficial for future work to compare the methods for evaluating legibility. The PJND method mentioned in this study, may be the best metric for use at present within JLR based on previous work into aligning the figure of merit to a suprathreshold condition and establishing 'pass-fail' criteria. However, there is the possibility that other metrics and visual performance models could be applied which give greater flexibility in defining character size and age of driver when defining the legibility of a display under high ambient daylight.

REFERENCES

Ambrose, G., Harris, P., 2006. The Fundamentals of Typography. AVA Publishing.

Andor, n.d. CCD Blooming and Anti-blooming [WWW Document]. Learn. Acad. URL http://www.andor.com/learning-academy/ccd-blooming-and-anti-blooming-the-principle-of-blooming (accessed 6.16.16).

Angus, R.C., 1995. Daylight Illuminance Modelling for the UK and Europe. Napier University.

ARRI, 2014. ARRI Daylight Compact 1200: Technical Details [WWW Document]. ARRI Rent. Light.

ARRI, 2005. Daylight Compact [Product Brochure].

Aydın, T.O., Myszkowski, K., Seidel, H.-P., 2009. Predicting Display Visibility Under Dynamically Changing Lighting Conditions. Eurographics 28.

Becker, M.C., Salvatore, P., Zirpoli, F., 2005. The impact of virtual simulation tools on problem-solving and new product development organization. Res. Policy 34, 1305–1321. doi:10.1016/j.respol.2005.03.016

Bell, R.I., Marsden, A.M., 1975. Disability glare: the relationship between veiling luminance and threshold rise. Light. Res. Technol. 7, 56–57.

Bell, S., 1999. A Beginner's Guide to Uncertainty of Measurement. Meas. Good Pract. Guid. 41. doi:10.1111/j.1468-3148.2007.00360.x

Bellia, L., Cesarano, A., Minichiello, F., Sibilio, S., 1997. Videography for sky luminance distribution measurement. Light. Res. Technol. 29, 40–46. doi:10.1177/14771535970290011001

Berrio, E., Tabernero, J., Artal, P., 2017. Optical aberrations and alignment of the eye with age. J. Vis. 10, 1–17. doi:10.1167/10.14.34

Beyer, H.G., Martinez, J.P., Suri, M., Torres, J.L., Lorenz, E., Müller, S.C., Hoyer-Klick, C., Ineichen, P., 2009. Report on Benchmarking of Radiation Products.

Bhise, V.D., Sethumadhavan, S., 2008. Predicting Effects of Veiling Glare Caused by Instrument Panel Reflections in the Windshields. SAE Int. J. Passeng. Cars - Electron. Electr. Syst. 1, 275–281.

Birman, V., Pala, S., Hildebrand, L., 2013. White shirt reflections and ambient illumination challenges in determining automotive display legibility performance, in: SID 20th Annual Symposium on Vehicle Displays October 2013. Society for Information Displays, University of Michigan-Dearborn, Dearborn MI, pp. 33–42.

Blackwell, H.R., 1946. Contrast Thresholds of the Human Eye. J. Opt. Soc. Am. 36, 624–643.

Blankenbach, K., 2012. Display Metrology, in: Handbook of Visual Display Technology. Springer-Verlag. doi:10.1007/978-3-540-79567-4

Bodart, M., Deneyer, A., Gilbert, V., 2008. Validation of the Belgian single-patch sky and sun simulator. Build. Environ. 43, 1892–1901. doi:10.1016/j.buildenv.2007.11.005

Boehm, B.W., 1976. Software Engineering. IEEE Trans. Comput. C-25, 1226–1241.

doi:10.1111/j.1365-2362.2005.01463.x

Boyce, P.R., 2003. Human Factors in Lighting, 2nd Ed. ed. Taylor & Francis, London; New York.

Boyce, P.R., 1973. Current knowledge of visual performance. Light. Res. Technol. 5, 204–212. doi:10.1177/096032717300500404

BSi, 1994. BS ISO 5725-2:1994. Accuracy (trueness and precision) of measurement methods and results - Part 2: Basic method for the determination of repeatability and reproducibility of a standard measurement method.

BSI, 2014. BS IEC 62679-3-1:2014. Electronic paper display Part 3-1: Optical measuring methods.

BSI, 2012. BS EN 61747-6-2:2011. Liquid crystal display devices -- Part 6-2: Measuring methods for liquid crystal display modules — Reflective type.

BSI, 2011. BS EN ISO 11664-2:2011. Colorimetry - Part 2 : CIE standard illuminants.

BSI, 2010. BS ISO 4513:2010. Road vehicles — Visibility — Method for establishment of eyellipses for driver's eye location.

BSI, 2009. BS EN ISO 15008:2009. Road vehicles — Ergonomic aspects of transport information and control systems — Specifications and test procedures for in-vehicle visual presentation.

BSI, 2005. BS ISO 23603:2005. Standard method of assessing the spectral quality of daylight simulators for visual appraisal and measurement of colour.

BSI, 1967. BS 950-1:1967. Artificial daylight for the assessment of colour — Part1: Illuminant for colour matching and colour appraisal.

Burton, K.B., Sloane, E., 1993. Aging and Neural Spatial Contrast Sensitivity : Photopic Vision. Vision Res. 33, 939–946.

Caberletti, L., Elfmann, K., Kummel, M., Schierz, C., 2010. Influence of ambient lighting in a vehicle interior on the driver's perceptions. Light. Res. Technol. 42, 297–311. doi:10.1177/1477153510370554

Cai, H., Green, P.A., 2009. Legibility Index for Examining Common Viewing Situations : A New Definition Using Solid Angle. LEUKOS J. Illum. Eng. Soc. North Am. 5, 279–295. doi:10.1582/LEUKOS.2008.05.04.002

Cai, H., Green, P.A., 2005. Character Heights for Vehicle Displays as Predicted by 22 Equations, in: SID 12th Annual Vehicle Display Symposium. Dearborne, MI.

Chen, J., Reilly, R.R., Lynn, G.S., 2005. The impacts of speed-to-market on new product success: The moderating effects of uncertainty. IEEE Trans. Eng. Manag. 52, 199–212. doi:10.1109/TEM.2005.844926

Chong, Y., Chen, C.-H., 2010. Customer needs as moving targets of product development: a review. Int. J. Adv. Manuf. Technol. 48, 395–406. doi:10.1007/s00170-009-2282-6

CIE, 2010. CIE 192:2010. Practical daylight sources for colorimetry.

CIE, 2009. CIE 184:2009. Indoor daylight illuminants.

CIE, 2006. CIE 171:2006. Test cases to assess the accuracy of lighting computer programs.

CIE, 2004. CIE 15:2004. Colorimetry.

CIE, 2002. CIE 145:2002. Correlation of models for vision and visual performance.

CIE, 1994. Part B: Research Class Stations, in: CIE 108:1994. Guide to Recommended Practice of Daylight Measurement. Commission Internationale de l'Éclairage, pp. 6–10.

CIE, 1989. CIE 85:1989. Solar Spectral Irradiance.

CIE, 1981. CIE 19/2:1981. An Analytic Model for Describing the Influence of Lighting Parameters upon Visual Performance.

Clear, R., 2012. Discomfort glare: What do we actually know? Light. Res. Technol. 45, 141–158. doi:10.1177/1477153512444527

Cooper, R.G., 2008. Perspective: The Stage-Gate® Idea-to-Launch Process—Update, What's New, and NexGen Systems*. J. Prod. Innov. Manag. 25, 213–232. doi:10.1111/j.1540-5885.2008.00296.x

Cooper, R.G., 1990. Stage-Gate Systems: A New Tool for Managing New Products. Bus. Horiz.

Cooper, R.G., 1988. Predevelopment activities determine new product success. Ind. Mark. Manag. 17, 237–247. doi:Doi: 10.1016/0019-8501(88)90007-7

Cooper, R.G., Edgett, S.J., Kleinschmidt, E.J., 2002. Optimizing the stage-gate process: What best-practice companies do - II. Res. Manag. 45, 43–49.

Cooper, R.G., Kleinschmidt, E.J., 1993. Major New Products: What Distinguishes the Winners in the Chemical Industry? J. Prod. Innov. Manag. 10, 90–111. doi:10.1111/1540-5885.1020090

Cooper, R.G., Kleinschmidt, E.J., 1988. Resource allocation in the new product process. Ind. Mark. Manag. 17, 249–262. doi:Doi: 10.1016/0019-8501(88)90008-9

Cucumo, M., De Rosa, A., Ferraro, V., Kaliakatsos, D., Marinelli, V., 2010. Correlations of direct solar luminous efficacy for all sky, clear sky and intermediate sky conditions and comparisons with experimental data of five localities. Renew. Energy 35, 2143–2156. doi:10.1016/j.renene.2010.04.004

Czichos, H., Wallard, A., Ramsey, M.H., Ellison, S.L.R., Hässelbarth, W., Ischi, H., Wegscheider, W., Brookman, B., Zschunke, A., Frenz, H., Golze, M., Hedrich, M., Schmidt, A., Steiger, T., 2011. Fundamentals of Metrology and Testing, in: Czichos, H., Saito, T., Smith, L. (Eds.), Springer Handbook of Metrology and Testing. Springer Berlin Heidelberg, Berlin, Heidelberg, pp. 3–138. doi:10.1007/978-3-642-16641-9

Dale, E., Chall, J.S., 1949. The Concept of Readability, in: Dale, E. (Ed.), Readability. National Conference on Research in English.; National Council of Teachers of English, Champaign, Ill., pp. 1–7.

Darula, S., Kittler, R., 2015. A Methodology for Designing and Calibrating an Artificial Sky to Simulate ISO/CIE Sky Types with an Artificial Sun. Leukos 11, 93–105. doi:10.1080/15502724.2014.977391

de Waard, P.W.T., Ispeerf, J.K., Berg, T.J.T.P. Van Den, Jong, P.T.V.M. De, 1992. Intraocular Light Scattering in Age-Related Cataracts. Invest. Ophthalmol. Vis. Sci. 33, 618–625.

Delacour, J., Fournier, L., Massakbi, M., 2005. Simulating Driver Vision Using a CAD Software - New Technologies for Predicting Visual Comfort , Distraction , and Glare in the Driving Environment. SAE Tech. Pap. 2005-01-0446.

Devlin, K., Chalmers, A., Wilkie, A., Purgathofer, W., 2002. Tone Reproduction and Physically Based Spectral Rendering. State Art Reports, Eurographics 2002 101–123. doi:≤

DiLaura, D., Houser, K., Mistrick, R., Steffy, G., 2011. The Lighting Handbook, 10th Edition. Illuminating Engineering Society of North America.

Dunsäter, A., Andersson, M., 2007. Daytime veiling glare in automobiles caused by dashboard reflectance. Linköpings Universitet, Sweden.

EKO Instruments, 2006. Data Sheet: MS-321LR Sky Scanner.

El-Sayed, M., 2011. Expanding Virtual Simulation in Product Realization. SAE Int. J. Mater. Manuf. 4. doi:10.4271/2011-01-0530

Elverum, C.W., Welo, T., 2014. The role of early prototypes in concept development: Insights from the automotive industry. Procedia CIRP 21 21, 491–496. doi:10.1016/j.procir.2014.03.127

Feister, U., Shields, J.E., Karr, M., Johnson, R., Dehne, K., Woldt, M., 2000. GROUND-BASED CLOUD IMAGES AND SKY RADIANCES IN THE VISIBLE AND NEAR INFRARED REGION FROM WHOLE SKY IMAGER MEASUREMENTS, in: Proc. Climate Monitoring–Satellite Application Facility Training Workshop, DWD, EUMETSAT, and WMO.

Ferraro, V., Mele, M., Marinelli, V., 2011. Sky luminance measurements and comparisons with calculation models. J. Atmos. Solar-Terrestrial Phys. 73, 1780–1789. doi:10.1016/j.jastp.2011.04.009

Freeman, C.M., Gaylard, A.P., 2008. Integrating CFD and Experiment : The Jaguar Land Rover Aeroacoustics Process, in: 7th MIRA International Conference on Vehicle Aerodynamics, 22-23 October 2008, The Ricoh Arena, Coventry, UK.

Gawlik, J., Rewilak, J., 1999. Repeatability and reproducibility (R & R) studies for the assessment of measurement system capability. e i Elektrotechnik und Informationstechnik 116, 266–270. doi:10.1007/BF03159516

Gibbs, N., 2015. How digital prototyping is cutting development time and costs for new models. Automot. News Eur.

Gueymard, C. a., Myers, D.R., 2008. Validation and Ranking Methodologies for Solar Radiation Models, in: Badescu, V. (Ed.), Modeling Solar Radiation at the Earth's Surface. Springer, pp. 479–510. doi:10.1007/978-3-540-77455-6_20

Hart, S., Jan Hultink, E., Tzokas, N., Commandeur, H.R., 2003. Industrial Companies' Evaluation Criteria in New Product Development Gates. J. Prod. Innov. Manag. 20, 22–36. doi:10.1111/1540-5885.201003

Hertel, D., Kelley, E.F., 2014. Viewing Direction Measurements with Hemispherical Diffuse Illumination on E-Paper Displays. SID Symp. Dig. Tech. Pap. 45, 532–535.

Hubbell, G.R., 2013. CCD Chip Performance, CCD Camera Basics, and Image Scaling Factors, in: Scientific Astrophotography: How Amateurs Can Generate and Use Professional Imaging Data. Springer Science+Business Media, New York, pp. 31–53. doi:10.1007/978-1-4614-5173-0_4

Hubel, P.M., Liu, J., Guttosch, R.J., 2004. Spatial frequency response of color image sensors: Bayer color filters and Foveon X3. Proc. SPIE 5301, 402–407. doi:10.1117/12.561568

ICDM, 2012. Information Display Measurements Standard, Version 1. ed. International Committee for Display Metrology.

Inanici, M.N., 2010. Evalution of High Dynamic Range Image-Based Sky Models in Lighting Simulation. LEUKOS J. Illum. Eng. Soc. North Am. 7, 69–84.

doi:10.1582/LEUKOS.2010.07.02001

Inanici, M.N., Galvin, J., 2004. EVALUATION OF HIGH DYNAMIC RANGE PHOTOGRAPHY AS A LUMINANCE MAPPING TECHNIQUE. Lawrence Berkeley Natl. Lab.

Ineichen, P., 1992. PRC Krochman Sky Scanner Characterisation (parts 1 & 2).

Ineichen, P., Molineaux, B., Perez, R., 1994. SKY LUMINANCE DATA VALIDATION: COMPARISON OF SEVEN MODELS WITH FOUR DATA BANKS. Sol. Energy 52, 337–346.

Instrument Systems, Konica Minolta, 2014. LumiCam 1300.

Jaguar Land Rover, 2016. Jaguar Land Rover Automotive PLC Annual Report.

Jones, G.R., Kelley, E.F., 1998. Reflection Measurement Problems Arising from Haze. SID'98 Dig. 33.4, 945–946.

Judd, D.B., MacAdam, D.L., Wyszecki, G., 1964. Spectral Distribution of Typical Daylight as a Function of Correlated Color Temperature. J. Opt. Soc. Am. 54, 1031–1040.

Kelley, E.F., 2007. Invited Paper : Metrology and Robustness of Bright-Room Contrast Measurements. SID Symp. Dig. Tech. Pap. 38, 1034–1037.

Kelley, E.F., 2002. Sensitivity of Display Reflection Measurements to Apparatus Geometry. SID Symp. Dig. Tech. Pap. 140–143.

Kelley, E.F., 2001a. Proposed Diffuse Ambient Contrast Measurement Methods for Flat Panel Displays, NISTIR 6738.

Kelley, E.F., 2001b. Electronic Display Metrology — Not a Simple Matter, in: Proc. SPIE 4450, Harnessing Light: Optical Science and Metrology at NIST, 44. San Diego, CA. doi:10.1117/12.431252

Kelley, E.F., Eghtesadi, C., Blubaugh, M., Reuschel, W., 2011. Character-contrast measurements on reflective displays using replica masks. J. Soc. Inf. Disp. 19, 685–692.

Kelley, E.F., Jones, G.R., Germer, T.A., 1998a. The Three Components of Reflection. Inf. Displays 10, 24–29.

Kelley, E.F., Jones, G.R., Germer, T.A., 1998b. Display reflectance model based on the BRDF. Displays 19, 27–34. doi:10.1016/S0141-9382(98)00028-6

Kelley, E.F., Lindfors, M., Penczek, J., 2006. Display daylight ambient contrast measurement methods and daylight readability. J. Soc. Inf. Disp. 14, 1019–1030.

Kelley, E.F., Penczek, J., 2004. Scalability of OLED Fluorescence in Consideration of Sunlight-Readability Reflection Measurements. SID Symp. Dig. Tech. Pap. 35, 450–453. doi:10.1889/1.1831011

Kenny, P., Olley, J., Lewis, J.O., 2006. Whole-Sky Luminance Distribution Maps from Calibrated Digital Photography, in: Proceedings of the EuroSun 2006 Conference (CD). International Solar Energy Society, Dublin.

Kent, M.G., Altomonte, S., Tregenza, P.R., Wilson, R., 2014. Discomfort glare and time of day. Light. Res. Technol. 47, 641–657. doi:10.1177/1477153514547291

Kim, S., Kelley, E.F., Penczek, J., 2009. Robustness of Display Reflectance Measurements : Comparison between BRDF and Hemispherical Diffuse Reflectance. SID Symp. Dig. Tech. Pap. 40, 325–327.

King, G., 2002. Systems Modelling and Simulation in the Product Development Process for Automotive Powertrains. University of Warwick.

Kobav, M.B., 2009. Development and validation of methods used to compute time values of indoor daylight illuminances. University of Ljubljana.

Kobav, M.B., Dumortier, D., 2007. USE OF A DIGITAL CAMERA AS A SKY LUMINANCE SCANNER, in: Proceedings of the 26th Session of the CIE in Beijing, China, 4-11 July 2007. Beijing, China.

Labayrade, R., 2014. Certificate of assessment of SPEOS against CIE 171:2006 test cases.

Labayrade, R., Launay, V., 2011. TEST CASES TO ASSESS THE ACCURACY OF SPECTRAL LIGHT TRANSPORT SOFTWARE, in: Proceedings of Building Simulation 2011. International Building Performance Simulation Association, Sydney, pp. 78–85.

Lee, R.L., Devan, D.E., 2008. Observed brightness distributions in overcast skies. Appl. Opt. 47, H116-27.

Li, H., Luo, M., Liu, X., Wang, B., Liu, H., 2016. Evaluation of colour appearance in a real lit room. Light. Res. Technol. 48, 412–432. doi:10.1177/1477153515571784

Littlefair, P.J., 1994. A Comparison of Sky Luminance Models with Measured Data from Garston, United Kingdom. Sol. Energy 53, 315–322.

Loch, C., 2000. Tailoring product development to strategy: case of a European technology manufacturer. Eur. Manag. J. 18, 246–258. doi:10.1016/S0263-2373(00)00007-4

Loch, C.H., Terwiesch, C., 1999. Accelerating the process of engineering change orders: capacity and congestion effects. J. Prod. Innov. Manag. doi:10.1016/S0737-6782(98)00042-3

Mardaljevic, J., 2013. Encyclopedia of Color Science and Technology, Encyclopedia of Color Science and Technology. Springer Berlin Heidelberg, Berlin, Heidelberg. doi:10.1007/978-3-642-27851-8

Mardaljevic, J., 2008. Sky model blends for predicting internal illuminance: a comparison founded on the BRE-IDMP dataset. J. Build. Perform. Simul. 1, 163–173. doi:10.1080/19401490802419836

Mardaljevic, J., 2006. Comment 2 on “Design of a new single-patch sky and sun simulator” by M Bodart, A Deneyer, A De Herde and P Wouters. Light. Res. Technol. 38, 87–88. doi:10.1177/136578280603800121

Mardaljevic, J., 2003. A Radiance Evaluation of Parallax Errors in Sky Simulator Domes, in: Radiance Workshop. Berkeley National Laboratory, USA, pp. 1–31.

Mardaljevic, J., 2002. Quantification of parallax errors in sky simulator domes for clear sky conditions. Light. Res. Technol. 34, 313–332. doi:10.1191/1365782802li055oa

Mardaljevic, J., 1999. Daylight Simulation: Validation, Sky Models and Daylight Coefficients. De Montfort University, Leicester.

Martin, A.C.M., Carvalho, M.M., 2006. Applying virtual simulation in automotive new product development process. Prod. Manag. Dev. 4, 79–86.

Martinez, A., 2010. Faster Photorealism in Wonderland: Physically based shading and lighting at Sony Pictures Imageworks. Siggraph 2010.

Mathur, A., Atchison, D.A., Charman, W.N., 2010. Effects of age on peripheral ocular aberrations. Opt. Express 18, 5840–5853.

Mcfadden, P., 2012. Making things: A reassessment of British manufacturing. London.

Mohr, D; Muller, N; Krieg, A; Gao, P; Kaas, H W; Krieger, A; Hensley, R., 2013. The road to 2020 and beyond: What's driving the global automotive industry?

Müller, S., Kresse, W., Gatenby, N., Schöffel, F., Muller, S., Kresse, W., Gatenby, N., Schoeffel, F., 1995. A radiosity approach for the simulation of daylight. Render. Tech. '95 (Proceedings Sixth Eurographics Work. Render. 137–146.

Muneer, T., 2004. Solar Radiation and Daylight Models, Second. ed. Elsevier Ltd, Oxford.

Murphy, B., Wakefield, A., Friedman, J., 2008. Best Practices for Verification, Validation, and Test in Model- Based Design. MathWorks, Inc. doi:10.4271/2008-01-1469

Murphy, S.P., Perera, T., 2002. Successes and failures in UK / US development of simulation. Simul. Pract. Theory 9, 333–348.

O'Day, S., Tijerina, L., 2011. Legibility: Back to the Basics. SAE Int. J. Passeng. Cars - Mech. Syst. 4, 591–604. doi:10.4271/2011-01-0597

Ogewell, V., 2015. PLM at Jaguar Land Rover – The Moment of Truth for Dassault's 3DEXPERIENCE Platform [WWW Document]. Eng. PLM/ERP. URL http://www.engineering.com/PLMERP/ArticleID/10233/PLM-at-Jaguar-Land-Rover-The-Moment-of-Truth-for-Dassaults-3DEXPERIENCE-Platform.aspx (accessed 5.13.16).

OPTIS, 2017. They trust us [WWW Document]. Showcase. URL http://www.optis-world.com/Showcase/They-trust-us (accessed 7.25.17).

OPTIS, 2016. SPEOS CAA V5 Based Visual Ergonomics User Guide.

OSRAM, 2016. HMI® 12000 W/SE, HMI® 6000 W/SE Brochure.

Owsley, C., 2011. Aging and vision. Vision Res. 51, 1610–1622. doi:10.1016/j.visres.2010.10.020

Pala, S., 2007. Light Wreaks Havoc with Automotive Display Standards Optimizing vehicular flat panel displays. Photonics Spectra.

Paulson Jr., B.C., 1976. Designing to Reduce Construction Costs. J. Constr. Div. 102, 587–592. doi:10.1080/19397030902947041

Penczek, J., Kelley, E.F., Boynton, P.A., 2015. General Metrology Framework for Determining the Ambient Optical Performance of Flat Panel Displays. SID Symp. Dig. Tech. Pap. 46, 727–730.

Photo Research Inc., 2002. PR-920 Digital Video Photometer (DVP).

Preetham, A.J., Shirley, P., Smits, B., 1999. A practical analytic model for daylight. Proc. 26th Annu. Conf. Comput. Graph. Interact. Tech. - SIGGRAPH '99 91–100. doi:10.1145/311535.311545

Pro-Lite Technology Ltd, 2011. ProMetric CCD Imaging Photometers [WWW Document]. Photometers Color.

Pro-Lite Technology Ltd, 2007. CCD Sensor Resolution, Type, Grey Levels and Speed.

Radiant Zemax, 2014. Guide to CCD-Based Imaging Colorimeters.

Radiant Zemax, 2012. PM-1600F ™ Series: Data Sheet.

Raynham, P., 2006. Comment 1 on "Design of a new single-patch sky and sun simulator" by M Bodart, A Deneyer, A De Herde and P Wouters. Light. Res. Technol. 38, 87–87. doi:10.1177/136578280603800120

Rea, M.S., 1986a. Practical implications of a new visual performance model. Light. Res. Technol. 18, 113–118. doi:10.1177/096032718601800301

Rea, M.S., 1986b. Toward a model of visual performance: Foundations and data. J. Illum. Eng. Soc. doi:10.1080/00994480.1986.10748655

Rea, M.S., Ouellette, M.J., 1991. Relative visual performance: A basis for application. Light. Res. Technol. 23, 135–144. doi:10.1177/096032719102300301

Rea, M.S., Ouellette, M.J., 1988. Visual performance using reaction times. Light. Res. Technol. 20, 9. doi:10.1177/096032718802000401

Reuding, T., Meil, P., 2004. Predictive Value of Assessing Vehicle Interior Design Ergonomics in a Virtual Environment. J. Comput. Inf. Sci. Eng. 4, 109. doi:10.1115/1.1710867

Robinson, S., 1997. Simulation model verification and validation. Proc. 29th Conf. Winter Simul. - WSC '97 53–59. doi:10.1145/268437.268448

Rogers, Z., Thanachareonkit, A., Fernades, L., 2013. Enhanced Skylight Modeling and Validation, Energy Research and Development Division FINAL PROJECT REPORT.

Rohrer, M.W., 2000. SEEING IS BELIEVING: THE IMPORTANCE OF VISUALIZATION IN MANUFACTURING SIMULATION, in: Joines, J.A., Barton, R.R., Kang, K., Fishwick, P.A. (Eds.), Proceedings of the 2000 Winter Simulation Conference. IEEE, Orlando, FL, USA, pp. 1211–1216. doi:10.1109/WSC.2000.899087

Roy, G.G., Hayman, S., Julian, W., 1998. Sky Modelling from Digital Imagery.

Rykowski, R., Kostal, H., 2008. LED Characterization for Production Quality Control [WWW Document]. Photonics Spectra. URL http://www.photonics.com/Article.aspx?AID=33008 (accessed 9.10.13).

SAE, 2010. SAE J941: Motor Vehicle Drivers' Eye Locations.

SAE, 2007. SAE J1757-1: Standard Metrology for Vehicular Displays.

Salvi, S.M., Akhtar, S., Currie, Z., 2006. Aging changes in the eye. Postgr. Med. J. 82, 581–587. doi:10.1136/pgmj.2005.040857

Sargent, R.G., 2011. Verification and validation of simulation models. Proc. 2011 Winter Simul. Conf. 2194–2205. doi:10.1109/WSC.2011.6148117

Sawicki, D., Wolska, A., 2015. Discomfort glare prediction by different methods. Light. Res. Technol. 47, 658–671. doi:10.1177/1477153515589773

Schumann, J., Flannagan, M.J., Sivak, M., Traube, E.C., 1996. UMTRI-96-13: Daytime veiling glare and driver visual performance - Influence of windshield rake angle and dashboard reflectance.

Sethi, R., Iqbal, Z., 2008. Stage-Gate Controls, Learning Failure, and Adverse Effect on Novel New Products. J. Mark. 72, 118–134. doi:10.1509/jmkg.72.1.118

Shahriar, A.N.M., Hyde, R., Hayman, S., 2009. Wide-angle Image Analysis for Sky Luminance Measurement. Archit. Sci. Rev. 52, 211–220. doi:10.3763/asre.2009.0021

Sharpe, R., Cartwright, C.M., Gillespie, A., Vassie, K., Christopher, W.C., 2003. Sunlight readability of displays, a numerical scale, in: Proc. SPIE 4826, Fourth Oxford Conference on Spectroscopy, 176 (July 28, 2003). pp. 176–180. doi:doi:10.1117/12.514544

Shimono, M., Imatani, S., Tezuka, A., Ohtani, H., Koyama, T., Hu, X., Nonomura, Y., Kohno, M., 2011.

Modeling and Simulation Methods, in: Czichos, H., Saito, T., Smith, L. (Eds.), Springer Handbook of Metrology and Testing. Springer Berlin Heidelberg, Berlin, Heidelberg, pp. 973–1157. doi:10.1007/978-3-642-16641-9

SMMT, 2016. SMMT Motor Industry Facts 2016.

Spasojević, B., Mahdavi, A., 2005. SKY LUMINANCE MAPPING FOR COMPUTATIONAL DAYLIGHT MODELING, in: Ninth International IBPSA Conference. Montreal, Canada, pp. 1163–1170.

TechnoTeam, 2014. LMK Video Photometers.

Thomke, S., 2007. Learning by experimentation: Prototyping and testing, in: Handbook of New Product Development Management. pp. 401–420. doi:10.1016/B978-0-7506-8552-8.50018-9

Thomke, S., Fujimoto, T., 2000. The Effect of "Front-Loading" Problem-Solving on Product Development Performance. J. Prod. Innov. Manag. 17, 128–142. doi:10.1111/1540-5885.1720128

Thomke, S.H., 1998. Simulation, learning and R&D performance: Evidence from automotive development. Res. Policy 27, 55–74. doi:10.1016/S0048-7333(98)00024-9

Tohsing, K., Schrempf, M., Riechelmann, S., Schilke, H., Seckmeyer, G., 2013. Measuring high-resolution sky luminance distributions with a CCD camera. Appl. Opt. 52, 1564–73.

Transport Knowledge Transfer Networks, 2012. Automotive Routes to Market as Illustrated by the Jaguar Land Rover Innovation System.

Tregenza, P.R., 1987. Subdivision of the sky hemisphere for luminance measurements. Light. Res. Technol. 19, 13–14. doi:10.1177/096032718701900103

Trombini, G., Zirpoli, F., 2013. Innovation Processes in the Car Industry: New Challenges for Management and Research. Automot. Transition. Challenges Strateg. Policy.

Trott, P., 2008. Innovation management and new product development, 4th ed. ed. Financial Times/Prentice Hall, Harlow, England.

UKAS, 2012. M3003: The Expression of Uncertainty and Confidence in Measurement, Edition 3. ed. United Kingdon Accreditation Service. doi:10.1109/IMTC.2000.848897

Unger, D.W., Eppinger, S.D., 2009. Comparing Product Development Processes and Managing Risk The MIT Faculty has made this article openly available . Please share Citation Publisher Version Accessed Citable Link Terms of Use Detailed Terms Comparing product development processes and managi. Int. J. Prod. Dev. 8, 382–402.

Van Oorschot, K., Sengupta, K., Akkermans, H., Van Wassenhove, L., 2010. Get fat fast: Surviving Stage-Gate in NPD. J. Prod. Innov. Manag. doi:10.1111/j.1540-5885.2010.00754.x

Vassie, K., 1998. Specification and assessment of the visual aspects of cockpit displays. SID Symp. Dig. Tech. Pap. 29, 1199–1203. doi:10.1889/1.1833704

Vassie, K., Christopher, C., 2000. Just acceptable and desirable luminance levels for fast jet cockpit displays, in: Hopper, D.G. (Ed.), Proc. SPIE 4022, Cockpit Displays VII: Displays for Defense Applications, 116 (August 28, 2000). pp. 116–125. doi:10.1117/12.397737

Vezifeh, E., Schuß, M., Mahdavi, A., 2015. AN EMPIRICALLY-BASED ASSESSMENT OF COMPUTATIONAL SKY LUMINANCE DISTRIBUTION MODELS, in: 14th Conference of International Building Performance Simulation Association. Hyderabad, India, pp. 2804–2808.

Vitek, J., Kalibera, T., 2011. Repeatability, reproducibility, and rigor in systems research, in:

Proceedings of the Ninth ACM International Conference on Embedded Software - EMSOFT '11. ACM Press, New York, New York, USA, p. 33. doi:10.1145/2038642.2038650

Wang, A.-H., Hwang, S.-L., Kuo, H.-T., 2012. Effects of text / background color combination , ambient illuminance , and display type on discriminating performance for young and elderly users. J. Soc. Inf. Disp. 20, 87–93. doi:10.1889/JSID20.2.87

Wang, A.-H., Hwang, S.-L., Kuo, H.-T., Jeng, S.-C., 2010. Effects of ambient illuminance and electronic displays on users' visual performance for young and elderly users. J. Soc. Inf. Disp. 18, 629–634. doi:10.1889/JSID18.9.629

Wang, A.-H., Kuo, H.-T., Jeng, S.-C., 2009. Effects of ambient illuminance on users' visual performance using various electronic displays. J. Soc. Inf. Disp. 17, 665–669. doi:10.1889/JSID17.8.665

Weale, R.A., 1961. Retinal Illumination and Age. Light. Res. Technol. 26, 95–100. doi:10.1177/147715356102600204

Weindorf, P., Hayden, B., 2013. Automotive Display Visibility Considerations. SID Symp. Dig. Tech. Pap. 44, 555–558.

Wheelwright, S.C., Clark, K.B., 1992a. Revolutionizing product development : quantum leaps in speed, efficiency, and quality. Simon and Schuster, New York.

Wheelwright, S.C., Clark, K.B., 1992b. Creating project plans to focus product development. Harv. Bus. Rev. 70, 70–82.

Williams, O.S., 2008. New Product Introduction Process Improvements in an Automotive Company. Cranfield University.

WMG, 2013. International Doctorate Centre Handbook 2013.

Wolf, D.C., 2014. Modelling Image Quality for Automotive Display Technologies. Abertay University.

Wyszecki, G., Stiles, W.S., 1982. Color Science: Concepts and Methods, Quantitative Data and Fromulae, 2nd ed. John Wiley & Sons.

Yazdani, B., 2006. Lean product development: Jaguar Land Rover, in: IET 2nd International Technology and Innovation Conference. IEE, pp. 113–132. doi:10.1049/ic:20060230

Youmans, R.J., 2011. The effects of physical prototyping and group work on the reduction of design fixation. Des. Stud. 32, 115–138. doi:10.1016/j.destud.2010.08.001

Zorriassatine, F., Wykes, C., Parkin, R., Gindy, N., 2003. A survey of virtual prototyping techniques for mechanical product development. Proc. Instn Mech Engrs 217, 513–530. doi:10.1243/095440503321628189

Appendix A MEASUREMENTS

A.1 MEASUREMENTS TAKEN IN AUSTRALIA

Test #	Vehicle Orientation		Date	Time (GMT+11)	Global Horizontal Illuminance (lm/m^2)	Interior illuminance (lm/m^2)
#1	East	Sun Passenger Side	14/01/2015	12:32 PM	127,000	3,560
#2	East	Sun Passenger Side	14/01/2015	1:08 PM	118,900	2,175
#3	East	Sun Passenger Side	14/01/2015	1:58 PM	121,500	1,566
#4	East	Sun Passenger Side	14/01/2015	2:29 PM	117,200	1,395
#5	East	Sun Passenger Side	14/01/2015	3:00 PM	113,600	1,268
#6	East	Sun Passenger Side	14/01/2015	3:38 PM	105,300	1,100
#7	East	Sun Passenger Side	14/01/2015	4:00 PM	105,100	1,082
#8	West	Sun Driver's Side	15/04/2015	9:59 AM	96,100	1,489
#9	West	Sun Driver's Side	15/04/2015	10:32 AM	111,500	1,451
#10	West	Sun Driver's Side	15/04/2015	10:59 AM	123,200	2,547
#11	West	Sun Driver's Side	15/04/2015	11:30 AM	124,500	2,121
#12	West	Sun Driver's Side	15/04/2015	12:00 PM	128,100	2,124
#13	West	Sun Driver's Side	15/04/2015	12:29 PM	129,500	2,255
#14	West	Sun Driver's Side	15/04/2015	1:00 PM	129,800	3,230
#15	West	Sun Driver's Side	15/04/2015	1:31 PM	68,500	5,610
#16	West	Sun Driver's Side	15/04/2015	2:00 PM	32,800	3,360
#17	West	Sun Driver's Side	15/04/2015	2:30 PM	54,800	3,330
#18	West	Sun Driver's Side	15/04/2015	3:00 PM	108,300	3,490
#19	West	Sun Driver's Side	15/04/2015	3:30 PM	101,000	5,670
#20	West	Sun Driver's Side	15/04/2015	4:00 PM	89,500	5,710
#21	South	Sun Rear	16/01/2015	10:00 AM	85,200	2,992
#22	South	Sun Rear	16/01/2015	10:29 AM	93,200	2,174
#23	South	Sun Rear	16/01/2015	11:01 AM	108,300	2,422
#24	South	Sun Rear	16/01/2015	11:32 AM	114,400	2,466
#25	South	Sun Rear	16/01/2015	1:02 PM	128,500	1,802
#26	South	Sun Rear	16/01/2015	1:31 PM	129,300	2,203
#27	South	Sun Rear	16/01/2015	2:01 PM	121,900	1,452
#28	South	Sun Rear	16/01/2015	2:30 PM	118,300	1,417
#29	South	Sun Rear	16/01/2015	2:59 PM	119,200	1,497
#30	South	Sun Rear	16/01/2015	3:29 PM	97,600	1,612
#31	South	Sun Rear	16/01/2015	4:01 PM	89,100	1,648

A.2 DISPLAY CENTRE LOCATIONS – LAB ASSESSMENTS

Measurement No.	Centre of nav. arrow		Centre of display		Distance from datum origin (mm)
	x	y	x	y	
#1	0.588	-0.381	0	0	0
#2	0.623	-0.346	0.035	0.035	0.04949747
#3	0.623	-0.346	0.035	0.035	0.04949747
#4	0.658	-0.346	0.070	0.035	0.07826238
#5	0.658	-0.346	0.070	0.035	0.07826238
#6	0.658	-0.346	0.070	0.035	0.07826238
#7	0.692	-0.346	0.104	0.035	0.10973149
#8	0.692	-0.311	0.104	0.07	0.12536347
#9	0.727	-0.311	0.139	0.07	0.15563097
#10	0.727	-0.311	0.139	0.07	0.15563097
#11	0.761	-0.381	0.173	0	0.17300000
#12	0.761	-0.416	0.173	-0.035	0.17650496
#13	1.246	-1.384	0.658	-1.003	1.19957201
#14	0.173	-0.623	-0.415	-0.242	0.48040504
#15	-0.415	-0.623	-1.003	-0.242	1.03178147
#16	-0.45	-0.623	-1.038	-0.242	1.06583676
#17	-0.519	-0.623	-1.107	-0.242	1.13314297
#18	-0.692	-0.623	-1.280	-0.242	1.30267571
#19	0.277	-0.381	-0.311	0	0.31100000
#20	0.311	-0.381	-0.277	0	0.27700000
#21	0.45	-0.381	-0.138	0	0.13800000
#22	0.588	-0.346	0	0.035	0.03500000
#23	0.623	-0.346	0.035	0.035	0.04949747
#24	0.657	-0.346	0.069	0.035	0.07736924
#25	0.657	-0.346	0.069	0.035	0.07736924
#26	0.692	-0.346	0.104	0.035	0.10973149
#27	0.692	-0.346	0.104	0.035	0.10973149
#28	0.692	-0.346	0.104	0.035	0.10973149
#29	0.692	-0.346	0.104	0.035	0.10973149
#30	0.103	-0.484	-0.485	-0.103	0.49581650
#31	0.691	-0.45	0.103	-0.069	0.12397580
#32	0.691	-0.45	0.103	-0.069	0.12397580
#33	0.795	-0.45	0.207	-0.069	0.21819716
#34	0.795	-0.45	0.207	-0.069	0.21819716
#35	0.83	-0.415	0.242	-0.034	0.24437676
#36	0.83	-0.415	0.242	-0.034	0.24437676
#37	1.349	-0.45	0.761	-0.069	0.76412172

Measurement No.	Centre of nav. arrow		Centre of display		Distance from datum origin (mm)
	x	y	x	y	
#38	1.349	-0.449	0.761	-0.068	0.76403207
#39	1.349	-0.449	0.761	-0.068	0.76403207
#40	1.349	-0.45	0.761	-0.069	0.76412172
#41	1.385	-0.45	0.797	-0.069	0.79998125
#42	1.42	-0.45	0.832	-0.069	0.83485628
#43	1.418	-0.449	0.83	-0.068	0.83278088
#44	1.418	-0.449	0.83	-0.068	0.83278088
#45	1.418	-0.449	0.83	-0.068	0.83278088
#46	1.419	-0.45	0.831	-0.069	0.83385970
#47	1.419	-0.45	0.831	-0.069	0.83385970
#48	1.419	-0.451	0.831	-0.070	0.83394304
#49	1.419	-0.451	0.831	-0.070	0.83394304
#50	0.623	-0.485	0.035	-0.104	0.10973149
#51	0.311	-0.52	-0.277	-0.139	0.30991934
#52	0.104	-0.554	-0.484	-0.173	0.51398930
#53	0.104	-0.623	-0.484	-0.242	0.54112845
#54	-0.036	-0.624	-0.624	-0.243	0.66964543
#55	-0.485	-0.589	-1.073	-0.208	1.09297438
#56	-0.52	-0.589	-1.108	-0.208	1.12735443
#57	-0.485	-0.554	-1.073	-0.173	1.08685694
#58	-0.52	-0.589	-1.108	-0.208	1.12735443
#59	-0.485	-0.554	-1.073	-0.173	1.08685694

A.3 DISPLAY CENTRE LOCATIONS – FIELD MEASUREMENTS

Measurement No.	Centre of nav. arrow		Centre of display		Distance from datum origin (mm)
	x	y	x	y	
#1	0.147	-0.104	0.32	-0.369	0.488427067
#2	0.156	0.017	0.329	-0.248	0.412001214
#3	0.13	0.06	0.303	-0.205	0.365833295
#4	0.121	0.096	0.294	-0.169	0.339112076
#5	0.121	0.096	0.294	-0.169	0.339112076
#6	0.112	0.078	0.285	-0.187	0.34087241
#7	0.112	0.078	0.285	-0.187	0.34087241
#8	-0.173	0.265	0	0	0
#9	-0.173	0.265	0	0	0
#10	-0.173	0.265	0	0	0
#11	-0.173	0.265	0	0	0
#12	-0.173	0.265	0	0	0
#13	-0.173	0.265	0	0	0
#14	-0.173	0.265	0	0	0
#15	-0.173	0.265	0	0	0
#16	-0.173	0.265	0	0	0
#17	-0.173	0.265	0	0	0
#18	-0.173	0.265	0	0	0
#19	-0.173	0.265	0	0	0
#20	-0.173	0.265	0	0	0
#21	-0.182	0.251	-0.009	-0.014	0.016643317
#22	-0.182	0.251	-0.009	-0.014	0.016643317
#23	-0.182	0.251	-0.009	-0.014	0.016643317
#24	-0.182	0.251	-0.009	-0.014	0.016643317
#25	-0.173	0.294	0	0.029	0.029
#26	-0.173	0.277	0	0.012	0.012
#27	-0.173	0.277	0	0.012	0.012
#28	-0.181	0.277	-0.008	0.012	0.014422205
#29	-0.181	0.277	-0.008	0.012	0.014422205
#30	-0.181	0.277	-0.008	0.012	0.014422205
#31	-0.181	0.277	-0.008	0.012	0.014422205

Appendix B SUB-DIVISION OF THE SKY

B.1 PATCH LOCATIONS TO THE TREGENZA SUB-DIVISION OF THE SKY

This table is adapted from Muneer (2004)

Patch #	1	2	3	4	5	6	7	8	9	10
Elevation	6	6	6	6	6	6	6	6	6	6
Azimuth	180	192	204	216	228	240	252	264	276	288
Patch #	11	12	13	14	15	16	17	18	19	20
Elevation	6	6	6	6	6	6	6	6	6	6
Azimuth	300	312	324	336	348	0	12	24	36	48
Patch #	21	22	23	24	25	26	27	28	29	30
Elevation	6	6	6	6	6	6	6	6	6	6
Azimuth	60	72	84	96	108	120	132	144	156	168
Patch #	31	32	33	34	35	36	37	38	39	40
Elevation	18	18	18	18	18	18	18	18	18	18
Azimuth	168	156	144	132	120	108	96	84	72	60
Patch #	41	42	43	44	45	46	47	48	49	50
Elevation	18	18	18	18	18	18	18	18	18	18
Azimuth	48	36	24	12	0	348	336	324	312	300
Patch #	51	52	53	54	55	56	57	58	59	60
Elevation	18	18	18	18	18	18	18	18	18	18
Azimuth	288	276	264	252	240	228	216	204	192	180
Patch #	61	62	63	64	65	66	67	68	69	70
Elevation	30	30	30	30	30	30	30	30	30	30
Azimuth	180	195	210	225	240	255	270	285	300	315
Patch #	71	72	73	74	75	76	77	78	79	80
Elevation	30	30	30	30	30	30	30	30	30	30
Azimuth	330	345	0	15	30	45	60	75	90	105
Patch #	81	82	83	84	85	86	87	88	89	90
Elevation	30	30	30	30	42	42	42	42	42	42

Azimuth	120	135	150	165	165	150	135	120	105	90
Patch #	91	92	93	94	95	96	97	98	99	100
Elevation	42	42	42	42	42	42	42	42	42	42
Azimuth	75	60	45	30	15	0	345	330	315	300
Patch #	101	102	103	104	105	106	107	108	109	110
Elevation	42	42	42	42	42	42	42	42	54	54
Azimuth	285	270	255	240	225	210	195	180	180	200
Patch #	111	112	113	114	115	116	117	118	119	120
Elevation	54	54	54	54	54	54	54	54	54	54
Azimuth	220	240	260	280	300	320	340	0	20	40
Patch #	121	122	123	124	125	126	127	128	129	130
Elevation	54	54	54	54	54	54	66	66	66	66
Azimuth	60	80	100	120	140	160	150	120	90	60
Patch #	131	132	133	134	135	136	137	138	139	140
Elevation	66	66	66	66	66	66	66	66	78	78
Azimuth	30	0	330	300	270	240	210	180	180	240
Patch #	141	142	143	144	145					
Elevation	78	78	78	78	90					
Azimuth	300	0	60	120	-					

Appendix C TESTS OF STATISTICAL SIGNIFICANCE

C.1 MATERIALS OF SIMULATED DISPLAYS

Two-Sample T-Test and CI: satBRDF_fL, sat.approx_fL

```
Two-sample T for satBRDF_fL vs sat.approx_fL

                N   Mean  StDev  SE Mean
satBRDF_fL     12   1539   1922      555
sat.approx_fL  12  224.7   32.0      9.2


Difference = μ (satBRDF_fL) - μ (sat.approx_fL)
Estimate for difference:  1315
95% CI for difference:  (93, 2536)
T-Test of difference = 0 (vs ≠): T-Value = 2.37  P-Value = 0.037  DF = 11
```

Two-Sample T-Test and CI: satBRDF_bL, sat.approx_bL

```
Two-sample T for satBRDF_bL vs sat.approx_bL

                N  Mean  StDev  SE Mean
satBRDF_bL     12  1333   1948      562
sat.approx_bL  12  22.7   12.0      3.5


Difference = μ (satBRDF_bL) - μ (sat.approx_bL)
Estimate for difference:  1311
95% CI for difference:  (73, 2548)
T-Test of difference = 0 (vs ≠): T-Value = 2.33  P-Value = 0.040  DF = 11
```

C.2 TURBIDITY OF SKY MODELS

Test for Equal Variances: T2, T4, T6

```
Method

Null hypothesis         All variances are equal
Alternative hypothesis  At least one variance is different
Significance level      α = 0.05

95% Bonferroni Confidence Intervals for Standard Deviations

Sample    N    StDev          CI
    T2  372  194.042  (112.782, 336.014)
    T4  372  163.434  ( 95.882, 280.383)
    T6  372  141.183  ( 84.305, 237.969)

Individual confidence level = 98.3333%

Tests

                          Test
Method                Statistic  P-Value
Multiple comparisons          —    0.603
Levene                     0.42    0.657
```

P value is greater than the significance level, $\alpha = 0.05$, therefore the null hypothesis is not rejected and variances can be assumed to be equal.

One-way ANOVA: T2_fL, T4_fL, T6_fL

```
Method

Null hypothesis         All means are equal
Alternative hypothesis  At least one mean is different
Significance level      α = 0.05

Equal variances were assumed for the analysis.


Factor Information

Factor  Levels  Values
Factor       3  T2_fL, T4_fL, T6_fL


Analysis of Variance

Source    DF    Adj SS  Adj MS  F-Value  P-Value
Factor     2     21227   10613     0.38    0.686
Error   1113  31273802   28099
Total   1115  31295029


Model Summary

      S   R-sq  R-sq(adj)  R-sq(pred)
167.627  0.07%      0.00%       0.00%


Means

Factor    N    Mean   StDev        95% CI
T2      372   272.5   194.0  ( 255.4,  289.5)
T4      372  278.08  163.43  (261.03, 295.13)
T6      372  283.14  141.18  (266.09, 300.19)

Pooled StDev = 167.627
```

One-way ANOVA: T2_bL, T4_bL, T6_bL

```
Method

Null hypothesis         All means are equal
Alternative hypothesis  At least one mean is different
Significance level      α = 0.05

Equal variances were assumed for the analysis.


Factor Information

Factor  Levels  Values
Factor       3  T2_bL, T4_bL, T6_bL


Analysis of Variance

Source    DF    Adj SS  Adj MS  F-Value  P-Value
Factor     2     33216   16608     0.55    0.575
Error   1113  33355700   29969
Total   1115  33388916


Model Summary

      S   R-sq  R-sq(adj)  R-sq(pred)
173.116  0.10%      0.00%       0.00%


Means

Factor    N   Mean   StDev       95% CI
T2_bL   372   73.6   198.5  (56.0,   91.3)
T4_bL   372  80.26  170.43  (62.65,  97.87)
T6_bL   372  87.01  146.52  (69.40, 104.62)

Pooled StDev = 173.116
```

Appendix D DAYLIGHT SPECIFICATIONS

D.1 CHROMATICITY CHARTS

Different phases of daylight span a wide range of chromaticities. The specifications give a tolerance that spans the region of the isothermal line of constant CCT that is representative of the D65 illuminant.

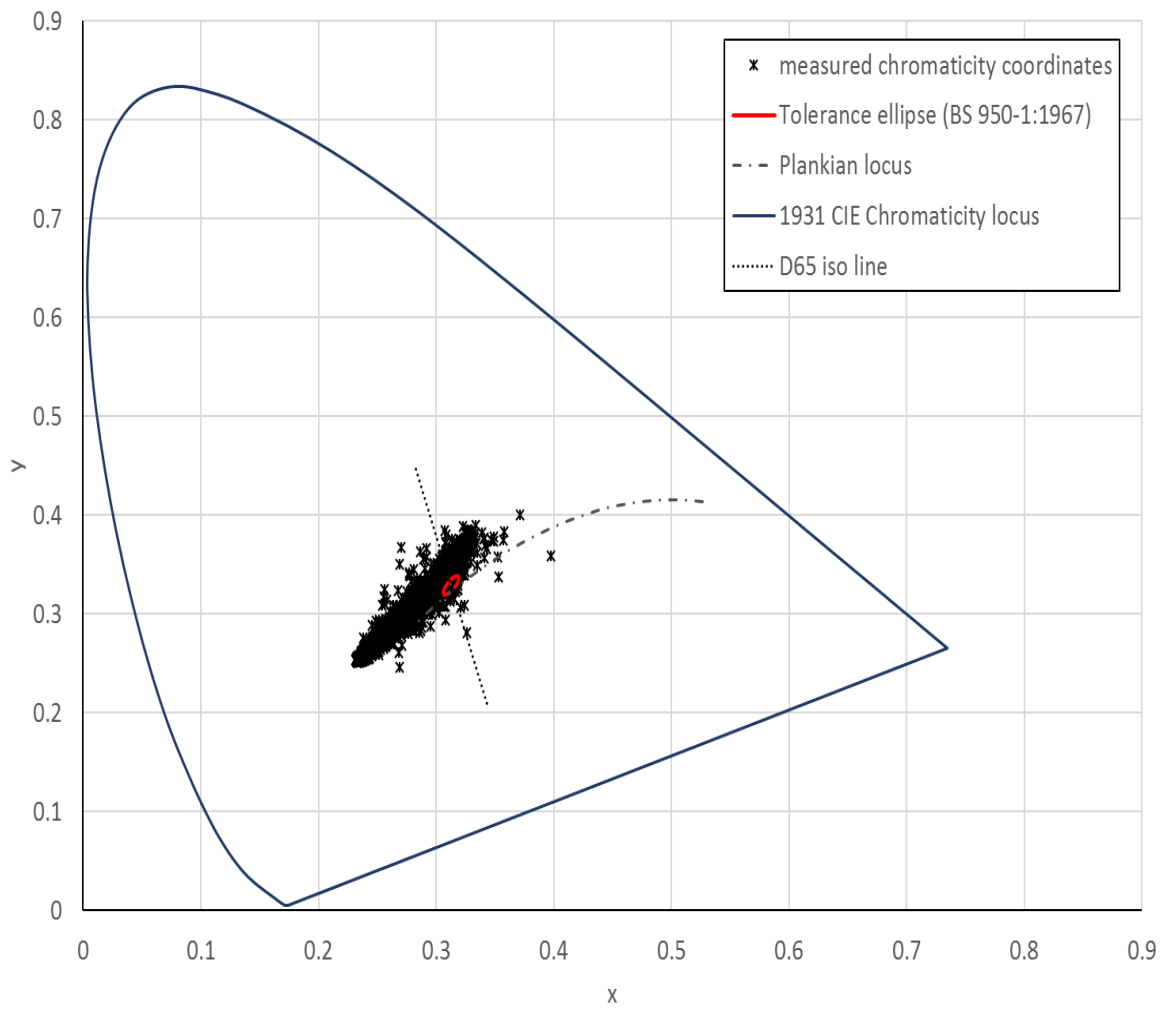

Figure D-1: Measured chromaticity and tolerance ellipse for daylight illuminant (BSI, 1967) *plotted on The CIE 1931 Chromaticity Diagram (range 0-0.9 x and y values)*

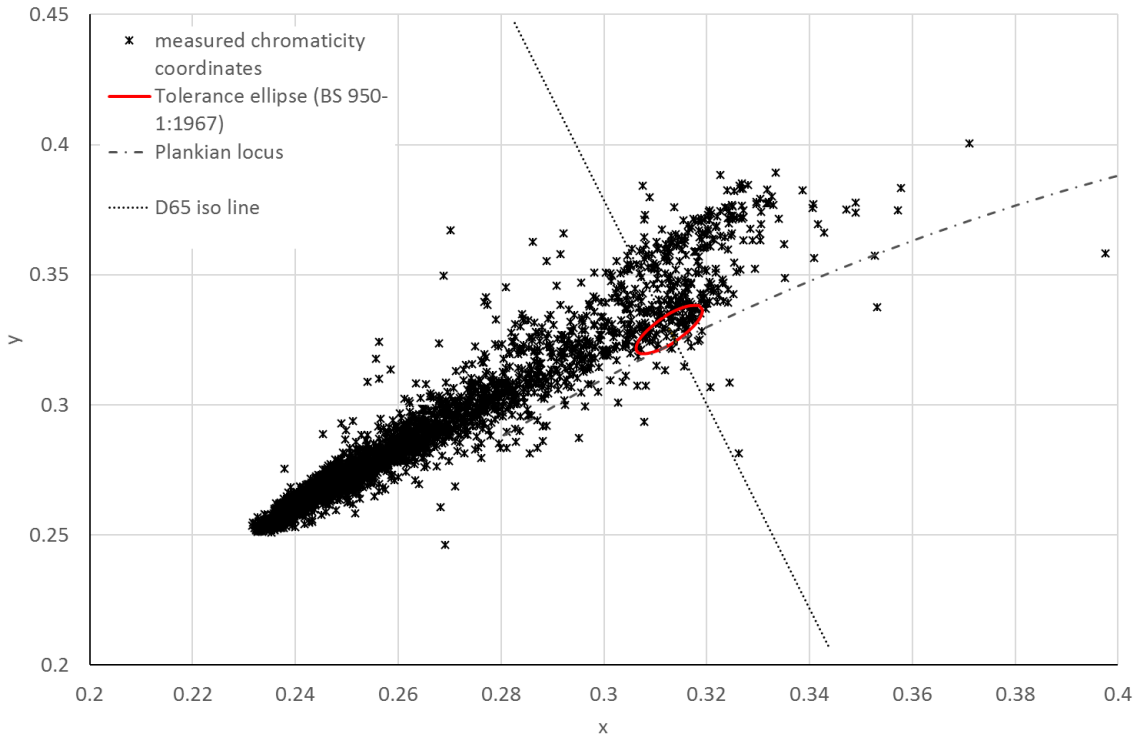

Figure D-2: Measured chromaticity and tolerance ellipse for daylight illuminant (BSI, 1967) *plotted on The CIE 1931 Chromaticity Diagram (range 0.2-0.45 x and y values)*

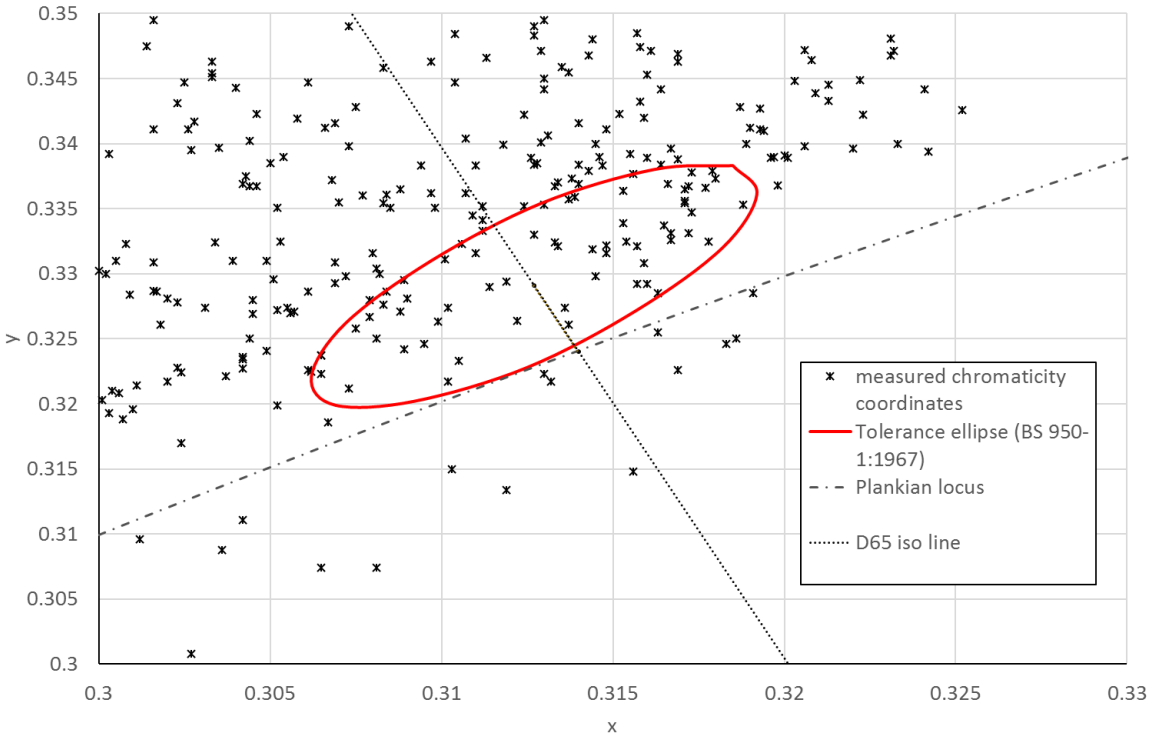

Figure D-3: Measured chromaticity and tolerance ellipse for daylight illuminant (BSI, 1967) *plotted on The CIE 1931 Chromaticity Diagram (range 0.3-0.35 x and y values)*

D.2 AVERAGE SKY VALUES FROM MEASUREMENT

Sky #	Mean global horizontal illuminance (lux)	CCT (K) [sky only]	CCT of 'sun' (assuming 10klux 'sky') *	CCT of 'sun' (assuming 5klux 'sky') *	Luminance (cd/m²) [Sky only]
1	127,000	21,264.39	5,238.09	5,894.90	4,080.85
2	118,900	23,522.73	4,936.85	5,752.73	2,922.04
3	121,500	27,903.11	4,580.44	5,581.41	2,621.77
4	117,200	28,633.43	4,435.31	5,513.66	2,792.61
5	113,600	29,349.90	4,294.41	5,447.98	2,860.97
6	105,300	31,659.92	3,859.92	5,245.77	2,751.22
7	105,100	28,383.32	4,198.91	5,406.93	2,971.92
8	96,100	22,424.22	4,650.50	5,626.00	4,029.54
9	111,500	22,688.80	4,905.04	5,739.96	3,136.96
10	123,200	19,494.61	5,352.07	5,950.31	4,865.64
11	124,500	18,164.30	5,481.28	6,011.95	3,990.47
12	128,100	18,336.17	5,497.78	6,019.25	3,924.40
13	129,500	18,047.30	5,533.70	6,036.25	3,947.56
14	129,800	16,162.06	5,693.48	6,112.90	4,653.82
18	108,300	14,021.59	5,734.83	6,135.93	5,099.38
19	101,000	12,014.05	5,894.06	6,212.81	6,987.07
20	89,500	12,433.33	5,753.67	6,148.92	6,339.15
21	85,200	11,728.36	5,804.74	6,174.04	5,891.97
22	93,200	15,032.42	5,474.47	6,016.30	4,647.23
23	108,300	12,226.40	5,917.46	6,222.83	6,118.88
24	114,400	12,193.76	5,954.62	6,239.77	5,550.03
25	128,500	13,571.42	5,903.26	6,213.71	5,449.92
26	129,300	15,030.11	5,784.99	6,156.87	4,654.73
27	121,900	18,629.21	5,416.07	5,981.21	3,145.29
28	118,300	22,684.85	5,005.55	5,785.75	2,708.23
29	119,200	23,219.53	4,968.91	5,767.97	2,727.77
30	97,600	19,997.69	4,959.17	5,771.18	3,046.33
31	89,100	21,042.39	4,661.52	5,635.41	2,808.06
Mean	112,682.14	19,637.83	5,210.40	5,885.81	4,097.28
Min	85,200	11,728	3,860	5,246	2,622
Max	129,800	31,660	5,955	6,240	6,987
SD	13762.40	5890.45	593.52	282.06	1297.84

* CCT relationship given by equation Equation D-1 (based on method used by (Kelley et al., 2006).

Equation D-1: CCT of sunlight combined with skylight to give average daylight CCT 6500 K

$$CCT_{Sun} = \frac{\left(6{,}500 \cdot \left(E_{Sky} + E_{Sun}\right)\right) - \left(E_{Sky} CCT_{Sky}\right)}{E_{Sun}}$$

D.3 SPECTRAL POWER DISTRIBUTIONS

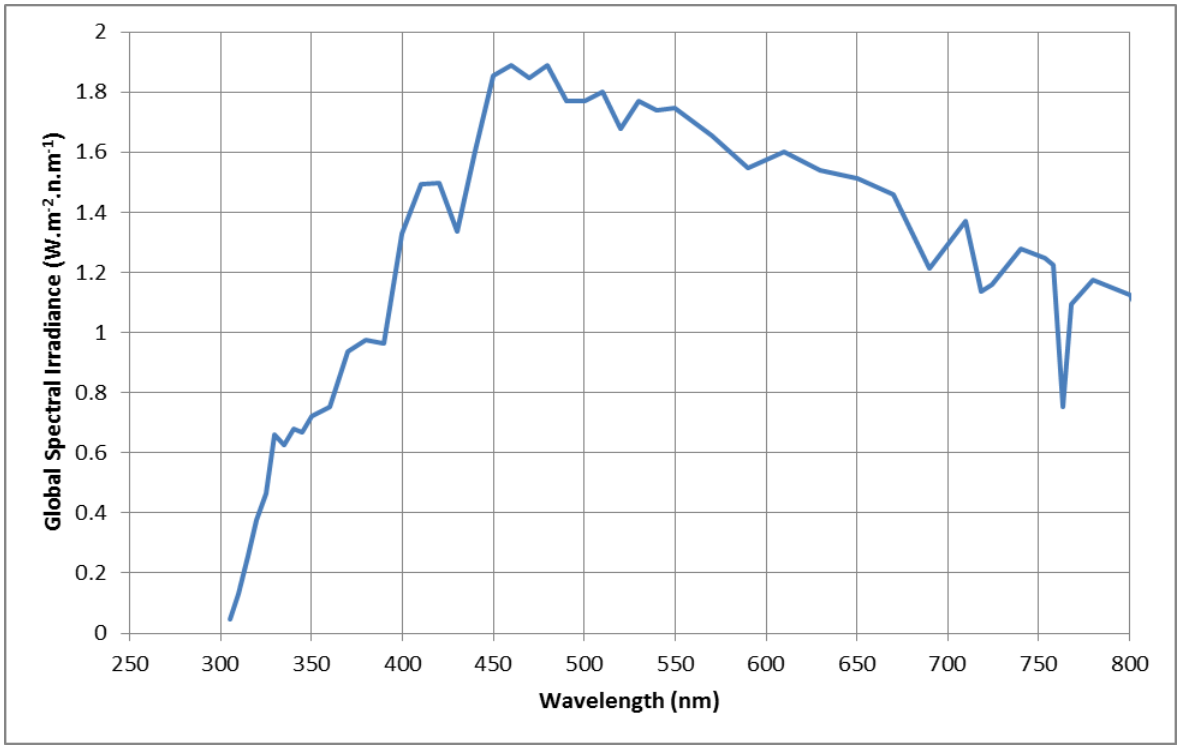

Figure D-4: Spectral irradiance distribution CIE 85 Table 4 (based on data from (CIE, 1989)*)*

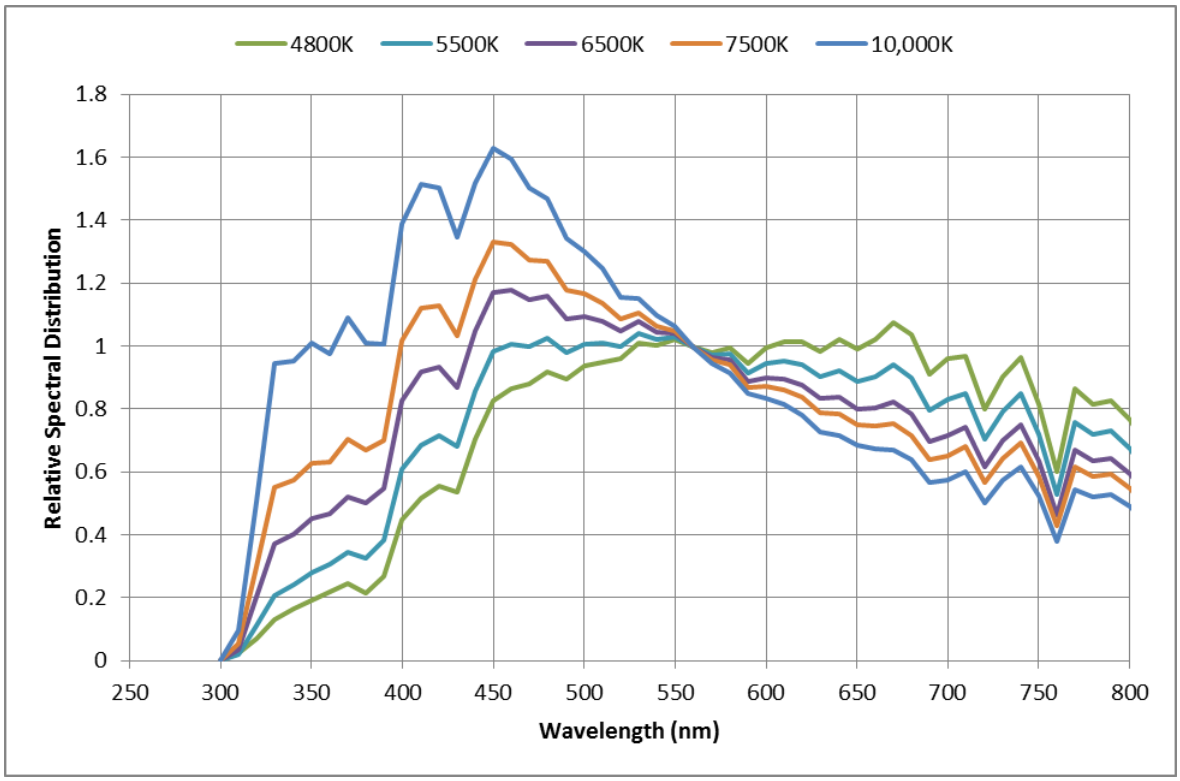

Figure D-5: Spectral irradiance distributions of the standard phases of daylight (data normalised to 560nm) (Judd et al., 1964)